Physicochemical studies on the recovery and immobilization of radiocesium

By

DAYAMOY BANERJEE

(CHEM01200604035)

BHABHA ATOMIC RESEARCH CENTRE

A thesis submitted to the
Board of Studies in Chemical Sciences

In partial fulfillment of requirements
For the Degree of

DOCTOR OF PHILOSOPHY
of
HOMI BHABHA NATIONAL INSTITUTE

May 2012

Homi Bhabha National Institute

Recommendations of the Viva Voce Board

As members of the Viva Voce Board, we certify that we have read the dissertation prepared by Shri **DAYAMOY BANERJEE** entitled **"Physicochemical studies on the recovery and immobilization of radiocesium"** and recommend that it may be accepted as fulfilling the dissertation requirement for the Degree of Doctor of Philosophy.

External Examiner	**Prof. (Dr.) S.R. Dharwadkar** Adjunct Professor of Chemistry, Department of Chemistry, Mumbai University, Mumbai, India.	
Chairman	**Prof. (Dr.) B.S. Tomar** Head, Radioanalytical Chemistry Division Bhabha Atomic Research Centre	10/10/2012
Guide	**Prof. (Dr.) D. Das** Head, Chemistry Division Bhabha Atomic Research Centre	10/10/2012
Member-1	**Prof. (Dr.) V. K. Jain** Head, Synthesis and Pure Material Section Chemistry Division Bhabha Atomic Research Centre	
Member-2	**Prof. (Dr.) P.K. Mohapatra** Head, Actinide Chemistry Section Radiochemistry Division Bhabha Atomic Research Centre	
Member-3	**Prof. (Dr.) C.P. Kaushik** Dy PS, WMFT(H) Waste Management Division Bhabha Atomic Research Centre	10/10/2012

Final approval and acceptance of this dissertation is contingent upon the candidate's submission of the final copies of the dissertation to HBNI.

I hereby certify that I have read this dissertation prepared under my direction and recommend that it may be accepted as fulfilling the dissertation requirement.

Date: October 10, 2012
Place: Mumbai

STATEMENT BY AUTHOR

This dissertation has been submitted in partial fulfillment of requirements for an advanced degree at Homi Bhabha National Institute (HBNI) and is deposited in the Library to be made available to borrowers under rules of the HBNI.

Brief quotations from this dissertation are allowable without special permission, provided that accurate acknowledgement of source is made. Requests for permission for extended quotation from or reproduction of this manuscript in whole or in part may be granted by the Competent Authority of HBNI when in his or her judgment the proposed use of the material is in the interests of scholarship. In all other instances, however, permission must be obtained from the author.

(Dayamoy Banerjee)
Author

DECLARATION

I hereby declare that the investigation presented in the thesis has been carried out by me. The work is original and has not been submitted earlier as a whole or in part for a degree / diploma at this or any other Institution / University.

(Dayamoy Banerjee)
Author

Dedicated to

“MRITTIKA”

ACKNOWLEDGEMENTS

I am deeply indebted to Dr.S.K. Samanta (presently at IAEA, Vienna on Foreign Service), who not only introduced me the subject of nuclear waste management but also encouraged me to do the Ph.D work on the title topic. He kindly accepted my registration for the Ph.D programme under his guidance and provided invaluable support and encouragement during the course of this work.

I am extremely grateful to Dr. D. Das, Professor HBNI and Head, Chemistry Division, Bhabha Atomic Research Centre, who accepted me wholeheartedly as his student, when Dr. Samanta was deputed on assignment to IAEA, Vienna. Without his deep involvement and invaluable guidance, this thesis would have never seen the light of day.

I wish to express my most sincere gratitude to Shri P.K. Wattal, Head Process Development Division, Bhabha Atomic Research Centre, who granted me permission to resister for Ph.D Programme and also gave me constant support and encouragement.

It gives me immense pleasure to place on record my heartfelt thanks to Shri S.D. Misra, Director, Nuclear recycle Group, Dr. I.J. Singh, former Head, Effluent Treatment and Matrix Development Section, Dr. C. Srinivas, Head Process Chemistry and Decontamination Studies Section and Dr. J.G. Shah, Head, Matrix Development Section, for their support and encouragement during the course of the work.

I am grateful to Dr. V. Sudarsan, Chemistry Division, for his invaluable support in helping me in understanding the structural characterization of glass samples and critical analysis of the manuscripts. His unfailing enthusiasm has helped complete the study.

I also wish to express my sincere gratitude to all members of my Doctoral committee for not only spending their valuable time in reviewing the progress of the work, but also for their invaluable suggestions and encouragement.

It has been a great experience to work as a team with Smt. Manjula A Rao, Smt. Sandhya Unnikrishnan and Smt. Annie Joseph. I acknowledge their invaluable contribution in conducting experiments and preparation of manuscripts. I also thank all members of Process Development Division, for their direct and indirect support during the course of the work. The support received from my colleagues Shri A.P. Anthony, Shri S.A. Khot, Shri Ajay Manjrekar and Smt. Pallavi Songire cannot be forgotten.

Many of my friends provided invaluable support by extending instrumental facilities available in their laboratories. I wish to express my appreciation of the help rendered by Dr. Balaji Mondal, Dr. Swarup Rakshit, Dr. R.K. Misra and Dr. V. Naidu.

I convey my heartfelt gratitude to my parents and all my family members and relatives who have always inspired my inquisitive mind throughout my childhood, study and career. Their inspiration, encouragement, blessings and support have helped me reach where I am today.

Last but not the least, I convey my heartfelt love to my daughter Shree who always inspired me with a smiling face even though I spent extended time at work and could not spare adequate playtime for her.

(Dayamoy Banerjee)

CONTENTS

Synopsis xii

List of tables xxiii

List of figures xxv

Abbreviation xxxi

1. Chapter 1 *Introduction* 1

1.1 Applications of radioisotopes 3

1.1.1 Radioisotopes for sealed sources applications 4

1.1.2 Radioisotopes for radiation technology applications 5

1.1.3 Uses of ^{60}Co in radiation technology application 6

1.1.4 Uses of ^{137}Cs in radiation technology application 7

1.2 Inventory of ^{137}Cs 8

1.2.1 Production 8

1.2.2 Reprocessing of spent fuel 8

1.2.3 Distribution of ^{137}Cs in different waste streams 9

1.2.4 Specific activity of ^{137}Cs in waste 10

1.3 Methods for Recovery of ^{137}Cs 11

1.3.1 Chemical precipitation based processes 11

1.3.2 Solvent extraction based processes 12

1.3.3 Ion exchange based processes 14

1.4 Selection of the source matrices 17

1.5 Matrices for immobilization of ^{137}Cs 18

1.6 Scope of the present work 21

2. Chapter 2 *Experimental* 26

2.1 Introduction 27

2.2 Preparation of AMP sorbents and RFPR Resins 27

2.3 Characterization of AMP sorbents and RFPR Resins 28

2.3.1 Determination of moisture content 28

2.3.2 Determination of batch distribution coefficient 28

2.3.3 Determination of cesium sorption isotherm 29

2.3.4 Column tests 29

2.3.5 Analysis and calculation 29

2.4 Preparation of glass 30

2.5 Chemical analysis of glass 31

2.5.1 Direct analysis 31

2.5.2 Indirect analysis 32
2.6 Density and molar volume 33
2.7 Chemical durability 33
2.8 Volatilization of Cs 35
2.8.1 Measurement of Cs volatility during glass preparation 35
2.8.2 Measurement of Cs volatility with preformed glass 37
2.9 Instrumental techniques used for analysis and characterization 40
2.9.1 Gamma ray detection system 40
2.9.2 Ion chromatograph 43
2.9.3 X-Ray diffraction 46
2.9.4 Thermal analysis 48
2.9.5 Vibrational spectroscopy 49
2.9.6 Nuclear magnetic resonance (NMR) spectroscopy 50
2.9.7 UV-VIS spectroscopy 54
2.9.8 Scanning electron microscopy (SEM) 54
3. Chapter 3 *Recovery of Cs* 57
3.1 Introduction 58
3.2 Theoretical estimation on Cs purification requirement 60
3.3 Separation of Cs from acidic waste streams 61
3.3.1 Characterization of AMP sorbents 61
3.3.2 General characteristics 61
3.3.3 Cesium sorption isotherm of AMP sorbents 62
3.3.4 Effect of HNO_3 concentration on Cs^+ uptake by AMP sorbent 64
3.3.5 Column tests on the separation of Cs from acidic solution using AMP-PMMA 65
3.3.6 Recovery of Cs^+ from Cs loaded AMP-PMMA column 66
3.4 Separation of Cs from alkaline waste streams 68
3.4.1 General characteristics of the RFPR 70
3.4.2 Effect of NH_4^+ ion on Cs^+ uptake by RFPR 71
3.4.3 Cesium sorption isotherm for RFPR 72
3.4.4 Correlation of batch data with Freundlich isotherm 73
3.4.5 Correlation of batch data with Dubinin-Radushkevich (D-R) isotherm 75
3.4.6 Prediction of column loading from batch results 78
3.4.7 Mechanism of Cs sorption 79
3.4.8 Column tests for separation of Cs 81
3.4.9 Recovery of Cs 84
3.5 Summary of the results and conclusions 89

4. Chapter 4 *Physicochemical properties of cesium borosilicate glasses containing TiO_2* 91
4.1 Introduction 92
4.2 Glass forming region of Na borosilicate system 94
4.3 Preparation of alkali borosilicate glasses 95
4.4 Preparation of TiO_2 containing glasses 96
4.5 Chemical analysis of glass 97
4.6 General characteristics of the glasses containing TiO_2 98
4.6.1 Density and molar volume 98
4.6.2 XRD analysis 99
4.6.3 Glass transition temperature 100
4.6.4 Chemical durability 101
4.7 Volatilization of Cs 103
4.7.1 Discussion on Cs volatilization results 108
4.8 Structural characterization of the glasses 114
4.8.1 FTIR study 114
4.8.2 NMR study 116
4.8.3 UV-Visible optical absorption study 118
4.9 Discussion on Cs leaching and volatilization from structural aspect 120
4.10 Summary of the results and conclusions 122
5. Chapter 5 *Physicochemical properties of cesium borosilicate glasses containing divalent metal oxides* 123
5.1 Introduction 124
5.2 Glasses of present study 126
5.3 Characterization of glasses 127
5.3.1 Chemical analysis of glass 127
5.3.2 Density and molar volume 128
5.3.3 Glass transition temperature 130
5.3.4 XRD study 131
5.3.5 FTIR study 131
5.3.6 ^{11}B MAS NMR study 134
5.4 Volatilization of Cs 136
5.4.1 Discussion on Cs volatilization results 143
5.5 Leaching study 147
5.5.1 Leaching tests in distilled water at 90^{o}C for 24 h 147

5.5.2 Leaching tests as a function of time 149
5.5.3 Discussion on leaching results 151
5.5.4 Mechanism of leaching process 151
5.5.5 Identification of leached layer 152
5.5.6 XRD study of the leached glass samples 154
5.5.7 FTIR study of the leached glass samples 155
5.5.8 ^{11}B MAS NMR study of the leached glass samples 157
5.6 Summary of the results and conclusions 159
6. Chapter 6 *Development of borosilicate glasses for use as a source in radiation technology applications* 161
6.1 Introduction 162
6.2 Properties of glasses containing a single additive 163
6.3 Properties of glasses containing more than one additive 165
6.4 Detailed characterization of the shortlisted glasses 167
6.4.1 XRD patterns 167
6.4.2 Leaching 168
6.4.3 Cs volatilization 169
6.5 Preparation of high Cs bearing glasses 172
6.6 Properties of high Cs bearing glasses 172
6.6.1 Formation temperature 172
6.6.2 Density and molar volume 173
6.6.3 Swelling factor 174
6.6.4 Volatilization of Cs 175
6.6.5 Leaching behavior 176
6.7 Summary of the results and conclusions 177
7. Chapter 7 *Conclusions and plan of future work* 179
7.1 Introduction 180
7.2 Recovery of ^{137}Cs 181
7.3 Preparation and characterization of Cs borosilicate glasses 183
7.4 Future work 186
Publications from present investigation 188
References 191

Synopsis

Fissoigenic radioisotope of cesium, ^{137}Cs, is one of the gamma emitting radionuclides which has immense potential for use as a sealed gamma source in radiation technology applications, notably, for irradiation of blood and foodstuffs, sterilization of medical supplies and radiation processing of sewage sludge [1]. Presently most of the irradiators are built with ^{60}Co and only a few are based on ^{137}Cs. This is mainly due to the ease of production of ^{60}Co in metallic form with high specific activity and also since it has 4 times higher gamma energy (2.5 MeV) than ^{137}Cs (0.662 MeV). However, the use of ^{137}Cs in place of ^{60}Co is exceptionally advantageous with respect to the source life (half life of ^{137}Cs :30 years; ^{60}Co: 5.2 years) which thereby minimizes source replacement frequency and reduces the total man rem expenditure. In fact, ^{137}Cs is the an ideal isotope for use in gamma chambers (GCs) and blood irradiators (BIs) where source strength requirement is not very high and source replacement will not be required during the useful life of the unit. Traditionally, ^{137}Cs in the form of CsCl powder encapsulated in double wall stainless steel capsule and has been used as source [2-4]. However, CsCl is a highly corrosive powder and can get easily dispersed. Moreover, the high solubility of the CsCl in water leads to release of activity to the environment and causes severe ecological consequences including fatal syndrome. It is therefore desirable to use ^{137}Cs in an immobilized form with suitable product characteristics ensuring high degree of safety during use.

The preparation of the ^{137}Cs based radiation sources therefore involves processes like separation of the radioelement from nuclear waste, immobilization of the recovered Cs in suitable solid matrix and encapsulation of the glass in source pencils. Many processes are known to be promising for the separation of ^{137}Cs from acidic as well as alkaline waste [5-13]. An ion exchange based process has been deployed successfully for the separation of the radioelement from alkaline waste streams generated from reprocessing plants in India [14-16]. However, it was found that the recovered ^{137}Cs product contained significantly higher concentration of sodium ions and hence is not suitable for the preparation of radiation source. Studies were therefore necessary to separate out sodium ions from the recovered Cs solution so that the final product after immobilization can be used as a gamma source. Additionally, the large-scale utilization of ^{137}Cs as a radiation source in industrial irradiators requires that an effective process be available for the recovery of this fission product in megacurie quantities from acidic high level waste. This aspect has been addressed during the course of the thesis work.

Second part of the work involves preparation of source matrices using the recovered ^{137}Cs product solution. In the present study, immobilization of the ^{137}Cs in glass matrix has been considered in view of its global acceptance for immobilization of high level waste. In contrast to high level waste bearing glasses, the Cs glasses will have significantly higher loading of alkali oxides loading including higher amount of Cs_2O and will be free from other radionuclides contamination. A high loading of Cs_2O is necessary to make sources of high specific activity. The high alkali oxide bearing soft glasses generally formed at relatively lower temperature are prone to chemical leaching in moist environment. Owing to the higher concentration of Cs in the glasses, a significant amount of Cs is likely to be volatilized during immobilization. Preparation of the glasses with higher chemical durability and minimum volatilization loss of Cs are the major challenges of the work. Several studies pertaining to minimization of Cs volatilization [17-22] in immobilization of high level waste and the improvement of chemical durability [23-29] of the glass have been carried out by the different investigators. These studies have revealed that the glass composition, including the nature and concentrations of the constituents in the waste played a major role in deciding the durability and Cs volatility from the high Cs bearing glasses. In the present study, detailed investigations on the durability and Cs volatilization behavior have been carried out by evaluating the effect of various additives on the physicochemical properties of the borosilicate glasses. Efforts were also made to evaluate the structural changes brought out by the incorporation of the different additives. The structural information obtained was used to explain the observed properties of the glasses. This study helped to shortlist some formulations suitable for possible application as a gamma source in radiation technology applications. In totality, work in the present dissertation addresses physicochemical studies on the recovery and immobilization of radiocesium. The dissertation is divided into 7 chapters each of which is briefly discussed below.

General and basic aspects of radiation source production including background of Cs separation from different waste streams are discussed in Chapter 1. The chapter begins with a brief introduction about the history of radioisotope production including radioisotope production in India. This is followed by a general introduction on sealed gamma sources and potential radioelements along with their characteristics. The radiochemical characteristics of ^{137}Cs clearly indicate that it is one of the suitable radioisotopes for use as a gamma source in radiation technology applications, particularly, where source strength requirement is not very high and the size of samples to be irradiated is small. As the present dissertation addresses to the preparation of ^{137}Cs based gamma sources, its production from fission reaction and also inventory are accounted for. However, the radioisotope gets distributed into the different waste streams generated during reprocessing of the spent fuel. For effective utilization of the radioisotope as gamma source, it is essential that it must be separated with highest possible chemical and radiochemical purities. A literature review has been carried out to account for the processes developed so far for the separation of the radioelement from different waste streams. Further, discussion is extended on preparation of radiation sources using the recovered ^{137}Cs. This includes selection criteria of the matrices along with a summary of the possible matrices for incorporation of the radioelement. Finally, the scope of the present work highlighting the specific work elements with respect to separation, recovery, immobilization and utilization of Cs are discussed.

Chapter 2 deals with the experimental methods and characterization techniques employed in the present study on preparation and characterization of glass samples. Generalized melt quenching techniques were used for the preparation of the glasses. Physicochemical characterization of glass samples carried out include determination of density, molar volume, glass transition temperature, leaching characteristics and extent of Cs volatilization. Structural aspects of the glasses were investigated using XRD, FTIR, ^{11}B MAS NMR and uv-visible optical absorption techniques. Brief description regarding various instrumental methods, such as powder X-ray diffraction (XRD), thermo-gravimetry (TG) and differential thermal analysis (DTA), Fourier transmission infrared spectroscopy (FTIR), UV-vis spectrophotometry, scanning electron microscopy (SEM), nuclear magnetic resonance (NMR) spectroscopy, which is used for characterization, is given in this Chapter. The results of the above investigations are described in Chapters 3-6 as summarized below.

Studies on the separation and recovery of ^{137}Cs from acidic as well as alkaline waste streams are discussed in Chapter 3 and are divided into two sections. First part of the work was devoted to develop a comprehensive flowsheet based on the use of inorganic sorbent Ammonium Molybdophosphate (AMP) for industrial-scale separation and recovery of ^{137}Cs from acidic high level waste. The AMP composites prepared by coating of AMP powder on poly methyl methacrylate (PMMA) beads were used in this study [30]. The characterization of the sorbent including equilibrium sorption isotherms for Cs^+ on AMP sorbents, effect of H^+ concentration on Cs^+ uptake and column behavior of the sorbent were examined. Recovery of Cs^+ from loaded AMP-PMMA column was carried out by dissolution of AMP using NaOH solution.

The second part of the study concentrated on the separation of Cs in chemically pure form from highly active alkaline solution so that it can be used in the preparation of radiation sources. In this study, the feasibility of ion exchange purification of the recovered Cs^+ solution was examined using Resorcinol Formaldehyde Polycondensate Resin (RFPR). It is noteworthy that the RFPR has extensively been used for the separation of ^{137}Cs from low and medium active alkaline waste solutions, wherein a maximum of 10^{-4} M Cs containing solution is used [31-34]. However, Cs solution obtained after its primary separation either from alkaline waste using RFPR or from acidic waste by the use of AMP, contains significantly higher concentration of Cs. The characteristics of RFPR for separation of Cs from high active solutions was therefore evaluated by conducting batch studies from test solutions containing varying Na (0.6-3.0 M) and Cs ($1x10^{-4}$ to 0.1 M) concentrations. Batch results have been used to establish Cs exchange isotherms of the resin and also to predict the column loading performance. This was further validated by conducting several column runs using different Cs bearing solutions. Sequential elution of Na and Cs resulted in a high Cs bearing concentrate containing very low concentration of sodium. The study established that RFPR can be used for production of a low Na bearing Cs concentrate suitable for the preparation of highly active radiation source. Further, results of these studies are useful in formulating a comprehensive scheme for the recovery of purified ^{137}Cs product from high level waste for large-scale utilization as a radiation source in industrial irradiators.

Chapter 4 describes the physicochemical characterization of sodium borosilicate glasses containing Cs_2O and also the glass samples prepared by incorporating TiO_2. From the detailed investigations on these glasses, the necessity of TiO_2 incorporation is established. It is clearly shown that the glasses prepared by addition of TiO_2 at the expense of B_2O_3 possess improved characteristics as compared to those obtained by incorporating

TiO_2 at the expense of SiO_2. The leach rates for Na and Cs have been found to decrease with incorporation of TiO_2. However, incorporation of the additive at more than 5 mole% results in higher Cs losses. Based on our studies, it can be inferred that the glass sample with 5 mole% TiO_2 content gives the optimum formulation with regard to the leaching and Cs volatilization losses. Structural studies revealed that TiO_2 in low concentration (upto 5 mole%) acts as a network modifier while it participates in network formation at higher concentrations. Unlike the glass without TiO_2, glasses containing TiO_2 have different distribution of alkali Na/Cs ion as the location of Na/Cs ions shift from the vicinity of BO_4^- structural units to that of Si/Ti structural units. This is one of the reasons for the decrease of leach rate of alkali ions from the glass. The interactions between the Ti^{4+} and Cs^+ ions may possibly be the reflection of lower Cs volatilization loss.

Chapter 5 describes the results of investigation on the effect of divalent oxides on physicochemical properties of the Cs-borosilicate glasses. Chemical durability of the glasses has been found to improve with incorporation of divalent modifier and this can been attributed to the formation of divalent metal and Si rich layer at the outer surface of the glass, as inferred from SEM/EDX analysis with CaO containing glass. Based on the chemical analysis of leachate and structural information obtained at the various stages of leaching, possible structural groups present in glasses have been formulated and relative stability of the different structural groups towards hydrolytic attack has been considered to explain observed leaching behavior. Studies of Cs volatilization as a function of temperature and heating duration helped in understanding the effect of composition. It is confirmed that the volatilization of Cs occurred predominantly through diffusion controlled process. From the temperature dependent volatility profiles of Cs, the activation energy and pre-exponential factor were calculated and found to be in the range of 300 – 500 kJ/mol and 10^3 - 10^{12} cm^2/s, lowest for ZnO and highest for CaO containing glasses. An interesting fact is that the pre-exponential factor and not activation energy controls the Cs loss. The observed variations in the activation energy and pre-exponential factor have been explained by a unique model structure and possible interactions of Cs with different structural units formed due to incorporation of different additives.

Chapter 6 deals with the preparation and characterization of borosilicate glasses incorporated with more than one additive and are divided in two sections. In the first section, cumulative effect of these additives on matrix properties mainly formation temperature, chemical durability and Cs volatilization have been examined. Based on these screening studies, four glass formulations have been shortlisted. Leaching tests for longer duration upto 21 days and measurement of the extent of Cs volatilization have been carried out with the shortlisted formulations. Result of the study is useful in selection of glass formulations for use as radiation source in blood irradiators.

Second part of this chapter discusses the preparation of high Cs loaded glasses for possible use as a gamma source in industrial radiation technology applications. In this study, the feasibility of incorporation of more Cs_2O by replacement of Na_2O is examined on one of the above mentioned shortlisted formulation. Properties of glasses measured include pour temperature, swelling factor, density, molar volume, Cs volatilization and chemical durability. Pour temperature, density, molar volume and Cs loss due to volatilization increased with increase of Cs_2O loading. The swelling factor was found to decrease gradually with increase of Cs_2O loading. Chemical durability of glasses, with respect to Na and Cs leaching in distilled water, decreased initially with incorporation of Cs_2O up to 4 mole%, and then increased slowly with the increase of Cs_2O loading. This anomalous leaching behavior is attributed to mixed alkali effect. Based on the formation temperature within 950^oC and good chemical durability, the highest Cs bearing glass containing 6 mole% (21 wt%) of Cs_2O and 14 mole% of Na_2O, can be selected for possible use as a gamma source in industrial radiation technology applications.

Chapter 7 gives the summary of the results from the above mentioned detailed investigations carried out on recovery of Cs and preparation and characterization of high Cs_2O incorporated borosilicate glasses. Future scope of the work with respect to further insight required for efficient separation and utilization of ^{137}Cs ions are discussed in detail in this chapter.

References

1. Feasibility of Separation and Utilization of Cesium and Strontium from High Level Liquid Waste. Technical Report Series, No. 356, IAEA, Vienna, 1993.
2. A.F. Rupp, Radioisotope program (8000) progress report for Dec1971, ORNL-TM-3677, 1972.
3. E. Lamb, ‘Cesium-137 Source Material for an Irradiator’, US DOE Report No. CONF-800964-1, Oak Ridge National Laboratory, USA, 1980.
4. H. Farrar IV, G. Subbaraman, C. C. Conners and J. P. Page, ‘The Cesium-137 Agricultural Commodities Irradiator’, pp. 551-56 in Proceedings of Waste Management Symposium, Vol-1, Edited by P. G. Roy, Tuscon, Arizona, 1985.
5. W. W. Schulz, L. A. Bray, Solvent Extraction recovery of Byproduct 137Cs and 90Sr from HNO3 Solutions—A Technology Review and Assessment, Separation Science and Technology, 22 (2&3), 191-214, 1987.
6. A. Clearfield, Inorganic Ion Exchangers, Past, Present, and Future, Solvent Extraction Ion Exchange, 18(4), 655-678, 2000.
7. V.N. Ramonovsky, Management of accumulated high level waste at the myak production Association in the Russian Federation’ in issues and Trends in Radioactive waste management, Proc. International conference, p-360, IAEA, Vienna, 2003.
8. R. S. Herbst, et al., Development and Testing of a Cobalt Dicarbollide Based Solvent Extraction Process for the Separation of Cesium and Strontium From of Acidic Tank Waste, Separation Science and Technology, 37(8), 1807-1831, 2002.
9. I. H. Gerow, G. E. Smith, and M. W. Davis, Extraction of Cesium (+1) and Strontium (+2) from Nitric Acid Solution using Macrocyclic Polyethers, Separation Science and Technology, 16(5), 519-548, 1981.
10. R. M. Izatt, et al., Selective M+□H+ Coupled Transport Through a Liquid Membrane by Macrocyclic Calixarene Ligands, Journal of American Chemical Society, 105, 1782, 1983.
11. J. F. Dozol, et al., A Solution for Cesium Removal from High-Salinity Acidic or Alkaline Liquid Waste: The Crown Calix[4]arenes, Separation Science and Technology, 34(6&7), 877-909, 1999.
12. P. V. Bonnesen, L. H. Delmau, B. A. Moyer, and R. A. Leonard, A Robust Alkaline-side CSEX Solvent Suitable for Removing Cesium from Savannah River High Level Waste, Solvent Extraction and Ion Exchange, 18 (6), 1079–1108, 2000.
13. M. A. Norato, et al., Demonstration of the Caustic-Side Solvent Extraction Process for Removing 137Cs from High-Level Waste at Savannah River Site, Separation Science and Technology, 38(12&13), 2647-2666, 2003.
14. S.K. Samanta, M. Ramaswamy, B.M. Misra, Studies on cesium uptake by phenolic resins, Separation Science and Technology, 27 (2), 255-267,1992.
15. D. Banerjee, S.K. Samanta, Proc. 14th Annual Conference of Indian Nuclear Society and 1st BRNS Conference on Nuclear Fuel Cycle, (INSAC 2003), IGCAR, Kalpakkam, Paper no. G14, 2003.

16. P.D. Ozarde, S.K. Samanta, and K. Raj, Management of intermediate level wastes from past reprocessing using cesium-specific resorcinol formaldehyde resin, International Conference on Issues and Trends in Radioactive Waste Management, December 9-13, International Atomic Energy Agency, Vienna, Austria. 2002.

17. R.C. Rastogi, J.D. Sehgal, K. Chandra and K.T. Thomas, "Investigation of Materials and Methods for the Fixation of Low and Medium Level Radioactive Waste in Stable Solid Media", BARC Report No. BARC-400, Bhabha Atomic Research Centre, India, 1969.

18. J.A. Kelly, "Evaluation of a Glass as a Matrix for Solidification of Savannah River Plant Waste", US DOE Report No. DP-1382, Savannah River Laboratory, Aiken, S.C., 1975.

19. W.J. Gray, "Volatility of Some Potential High Level Radioactive Waste forms", Radioact. Waste Manage., 1[2], 147-69, 1989.

20. H. Kamizono, S. Kikkawa, Y. Togashi, S. Tashiro, "Volatilization of ^{137}Cs and ^{106}Ru from Borosilicate Glass Containing Actual High-Level Waste", J. Am. Ceram. Soc., 72 (8), 1438–41, 1989.

21. H. Kamizono, S. Kikkawa, S.Tashiro, H. Nakamura and H. Kanazawa, "Air contamination by cesium in a canister containing nuclear waste glass", J. Nucl. Mater., 149, 113-16, 1987.

22. M.H. Langowski, J.G. Darab and P.A. Smith, "Volatility Literature of Chlorine, Iodine, Cesium, Strontium, Technetium and Rhenium; Technetium and Rhenium Volatility Testing", US DOE Report No. PNNL-11052, Pacific Northwest National Laboratory, USA, 1996.

23. L. L. Hench, D. E. Clark and J. Campbell, 'High Level Waste Immobilization Forms', Nucl. Chem. Waste Manage., 5, 149-73, 1984.

24. A. Paul, 'Chemical Durability of Glasses: A Thermodynamic Approach', J. Mater. Sci., 12, 2246-68, 1977.

25. L. A. Chick, B. F. Pieple, G. B. Mellinger, R. P. May, W. J. Gray and C. Q. Buckwalter, 'The Effects of Composition on Properties in an 11 Component Nuclear Waste Glass System', US DOE Report No. PNL-3188, Pacific Northwest Laboratory, WA, USA , 1981.

26. J.O. Israd, W. Muller, Influence of alkaline earth ions on the corrosion of glasses, Phys. Chem. Glasses. 27 (2), 55-58, 1986.

27. M.A. Rana, R.W. Douglas, The reaction between glass and water. Part I. Experiment methods and observations, Phys. Chem. Glasses. 2 , 179-195, 1961

28. N.E. Bibler, W.G, Ramsey, T.F. Meaker, J.M. Pareizs, 'Durabilities and microstructures of radioactive glasses for immobilization of excess actinides at the Savannah River site', Proceedings of the 1995 MRS Fall Symposium; Boston, MA, USA; 27-30 Nov. 1995, Materials Research Society, Pittsburgh, PA, United States.

29. B.M.J. Smets, M.G.W. Tholen and T.P.A. Lommen, 'The effect of divalent cations on the leaching kinetics of Glass', J. Non-Cryst. Solids, 65, 319-332, 1984.

30. J. Gabriel, G.J. Shah and T.P. Valsala, Spherical AMP composite ion exchange material for treatment of acidic intermediate level waste, Proc. Nuclear and

Radiochemistry Symposium (NUCAR 2003), p. 32, Bhabha Atomic Research Centre, Mumbai, 2003.

31. J.P. Bibler, R.M.Wallace, L.A. Bray, Testing a new cesium-specific ion exchange resin for decontamination of alkaline high-activity waste. Proc. Waste Management symp, Post, R.G. (Ed.), Vol. 2, 747. 1990
32. N.M. Hassan, K. Adu-Wusu, J.C. Marra, Resorcinol - Formaldehyde adsorption of cesium from Hanford waste solutions: Part I. Batch equilibrium study. Journal of Radioanalytical and Nuclear Chemistry, 262 (3), 579-586, 2004.
33. S.K Samanta, T.K. Theyyunni, B.M. Misra, Column behaviour of resorcinol-formaldehyde polycondensate resin for radiocesium removal from simulated radwaste solution. Journal of Nuclear Science and Technology, 32 (5), 425-429, 1995.
34. S.K. Fiskum, S.T. Arm, M.J. Steele, M.R. Thorson, Spherical resorcinol-formaldehyde performance testing with Hanford tank waste. Solvent Extraction and Ion Exchange, 26 (4), 435-452, 2008.

List of tables

Table 1-1: Commonly used radioisotopes in sealed source applications 5

Table 1-2: Characteristics of ^{60}Co and ^{137}Cs 7

Table 1-3: Typical distribution of Cs isotopes in spent fuel irradiated in PHWR.................10

Table 2-1: Chemicals used for glass preparation..30

Table 3-1: Characteristics of AMP sorbents..62

Table 3-2: Recovery of Cs^+ from loaded AMP-PMMA column...67

Table 3-3: Chemical composition of the recovered Cs solution resulting from the dissolution of Cs-loaded AMP bed 68

Table 3-4: Typical composition of the eluate resulting from primary separation of Cs from ILW before and after neutralization 69

Table 3-5: Characteristics of the RFPR...70

Table 3-6: Freundlich constants for Cs sorption by RFPR..75

Table 3-7: D-R isotherm parameters for Cs sorption by RFPR...77

Table 3-8: Ion exchange purification of Cs^+ in dissolved AMP solution.............................85

Table 3-9: Composition of waste and purified Cs solution before and after ion exchange processing 88

Table 4-1: Additives influence on the change of properties of borosilicate glasses 94

Table 4-2: Characteristics of the Cs-borosilicate glasses prepared as per formulation (wt%) 10 Cs_2O + 15 Na_2O + (75-x) SiO_2 + x. B_2O_3 96

Table 4-3: Characteristics of the Cs-borosilicate glasses prepared from base glass by incorporating TiO_2 97

Table 4-4: Chemical analysis (wt%) of Na and Cs in as melted glasses...............................98

Table 4-5: Distribution of Cs in vapor and glass during formation of the Cs-borosilicate glasses 105

Table 4-6: Elemental composition of the scrub solutions (in ppm) analyzed by using ion chromatography 106

Table 4-7: Cumulative loss of Cs (mg/cm^2) from the preformed Cs borosilicate glasses after 24 hours of heating at different temperatures 108

Table 4-8: Activation energy and pre exponential factor for Cs volatilization from the glasses 112

Table 4-9:: Concentrations of BO_4 and BO_3 structural units in the Cs-borosilicate glasses containing different concentrations of TiO_2 determined from ^{11}B MAS NMR profiles 117

Table 5-1: Nominal compositions of the Cs-borosilicate glasses (mole%) containing different divalent metal oxides 127

Table 5-2: Chemical analysis results of the Cs-borosilicate glasses (wt%) containing different amount of CaO 128

Table 5-3: Cumulative loss of Cs (mg/cm^2) from the preformed Cs borosilicate glasses after 24 hours of heating at different temperature. General formula of the glasses: $(SiO_2)_{0.45}$ $(B_2O_3)_{0.3}$ $(Na_2O)_{0.175}$ $(Cs_2O)_{0.025}$ $(MO)_{0.05}$..138

Table 5-4: Activation energy and pre exponential factor for Cs volatilization from the glasses of general formula: $(SiO_2)_{0.45}$ $(B_2O_3)_{0.3}$ $(Na_2O)_{0.175}$ $(Cs_2O)_{0.025}$ $(MO)_{0.05}$...............143

Table 6-1: Effect of additives on Na and Cs leach rates of CBS glasses of general formulation: 2.5 Cs_2O + 17.5 Na_2O + 45 SiO_2 + (35-x) B_2O_3 + MO. The values in the table represent the factor by which leach rate of the different glass samples decrease with respect to the base glass. 164

Table 6-2: Properties of the Cs borosilicate glasses containing more than one additive 166

List of figures

Figure 1-1: Typical distribution of ^{137}Cs in different waste available for recovery at Trombay 10

Figure 2-1: Teflon-lined stainless steel container used in leaching study 34

Figure 2-2: Schematic of experimental setup to study the Cs volatilization during glass preparation 36

Figure 2-3: Volatilization setup for heating preformed glass in alumina crucible 39

Figure 2-4: Block diagram of radiation counting system 41

Figure 2-5: Typical planner configuration of HPGe detector applied in reverse bias 42

Figure 2-6: Schematic of ion chromatography system 44

Figure 2-7: Typical chromatogram of a standard sample containing 5 ppm Na, 10 ppm Cs 10 ppm Ca and a glass leaching sample 45

Figure 2-8: X-Ray diagram of a typical reflection mode diffractometer 47

Figure 2-9: Principle of MAS NMR experiment 52

Figure 2-10: Schematic representation of SEM microscope 54

Figure 2-11: Interaction of electron beam with sample 55

Figure 3-1: Estimated activity of ^{137}Cs in borosilicate glass as a function of Na/Cs ratio of the waste solution 61

Figure 3-2: Equilibrium sorption isotherms for Cs on AMP sorbents 63

Figure 3-3: Effect of HNO_3 on Cs uptake by AMP(Lab)-PMMA beads 64

Figure 3-4 : Column separation of Cs from acidic solution using AMP-PMMA beads 65

Figure 3-5: Ion exchange cycle for RFPR 69

Figure 3-6: Uptake of Cs and Sr by RFPR from simulated alkaline ILW of composition 2.5 M $NaNO_3$ + 1.0 M NaOH + 0.15 M Na_2CO_3 and 1 mg/L Cs and spiked with ^{134}Cs and $^{85+89}$Sr tracer 71

Figure 3-7: Batch uptake of Cs by RFPR from dissolved AMP and neutralized eluate solution 73

Figure 3-8: Cs exchange isotherm for RFPR from solutions containing Cs concentration in the range of 1×10^{-4} to 0.1 M and having different Na concentrations. 74

Figure 3-9: D-R isotherm plot for the Cs uptake by RFPR from solutions containing Cs concentration in the range of 1×10^{-4} to 0.1 M and having different Na concentrations. 76

Figure 3-10: Maximum possible loading of Cs on 1 L RFPR column as a function of Cs concentration in solution containing 0.5 M $NaNO_3$+ 0.1 M NaOH; The loading predicted from D-R isotherm and Freundlich isotherm equation is indicated by blue (solid) and red (doted) line, respectively. The star is showing the values calculated from column run. 78

Figure 3-11: Effect of Na concentration in solution on Cs uptake by the RFPR 79

Figure 3-12: Uptake of Na and Cs by RFPR: (a) and (b) are gamma spectra and concentrations (meq/ml) of Na solution before and after equilibration of RFPR (H-form) with 0.6 M Na solution spiked with ^{22}Na tracer; (c) and (d) are the gamma spectra and Na and Cs concentration of in solution with the progress of equilibration of the Na-form resin with Cs solution spiked with 134Cs radiotracer. Gamma spectrum for "0" minute are in actual energy scale, other are shifted to 15 Kev for ease of representation. 80

Figure 3-13: Cs separation behavior of RFPR column (Bed volume: 5 mL) from solutions containing 0.5 M $NaNO_3$+ 0.1 M NaOH and varying concentration of Cs at the flow rate of 4 bed volume per hour. 82

Figure 3-14: Loading of Cs^+ on RFPR column from dissolved AMP solution 83

Figure 3-15: Elution profile of Cs and Na from RFPR column (Bed volume: 5 mL) at the flow rate of 4 bed volume per hour, fraction volume = 10 ml. 85

Figure 3-16: Elution profile of Cs and Na from RFPR column (Bed volume: 10 mL) at the flow rate of 4 bed volume per hour, fraction volume = 10 ml. The column was loaded with 0.6 g Cs from dissolved AMP solution containing 2.15×10^{-2} M Cs. 86

Figure 3-17: Elution profile of Cs and Na from RFPR column (Bed volume: 5 mL) at the flow rate of 4 bed volume per hour, fraction volume = 10 ml. The column was loaded with 0.06 g Cs from neutralized eluate containing 2.57×10^{-4} M Cs. 87

Figure 4-1: Ternary diagram of sodium borosilicate glass highlighting region of interest of some important class of glasses 95

Figure 4-2: Density and molar volume of the Cs borosilicate glasses (*$(SiO_2)_{0.4}$ $(B_2O_3)_{0.35-x}$ $(Na_2O)_{0.175}$ $(Cs_2O)_{0.025}$ $(TiO_2)_x$)* containing different concentration of TiO_2, ...99

Figure 4-3: XRD profiles of the Cs borosilicate glasses of general formula $(SiO_2)_{0.45}$ $(B_2O_3)_{0.35-x}$ $(Na_2O)_{0.175}$ $(Cs_2O)_{0.025}$ $(TiO_2)_x$ with x varying from 0.0 to 10.0 100

Figure 4-4: TG-DTA profile for the Cs-borosilicate glass containing 7.5 mole% TiO_2 (Batch No. Ti-7.5) 101

Figure 4-5: Glass transition temperature of Cs-borosilicate glasses containing varying amount of TiO_2, line is guided to eye 101

Figure 4-6: Leaching of Na and Cs from Cs-borosilicate glasses in distilled water at 90°C for 24 hours, lines are guided to eye, general formula of the glasses: $(SiO_2)_{0.4}$ $(B_2O_3)_{0.35-x}$ $(Na_2O)_{0.175}$ $(Cs_2O)_{0.025}$ $(TiO_2)_x$ 102

Figure 4-7: Cs loss profile as a function of square root of heating time for glass sample of molecular formula $(SiO_2)_{0.45}$ $(B_2O_3)_{0.35}$ $(Na_2O)_{0.175}$ $(Cs_2O)_{0.025}$ in dry air at different temperature 112

Figure 4-8: Cs loss profile as a function of square root of heating time for glass sample of molecular formula $(SiO_2)_{0.45}$ $(B_2O_3)_{0.30}$ $(Na_2O)_{0.175}$ $(Cs_2O)_{0.025}$ $(TiO_2)_{0.05}$ in dry air at different temperature 113

Figure 4-9: Plot of ln(D) against 1/T for the base glass and glass sample containing 5 mole% TiO_2 113

Figure 4-10: FTIR patterns of Cs-borosilicate glasses containing different amounts of TiO_2 over the region of 400-2000 cm^{-1} 114

Figure 4-11: FTIR spectrum of Cs-borosilicate glasses containing different amounts of TiO_2 (normalized at peak 970-1010 cm^{-1} 115

Figure 4-12 : ^{11}B MAS NMR profile of the glasses containing varying concentration of TiO_2...117

Figure 4-13: UV-visible optical absorption spectra of Cs borosilicate glasses containing different amounts of TiO_2. 118

Figure 4-14: Tauc plots for Cs borosilicate glasses containing different amounts of TiO_2.120

Figure 5-1: Density and molar volume of the Cs borosilicate glasses as a function of the incorporated CaO...129

Figure 5-2: Density and molar volume of the Cs borosilicate glasses as a function of the incorporated MO in $(SiO_2)_{0.45}$ $(B_2O_3)_{0.30}$ $(Na_2O)_{0.175}$ $(Cs_2O)_{0.025}$ $(MO)_{0.05}$, where M=Mg^{2+}, Ca^{2+}, Sr^{2+}, Ba^{2+} or Zn^{2+}..........129

Figure 5-3: DSC pattern of the 5 mole% CaO containing Cs borosilicate glass sample, The inset plot represents values of glass transition temperature for the glass samples containing different amount of CaO..........130

Figure 5-4: FTIR spectrum of Cs-borosilicate glasses containing varying concentrations of CaO over the region of 400-2000 cm^{-1}..........131

Figure 5-5: FTIR spectrum of Cs-borosilicate glasses containing varying concentrations of CaO (normalized at peak 970-1000 cm^{-1}..........132

Figure 5-6: FTIR spectrum of the Cs-borosilicate glasses containing different MO, where M= Ca, Ba and Zn..........133

Figure 5-7: ^{11}B MAS NMR pattern of the Cs-borosilicate glasses of formula :$(SiO_2)_{0.45}$ $(B_2O_3)_{0.35-x}$ $(Na_2O)_{0.175}$ $(Cs_2O)_{0.025}$ $(CaO)_x$..........134

Figure 5-8: ^{11}B MAS NMR patterns of the Cs borosilicate glasses incorporated with different divalent cation (MO)..........135

Figure 5-9: Loss of Cs from preformed Cs borosilicate glasses during heating at 950°C, Batch size: 25 g..........136

Figure 5-10: Cs loss from preformed borosilicate glasses incorporated with different divalent cations at 900°C...........137

Figure 5-11: Cs loss profile as a function of square root of heating time for glass sample of molecular formula $(SiO_2)_{0.45}$ $(B_2O_3)_{0.35}$ $(Na_2O)_{0.175}$ $(Cs_2O)_{0.025}$ in dry air at different temperature..........139

Figure 5-12: Cs loss profile as a function of square root of heating time for glass sample of molecular formula $(SiO_2)_{0.45}$ $(B_2O_3)_{0.3}$ $(Na_2O)_{0.175}$ $(Cs_2O)_{0.025}$ $(CaO)_{0.05}$ in dry air at different temperature..........140

Figure 5-13: Cs loss profile as a function of square root of heating time for glass sample of molecular formula $(SiO_2)_{0.45}$ $(B_2O_3)_{0.3}$ $(Na_2O)_{0.175}$ $(Cs_2O)_{0.025}$ $(BaO)_{0.05}$ in dry air at different temperature..........140

Figure 5-14: Cs loss profile as a function of square root of heating time for glass sample of molecular formula $(SiO_2)_{0.45}$ $(B_2O_3)_{0.3}$ $(Na_2O)_{0.175}$ $(Cs_2O)_{0.025}$ $(ZnO)_{0.05}$ in dry air at different temperature 141

Figure 5-15: Plot of ln D vs 1000/T for Cs borosilicate glasses with different additive.....142

Figure 5-16: Model structural unit of the base glass 144

Figure 5-17: Model structural unit of the Cs borosilicate glass containing CaO along with its formation from base glass...145

Figure 5-18: Model structural unit of the Cs borosilicate glass containing CaO along with its formation from base glass...146

Figure 5-19: Leaching of Na and Cs from Cs-borosilicate glasses in distilled water at 90°C for 24 hours, lines are guided to eye...147

Figure 5-20: Elemental leach rates from the borosilicate glasses against the atomic radii of the incorporated bivalent cation (MO) 149

Figure 5-21: Elemental leaching profiles of the Cs borosilicate glasses containing varying concentrations of CaO as a function of leaching time. (*leaching in distilled water at 90^{o}C*). 150

Figure 5-22: Kinetics of Cs extraction from ZnO and CaO bearing Cs-borosilicate glasses in distilled water at 90^{o}C..152

Figure 5-23: SEM micrograph of 5 mole% CaO containing glass sample (after 5 days leaching in distilled water at 90^{o}C). Here, G, S and R represents bulk glass, outer surface and resin, respectively 153

Figure 5-24: EDX spectra recorded at the interface. The line spectrum 1 and line spectrum 2 represent outer surface layer and bulk glass, respectively..154

Figure 5-25: XRD pattern of the Cs-borosilicate glasses before and after leaching 155

Figure 5-26: FTIR spectram of the base Cs-borosilicate glass without CaO before and after leaching..156

Figure 5-27: FTIR spectram of the Cs-borosilicate glass containing 5 mole% CaO before and after leaching..157

Figure 5-28: ^{11}B MAS NMR pattern of base (without CaO) and 5 mole% CaO containing glasses before and after leaching 158

Figure 6-1: Optimization of CaO, TiO_2 and MnO_2 concentrations for the production of a chemically durable Cs-borosilicate glass containing constant levels of other oxides (mole%) 45 SiO_2-10 B_2O_3-15 Na_2O-10 Cs_2O. The number inside the circle represents batch number along with the corresponding chemical durability improvement index. 167

Figure 6-2: XRD patterns of the three shortlisted glasses 168

Figure 6-3: Na and Cs leach rates in distilled water at 90^{o}C as a function of leaching time upto 21 days for the three shortlisted glasses. 169

Figure 6-4: Cs volatilization loss during glass preparation including soaking at 950 ^{o}C for 4 hours. 170

Figure 6-5: Cs volatilization during preparation of glass#15, as a function of soaking time. About 2 g glass was prepared in silica boat at 900^{o}C. 171

Figure 6-6: Composition of the glass used in Na and Cs variation study 172

Figure 6-7: formation temperature and source strength of the glasses as a function of Cs_2O content in glass 173

Figure 6-8: Density and molar volume of the mixed alkali Na-Cs borosilicate glasses 174

Figure 6-9: Swelling factor of the mixed alkali Na-Cs borosilicate glasses 175

Figure 6-10: Cs volatilization of the mixed alkali Na-Cs borosilicate glasses 176

Figure 6-11: Leaching profile of Na and Cs from mixed alkali Na-Cs borosilicate glasses 177

Figure 7-1: Process schematic for recovery ^{137}Cs from acidic HLW and production of source pencils 183

Abbreviation

AERB : Atomic Energy Regulatory Board

AMP : Ammonium Molybdophosphate

BRIT : Board of Radiation and Isotope Technology

BI : Blood Irradiator

BWR : Boiling Water Reactor

CBS : Cesium Borosilicate

CSEX : Caustic Side Solvent Extraction

DSC : Differential Scanning Calorimetry

FTIR : Fourier Transform Infered Spectroscopy

GC : Gamma Chember

HLW : High Level Waste

ILW : Intermediate Level Waste

PCT : Product Consistency Test

PHWR : Pressurized Heavy Water Reactors

PMMA : Polymethylmethacrylate

RFPR : Resorcinol Formaldehyde Polycondensate Resin

SEM : Scanning Electron Microscopy

Chapter 1

Introduction

Introduction

Several radionuclides are present in nuclear waste in substantial quantities, some of them being highly valuable mainly with respect to their potential application in our daily life, ^{137}Cs being one of them. In view of the potential use of ^{137}Cs, several independent programmes have been pursued since late 1950 for the recovery of this valuable radionuclide from waste streams and used in various peaceful applications notably, for irradiation of blood and foodstuffs, sterilization of medical supplies and radiation processing of sewage sludge, brachytherapy, gamma knife, etc[1]. It is desirable that the recovery of the valuables should also address the end-routing of the remaining waste streams as well as the generated secondary waste streams. Different countries have adopted various processes for separation of the radionuclides and matrices. Indeed, India is one of the few countries in the world having mature technology for the management of the waste. Several hundreds of ^{137}Cs based brachytheraphy sources have been prepared in our laboratories and used in treatment of cancer[2]. Recent interest is focused on the use of ^{137}Cs as a gamma source in radiation technology applications. The preparation of ^{137}Cs based radiation sources requires mega curie quantities of the radioisotope and hence involves processes like separation of the radioelement from nuclear waste, immobilization of the recovered Cs in suitable solid matrix and encapsulation of the glass in source pencils. In this context, efforts have been made to address the subject in totality under the title topic 'Recovery and immobilization of radiocesium' of the thesis work.

As an introductory note for the work, application of radioisotopes including ^{137}Cs, production of ^{137}Cs and processing of the spent fuel is discussed. This gives a quantitative account of the inventory of radioisotopes and its distribution in different waste streams. Further, state of art processes and technologies prevailing in this field including separation and recovery of ^{137}Cs from different waste streams and its conversion in source form are highlighted. This helps to define the scope of the work which needs to be addressed to utilize this useful byproduct of nuclear energy production.

1.1 Applications of radioisotopes

The discovery of radioactivity by Henri Becquerel in 1896 followed by the production of the first artificially produced radioisotope of ^{30}P by Irene Curie Joliot gave impetus to the application of radioisotope for the betterment of human lives. Later on, the invention of cyclotron by E.O. Lawrence increased the range of man-made radioisotopes. The discovery of nuclear fission by O. Hahn and F. Strassmann in 1939 and subsequent setting up of the nuclear reactor at Chicago by Fermi and coworkers in 1942 opened up immense opportunities for the production of radioisotopes. As of today, more than 450 nuclear reactors are in operation all over the globe adding a quantum to the total energy demand. Consequently, hundreds of radioisotopes in substantial quantities are produced daily along with energy production through fission as well as neutron activation utilizing the high neutron flux during operation of such reactors. Almost all the radioisotopes produced are being used for the betterment of human society in fields like healthcare, radio-diagnostics, radiopharmaceuticals, radiotherapy, brachytherapy, radioimmuno- assay, radio-analytical techniques, sterilization of medical products, radiation processing in industry, radiotracer applications in industry, food preservation, agriculture and radiation technology.

Indian atomic energy programme was initiated by the great visionary and father of Indian nuclear energy programme, Dr. Homi Jahangir Bhabha, in 1954[3] who envisioned the peaceful uses of atomic energy including generation of nuclear power and applications of radioisotopes in various fields. The first research reactor “APSARA” was dedicated to the nation in 1956 and thereafter several reactors have been added to the list. At present, 20 reactors including 17 power reactors utilizing natural uranium fuel in Pressurized Heavy Water Reactors (PHWR) as well as enriched uranium in Boiling Water Reactors (BWR) are in operation. The power generated from these reactors accounts for about 3% of total energy production (4.7 GWe). Along with the generation of power, these reactors are also used to produce radioisotopes from neutron activation. The produced isotopes are used in a variety of applications in the field of healthcare, agriculture, industry and research. A numbers of radioisotopes generated from fission reaction have been known to be useful for application in various fields as mentioned above. In the present context, further discussions are restricted with the isotopes which are suitable for use as a sealed source in gamma radiation technology applications.

1.1.1 Radioisotopes for sealed sources applications

Definition and classification of sealed sources

The sealed radiation source is defined as one in which the radioactive material is encapsulated or sealed in a capsule. The minimum criterion for the sealed sources is that the capsule should be strong enough to be leak proof under the conditions of use. Further, on the basis of intended application under various environmental conditions, several performance classification requirements are specified for the various sources, so that integrity of the sources remains intact even under reasonable accidental conditions.

Depending upon the strength of the source, the sources can broadly be classified in three groups as follows[4]:

(i) Low level source: Activity level are in few μCi.

(ii) Medium level source: Activity level are in few mCi to few Ci.

(iii) High level source: Activity level are in several kCi.

The low level sources are exempted from any tests except loose contamination, which should be less than limits prescribed. For others, it is necessary to qualify performance tests which include temperature, pressure, impact, vibration and puncture tests as per technical specification prescribed by AERB [5, 6].

1.1.2 Radioisotopes for radiation technology applications

Primary requirement for a radioisotope that can be used as a gamma source should have following characteristics

(i) High gamma energy

(ii) Long half life

(iii) High specific activity

(iv) Availability in substantial quantities

Based on the available information in literature, a list of radioisotopes useful for sealed gamma sources are summarized in Table 1-1. The radionuclides which have half life less than a year are not included in the list. It can be seen that the choices of radionuclides for sealed source applications are limited. Further considering the application as gamma source for irradiators, the choices are only ^{60}Co and ^{137}Cs.

Table 1-1: Commonly used radioisotopes in sealed source applications

Radioisotopes	Half life (y)	Gamma energy (MeV)
^{22}Na	2.6	0.51 and 1.27
^{60}Co	5.27	1.17 and 1.33
^{133}Ba	10.6	0.36
^{137}Cs	30	0.66

1.1.3 Uses of ^{60}Co in radiation technology application

^{60}Co is the radioisotopes used most extensively in gamma radiation technology application. This is mainly because of its favorable decay characteristics (Table 1-2) and ease of availability. Production of ^{60}Co is carried out by irradiation of metallic pellets of ^{59}Co. The rate of growth of activity in the target can be obtained from following equation[7]:

$$S = \frac{0.6\sigma\varphi}{A}\left(1 - e^{-\lambda t}\right) \qquad \ldots(1)$$

where s: specific activity in Bq/g, σ: neutron absorption cross section in barn, ϕ: neutron flax in n/cm^2/sec, A:Mass number, λ: decay constant and t is the period of irradiation. In practice, the target is irradiated for 1-2 half lives of the radioelement. It is clear from above equation that high neutron flux is needed for the production of high specific activity ^{60}Co source and therefore a major part of the isotope is prepared in the power reactor. In India, both the metallic pellets in the form of 1 mm dia x 1 mm height and 6 mm dia x 25 mm long slugs are used for irradiation[8]. These targets are encapsulated in suitable irradiation containers, loaded in the specially designed assemblies and irradiated for period of 5 to 7 years. Cobalt pellets provide very high specific activity (200-300 Ci), while the specific activity for slugs are in the range of 50-100 Ci. Currently, about 2 MCi of ^{60}Co is produced annually from different power reactors. Board of Radiation and Isotope Technology (BRIT), a unit of Department of Atomic Energy is responsible for the production, fabrication and supply of laboratory irradiators like Gamma Chambers (GC) and Blood Irradiators (BI). These units are useful for the radiation damage studies on various materials and for blood irradiation where T-lymphocytes are made inactive before transfusion of blood in the organ transplanted patients. BRIT is also supplying the industrial irradiator sources for sterilization of medical products and food irradiation. Since ^{60}Co has half life of 5.27 years which necessitates replacement of the source every 5-7 years depending on the requirement.

Table 1-2: Characteristics of ^{60}Co and ^{137}Cs

Characteristics	**^{60}Co**	**^{137}Cs**
Half life	5.27 years	30 years
Energy of γ rays	1.17 and 1.33 MeV.	0.662 MeV.
Production	^{59}Co (n,γ) ^{60}Co	Fission of ^{235}U
Dose rate from 1 Ci at 1 meter	1.32 R/hr	0.34 R/hr
Specific activity	25-300 Ci/g for metallic cobalt	20 Ci/g for CsCl powder 5-10 Ci/g for glass matrix

1.1.4 Uses of ^{137}Cs in radiation technology application

Unlike ^{60}Co, ^{137}Cs has a long half life of 30 years and emits γ radiation of relatively low energy of 0.662 MeV. The use of ^{137}Cs in place of ^{60}Co can minimize the source replacement frequency and thereby reduce the total man rem expenditure. In fact, ^{137}Cs is an ideal isotope for use in GCs and BIs where source strength requirement is not very high and source replacement will not be required during the useful life of the unit. These irradiators are useful for the irradiation of blood and foodstuffs, sterilization of medical supplies (such as syringes, bandages and other disposal material where sterilization is carried out after final packing of the product) and radiation processing of sewage sludge. Though low gamma energy of ^{137}Cs is disadvantageous in irradiation technology application, it is advantageous for GC and BI because of low shielding requirement. The use of ^{137}Cs makes it possible to build such units in smaller size as well as mobile units. As the radioisotope is produced only in nuclear fission reaction, separation of the isotope from fuel

1.2 Inventory of ^{137}Cs

The suitability of a radioisotope for industrial scale uses is mainly decided by the availability of the radioelement and its production cost.

1.2.1 Production

^{137}Cs is produced in substantial quantities from nuclear fission reaction. The fission yield of ^{137}Cs is about 6% from thermal neutron fission of ^{235}U. In terms of weight, it was estimated that about 240 g of ^{137}Cs is produced from 1 tonne of fuel irradiated in PHWR at the rate of 6,700 MWD/tonne. However, this is not the only radioelement produced in fission. It is known than several hundreds of radioelement, including three major isotopes of Cs and a series of activation products and actinides are produced in fission. Interestingly, all these are confined within the fuel element. For use of the ^{137}Cs, it is to be separated from the host of the other radioelement. In fact, the spent fuel is then processed, known as reprocessing, for separation of fissile elements. A brief description of the reprocessing is given below to track the routing of ^{137}Cs and its inventory.

1.2.2 Reprocessing of spent fuel

The spent fuel after removal from reactors is cooled for some time for decaying short-lived fission products and then taken for reprocessing. Reprocessing of spent fuel involves various processes including decladding, dissolution of the fuel in concentrated HNO_3 and solvent extraction for the recovery of Uranium and Plutonium. This is done through a series of solvent extraction steps by contacting the acidic solution with 30% TBP/dodecane mixture. During solvent extraction, all the fission products including ^{137}Cs remain in the aqueous streams, while Pu and U go to the organic. The Pu and U lean acidic raffinate resulting from the first step of solvent extraction is subjected to evaporation for volume reduction. The evaporator concentrate is designated as acidic high level waste which contains more than 99% of the total fission products activities. The evaporator condensate is mixed with the acidic raffinate of second and third steps of solvent extraction and subjected to evaporation. The concentrated part is neutralized using Na_2CO_3 and NaOH and stored in carbon steel tank as intermediate level waste, while the condensate is sent as low level waste for further treatment and discharged. In addition, some other waste streams are also generated during reprocessing. Detailed descriptions of these waste streams are not included in view of their low inventory of ^{137}Cs in such waste.

1.2.3 Distribution of ^{137}Cs in different waste streams

Among the different wastes generated, three waste streams are important with respect to Cs recovery point of view. These waste streams are (i) Acidic high level waste (ii) Alkaline ILW and (iii) Alkaline declad waste. The radioactive liquid waste containing more than 1 Ci/L of total activity is generally classified as high level waste. The acidic HLW generated from reprocessing plants in India have gross β activity in the range of 10-30 Ci/L which is due to the presence of major radionuclides ^{137}Cs (3-10 Ci/L), ^{90}Sr (3-10 Ci/L), fission products and several actinides[9]. The ILW generated at the back end of nuclear fuel cycle is alkaline in nature and characterized with high salt loads. The waste has gross β activity in the range of 4-50 mCi/L with ^{137}Cs as the major radionuclide and traces of ^{90}Sr, ^{106}Ru etc[10]. The declad waste, generated from the chemical dissolution of aluminium cladded natural uranium fuel irradiated in research reactors, is characterized by much higher concentration of NaOH, Al and Na-salts[11]. However, with respect to activity content, it is similar to that of ILW. It is worth mentioning here that although ^{137}Cs concentration in both the alkaline streams are quite low, total inventory of ^{137}Cs in these waste streams are quite significant because of high waste volumes. A typical distribution scheme of radioisotopes in these waste streams is shown in Fig.1-1. It can be seen that the acidic High Level Waste (HLW) generated from reprocessing plants is the main source for ^{137}Cs.

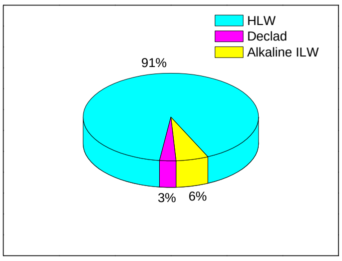

Figure 1-1: Typical distribution of ^{137}Cs in different waste available for recovery at Trombay

1.2.4 Specific activity of ^{137}Cs in waste

The concentration of ^{137}Cs in different waste streams has been discussed above. Specific activity of the radioelement is one of the important parameters from application point of view. The specific activity of pure ^{137}Cs calculated from radioactive decay equation is about 87 Ci/g but its specific activity in waste will vary depending upon the concentration of other Cs isotopes and age of the waste. Three isotopes of Cs are known to be produced in substantial quantities during fission reaction. The details of the isotopes produced in thermal neutron fission of ^{235}U in PHWR[12] are shown in Table 1-3. After 10 years of cooling the specific activity of Cs in waste would be around 35 Ci/g.

Table 1-3: Typical distribution of Cs isotopes in spent fuel irradiated in PHWR

Mass No.	**$t_{1/2}$ (years)**	**Thermal neutron fission of ^{235}U**	
		Fission yield (atom%)	Quantity* (g/tonne)
133	stable	6.7	240
135	2.3×10^6	6.6	20
137	30.2	6.2	240

**Typical distribution of Cs isotopes in spent fuel at the end of irradiation in PHWR (6700 MWD/tonne).*

1.3 Methods for Recovery of ^{137}Cs

A large number of processes for the recovery of ^{137}Cs from acidic as well as alkaline waste streams have been developed till date, many have been used and some have been advocated for the large scale recovery of the radioelement[13,14]. Based on the methods of recovery, processes are categorized in three groups and discussed in detail below.

1.3.1 Chemical precipitation based processes

Precipitation is generally the method of choice for separation of the traces of radioelements from large volumes of waste solution. In this process, solutions of more than one precipitating agents in solution form are added to waste and the medium is maintained in such a manner which is conducive for the formation of an insoluble compound. This compound, initially in the form of fine particle or colloids gets subsequently agglomerated and form large flocks. The radionuclides are entrapped into the precipitate by the mechanisms like (i) ion exchange, (ii) co-precipitation and (iii) sorption, leaving the bulk liquid free of radionulide contamination. This process is generally used for decontamination of low level effluents. Nevertheless, several precipitation based processes have been used in large scale recovery of ^{137}Cs with some of them are highlighted below.

(1) Precipitation of Cs by transition metal hexacyanoferrates are known for a long time. Formation of the precipitate is generally carried out by addition of potassium salt solution of hexacyano ferrate and nitrate salt solution of the transition metal (Cu, Co, Ni, Zn, etc)[15] to waste. Separation of Cs^+ by the precipitate occurs vide ion exchange mechanism as shown below:

$$K_4Fe(CN)_6 + CuSO_4 \Leftrightarrow K_2CuFe(CN)_6\downarrow + K_2SO_4$$

In 1959, a process involving precipitation of ^{137}Cs by zinc hexacyanoferrate was adopted at US DOE laboratory for the large scale recovery of ^{137}Cs from purex raffinate at pH 2[16]. After separation of the precipitate from the bulk solution, it was then washed in water and then hydrolyzed by steam at 250-300°C. The leached Cs solution was processed further to obtain ^{137}Cs product in the form of CsCl powder.

(2) The use of phosphotunstic acid, $H_3[PW_{12}O_{40}]$, for selective precipitation of ^{137}Cs from acidic raffinate was adopted at US DOE laboratory[13]. In acidic solution, the replacement of one or more hydrogen of $H_3[PW_{12}O_{40}]$ by Cs^+ leads to the formation of an insoluble precipitate. The precipitate after separation from bulk liquid was dissolved in NaOH and processed further for the recovery of ^{137}Cs.

(3) Sodium tetraphenyl boron, $Na(C_6H_5)_4B$, is an well known reagent which can selectively form an insoluble compound with Cs. This process has extensively been tested at Savannah River laboratory, USA[17].

The use of precipitation based process have been discontinued in recent times because of its inherent disadvantages like bulkiness of process pot, higher shielding requirements and complexity of filtration/centrifugation in high radiation fields.

1.3.2 Solvent extraction based processes

Solvent extraction based processes are the most promising as far as selective separation of radionulides are concerned. Technology for large scale applications of the process are well established as one of the biggest solvent extraction based process, i.e., PUREX process for separation of U and Pu from dissolved spent fuel solution has been operational over the last five decades.

In this process, an organic stream containing solvent, traces of selective extractant and the aqueous waste are kept in intimate contact by employing strong external agitation. During this agitation, the metal ions come in contact with the extractant and are extracted into the organic phase by formation of an organic phase soluble metal-extractant complex.

On standing, the organic phase separates out and the metal ion is stripped from organic phase to aqueous phase by disturbing the stability of the metal-extractant complex.

A variety of extractants have been evaluated in recent years for the separation of ^{137}Cs from acidic as well as alkaline waste streams. Amongst others, two extractants, viz., (i) chlorinated cobalt dicarbollide (CCD) and (ii) calix-crown are widely popular for their very high selectivity for Cs from acidic solution.

The process based on use of CCD in polar diluent (metanitrobenzotrifluoride) was developed at the Nuclear Research Institute in Czechoslovakia[18] and successfully adopted in the commercial separation plant at Mayak PA in Russia[19]. The loaded Cs on CCD can be stripped using 5-6 M HNO_3. A total of about 15 MCi of ^{137}Cs-^{90}Sr, was separated from 400 M^3 of HLW at UE-35 operation, using CCD along with PEG[20]. A similar process was developed and tested with high degree of Cs recovery at INEEL[21].From this encouraging result, it can be inferred that the use of CCD can be adapted for selective recovery of ^{137}Cs for its utilization as a radiation source.

The discovery of crown ethers by Pederson attracted researchers interest in developing suitable extractants for selective separation of alkali and alkaline earth metal, notably cesium and Sr [22]. Various crown ethers have been identified as effective extractants for separation of Cs[23]. A process (CSEX) based on the use of di-benzo-18- crown-6 has been developed at ANL and tested with simulated waste along with SREX (Sr extraction by using di-t-butylcyclohexano-18- crown-6) in an isopraraffinic hydrocarbon diluents with TBP solvent phase modifier[24, 25]. Because of the poor stability of the cesium extractant in nitric acid, development work was not pursued further.

The development of calixarenes by Izatt in mid 1980, heralded the next generation extractant for selective separation of Cs from acidic as well as basic solutions[26]. In this new class of compounds, Calix[4] arene-bis (t-octylbenzo-crown-6) has been evaluated as superior extractant for Cs separation[27, 28.] Researchers at Oak Ridge National laboratory successfully developed a caustic side solvent extraction (CSSX) process for the separation of ^{137}Cs from alkaline waste streams[29]. This process was demonstrated in a small scale centrifugal contactor using actual waste at Savannah River site[30]. It has also been demonstrated at the Oak Ridge National Laboratory that the calix[4]arene-crown ethers are highly effective for selective separation of Cs from acidic solution[31]. The attractive feature of the process is that Cs can easily be stripped from organic phase by using dilute HNO_3. The present limitation of employing solvent extraction on industrial scale is the commercial non -availability of these specific solvents in our country.

1.3.3 Ion exchange based processes

Ion exchange is the process of reversible exchange of ions between electrolyte solution and solid ion exchanger, as illustrated for the separation of Cs from waste below.

$$R\text{-}O^-X^+ \text{ (Solid)} + Cs^+ \text{ (sol)} = R\text{-}O^-Cs^+ \text{ (solid)} + X+ \text{ (sol)}$$

where R is the polymer matrix, X^+ is the exchangeable ion, Cs^+ is the ion of interest to be separated from waste solution. The effective separation of Cs^+ by the ion exchanger depends on various factors like nature of ion exchanger and functional group, nature and composition of the waste including concentration of the Cs^+ and concentration of competing ions in the solution. Nuclear wastes of reprocessing plant origin including the acidic HLW and alkaline ILW contains, very low concentration of Cs^+ and significantly higher concentrations of competing Na^+ ions. It is therefore a prerequisite for waste treatment application that the ion exchangers should have very high affinity for Cs^+. In addition to this, elution of Cs^+ is also desirable when recovery of Cs^+ is the main objective. Highlights of the promising ion exchange based processes evaluated till date is given below.

(1) The first successful application based on the fixed bed use of ion exchange column was reported from Hanford site for recovery of mega curies of ^{137}Cs from alkaline waste. The process utilized a commercially available zeolite of chabazite type, Linde AW 500, for loading of ^{137}Cs from alkaline solution.

Recovery of loaded ^{137}Cs was carried out by elution using $(NH_3)_4CO_3$ followed by neutralization of the eluate using HCl resulting in a CsCl solution, which as CsCl powder was obtained[13].

(2) Another ion exchange based process based on the use of copper hexacyano ferrate on silica support was adopted in Russia for recovery of ^{137}Cs from acidic solution. In this process, ^{137}Cs in acidic waste stream was loaded on the sorbent column and then eluted by using 8.0 M HNO_3. In HNO_3 medium, the affinity for Cs with the compound is reduced due to oxidation of $Fe^{II}(CN)_6$ to $Fe^{III}(CN)_6$, leading to effective elution. The sorbent was then regenerated by passing a reducing mixture $NaNO_2$ and KNO_3. During industrial scale use of the process at Mayak (Russia), about 7 MCi of ^{137}Cs was recovered using a 120 L column in sorption-desorption-regeneration cycles[32].

(3) The inorganic sorbent ammonium molybdophosphate (AMP) has been known for a long time as a promising candidate for selective separation of ^{137}Cs from acidic solutions[33]. However, its industrial application has been limited by the fact that the sorbent has poor column properties owing to its microcrystalline nature. Several efforts have been made over the years to prepare the sorbent in column-usable granular form, either by precipitation inside the pores of silica gel[34], alumina[35], polymeric resins[36] and anion exchangers[37] or by granulation using an organic binder like polyacrylonitrile (PAN)[38,39], calcium alginate[40], etc. Amongst these AMP sorbents, AMP–PAN has been extensively tested for Cs removal from simulated as

well as actual acidic waste at Idaho National Engineering and Environmental Laboratory (INEEL), USA [41]. An innovative process for preparing AMP-coated on polymethylmethacrylate (PMMA) beads has been developed from our laboratory and found to be promising for use in fixed bed column for separation of Cs from high level waste[42]. A significant amount of work has also been carried out using titanates and silicotitanates for separation of Cs from acidic medium[43,44,45]. However, none of them have been found to be promising from recovery point of view as Cs cannot be removed from these exchangers.

(4) Separation of ^{137}Cs from alkaline waste: The use of resorcinol formaldehyde polycondensate resin (RFPR), an alkali catalyzed polycondensation product of resorcinol and formaldehyde[46,47,48,49], is well established. The resin possesses very high affinity for Cs^+ ions even in presence of molar levels of Na^+ ions[50],[51]. This signifies that the deleterious effect of Na on Cs uptake by RFPR is quite low and hence advantageous for its application because Na is the major non-radioactive constituent present in most of the effluents generated at the back end of nuclear fuel cycle. Further, the weakly acidic nature of the functional groups facilitates the recovery of Cs^+ ions from loaded resin by elution in small volumes of dilute acid. The regenerated resin is as effective as fresh resin and can be used for the separation of Cs in repeated loading-elution-regeneration cycles[52]. In India, extensive studies have been carried out in the authors' laboratory on the preparation, characterization and testing of the resin for the separation of ^{137}Cs from alkaline radioactive waste solutions of reprocessing plant origin. Industrial scale application of the resin for separation of ^{137}Cs from alkaline ILW solution in repeated loading-elution-regeneration cycles has also been demonstrated successfully[10, 53, 54]. The use of RFPR in repeated loading-elution-regeneration cycles served twin objectives viz.,

efficient decontamination of the ILW and recovery of ^{137}Cs in a small volume of dilute nitric acid solution. However, the eluate contains a substantial amount of Na ions. Presence of Na entails further purification of the solution to make it suitable for use as a gamma source in radiation technology application. A significant amount of work has also been carried out in US-DOE laboratories with simulated and actual tank effluent[55,56,57,58,59,60]. In all these work, decontamination of the waste were the main objective. In summary, RFPR has successfully been used for the separation of ^{137}Cs from either waste simulant or actual waste containing Cs concentrations $<7.5\times10^{-5}$ M and the recovery of the Cs is possible in a small volume of dilute acid. Since this recovered ^{137}Cs solution contains a substantial amount of Na ions, further processing is required to make it suitable for use as source in radiation technology application.

After separation from waste by any of the processes discussed above, the Cs is to be incorporated in a solid matrix for use as a radiation source. In the following discussion therefore an overview of the matrices suitable for the application are highlighted.

1.4 Selection of the source matrices

Higher stability at elevated temperature and low solubility in common aqueous solvents are the two major considerations for the selection of source matrices. Other considerations includes higher loading of ^{137}Cs per unit volume of the matrix, high radiation resistance, ease of preparation at relatively lower temperature and minimum loss of Cs due to volatilization. Fundamentally, matrices with high thermal stability, low solubility and good mechanical properties are generally characterized by a combination of (i) strong ionic bond, (ii) large lattice energy and (ii) high ionic potential (charge/radius ratio).

1.5 Matrices for immobilization of ^{137}Cs

Although CsCl (melting point: 646°C) powder does not satisfy most of the above criteria, it has been the choice for radiation source application[61, 62], mainly because of highest weight ratio of ^{137}Cs per unit volume (~100 Ci/cm^3), excellent compatibility with stainless steel at ambient temperature and ease of preparation. However, CsCl powder is highly corrosive at elevated temperatures and can be easily dispersed. Moreover, the high solubility of the CsCl in water may lead to release of the activity from its defective capsule to the environment and cause severe ecological consequences including fatal syndrome[63].

Several matrices have been identified as potential candidates for Cs sources. This includes cesium tantalates, cesium saturated calcinated zeolites, synthetic pollucite, ceramic oxides, aluminosilicate glass, aluminophosphate glasses, glass ceramics and Zn borosilicate glasses. A brief description of the preparation of such matrices is given below.

(1) Cesium tantalates can be prepared either by molten salt reaction or slurry reaction as shown below[64]:

In molten salt reaction, the molten CsOH reacts with Ta_2O_5 and forms the corresponding Cs compound. For example,

$2CsOH\ (melt) + Ta_2O_5\ (g) \rightarrow 2CsTaO_3\ (g) + H_2O\ (g)$

(ii) The slurry reaction method involves a reaction of aqueous solution of CsOH or Cs_2CO_3 and suspended particle of Ta_2O_5, as shown below.

$Ta_2O_5 + xH_2O + 2CsOH \rightarrow 2CsTaO_3 \downarrow + H_2O\ (g)$

The products from both methods were calcined at 700-1000°C. The characteristic properties of Cs tantalite such as high density (about 70 Ci/cm^3 volumetric specific activity for Cs), high melting temperature (1400°C) and relative insolubility in water makes it one of the promising candidates for immobilization of Cs. The main drawback is that the mass absorption coefficient for Cs (owing to higher molecular weight) is quite high. However, proper irradiator design can make the compound useful as a radiation source.

(2) Preparation of ceramic matrices as host for cesium is known to be advantageous mainly with respect to Cs stability. The ceramic matrices include aluminosilicate, synthetic zeolites, pollucite type compounds and synroc. The preparation of most of the ceramic compounds involves reactions at elevated temperature and pressure. A brief description of the matrices is given below.

Pollucite ($CsAlSi_2O_6$) is a chemical form of Cs existing as ore. The compound has very high melting temperature (1700^{o}C) and it is insoluble in water. In 1967, Olombel et al developed a method for synthesizing pollucite for use as X-ray source[65]. Shigemasa et al proposed a simple method for preparation of pollucite using synthetic zeolite[66], where zeolite powder was pressed at about 0.5 tonne to make pellet and calcined at 600^{o}C for 2 hours, then the pellet was immersed in $CsNO_3$ solution followed by heating at 1100^{o}C for 2 hours. The pellet obtained was found to have bulk density of about 2.4 g/cm^3, specific activity of Cs is about 12 Ci/g and water solubility quite similar to that of natural pollucite.

Similarly, a synthetic zeolite of chabazite type (AW-500) was also used to load Cs in which the zeolite sample was fired at 1100^{o}C[67]. The product formed was found to have excellent leach rate characteristics but the Cs storage density was quite low.

Preparation of pollucite directly from CsCl was also reported by mixing 3M CsCl solution with bentonite clay followed by drying and firing at 1000^{o}C[67]. The Cs storage density was quite low but the product had excellent stability against hydrolytic attack.

(3) Immobilization of Cs in synthetic rock (synroc) [68] is one of the best options which make the final product water insoluble. Among others, Cesium titanate hollandite,

($Cs_xTi_8O_{16}$, x=1.36) is one of the promising synroc material for immobilization of Cs. Hollandite can be prepared by solid state reaction between Cs and solid TiO_2 under reducing conditions at about 1250°C. Though Cs ions are highly stable in hollandite as it is encapsulated within the one dimensional oxygen cavity formed by ledge-sharing TiO_6 octahedral, high processing temperature is the main drawback from processing point of view. A simplified process involving electrolysis of a mixture of Cs_2O, MoO_3 and TiO_2 at 900°C was reported recently for the preparation of single crystalline hollandite[69]. However, feasibility of the process for large scale preparation of the compound from CsCl/$CsNO_3$ solution is still to be evaluated.

(4) Glass as a matrix can be considered another choice for immobilization of cesium. Primary reason for this being that glasses produced by the nature thousands of years ago are found to be stable even today. Taking this analogy, scientists have synthesized glasses in laboratory which are being used almost in every part of our daily life. Secondly, glass is unanimously accepted as a primary matrix for immobilization of the high level waste. Depending upon the nature and composition of major glass forming constituents, different glasses such as silicate, aluminosilicate, borosilicate, phosphate, etc have been developed. A brief description of each of the glasses with relevance to either immobilization of nuclear waste or radiocesium is discussed below.

France has considered preparation of aluminosilicate glasses for conditioning of Cs[70]. The loading of Cs used in preparation of such glasses were in the range of 3-10 wt% and all the glasses were fabricated at 1400-1600°C. However, use of such glasses as radiation source has not been reported.

Borosilicate based matrices have been widely used for the immobilization of high level radioactive liquid waste mainly because of its excellent glass forming ability with regard to many different types of waste elements coupled with good chemical durability, mechanical integrity, thermal and radiation stability. Pour temperature of such glasses are in the range of 950-1100^{0}C. However, such matrices have limited use in preparation of ^{137}Cs based radiation sources. This may possibly be due to the lower loading of Cs_2O in borosilicate based glasses which are formed within 1000^{0}C, and notably higher loss of Cs due to volatilization. In UK, Zn-borosilicate matrix has been chosen for preparation of Cs-based sources. The Cs activity in such sources is less than 3 Ci/g[71].

1.6 Scope of the present work

Present work deals with the development of a high ^{137}Cs loaded matrix for use as a gamma source in medical and industrial irradiators. Among the possible solid matrices, immobilization of ^{137}Cs in glass matrix is considered in this study in view of its global acceptance for immobilization of high level waste as well as its attractive properties including (i) high chemical durability (ii) high radiation stability (ii) good thermal conductivity (iv) high mechanical strength (v) easy availability of raw materials (vi) ease of processing within acceptable temperature range. The glasses developed so far for the immobilization of HLW contains about 15-30 wt% waste oxide. In terms of Cs_2O and Na_2O content, this corresponds to about 1-3% and 15-20 wt%, respectively, whereas glasses required for radiation source application should have a minimum of 10 wt% Cs_2O loading and free from other radionuclide contamination. Higher loading of Cs_2O will make sources with higher specific activity. Contamination from other radionuclides should be strictly avoided to meet the source specifications as per regulatory guidelines for product use in public domain. This will therefore restrict the use of immobilized high level waste product as a radiation source even-though specific activity requirement will be fulfilled. In order to meet these basic requirements, it is necessary to use radiochemically pure ^{137}Cs in source preparation.

At the onset of the work, efforts have been made to develop suitable processes for the separation ^{137}Cs from waste streams (alkaline intermediate level waste (ILW) and acidic high level waste (HLW)) generated from reprocessing plants in India. For industrial scale separation of Cs from alkaline ILW the process used in India is based on the use of highly Cs-selective resorcinol formaldehyde polycondensate resin (RFPR) in loading–elution cycle[53]. Owing to the high Cs-selectivity of RFPR, one would normally expect that the recovered ^{137}Cs product will be radiochemically pure. However, the substantial amount of Na ions, which are present in the resin bed as counter ions, accompanies the ^{137}Cs during the elution. Presence of higher Na content in the eluate restricts its direct use in source preparation as total limit of alkali oxide (Na_2O+Cs_2O) loading in glass is used up by Na_2O and results in low ^{137}Cs bearing product glass. It therefore requires specific efforts to separate out Na ions from the eluate.

In order to separate out Na from eluate, studies were carried out with RFPR to devise suitable conditions for selective elution of Na and Cs ions. Some characteristics properties of the resin with high Cs^+ bearing solution have been determined. This includes evolution of the ion exchange isotherm, column loading behavior as a function of Cs concentration and selective elution of Na^+ and Cs^+ ions from RFPR column. Results of the study helped finalize a process for production of a chemically and radiochemically pure ^{137}Cs product. The composition of final ^{137}Cs product obtained in this process has been used as an input parameter in preparation of ^{137}Cs based glass matrices. Details of the experimental results are incorporated in Chapter 3.

Studies have also been carried out for separation of ^{137}Cs from acidic high level waste streams which is the main reservoir for ^{137}Cs as it contains more than 99% of the total

^{137}Cs produced from nuclear fission reaction. Development of a practically viable process for the recovery of ^{137}Cs from HLW is thus one of the important considerations for its utilization as a gamma source in radiation technology applications. Ammonium molybdophosphate coated on PMMA beads has been used in this study. The reason behind the selection of the sorbent among others discussed in section 1.3.3 of this chapter is that the inorganic sorbent possesses very high affinity for Cs from acidic solution, high radiation stability and most importantly its availability and ease of preparation in column useable granular form. Several batch and column studies have been carried out to confirm the suitability of the sorbent for separation of Cs from acidic HLW. It is known that recovery of loaded Cs from AMP is possible either by elution using concentrated NH_4NO_3 or by dissolution of AMP in NaOH. Because of safety issues, the Cs in NH_4NO_3 cannot be used for immobilization. On the other hand, no process for the separation of chemically pure ^{137}Cs from dissolved AMP has been worked out till date to the best of the author's knowledge. In the present investigation, efforts have therefore been made to work out a scheme for the recovery of ^{137}Cs from acidic HLW. The investigation envisaged (i) evaluation of Cs loading behavior of the granular AMP sorbent prepared by coating of AMP powder on PMMA beads (ii) recovery of Cs from loaded AMP by dissolution in NaOH solution and (iii) purification of Cs from dissolved AMP solution using RFPR column. Based on the results, an integrated process flow sheet has been developed for the first time and demonstrated in the laboratory. Results of the study are also incorporated in Chapter 3.

A major part of the present investigation was devoted to the development of glass matrices for immobilization of the Cs product solution obtained from above mentioned Cs separation studies (Chapter 3). In initial part of the study, the matrix development work was pursued with a nominal loading of about 10 wt% of Cs_2O and 15wt% of Na_2O in borosilicate glass for its possible application as a source in blood irradiators. The glasses of this type can be categorized as high alkali oxide bearing glasses. In general, the high alkali oxide bearing glasses are formed at relatively lower temperature and resultant glasses are chemically less durable. Though processing temperature up to 1000^{o}C is acceptable from application point of view, a lower processing temperature for the production of cesium glasses is always preferable as loss of Cs due to volatilization will be less at lower temperature. Although no limit on chemical durability has yet been imposed for this specific application, it is one of the objectives of the work to make glasses as corrosion resistant as possible. The chemical durability of the cesium glasses, like other nuclear waste bearing glasses, can be considered as one of the important characteristics so that the glasses can eventually be disposed off after life-time use as a radiation source. Evaluation of formulation was therefore based on (i) low pouring temperature (ii) good chemical durability and (iii) low Cs-loss due to volatilization.

The matrix development work was carried out by adopting a simple practical approach that includes optimization of a borosilicate glass formulation and thereafter efforts were made to improve the properties of the optimized formulation by inclusion of additives. The additives used in this study include TiO_2, alkaline earth metal oxides, ZnO and MnO. In this study, efforts were also made to extend our understanding on change of physicochemical properties of the borosilicate glasses as a function of the incorporated additives. Physiochemical properties of the glasses measured include chemical durability, density, molar volume, glass transition temperature (Tg) and Cs loss due to volatilization. Chemical durability of the glasses have been determined by conducting leaching tests for varying time periods up to 21days. Thermophysical properties like glass transition temperature (T_g) was measured by differential scanning calorimeter (DSC) and TG-DTA techniques. The loss of Cs due to volatilization has been measured as a function of (i) matrix composition (ii) formation temperature and (iii) soaking time. Powder XRD pattern was used to ascertain the amorphous nature of the glasses. Scanning electron microscopy (SEM) was used to examine the surface profile of the glasses. Structural characterizations of the glasses have been done by using FTIR and NMR spectroscopy techniques. Results of the study are discussed in detail in Chapter 4, 5 and 6. Results were used to arrive at some short-listed formulations for possible application as a source in blood irradiators.

Further, formulation development work has been pursued for the preparation of source matrix for use in industrial irradiators. High loading of ^{137}Cs is required for such application. For preparation of such glasses, a series of glasses were prepared by varying concentration of Na and Cs keeping total alkali oxide concentration constant (20 mole%). Results of the study also included in Chapter 6.

Chapter 2

Experimental

Experimental

2.1 Introduction

The chapter covers the descriptions pertaining to the experiments carried out during the course of this thesis work. A brief description of experimental procedures for the preparation and characterization of ion exchange resins/ sorbents and glasses are discussed. Various instrumental techniques used for characterization and analysis are also discussed along with the working principle and overall block diagram of the instrument.

2.2 Preparation of AMP sorbents and RFPR Resins

AMP sorbents used in this work are (i) AMP(*Lab*) - AMP powder prepared in the laboratory using citromolybdate procedure[72] (ii) AMP(*V1*) and AMP(*V2*) - AMP powders procured from two vendors and (iii) AMP(*V2*)-PMMA and AMP(*Lab*)-PMMA beads - prepared by coating AMP(*V2*) and AMP(*Lab*) powder on PMMA beads, respectively. PMMA beads, procured from a commercial source and sieved to 0.30-0.42 mm size, were used in the preparations. The preparation of AMP-PMMA beads was done as per the procedure described[42]. Based on the weight of AMP used in the preparations, the nominal loading of AMP was estimated to be 37% on the coated bead products. After preparation, the AMP-PMMA beads were taken in sintered disc funnel and conditioned by passing 20 bed volumes of 1.0 M NH_4NO_3 + 0.1 M HNO_3 solution followed by 20 bed volumes of 0.1 M NH_4NO_3 + 0.1 M HNO_3 solution, air-dried, sieved and stored in stoppered bottles. AMP powders were microcrystalline in nature. The particle sizes of AMP-coated PMMA products, viz., AMP(*V2*)-PMMA and AMP(*Lab*)-PMMA, were in the range of 0.30-0.60 mm and 0.30-0.85 mm, respectively.

The Resorcinol formaldehyde polycondensate resin (RFPR) was made and processed in the laboratory as per the procedure described elsewhere[48]. The particle size of RFPR was in the range of 0.30-0.85 mm.

2.3 Characterization of AMP sorbents and RFPR Resins

2.3.1 Determination of moisture content

Moisture contents of the sorbents and RFPR were determined by measuring the loss in weight after heating at 100±2°C for 6 hours.

2.3.2 Determination of batch distribution coefficient

Batch distribution coefficient is the ratio of metal ion concentration (e.g. Cs) between resin and solution phase. It is generally determined by conducting batch tests. In the present study, batch tests were conducted by equilibrating 0.1 g of sorbent and 10 mL of test solution in stoppered polypropylene vials. The mixture was shaken in wrist action shaker for 7 hours and left standing overnight. The mixture was then filtered through Whatman 42 filter paper and the activity of ^{134}Cs in filtrate was measured.

The distribution coefficient (K_d, cm^3/g dry resin) was calculated using the equation:

$$K_d = \frac{C_i - C_f}{C_f} \times \frac{V}{W_r} \times \frac{100}{100 - W_m} \qquad \ldots(2)$$

where C_i and C_f are the activities of ^{134}Cs in the solution before and after equilibration (counts/min/cm^3), V is the volume of equilibrating solution (cm^3), W_r is the weight of resin (g) and W_m is its moisture content (% wt/wt).

2.3.3 Determination of cesium sorption isotherm

Batch equilibration tests were carried out to determine the cesium sorption isotherms. Test solutions containing varying concentrations of Cs and Na were used. Details of tests solution are given in Chapter 3 along with the results of these batch tests.

2.3.4 Column tests

Laboratory scale glass columns having 12 mm internal diameter (ID) and equipped with PTFE stopcock and sintered disc support at the bottom were used. The columns were loaded with requisite quantity of sorbent. For AMP sorbent, column was conditioned by passing 5 bed volumes of 1.0 M HNO_3, whereas 1.0 M NaOH was used for conditioning the RFPR bed. After conditioning, the bed volume was noted. The feed solution was passed through the column from top to bottom at a flow rate of about 5 bed volume /hour. Effluent samples were collected periodically and analyzed. The loading was followed by rinsing the column with 3 bed volumes of 0.1 M HNO_3 for AMP and 0.1 M NaOH for RFPR bed, respectively.

Recovery of loaded Cs^+ from AMP bed was carried out by caustic dissolution of AMP. For dissolution, 1.0 M NaOH followed by 0.1 M NaOH solution was passed through the bed from bottom to top at the flow rate of 5 bed volume/hour.

For the case of RFPR, elution of loaded Cs was carried out by passing either 20 bed volumes of 0.5 M HNO_3, or 8 bed volumes of 0.1 M HNO_3 followed by 12 bed volumes 0.5 M HNO_3.

2.3.5 Analysis and calculation

All the experiments were carried out with test solutions containing requisite amount of inactive $CsNO_3$ and ^{134}Cs tracer procured from the Board of Radiation and Isotope Technology

(BRIT), Mumbai. The gamma activity of ^{134}Cs (E_γ= 604 and 795 KeV, $t_{½}$ =2 years) in solution was measured using NaI/Tl scintillation detector coupled with single channel analyzer. The measured activities of ^{134}Cs in solution before and after separation and initial concentration of Cs^+ in solution were used to calculate the molar concentration of Cs^+ in the equilibrated solutions. The calculated molar concentration of Cs^+ was expressed in terms of Ci of ^{137}Cs assuming 35 Ci/g as the typical specific activity of ^{137}Cs in waste (section 1.2.4).

2.4 Preparation of glass

Glasses were prepared in batches in platinum crucible (batch size: 50 g) using AR grade chemicals. The chemical mixture was heated in muffle furnace at 900°C for 2 hours followed by 1000°C for about 15 min and then poured on a steel plate. The sources of AR grade chemicals from where they are procured are given in Table 2-1.

Table 2-1: Chemicals used for glass preparation

Oxides	**Chemical used**	**Make**
SiO_2	SiO_2	S. D. fine, India
B_2O_3	H_3BO_3	S. D. fine, India
Na_2O	$NaNO_3$	S. D. fine, India
Cs_2O	$CsNO_3$	Chempur, Germany
CaO	CaO	BDH
BaO	$Ba(NO_3)_2$	S. D. fine, India
ZnO	$ZnNO_3$	B D H
MgO	$Mg(NO_3)_2$	S. D.fine, India
SrO	$Sr(NO_3)_2$	S. D.fine, India
TiO_2	TiO_2	S. D.fine, India
MnO	$MnCO_3$	Alphabio

2.5 Chemical analysis of glass

Glass is a tailor made product design to meet specific requirements concerning their physical and chemical properties. The properties of the glasses are decided by the chemical composition. Further, structure of the glass also depends on its chemical composition. Calculating chemical composition of the final glass from batch composition is not desirable as the composition of the final glass product always differ from batch composition mainly because of the two reasons, viz., (i) during the melting process some constituents (alkaline oxides, boron oxides) are partially volatilized and (ii) mistake caused by human error and instrument during weighing of chemicals, and contamination. In the case of Cs glasses used in present study, it is of paramount importance because Cs is one of the highly volatile elements at elevated temperatures. In addition, boron is another constituent which also known to volatilize significantly. It is therefore always desirable to determine the chemical composition of the glasses prepared. In general, two approaches, viz., indirect analysis and direct analysis are used to determine the glass composition. A brief discussion of these approaches is given below.

2.5.1 Direct analysis

In this analysis method, the glass sample is exposed to radiation (such as X-ray, laser light) or particle beam (e.g, electron, neutron, ions) and response from the sample in the form of secondary emission, backscattering etc. is measured. The change in intensity of the signal when compared to standard sample is used to measure the chemical composition. X-ray fluorescence (XRF), Electron probe microanalysis (EPMA) are the methods generally performed. Although these techniques are very simple and quick, quantitative analyses are often limited due to lack of similar standard. Among the advanced techniques, laser induced breakdown spectroscopy (LIBS) is the most promising for analysis of glass samples. The method is suitable for online determination of the chemical composition. In this technique, a small amount of glass is evaporated by a pulsed laser beam at high energy density and this generates a plasma discharge. The plasma emits light that contains spectral lines specific to the elements present in the sample. No specific efforts have been made during the present study to analyze the glass sample by direct analysis method.

2.5.2 Indirect analysis

In indirect analysis, the glass sample is quantitatively brought into solution and the composition of the solution is analyzed. This method is straightforward and compatible with great variety of common analytical methods for analysis of the solution samples. However, the difficulty lies in dissolution of glass samples. The method adopted for digestion and analysis of the glass samples of present study is described below[73].

2.5.2.1 Sample preparation for digestion

The glass sample (about 0.1 g, -200 mesh) was crushed and washed with acetone and dried at 120^{o}C. The dissolution of the dried glass samples were carried out by adopting processes as described below.

2.5.2.2 Determination of alkali and alkaline earth metal ion

Although acid digestion including heating is generally followed for analysis of alkali metal ion, this procedure is modified to avoid loss of Cs during digestion. In this study, for determination of Na, Cs and Ca concentrations, the glass sample (about 0.1 g, -200 mesh) was soaked in 3 ml of HF and 2 ml HNO_3 mixture at ambient conditions for 2 days and then volume was made up to 100 ml using distilled water. The solution after filtration was used for analysis using ion chromatograph (IC-1000, Dionex make) as per the procedure described in section 2.8.2 below.

2.5.2.3 Determination of boron

For determination of boron, sodium hydroxide fusion at 450°C followed by dissolution of the fused mass in HNO_3 has been used. Estimation of Boron was done by Ion chromatograph as per the procedure discussed in section 2.8.2 below.

2.5.2.4 Determination of silicon

For estimation of silicon, the glass sample was subjected to Na_2CO_3 fusion at 1000 °C followed by its dissolution of the fused mass in HCl and estimation of Si by measuring the color intensity of the molybdenum blue complex spectrophotometrically at 565 nm[74].

2.6 Density and molar volume

Density of the glass samples were measured by Archimedes method, with around 0.5 g of glass samples having grain size ~100+200 mesh (ASTM) using water as immersing liquid (temperature:33°C). Density measurements for each glass were made in triplicate and the average value is presented. The error in the density values was found to be ± 0.5%. The measured density (g/cm^3) and calculated molecular weight (g) from batch composition of the glasses were used to calculate the molar volume (cm^3) of the glasses by using the following equation:

$$\text{Molar volume} = \text{Molecular weight} / \text{density}$$

2.7 Chemical durability

Chemical durability is one of the important properties which used to determine long term stability of the glasses. Several experimental test conditions have been proposed to determine the chemical durability and broadly they can be categorized in two groups, viz., static and dynamic. Under static methods, ASTM standard product consistency is most commonly used. This method is most suitable for rapid evaluation of composition.

Figure 2-1: Teflon-lined stainless steel container used in leaching study

In present study, the product consistency test (PCT-B) as per the procedure described in ASTM-1285-94, was followed to measure the chemical durability of the matrices[75]. In this test, 1.0 g glass sample (-100+200 mesh ASTM) and 10 cm^3 of ultrapure water in Teflon-lined stainless steel container (Fig.2-1) was heated in air-oven at 90°C for 24 hours (in some cases duration of leaching was varied, which will be mentioned in the appropriate sections). These short duration leaching tests were performed for the comparative evaluation of composition. The clear leachate obtained after centrifugation was used for measurement of pH as well as the concentrations of the elements such as Na, Cs, B, Ca, Ba and Si. From the measured concentration, the normalized elemental leach rate (LR_i) was calculated as $g/cm^2/d$ using the following equation.

$$LR_i = \frac{C_i \times V}{f_i \times A \times t} \qquad \ldots(3)$$

where C_i = the concentration of i^{th} element in the leachate (μg/ cm^3), f_i = the mass fraction of the i^{th} element in glass (unit less) calculated from batch composition as taken, A= the calculated surface area of the glass considering their spherical geometry (cm^2), V= the volume of leachant (cm^3) and t =the duration of leaching (day).

2.8 Volatilization of Cs

Being an alkali metal ion, Cs is highly volatile at elevated temperatures with the highest volatility among the glass constituents used in the present study. In order to determine Cs volatility during different stages of glass formation and also to understand the effect of matrix composition and process variables such as temperature and time, efforts have been made to measure Cs volatility under different conditions such as (i) measurement of Cs volatility during glass preparation starting from glass chemicals and (ii) measurement of Cs volatility with preformed glass. Detailed descriptions of each of the processes are given below.

2.8.1 Measurement of Cs volatility during glass preparation

In this method, the requisite amounts of glass forming chemicals (starting materials) were mixed and taken in silica/platinum boat and the boat was heated to fusion temperature. The elements volatilized during glass preparation were collected and analyzed.

A resistant heating based tubular furnace assembly (Fig.2-2) equipped with an 800 mm long fused silica tube connected with two gas absorption bubblers, each containing about 50 ml of 1.0 M NaOH solution, was used in this study. Requisite amount of glass forming chemicals except $NaNO_3$ and $CsNO_3$ for 2 g glass batch was taken in the platinum boat (60 x 10 x 20 mm). A solution (2 mL) containing $NaNO_3$ and $CsNO_3$ and ^{137}Cs radiotracer was added to the chemical mix. The radiotracer was used for ease of measurement of Cs concentration.

The boat was then placed under IR lamp till dryness and thereafter it was placed inside the fused silica tube and heated to 900°C for duration of 2 hours. Gas evolved during heating was withdrawn by applying vacuum and passed through the bubblers. At the end of the experiment, the boat was taken out and weighed. The resultant glass in boat was dissolved in 40% HF under ambient conditions. The tube assembly was washed with 0.5 M HNO_3 to collect Cs, if any, deposited on the cooler part of the tube including the Cs collected in scrubber solutions. The concentration of ^{137}Cs in the washed solutions and in dissolved glass solution was determined by counting in NaI/Tl scintillation detector coupled with single channel analyzer and used was to represent the mass balance of Cs during preparation of the glass. For some selected batches, detailed elemental analysis of solutions obtained from washing of silica tube was carried out.

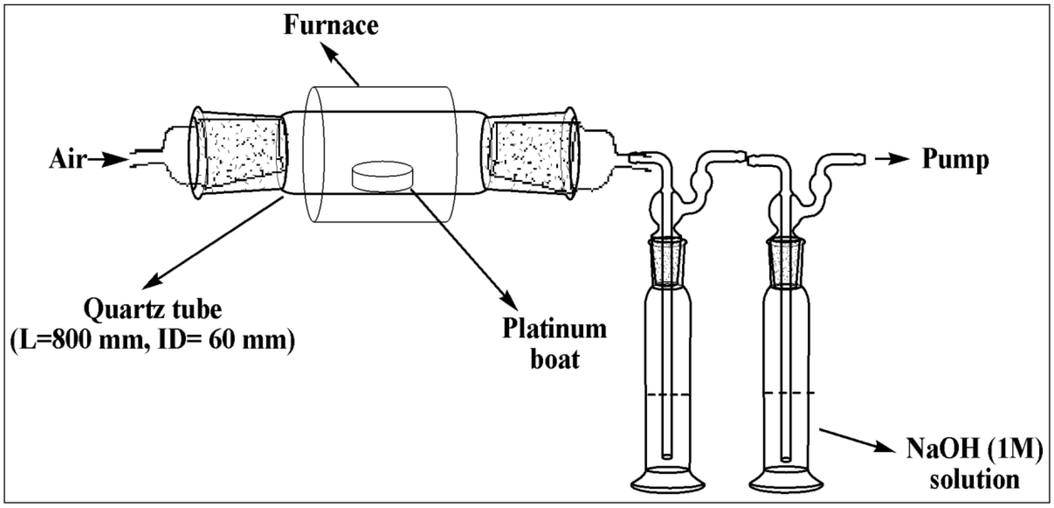

Figure 2-2: Schematic of experimental setup to study the Cs volatilization during glass preparation

2.8.2 Measurement of Cs volatility with preformed glass

Although the direct measurement of Cs volatilization described above (section 2.8.1) as the glass forming mixture is heated, involving collection and chemical analysis of the evolved gasses, the method is tedious particularly since dissolution of glass and analysis of the sample for material balance is involved. Further, this method gives cumulative loss of Cs due to volatilization from all four stages (evaporation, calcination, fusion and soaking) of glass formation. Though significant losses are incurred in all stages of glass formation, losses during fusion and soaking steps solely depend on the composition of the melt. Evaluation of Cs loss during fusion stage is difficult as it occurs in a short time span and is associated with significant froth formation. In contrast, soaking stage involves long time duration for better homogenization and minimum turbulence from froth formation/bubble evolution. The effect of temperature is more prominent at this stage. In view of the above, efforts have been made to measure the Cs volatilization loss as a function of matrix composition and temperature with preformed glasses as described in detail below.

2.8.2.1 Thermogravimetry method

In this method, about 40 mg of glass sample in platinum crucible was placed in TG-DTA instrument (Setaram make) and heated under static air to 900^{o}C at the heating rate of 10^{o}C/min and then isothermal heating was continued at 900^{o}C for 2 hours. The loss of weight of glass due to heating was considered as volatilization loss. Thermal analysis is highly sensitive technique used to measure very small amount of weight change involved, if any, during heating. In addition, it gives an idea about the nature of the reaction responsible for the weight change. Although this method is highly sensitive with regard to very small amount of weight change, it gives an indirect indication about the Cs volatility. A total of five samples were investigated during the course of present study. In view of the negligible amount of weight loss recorded from all the samples, this method was not continued further.

2.8.2.2 Chemical analysis method

The themogravimetry study described above showed no measurable amount of weight loss. This may possibly be due to very low quantity of the sample and lower temperature. Hence, feasibility of using a combination of the two above mentioned methods was examined. In this method, the preformed glass sample (25 g glass) was heated in fused silica volatilization assembly and the amount of Cs volatilized is analyzed by chemical method. This method is therefore can be called as modified procedure of that used by Oldfield *et al*[76]. The glass samples were prepared in independent cylindrical alumina crucibles (ID: 36 mm, OD: 40 mm, length: 60 mm) by heating the requisite amount of chemicals for 25 g of glass in a muffle furnace at 900° C for 2 hours followed by 1000° C for 20 minutes. Then the crucible was removed to ambient conditions for rapid cooling. The preformed glasses in the alumina crucible were examined visually and found to be transparent, colorless and homogeneous. The crucible containing preformed glass was then placed in the silica pot (Length: 12 cm, dia: 50 cm) to complete the volatilization set up as shown in Fig. 2-3. A top loading resistance heating based furnace was used for heating the pot and to a predetermined temperature for about 6 hours per day up to 4 days. The gas evolved during heating was passed through a connector followed by two ice cooled bubblers (containing air only) for the trapping of Cs vapor. The temperature gradient inside the assembly propelled the evolved gasses. After 6 hours of heating, the silica pot containing the crucible was taken out of the furnace to ambient conditions for rapid cooling of the glass. After cooling, the whole set-up including silica pot, connectors and bubblers, was washed using 250 ml of 0.1 M HNO_3 solution. The concentration of Cs in the washed solution was measured by using ion chromatograph or radiometrically. From the measured concentration of Cs in solution, the total amount of Cs volatilized (mg) was calculated and normalized for 25 g of glass. This normalized value of Cs (mg) was divided by geometrical the surface area of the crucible (πr^2, cm^2) and is expressed in terms of the mg/cm^2. It is noted that actual exposed area of the glass was likely to be slightly higher than the geometrical area of the crucible because of the meniscus formation of the glass melt. The error in calculating surface area without considering meniscus formation is considered marginal as the diameter of crucible used was quite large. In order to minimize this error, all crucibles used were of identical size.

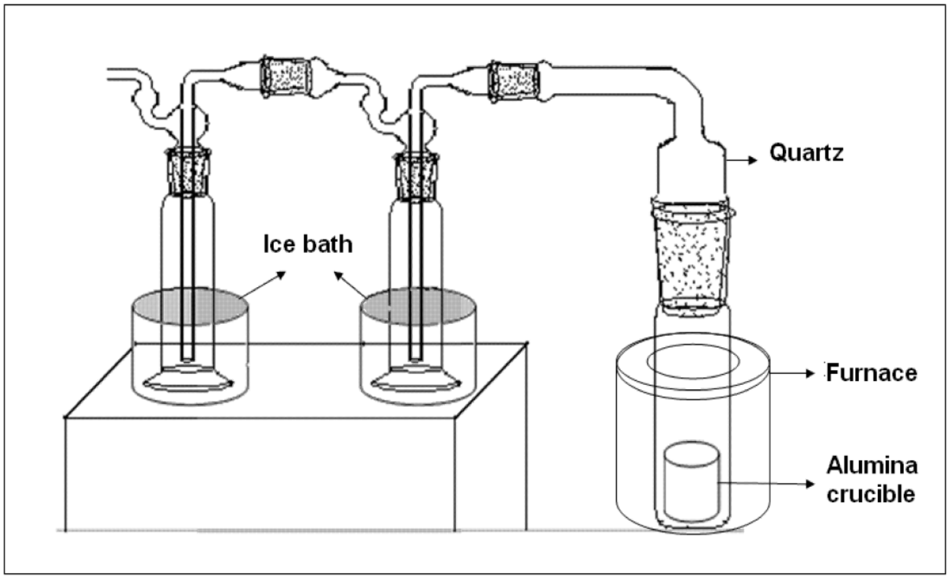

Figure 2-3: Volatilization setup for heating preformed glass in alumina crucible

2.9 Instrumental techniques used for analysis and characterization

2.9.1 Gamma ray detection system

Detection of gamma rays is based on the principle of charge produced by the interaction of radiation with detector volume. The principle mode of interaction of gamma rays with detector material utilized in detection is photoelectric effect. In this interaction, the whole energy of the gamma rays is transferred to the detector material and ejects energetic electron from one of the bound shell of the atom. Various detector systems are being employed to collect the charge and the intensity is used to quantity the radionuclide. Two detector systems, viz., (i) NaI/Tl scintillation detector and (ii) High purity HpGe detector have been used in the present study to measure the concentration of ^{134}Cs and ^{22}Na. A brief description of these two detector system is given below[77].

2.9.1.1 Scintillation detector

Sodium Iodide (NaI) activated with thalium (Tl) is the most widely used inorganic scintillation material for measurement of gamma activity in sample. The main reason is that the high atomic number of its iodine constituent ensures that photoelectric absorption will be more efficient for detection of gamma rays. Furthermore, the high light output and smaller decay time have contributed to the success of development NaI/Tl scintillation spectrometers. The principle of gamma rays detection by NaI/Tl can be explained as follows.

The interaction of gamma rays with NaI produce energetic electron through photoelectric effect (there are several other types of interaction takes place, which are not utilized in gamma rays detection and hence not mentioned). The electron while passing through the medium (NaI crystal) will form large number of electron and hole pair by elevation of electron from valence band and conduction band. Deexcitation of electron leads to emission of photon in the visible region. The shifting of wavelength of emitted photon to visible range is accomplished by the presence of Tl activator which forms the intermediate band. The emitted photon is then collected by photomultiplier tube, wherein the photon is converted to electron with some added multiplication. The electron is thereafter amplified and counted by the detector assembly system (Fig.2-4). The well type NaI/Tl crystal (3x3 inch) coupled with single channel analyzer is used for measurement of ^{134}Cs activity in liquid samples generated during the course of present study.

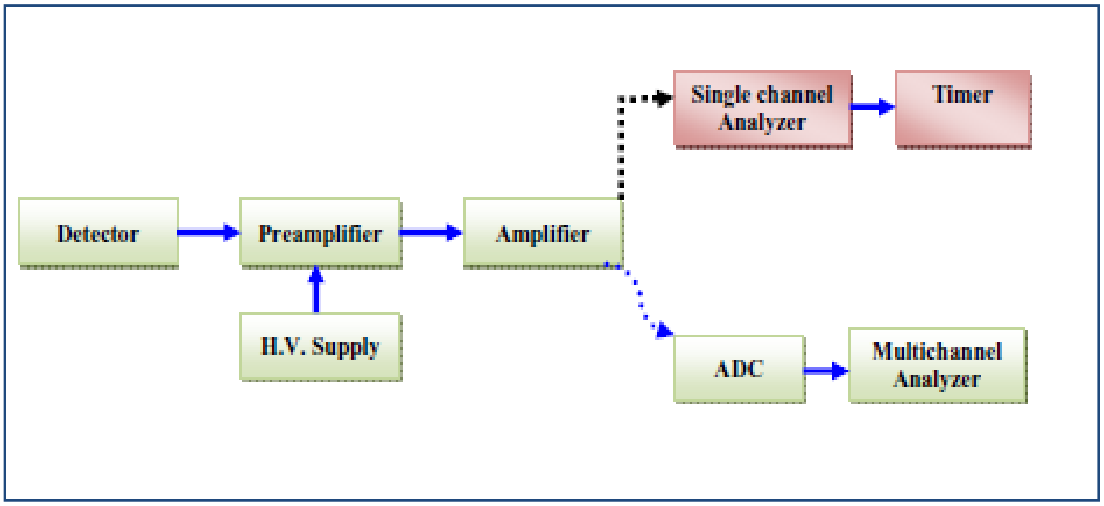

Figure 2-4: Block diagram of radiation counting system

The NaI/Tl detector, although has significantly high detection efficiency, is not useful for gamma rays spectroscopy because of the poor resolution. Therefore the samples containing more than one radionuclide (for example, ^{134}Cs and ^{22}Na in present study) are counted in high resolution HPGe detector assembly, principle of which is described below.

2.9.1.2 High purity HPGe detector

High purity germanium detector with impurity levels of around 10^9 atoms/cm^3 are used in gamma ray spectroscopy. Intrinsic property of the germanium crystal is that it generates electron and whole pair under ambient conditions (band gap is 0.7 ev). In order to minimize this, the detector is generally kept under liquid nitrogen temperatures. Further, detector depletion region is made by reverse biasing of the n-p junction. A typical planner configuration of HPGe detector applied in reverse bias is shown in Fig.2.5. The interaction of gamma rays with the detector materials are similar to that of solid materials such as photoelectric effect, compton scattering and pair production. The charge produced due to these interactions is collected and processed with the use of advanced electronics. A block diagram of charge collection and data processing system is similar as shown in Fig.2-4.

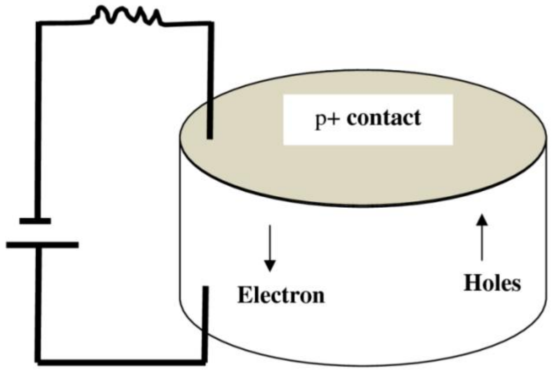

Figure 2-5: Typical planner configuration of HPGe detector applied in reverse bias

It can be noted that the lower atomic number of Ge results in a photoelectric cross section smaller by a factor of about 20 compared with sodium iodide and results in much smaller the intrinsic peak efficiency. Nevertheless, the peaks are still prominent and obvious part of the spectrum is that the line width is so small due to superior energy resolution (around 2 kev at 1332 Kev). The high resolution also helps to identify the other interaction of gamma rays with detector materials, such as compton continuum, pair production, X-ray emission, annihilation and escape peaks etc.

2.9.2 Ion chromatograph

The ion chromatograph system (Dionex make, ICS-1000) used in present study is capable to perform isocratic ion chromatography separations of the ions followed by their detection by conductivity measurements. The data collection is performed by computer running chromatography software (chromeleon), which produces a plot of the detector output vs. time (chromatogram). Before analysis, system is calibrated by running standard samples of at least four different concentrations and used to draw calibration curve. For unknown sample, identification of the ion is done by comparing their retention time with respect to standard sample and area under the peak is used for quantification.

The schematic of ion chromatography system is shown in Fig. 2-6. It has six main subsystem, viz. (i) eluent delivery system (ii) sample injection system (iii) ion separation system (iv) suppressor (v) conductivity detector and (vi) data collection system.

The eluent is passed continuously through the system by the use of pump. While analysis, the liquid sample is manually loaded into the sample loop and then the sample injects into the system by computer operated software. The sample is carried by the eluent to guard and separation column. The guard column removes insoluble mater only. The separation of ions occurred by ion exchange mechanism while travelling through separation column. Then the separated ions enter in suppressors, wherein, ions are electrolytically dissociated and separated through a series of membranes. In this process, ions of eluents are removed and only sample ions reach the detector. The role of suppressor can be illustrated by the following example of cation analysis process using H_2SO_4 as eluent. In electrolytic suppressor, only cations are allowed to pass and anions are rejected. The cations are then combined with OH^- ions (produced from electrolysis of H_2O) and enter in conductivity cell. The anions are combined with H^+ (produced from electrolysis of H_2O) and come out as waste. In conductivity cell, the electrical conductance of ions is measured and the signal is transmits to a data collection system, to produce the conductivity against time.

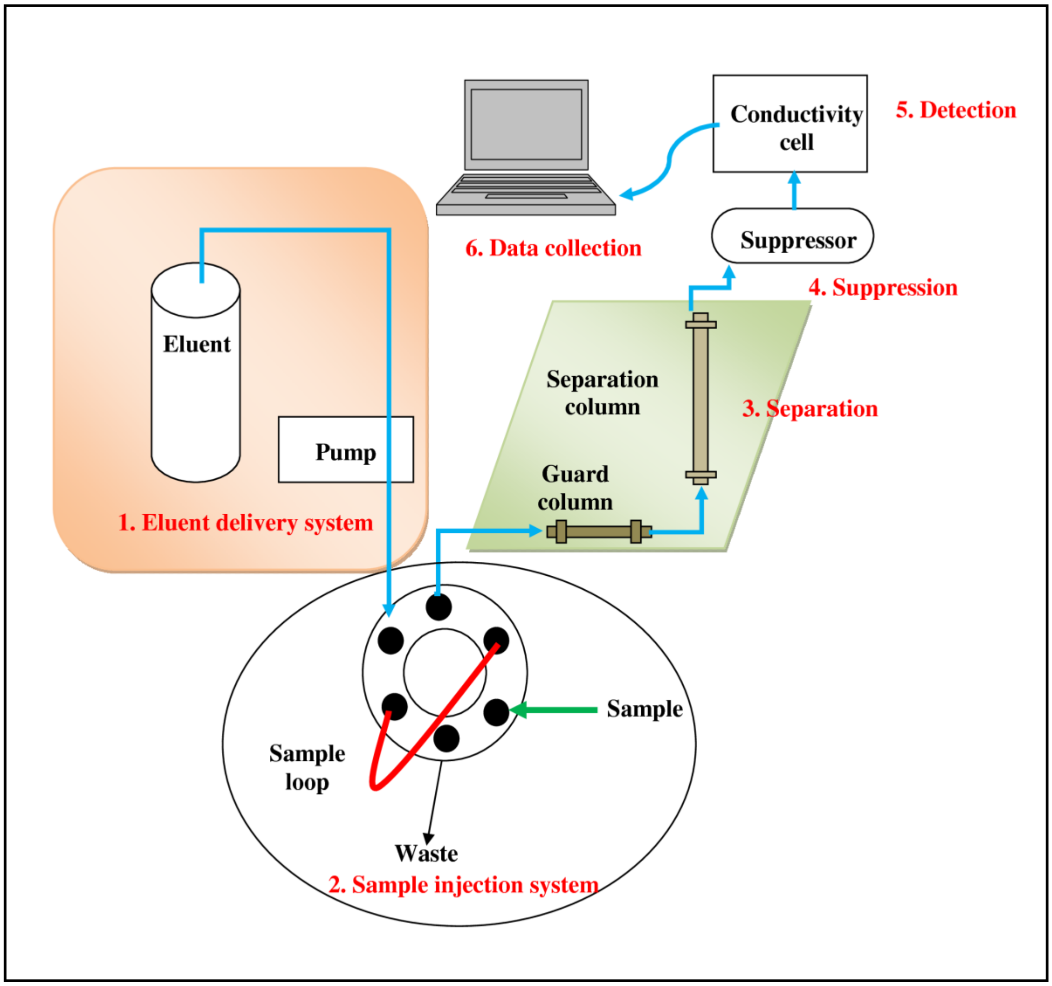

Figure 2-6: Schematic of ion chromatography system

In the present study, analysis of Cs and Na was performed by using sulphuric acid (7 mM) as eluent. All samples were suitably diluted prior to injection in to the system. All dilution was done by using eluent. The standard calibration curve was drawn from the analysis of four standard samples containing 5 to 20 ppm of Cs, 2.5 to 10 ppm Na and 5 to 20 ppm Ca. A typical chromatogram of Na and Cs analysis is shown in Fig.2-7.

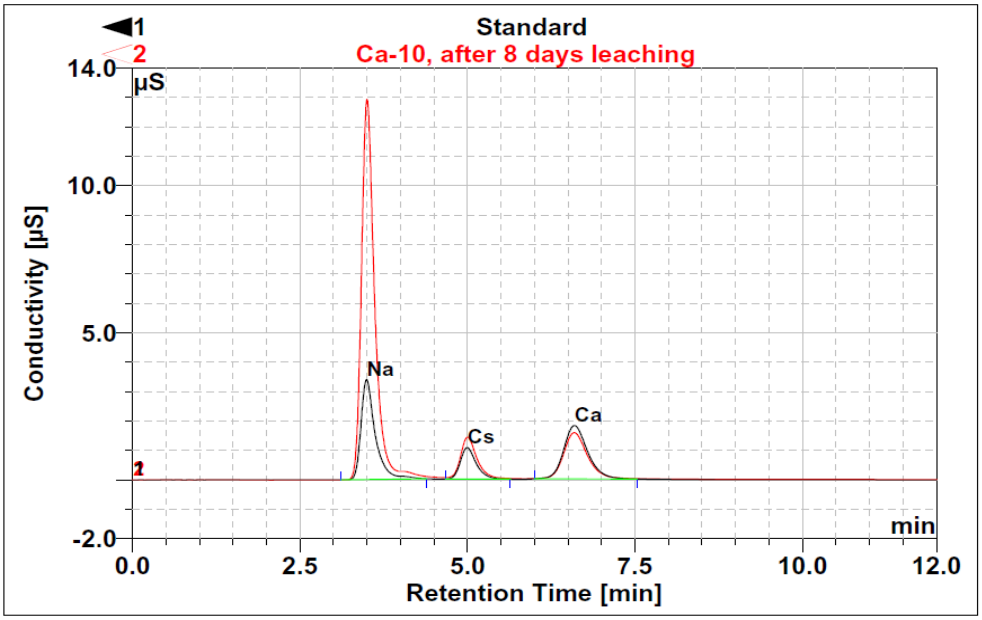

Figure 2-7: Typical chromatogram of a standard sample containing 5 ppm Na, 10 ppm Cs 10 ppm Ca and a glass leaching sample

For estimation of boron, a known volume of solution was heated to dryness to remove the HNO_3 and then a known volume of solution containing mannitol (0.56 M) and $NaHCO_3$ (6.5 mM) was added to bring the weakly borate anion to highly dissociated borate-mannitol anion in solution. Estimation of this borate-mannitol anion was done using a solution containing mannitol (0.56 M) and $NaHCO_3$ (6.5 mM) as eluent[78].

2.9.3 X-Ray diffraction

X-rays are electromagnetic radiation having wavelength (λ) ranging from approximately 0.04 Å to 1000 Å. X-rays are produced when fast moving electrons hit on hard metallic targets, called cathode and ejects core electron from the target. Consequently, inner level electronic transitions take place to fill the gap and thereby emit characteristic X-rays. These characteristic X-rays are superimposed over a broad background (known as white radiation) which is produced due to the acceleration or deceleration of incident charged particles. When the X-rays are incident on a solid material (grating), they are either elastically/in-elastically scattered or absorbed. The elastic scattering of X-rays is known as Bragg scattering and follows the Bragg equation $n\lambda = 2d \sin\theta$. Where λ is the wavelength of X-rays, θ is glancing angle, d is inter planar distance and n is order of diffraction. Depending on the interplanar distance and angle of diffraction, the diffracted/ scattered beam will interfere with each other giving constructive interference and destructive interference. When the path difference between the two rays, differ by an integral number of wavelength, constructive interference takes place.

A block diagram of the typical powder diffractometer, consisting of an X-ray source, sample under investigation and a detector to pick up the diffracted X-rays is shown in the Fig. 2-8. The X-ray beam passes through the soller and divergence slits and then fall on the sample which is spread uniformly over a rectangular area of a glass slide. The scattered X-rays (diffracted) from the sample pass through the soller and receiving slits and then fall on a monochromator before detection. The monochromator separates out the stray wavelength radiation as well as fluorescent radiation emitted by the sample. The output of the diffraction diffraction measurement is obtained as plot of intensity of diffracted x-rays versus Bragg angle.

The details of the X-ray production and the typical X-ray spectra are explained in several monographs[79, 80].

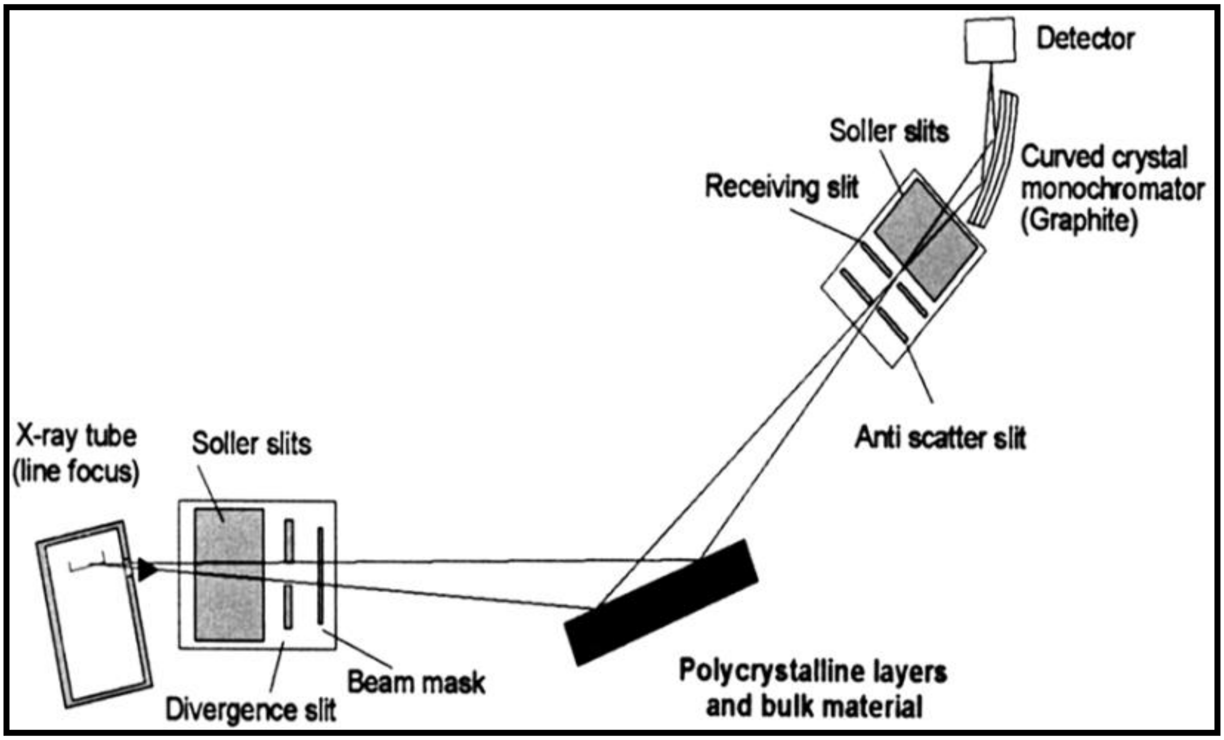

Figure 2-8: X-Ray diagram of a typical reflection mode diffractometer

In the present study, Philips 1710 diffractometer based on the Bragg-Brentano reflection geometry, was used for the characterization of all the glass samples. The Cu-Kα from sealed tube was used as the incident beam. A Ni foil was used as a filter and the diffracted beam was monochromatised with a curved graphite single crystal. The Philips (PW-1710) diffractometer is attached with a proportional counter (Argon filled) for the detection of X-rays. The X-ray tube rating was maintained at 30 kV and 20mA. The goniometer was calibrated for correct zero position using silicon standard. Samples are well grounded and made in the form of a slide. The X-ray beam falling on the sample at a particular angle leads to the simultaneous exposure of several stacks of plane. The sample is scanned for varying incident angle and intensity of the diffracted beam is measured and plotted against 2 theta angle.

2.9.4 Thermal analysis

Thermal analysis methods are used to investigate loss of water or volatile element and determination of glass transition temperature. Thermal analysis is generally performed by using (TGA-DTA) thermo gravimetric analyzer (TGA) coupled with differential thermal analysis (DTA) and Differential scanning calorimetric (DSC) technique. The thermal analysis techniques used in the present study and their principle are briefly discussed below.

2.9.4.1 Thermo gravimetric analysis (TGA)

In TGA, the weight of a sample is monitored as a function of time as the temperature is increased at a controlled uniform rate. The loss of water of crystallization or volatiles shows up as weight loss.

2.9.4.2 Differential thermal analysis (DTA)

In this technique, sample and an inert reference material such as alpha alumina, in two different crucibles are heated simultaneously at a controlled uniform rate in a furnace. The temperature difference (ΔT) between sample and reference is recorded against time or temperature. A phase change produces either absorption or an evolution of heat or any reaction involving heat change in the sample will be represented as a peak in the plot of ΔT vs T. Exothermic reactions give an increase in temperature, and endothermic reaction leads to a decrease in temperature and the corresponding peak appear in opposite directions.

In the present study, thermal analysis of the glasses was performed using Setaram make TG-DTA instrument. In this analysis, the glass sample was heated under static air to 900^{o}C at the heating rate of 10 ^{o}C/min and then isothermal heating was continued at 900^{o}C for 2 hours.

The TG profile was used to evaluate the loss of Cs on weight loss basis. The glass transition temperature (Tg) was determined from the onset of the first endothermic peak of DTA profile.

2.9.4.3 Differential scanning calorimetry:

Differential scanning calorimetry (DSC-131, Setaram, France) was also used to determine the glass transition temperature of some of the glass sample of present study. In this experiment, about 30 mg of glass sample was taken in an aluminium crucible and heated up to 600 ^{o}C at a heating rate of 10 ^{o}C/min in flowing Ar atmosphere. Prior to DSC study, the instrument was calibrated for temperature and the maximum error in the measured temperature would be less than ±1 ^{o}C.

2.9.5 Vibrational spectroscopy

Vibrational spectroscopic techniques are useful to identify the nature of different linkages present in a material. These methods can also give information regarding the symmetry of different vibrational units. The vibrational technique used in the present study is briefly described below.

Vibrations of bonds and groups which involve a change in the dipole moment result in the absorption of infrared radiation which forms the basis of IR spectroscopy. Modern IR instruments are based on Fourier transformation method to improve the signal to noise ratio. Unlike conventional IR instrument, in FTIR instrument, all the frequencies are used simultaneously to excite all the vibrational modes of different types of bonds/linkages present in the sample. This reduces the experimental time considerably. In the present study, infrared experiments were carried out using a FTIR spectrometer (model: Jasco-660) having a range of 200-4000 cm^{-1} and with resolution of 4 cm^{-1}. IR radiation was generated from globar source (silicon carbide rod). The instrument used CsI single crystal, as the beam splitter and deuterated triglycine sulphate (DTGS) as a detector. Prior to IR measurements, the samples were ground thoroughly by mixing with dry KBr powder, made in the form of a thin pellet and introduced into the sample chamber of the instrument. The background of the sample was corrected from the spectra of KBr.

2.9.6 Nuclear magnetic resonance (NMR) spectroscopy

Nuclear magnetic resonance spectroscopy is a technique that exploits the nuclear magnetic property of atomic nuclei and gives information about chemical environment of around a particular nucleus in a molecule. For analysis of solid samples, well established magic angle spinning (MAS) technique is used. Three different interactions between nuclei themselves or their environment can be used to probe the structure of the solid. These interactions are (i) dipole coupling (ii) anisotropy of the chemical shift and (iii) quadrupole interaction (present only for nuclei with spin $I>1/2$). The dipole coupling is proportional to $1/r^3$ (r is the distance between two nuclei).

The chemical shift of any nucleus is defined as the difference between its resonance pre-exponential and the resonance pre-exponential of the same nuclei in a reference sample and can be expressed as $\delta = [(\omega-\omega_0)/\ \omega_0] * 10^6$, where ω, ω_0 represent resonance frequencies of nuclei in the sample and in the reference, respectively. The quadruple interaction is governed by the electric charges around the resonant nucleus.

Chemical shift arises because of the effective magnetic field felt by nuclei is brought about by the polarization effect of electron cloud around the nuclei created by the applied magnetic field. Since this is particularly sensitive to the configuration of valance electrons, which is governed by the nature of chemical bonding, this aspect has been labeled as chemical shielding interaction. The Hamiltonian for this interaction can be written as[81]

$$H_{cs} = \gamma I_z \sigma B_0 \qquad \ldots(4)$$

where σ is a second rank (3x3) tensor known as the chemical shielding tensor. This tensor can be diagonalised for a specific principal axis system and σ_{11}, σ_{22}, σ_{33} are the corresponding diagonal components. The isotropic component of the chemical shift tensor can be expressed by the relation

$$\sigma_{iso} = \frac{1}{3}\left(\sigma_{11} + \sigma_{22} + \sigma_{33}\right) \qquad \ldots(5)$$

The symmetry parameter is defined as as

$$\eta = \frac{\sigma_{22} - \sigma_{11}}{\sigma_{33} - \sigma_{iso}} \qquad \ldots(6)$$

Due to the presence of chemical shielding anisotropy, the nuclear precession pre-exponential depends on the orientation of principal axis system with respect to the external applied magnetic field and can be expressed by the relation:

$$\omega_p(\theta,\phi) = \gamma B_0 \left\{ \left(1-\sigma_{11}\right)^2 cos^2\phi \sin^2\theta + \left(1-\sigma_{22}\right)^2 \sin^2\phi \sin^2\theta + \left(1-\sigma_{33}\right)^2 \cos^2\theta \right\}^{1/2} \qquad \ldots(7)$$

where θ and Φ represent the orientation of principal axis system with applied magnetic field direction. For axial symmetry η = 0 and the precession pre-exponential can be expressed by the relation

$$\omega_p(\theta) = \gamma B_0 \left[1 - \sigma_{iso} - \Delta\sigma.\left(3\cos^2\theta - 1\right)/3\right] \qquad \ldots(8)$$

For values of $\theta = 54.7°$ the term $3\cos^2\theta\text{-}1$ becomes zero and the dependence of chemical shielding anisotropy term on Larmor frequency gets averaged out to very small value.

In solution NMR spectroscopy, dipolar interactions and anisotropic effects are averaged out by the molecular motion, but this is not so in the solid state and the NMR spectra of solids tend to be broadened because of (a) magnetic interactions of nuclei with the surrounding electron cloud (chemical shielding interaction), (b) magnetic dipole – dipole interactions among nuclei and (c) interactions between electric quadrupole moment and surrounding electric field gradient. Hence it is difficult to get any meaningful information from such patterns.

However, the use of magic angle spinning nuclear magnetic resonance (MAS NMR) technique, such interactions can be averaged out, thereby improving the information obtained from solid state NMR patterns. In the following section brief account of the MAS NMR technique has been given.

Magic Angle Spinning Nuclear Magnetic Resonance (MAS NMR): MAS NMR technique involves rotating the powder samples at high speeds, at an angle of 54.7° (magic angle) with respect to the applied magnetic field direction. When $\theta=54.7°$, the term $3\cos^2\theta$ becomes unity. Since Hamiltonian for different anisotropic interactions have $3\cos^2\theta - 1$ term, these anisotropic interactions get averaged out in time during fast spinning. This is schematically shown in Fig.2.9 and explained below.

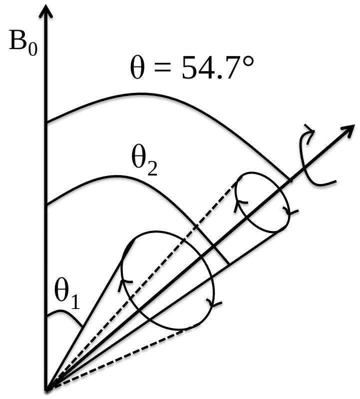

Figure 2-9: Principle of MAS NMR experiment

At sufficiently fast spinning speeds, the NMR interaction tensor orientations with initial angles of θ_1 and θ_2 relative to B_0 have orientational averages of 54.7°, resulting in the conversion of $3\cos^2\theta - 1$ term in expressions corresponding to various interactions to a very small value, thereby giving rise to sharp NMR peaks. Thus the MAS NMR technique simplifies the solid state NMR patterns and individual chemical environments can be correlated with corresponding chemical shift values obtained from these samples[82, 83].

Although, MAS is an efficient technique employed for getting high resolution NMR patterns from solid samples, in many cases, due to spinning, side bands, which are mirror images of the isotropic peak and spread from the isotropic peak by integer multiples of the spinning frequency, appear along with the central isotropic peak for nuclei having wide range of chemical shift values. For nuclei which is having a nuclear spin value ½, sideband pattern is a measure of the chemical shift anisotropy and valuable information regarding the symmetry of the electronic environment around a probe nuclei can be obtained from the intensity distribution of sidebands. However, in presence of large number of isotropic peaks, the number of sidebands also increases, and there can be overlap between the sidebands and isotropic peaks, which makes the MAS NMR pattern complicated.

In the present study, ^{11}B MAS NMR spectra of the sample were recorded using a 500 MHz Bruker make NMR spectrometer. Powdered samples were packed inside zirconia rotors and subjected to spinning speed of 10 kHz. A solution of H_3BO_3 (~0.1M) was used as the chemical shift reference. Typical 90° pulse duration of 4.5 µs with a relaxation delay of 3s was employed for all ^{11}B MAS NMR experiments. Relative concentration of BO_3 and BO_4 structural units were obtained from the ^{11}B MAS NMR patterns after subtracting the background arising from the BN stator of the solid state NMR probe.

2.9.7 UV-VIS spectroscopy

UV-VIS spectrophotometer, (Model V-650) was used to record UV-VIS spectra of the glass sample. The equipment records absorbance or transmission spectra in wavelength range of 190 nm to 900 nm using Deuterium and Tungsten lamps as source for UV and Visible regions respectively. A photomultiplier tube is used for detection of transmitted radiation. The specimen investigated in the present study was glass plate, prepared by melt quenching on steel plate. The thickness of the plate was measured before transmission measurement study. The spectra was recorded from 800 to 200 nm at a rate of 400 nm/minute scanning speed.

2.9.8 Scanning electron microscopy (SEM)

In a typical scanning electron microscope (Fig.2-10) consists of five major components, viz., electron gun, beam shaping column, scanning system, detector and turbo molecular high vacuum system. The generated electrons from tungsten filament in the gun are accelerated

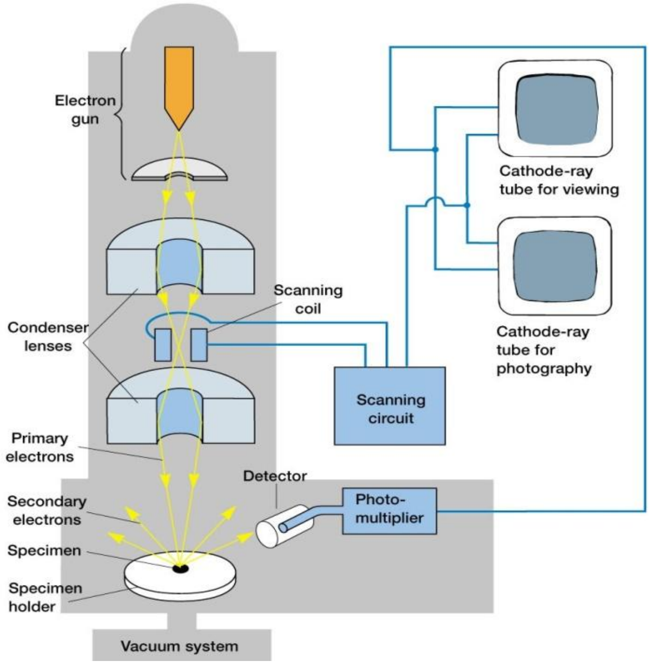

Figure 2-10: Schematic representation of SEM microscope

towards the specimen by high negative potential applied to the filament. The electron is thereby collimated by passing through magnetic field using electromagnetic lenses and finally the well-focused incident electron beam is used for scanning on the sample. The possible interactions of the energetic electron with sample are shown in Fig.2-11. The emitted secondary electrons are detected by scintillation detector and fed to a synchronously scanned cathode ray tube (CRT) as intensity modulating signals[84, 85] and the specimen image is displayed on the CRT screen. The X-rays produced due to emission of secondary electron are collected by semiconductor detector (Si/Li) to get the elemental composition of the sample.

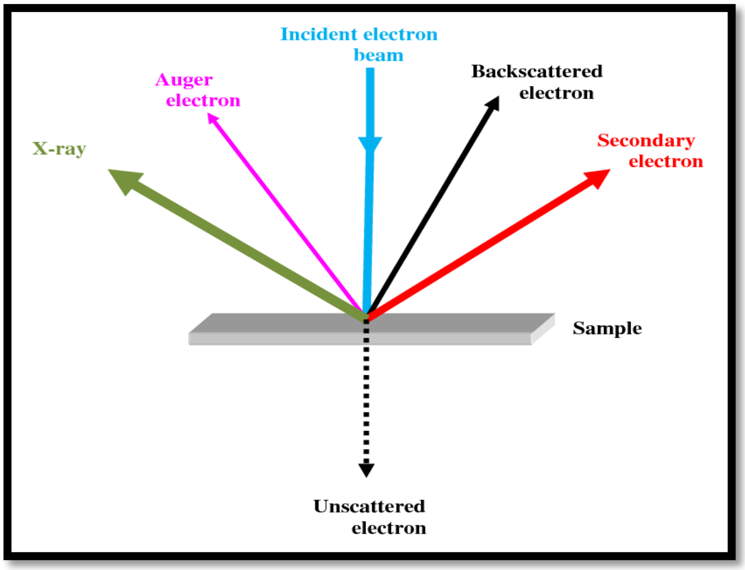

Figure 2-11: Interaction of electron beam with sample

In this study, SEM technique was used to study the change of glass surface morphology due to leaching and EDS (energy dispersive X-ray spectroscopy) was used for the compositional analysis. SEM micrographs were recorded using Seron Inc. make (Model AIS 2100) having standard tungsten filament. An accelerating voltage of 20 kV and magnification of 5000x was used for recording the micrographs. The glass samples (synthesized in bead form) cross section was cut by using diamond saw to observe and to study the interface. As glass sample is non conductive in nature, the surface was made conducting by applying thin gold coating (~50 nm) prior to loading the sample.

Chapter 3

Recovery of Cs

Recovery of Cs from alkaline and acidic waste streams

3.1 Introduction

Overviews of the processes used for the separation of ^{137}Cs from nuclear waste (acidic as well as alkaline) have been highlighted in chapter 1. In this chapter, results of present studies on separation of Cs from acidic as well as alkaline waste solution are discussed. As ^{137}Cs present in acidic waste of reprocessing plant origin is the main source of the radioelement, unambiguously it can be stated that large-scale utilization of ^{137}Cs as a radiation source in industrial irradiators requires an effective process for recovery of the fission product in mega curie quantities from acidic high level waste. First part of the work is therefore devoted to develop a comprehensive flow sheet based on the use of inorganic sorbent Ammonium Molybdophosphate (AMP) for industrial-scale separation and recovery of ^{137}Cs from acidic high level waste. The AMP powder coated on Poly methyl methacrylate (PMMA) beads has been used in this study. During the course of this study, major emphasis has been placed to generate data in the following areas: (a) Separation of ^{137}Cs from acidic waste using AMP-PMMA bead columns and (b) Recovery of ^{137}Cs from the loaded column by dissolution of the sorbent in alkali. (c) Ion exchange purification of ^{137}Cs in the resulting alkaline solution using RFPR resin.

In second part of the study, separation and recovery of ^{137}Cs from high active alkaline waste streams is addressed. The high active waste streams are generated during separation of Cs from nuclear waste, such as dissolution of Cs loaded AMP column as mentioned above and also separation of Cs from alkaline intermediate level waste solution. Studies on the separation of Cs from alkaline ILW using RFPR, hereinafter designated as “primary separation of Cs, have extensively been carried out in authors’ laboratory and the process has successfully been implemented in industrial scale treatment of the waste[48, 51-53]. In primary separation process, recovery of loaded Cs from resin bed is carried out by elution using dilute HNO_3. Although quantitative recovery of Cs from the loaded resin was accomplished, the recovered ^{137}Cs solution was found to contain a substantial amount of Na (Na/Cs ratio ≈ 65 wt/wt) and thus not suitable for preparation of radiation source. In order to make the ^{137}Cs product suitable for preparation of radiation source after immobilization in glass, further processing of the eluate solution is necessary to reduce Na^+ concentration to still lower levels. In the present study, feasibility of using RFPR for separation of Cs from high active concentrate has been examined. The main reasons behind the selection of the ion exchangers are (i) high selectivity for Cs (ii) high ion exchange capacity (iii) high radiation stability and (iii) ease of availability.

It can be noted that RFPR has been used for separation of ^{137}Cs solution from alkaline ILW, where Cs concentration are in the range of 4-50 mCi/L. In contrast, the Cs concentration in the eluate solution is about 1-5 Ci/L, whereas the dissolution of Cs loaded AMP column resulted in about 50-100 Ci/L. The Cs separation behavior of RFPR from such high Cs bearing solution has not been evaluated till date. In this work, efforts have therefore been made to devise a suitable scheme for processing of the eluate solution to obtain a concentrated ^{137}Cs product, with very low sodium content as required for immobilization in glass. This study includes evaluation of Cs separation behavior of the RF resin using solutions containing varying concentrations of Cs and Na ions, determination of ion exchange isotherm of the resin, prediction of column loading performance from the results of batch tests and evaluation of the column performance of RFPR from high Cs bearing solutions. In all the cases, elution was carried out by adopting sequential elution process. Results of this study established that RFPR is promising for the recovery of ^{137}Cs from high Cs bearing solution and the recovered ^{137}Cs solution obtained in this process contains very low concentration of accompanying Na ions and thus suitable for use as a gamma radiation source after immobilization. Highlights of the above results are presented in this Chapter.

3.2 Theoretical estimation on Cs purification requirement

It was discussed above that the eluate solution obtained from primary separation process contains a significant amount of sodium along with Cs ion and further processing of the solution is necessary for its utilization as radiation source in the form of glass immobilized matrix. In this section, an effort has therefore been made to put a pointer which will satisfy our minimum need. To arrive this, it is assumed that the final product glass will have a maximum of 15 wt% Cs_2O loading and the total alkali oxides in the glass will be 25 wt%. The matrix is defined by the following equation:

$$Na_2O + Cs_2O = 25 \text{ wt\%, where } Cs_2O \leq 15 \text{ wt\%}$$

It is obvious that the Cs oxide loading and hence specific activity of ^{137}Cs in the product glass will be governed by the above equation and the Na/Cs ratio in the eluate. Based on these considerations, the specific activity of ^{137}Cs in glass (Ci/g) has been calculated as a function of Na/Cs ratio in the concentrate. A 10% loss of Cs has been assumed in the calculations to account for its possible loss due to volatilization. The results of the calculation are shown graphically in Fig.3-1. The importance of having low Na/Cs in the concentrate in order to achieve a high loading of ^{137}Cs in the glass is clearly evident. Based on source strength requirement, it is found that the Na/Cs of less than 2 is necessary for preparation of source for blood irradiators.

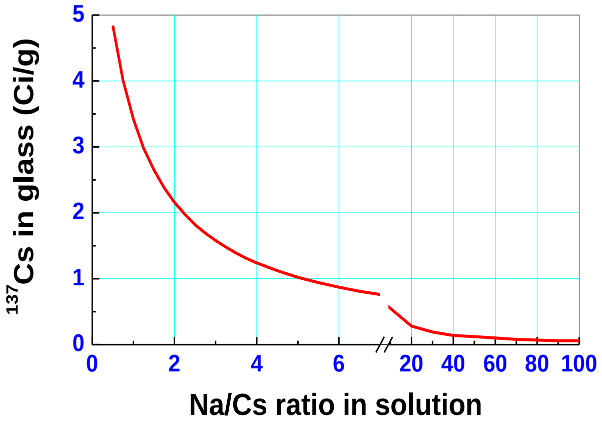

Figure 3-1: Estimated activity of ^{137}Cs in borosilicate glass as a function of Na/Cs ratio of the waste solution

3.3 Separation of Cs from acidic waste streams

3.3.1 Characterization of AMP sorbents

Details pertaining to the AMP sorbents and experimental procedure are discussed in section 2.2. The results of characterization tests are discussed below.

3.3.2 General characteristics

The characteristics of AMP sorbents used in this study are given in Table 3-1. Moisture contents of the AMP sorbents were determined by measuring the loss in weight after heating at 100±2 ^{0}C for 6 hours.

Table 3-1: Characteristics of AMP sorbents

Sl. No.	**Sorbents**	**Form**	**Moisture content (%wt/wt)**
1	AMP (*Lab*)	Powder	3.8
2	AMP (*V1*)	Powder	9.5
3	AMP (*V2*)- PMMA	Bead (0.30-0.60)	1.3
4	AMP (*Lab*)- PMMA	Bead (0.30-0.85)	2.5

3.3.3 Cesium sorption isotherm of AMP sorbents

The detailed characterizations of sorbents with respect to their Cs^+ sorption isotherms was done by conducting batch equilibration tests as mentioned earlier. Test solutions containing varying concentrations of Cs^+ ranging from 4.0 x10^{-3} M to 5.0 x10^{-2} M in 1.0 M HNO_3 and ^{134}Cs tracer were used in this study. After equilibration, the mixture was then filtered through Whatman 42 filter paper and the activity of ^{134}Cs in filtrate was measured. The results were used to calculate Cs-uptake, expressed as meq/g (dry).

Fig.3-2 shows the Cs^+ sorption isotherms for AMP sorbents. It is seen that equilibrium Cs-uptake capacity of AMP sorbents increases with the concentration of Cs^+ ions in solution and gradually approaches saturation capacity. From the molecular formula of AMP, $(NH_4)_3[PMo_{12}O_{40}].2H_2O$, the theoretical Cs uptake capacity can be calculated as 1.57 meq/g considering all the three NH_4^+ ions to be exchangeable. For AMP(*Lab*), saturation capacity is found to be 0.94 meq/g. This value corresponds to the exchange of nearly two of the three NH_4^+ ions present in AMP and is in good agreement with the experimental Cs^+-uptake capacity of AMP reported in literature[86]. The Cs^+-uptake capacity of AMP(*Lab*)-PMMA beads was found to be 0.38 meq/g. Considering that AMP loading on the beads is 37% (wt/wt), the capacity in terms of AMP can be calculated as 1.02 meq/g, indicating that Cs^+-uptake capacity of AMP powder is unaffected even after coating on PMMA beads. The lower capacities of AMP(*V1*) and AMP(*V2*)-PMMA beads are possibly due to inadequate control during preparation of AMP powder by the vendor and/or partial wash-out of AMP during conditioning of the coated beads.

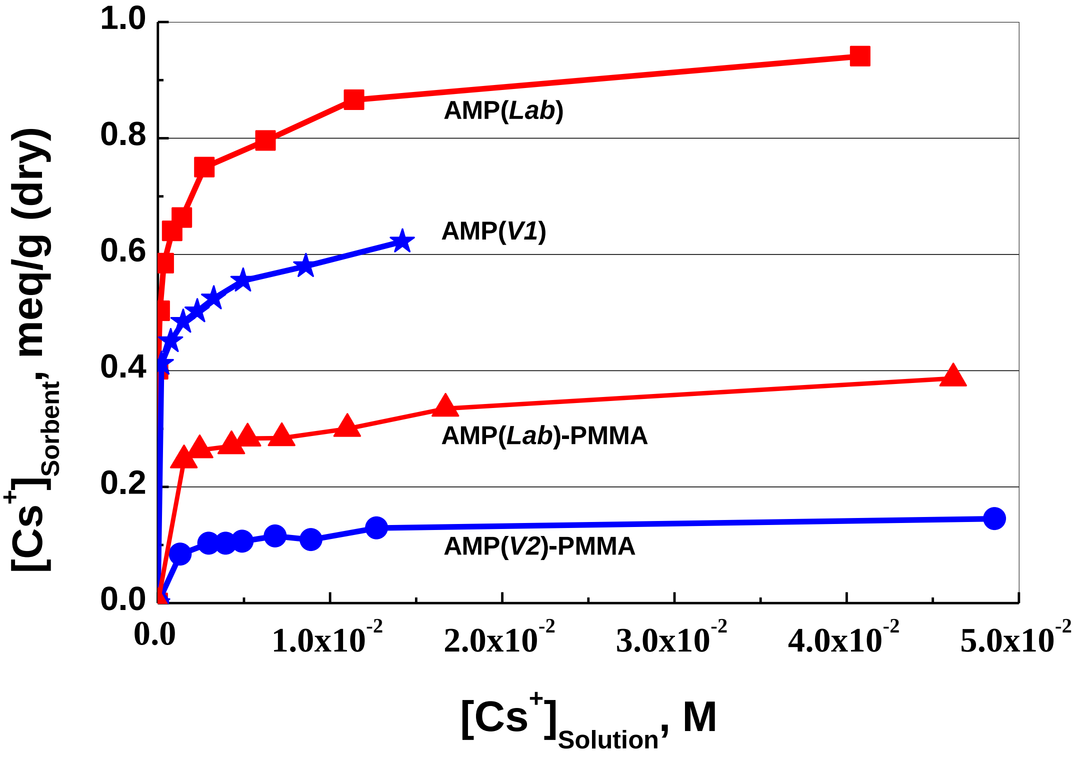

Figure 3-2: Equilibrium sorption isotherms for Cs on AMP sorbents

(*Test solution: $CsNO_3$ in 1.0 M HNO_3 with ^{134}Cs radiotracer; contact time: 24 hours*)

3.3.4 Effect of HNO_3 concentration on Cs^+ uptake by AMP sorbent

The uptake of Cs^+ by AMP(*Lab*)-PMMA beads was studied as a function of nitric acid concentration in solution over the range of 0.1-5.0 M. The results are shown in Fig.3-3. It is seen that the equilibrium uptake of Cs^+ by AMP-PMMA is highest at 0.1 M HNO_3, which is the lowest acidity used in this study. With increase in acidity, the uptake of Cs^+ is found to decrease slightly, possibly due to increasing competition from H^+ ions. However, in spite of the marginal reduction, the uptake remains adequately high in the region of 1-4 M HNO_3 which is the region of interest for separation of Cs^+ from high level waste.

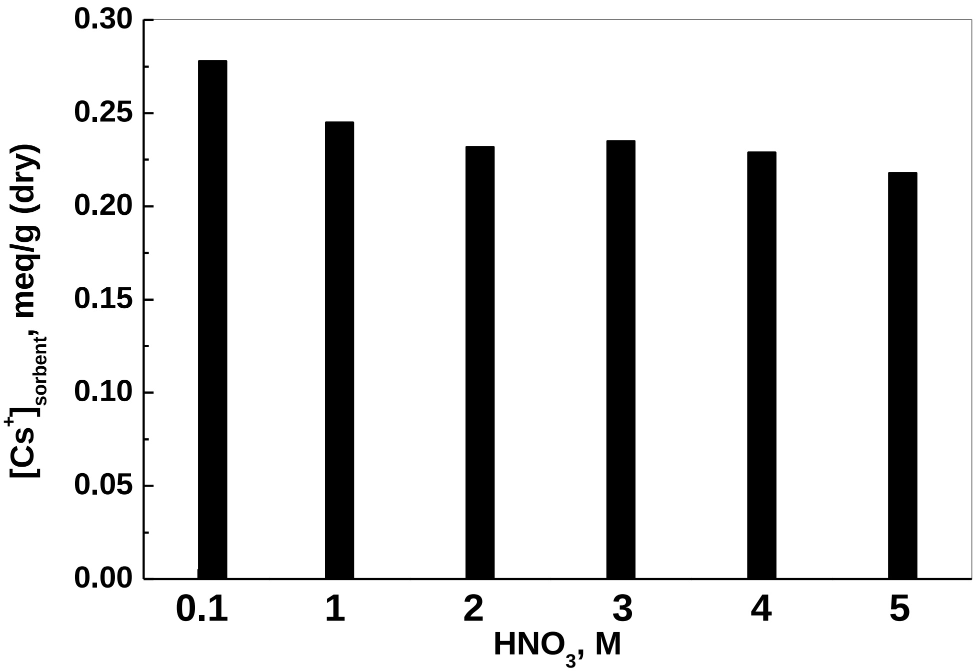

Figure 3-3: Effect of HNO_3 on Cs uptake by AMP(Lab)-PMMA beads

(*Test solution: 4.6 x10^{-3} M of $CsNO_3$ in HNO_3 with ^{134}Cs radiotracer; contact time: 24 hours*)

3.3.5 Column tests on the separation of Cs from acidic solution using AMP-PMMA

Two column runs were conducted to establish the column performance of AMP-PMMA beads for separation of Cs^+ from acidic solution. The results of column runs are shown as breakthrough curves in Fig.3-4. The breakthrough of Cs^+ occurred after 20 bed volumes for AMP(*V2*)-PMMA and 66 bed volumes for AMP(*Lab*) -PMMA, the difference being in line with the lower batch capacity of AMP(*V2*)-PMMA as noted above. The breakthrough capacities for AMP(*V2*)-PMMA and AMP(*Lab*)-PMMA are 0.043 and 0.142 meq/mL sorbent, respectively. For both sorbents, the breakthrough capacities correspond to about 65% of their

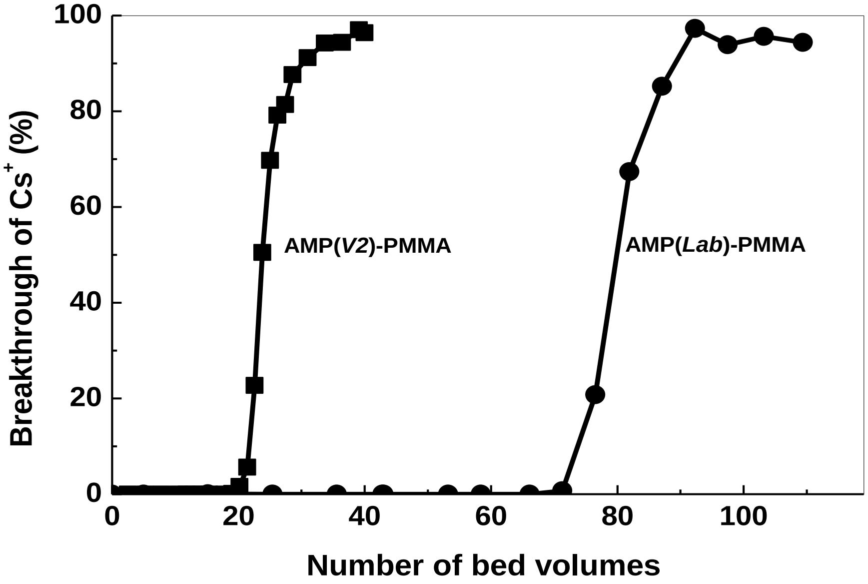

Figure 3-4 : Column separation of Cs from acidic solution using AMP-PMMA beads

(Feed solution: 2.15 x10^{-3} M $CsNO_3$ in 1.0 M HNO_3 and ^{134}Cs radiotracer; bed volume: 10 mL; flow rate: 5 bed volume/hour).

batch capacities for the concentration used in column runs. From the measured Cs concentration in the feed and accumulated effluent, the maximum possible loading of Cs^+ on the bed (saturation capacity) under the test conditions was calculated to be 0.0525 meq/mL (244 Ci ^{137}Cs/L bed) for AMP(*V2*)-PMMA and 0.1723 meq/mL (802 Ci ^{137}Cs/L bed) for AMP(*Lab*)-PMMA (Table 3-2). At saturation, about 80% of the batch capacity was realized for both the sorbents. It is possible that loading will be somewhat lower when ^{137}Cs of the same concentration is separated from high level waste, which has a more complex chemical composition as compared to the simple test solution used in the present case.

3.3.6 Recovery of Cs^+ from Cs loaded AMP-PMMA column

AMP dissolves in alkali solution. This property of AMP is utilized for recovery of Cs^+ from Cs-loaded AMP column. Initially, the dissolution behavior of AMP(*Lab*) powder was tested using 1.0 M NaOH solution. Complete dissolution of 1.0 g AMP powder was achieved in 12.0 mL of 1.0 M NaOH, resulting in a clear colorless solution (pH 7.2). The amount of NaOH consumed for dissolution is in good agreement with the value calculated from the following reaction[87].

$(NH_4)_3[PMo_{12}O_{40}].2H_2O + 23\ NaOH = 11Na_2MoO_4 + (NH_4)_2MoO_4 + NaNH_4HPO_4 + 11H_2O$

The dissolution behavior of Cs-loaded AMP-PMMA column in NaOH solution was investigated in order to ascertain the quantitative release of sorbed cesium from the two columns. Dissolution was carried out by passing 1.0 M NaOH followed by 0.1 M NaOH solution. At first, 1.0 M NaOH solution was passed till a clear colorless solution of pH 13 was obtained and then 0.1 M NaOH was passed to remove any remaining Cs activity from the bed with minimum increase of Na^+ concentration in the final solution. The volumes of NaOH solutions used are included in Table 3-2 along with the expected activities of ^{137}Cs in the final solutions that would be obtained after complete dissolution of AMP loaded to the levels shown therein. The volume of the sorbent bed did not change after passing NaOH solution. Complete dissolution of AMP was evident from the conversion of the yellow sorbent back to the original white colored PMMA beads. From the measured activity of ^{134}Cs in the final solution the concentration of Cs^+ was calculated and used to estimate the corresponding activity of ^{137}Cs. As can be seen from Table 3-2, quantitative recovery of cesium was achieved for AMP(*V2*)-PMMA. For AMP(*Lab*)-PMMA, the recovery was 95.5% of the amount loaded. It is felt that quantitative recovery can be ensured by increasing the volume of 1.0 M NaOH solution. From these results it can be concluded that AMP-PMMA can be used to effectively separate and recover ^{137}Cs from acidic high level waste.

Table 3-2: Recovery of Cs^+ from loaded AMP-PMMA column

Sorbents	**$^{137}Cs^{\#}$ loading on 10 mL bed**	**Volume of NaOH solution passed for dissolution of AMP (mL)**			**$^{137}Cs^{\#}$ in final solution (Ci/L)**	
	Ci	1.0 M	0.1 M	Total	Expected	Measured
AMP(*V2*)-PMMA	2.44	29	16	45	54.2	54.4
AMP(*Lab*)-PMMA	8.02	54	21	75	106.9	102.1

Specific activity of ^{137}Cs in waste of 35 Ci/g is used to arrive at the ^{137}Cs activities from measured values for loading/recovery of Cs^+ ions.

The estimated chemical composition of the recovered Cs solution resulting from the dissolution of Cs-loaded AMP bed is shown in Table 3-3. It can be seen that the concentration of Cs in this solution is quite high (~50-100 Ci/L), but the Na/Cs > 6 and the solution contains higher amounts of Mo, and hence it cannot be used for the preparation of radiation source. Purification of the solution is therefore addressed during the course of the work and the results are discussed in detail below.

Table 3-3: Chemical composition of the recovered Cs solution resulting from the dissolution of Cs-loaded AMP bed

Component	**Concentration**
Cs^+	2-3 g/L
Na^+	17 g/L
NH_4^+	0.06 M
MoO_4^{2-}	0.28 M
PO_4^{3-}	0.02 M

3.4 Separation of Cs from alkaline waste streams

The main objective of the work to evolve conditions for separation of Cs from high active waste streams resulting from primary separation process. Two waste streams, viz., (i) eluate solution resulting from separation of ^{137}Cs from alkaline waste and (ii) dissolved AMP solution generated from separation of ^{137}Cs from acidic waste have been considered as sources of high Cs bearing waste. The Cs separation study was carried out using resorcinol formaldehyde polycondensate resin (RFPR). The resin is an alkali catalyzed polycondensation product of resorcinol and formaldehyde, in which the phenolic OH group of resorcinol ionizes under alkaline conditions and functions as cation exchanger. Further, the weakly acidic nature of the functional groups facilitates the recovery of Cs^+ ions from loaded resin by elution in small volumes of dilute acid[52]. The ion exchange cycle for the separation of ^{137}Cs by RFPR can be represented as follows (Fig.3-5):

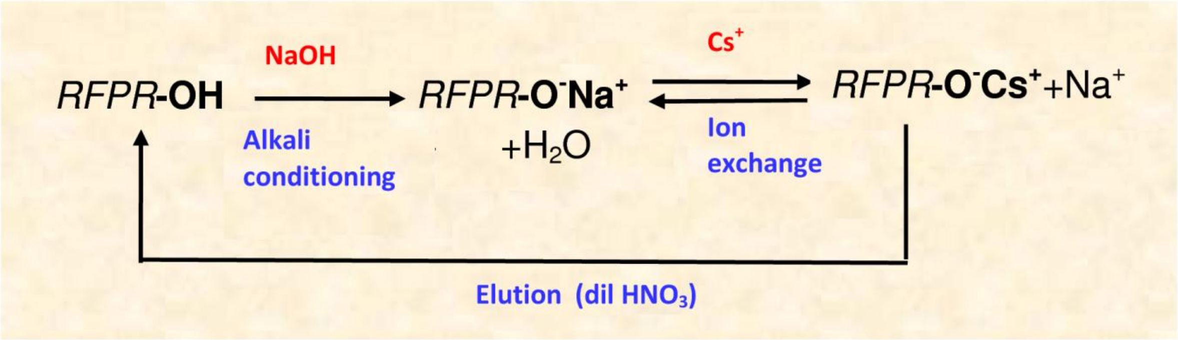

Figure 3-5: Ion exchange cycle for RFPR

As the resin can only process alkaline solution, it is considered that the acidic eluate will be neutralized prior to Cs separation. A typical composition of the eluate before and after neutralization is shown in Table 3-4. For Cs separation study, the neutralized eluate was

Table 3-4: Typical composition of the eluate resulting from primary separation of Cs from ILW before and after neutralization

Component	**Ion exchange column eluate**	
	As generated	After neutralization
Nature	Acidic (0.4 M)	Alkaline (0.1 M)
^{137}Cs (Ci/L)	0.035	0.035
$NaNO_3$ (M)	0.1	0.5
Na (g/L)	2.3	12
Na/Cs	64	300
Elution using 20 bed volumes of 0.5 M HNO_3 and neutralization using 4 M NaOH		

prepared in laboratory by dissolving requisite quantity of AR grade salt and used. The dissolved AMP solution (Table 3-3), being alkaline, was processed as such. As noted above, the Cs separation behavior of RFPR under high Cs environment is not known, some typical characteristics of the resin was therefore determined as described below.

3.4.1 General characteristics of the RFPR

Characteristics of the resin used in present study are shown in Table 3-5. The total ion exchange capacity of the resin is expressed in terms of the Na exchange capacity, which was found to be about 6 meq/g. Uptake of Cs by the resin was determined from a typical simulated ILW solution containing 3.8 M Na (2.5 M $NaNO_3$ + 1.0 M NaOH + 0.15 M Na_2CO_3) and 1 mg/L Cs and expressed in terms of batch distribution coefficient of Cs(K_d). The K_d for Cs was found to be around 10000 ml/g. This high Kd value for Cs even in presence of significantly higher concentration of Na ions suggests that RFPR is highly selective for Cs. Strontium being one of the most common radionuclides present along with Cs in nuclear effluents[88], Sr uptake by the resin under similar conditions was measured by adding $^{85+89}Sr$ tracer in the waste and found to be marginal (K_d= 90 ml/g), as can be seen from Fig.3-6.

Table 3-5: Characteristics of the RFPR

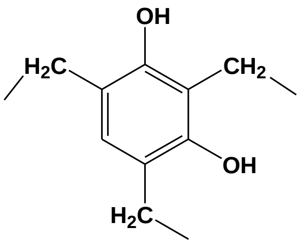	Particle size	: 0.3-0.85 mm
	IX Capacity ($H^+ \rightarrow Na^+$)	: 6 meq/g
	Moisture content	: 20 % wt/wt
	K_d(Cs)*	: 10000 mL/g

Composition of test solution: 2.5 M $NaNO_3$ + 1.0 M NaOH + 0.15 M Na_2CO_3+ 1 mg/L Cs + ^{134}Cs tracer

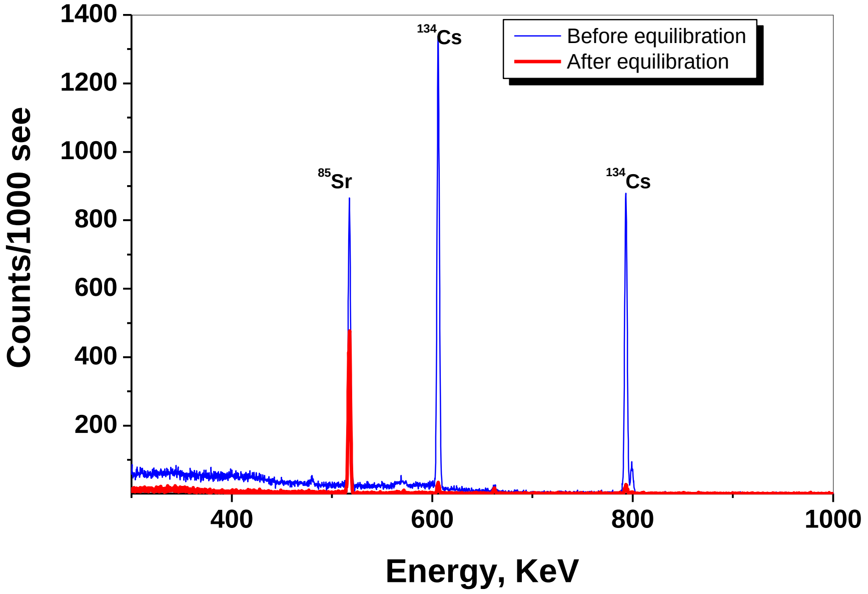

Figure 3-6: Uptake of Cs and Sr by RFPR from simulated alkaline ILW of composition 2.5 M $NaNO_3$ + 1.0 M NaOH + 0.15 M Na_2CO_3 and 1 mg/L Cs and spiked with ^{134}Cs and $^{85+89}$Sr tracer

3.4.2 Effect of NH_4^+ ion on Cs^+ uptake by RFPR

Owing to the close similarity in ionic radii of Cs^+ (1.69 Ǻ) and NH_4^+ (1.49 Ǻ)[89], the possible effect of competing NH_4^+ ions present in dissolved AMP solution on the uptake of Cs^+ by RFPR was investigated. Two test solutions, each containing $CsNO_3$ (1.0 x10^{-2} M) and ^{134}Cs radiotracer in dissolved AMP solution, were used for equilibration with RFPR (0.1 g resin + 10 mL solution). One of the solutions was heated to boiling to drive out NH_3 from the solution. The uptake of Cs^+ was determined by measuring the activities of the solutions before and after equilibration. The same Cs-uptake value (0.72 meq/g) was obtained in both the cases, indicating thereby that the uptake of Cs^+ by RFPR from dissolved AMP solution is not affected by the presence of NH_4^+ ions.

3.4.3 Cesium sorption isotherm for RFPR

Depending upon the concentration of Cs^+ in waste and extent of the loading run, ^{137}Cs loading on AMP columns and on RFPR in the primary separation step would vary and this would result in varying activities of ^{137}Cs in the recovered solution. Hence, the uptake of Cs^+ was measured by conducting batch equilibrium tests. The compositions of the test solution used were (i) 0.6 M Na (0.1 M NaOH + 0.5 M $NaNO_3$) (ii) 1.0 M Na (0.1 M NaOH + 0.9 M $NaNO_3$) (iii) 2.0 M Na (0.1 M NaOH + 1.9 M $NaNO_3$) (iv) 3.0 M Na (0.1 M NaOH + 2.9 M $NaNO_3$) and (v) dissolved AMP solution. The 1st solution used was obtained upon neutralization of the eluate using NaOH (Table 3-4). The other solutions used are considered to be obtained by evaporation of the eluate followed by neutralization. The chemical composition of dissolved AMP solution used in this study is similar to that of the solution generated after dissolution of AMP(*Lab*) (Table 3-3). In each of these compositions, different test solutions of varying Cs concentrations ranging from 1.00x 10^{-4} to 0.10 M were prepared using inactive $CsNO_3$ and spiked with ^{134}Cs tracer. The initial concentration of Cs in solution and the ^{134}Cs activities in solutions before and after equilibration was used to calculate the Cs uptake (meq/g dry resin) by the resin as follows:

$$[Cs]_R = \{ [Cs]_{initial} - [Cs]_{eq.\ sol} \} \times \frac{V_{sol}}{W_r\ (1 - W_m / 100)} \qquad \ldots(9)$$

where,

$$[Cs]_{eq.\ sol} = [Cs]_{initial} \times \frac{^{134}Cs\ \text{after equilibration}}{^{134}Cs\ \text{before equilibration}} \quad \text{(M)}$$

W_r is weight of resin (g), W_m is the moisture content of resin (weight %), V_{sol} is the volume of solution in mL used for equilibration (V_{sol} =10 mL).

The results of batch uptake for Cs from neutralized eluate and from dissolved AMP solution are shown in Fig.3-7. It can be seen that Cs uptake of RFPR increases with the increase of Cs concentration in solution. It is also evident that the Cs uptake decreased significantly with the increase of Na concentration.

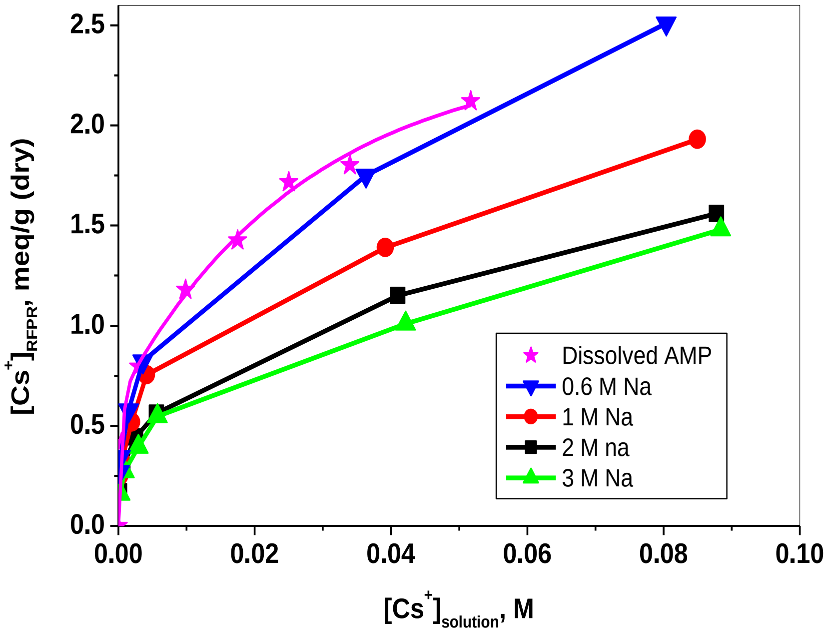

Figure 3-7: Batch uptake of Cs by RFPR from dissolved AMP and neutralized eluate solution

3.4.4 Correlation of batch data with Freundlich isotherm

In order to correlate the batch data with different well known absorption isotherms, the batch results with neutralized eluate is therefore plotted in log-log plot (Fig. 3-8). The linear relationship seen in the figure suggests that Freundlich isotherm equation hold good for Cs sorption under the above mentioned test conditions. The Freundlich isotherm equation can be written as follows:

$$\log q = \log K + \frac{1}{n}\log\,[Cs]_{eq} \quad \ldots(10)$$

where q is the amount of Cs sorbed by the unit weight of the dry resin in mmol/g, $[Cs]_{eq}$ is the equilibrium concentration of Cs in mol/L, K and n are constants. From the intercept and slope of each of the straight lines, K and $1/n$ were calculated and tabulated in Table 3-6. It can be seen that the values of $1/n$ are almost same for all the isotherms. This suggests that the extent of Cs exchange reached a saturation limit, even though the surface coverage as per Freundlich equation is unlimited. Further, '*n*' value greater than unity reflects the Cs sorption by RFPR under the test conditions is multilayered in nature. The values of K can be related to the Cs exchange capacity of the resin. The decrease of K value with the increase of Na ion concentration in solution is due to the increasing competition between Na and Cs ions.

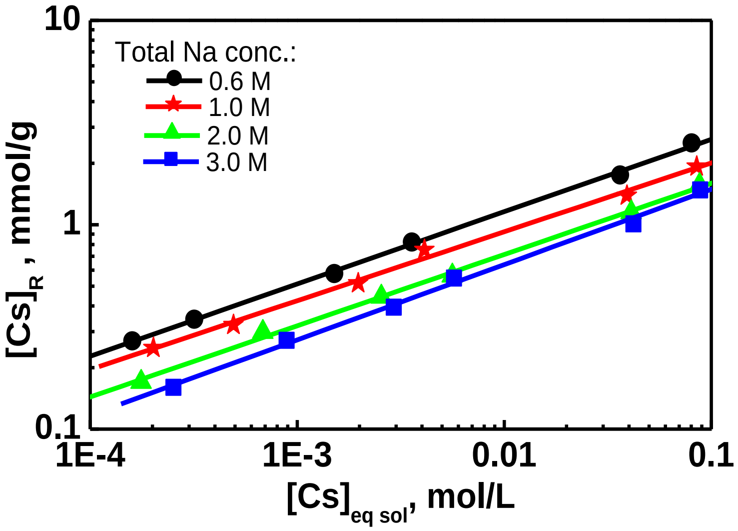

Figure 3-8: Cs exchange isotherm for RFPR from solutions containing Cs concentration in the range of 1×10^{-4} to 0.1 M and having different Na concentrations.

Table 3-6: Freundlich constants for Cs sorption by RFPR

Total Na * (M)	**K**	**1/n**
0.5	5.90	0.3535
1.0	4.37	0.3372
2.0	3.56	0.3485
3.0	3.48	0.3683
**The total Na in solution is due to the presence of 0.1 M NaOH and remaining* $NaNO_3$*, the solutions also contains* ^{134}*Cs tracer and varying Cs in the range of* $1x10^{-4}$ *to 0.1 M.*		

3.4.5 Correlation of batch data with Dubinin-Radushkevich (D-R) isotherm

It is worth mentioning at this point that the Cs exchange reaction by RFPR is a thermodynamically favorable process[51]. The energy associated with the Cs exchange reaction is an important parameter controlling the extent of sorption. In order to evaluate such data, the results of batch tests are plotted in Fig.3-9 in the form of Dubinin-Radushkevich (D-R) isotherm[90].

The linear form of D-R isotherm is represented by the following equation:

$$\ln q = \ln q_m - \beta\varepsilon^2 \qquad \ldots(11)$$

where q_m is the maximum sorption capacity (mol/g dry resin in H^+-form), β is the constant related to sorption energy (mol^2/kJ^2) and ε is Polani potential which is represented as follows[91]:

$$\varepsilon = RT \ \ln\ (1 + \frac{1}{[Cs]_{eq}}) \qquad \ldots(12)$$

where R is the gas constant in $kJ.mol^{-1}$, T is the absolute temperature in Kelvin and $[Cs]_{eq}$ is the equilibrium concentration of Cs in mol/L. All the batch data plotted in Fig. 3-9 showed a linear relationship between ln (q) and ε^2, indicating D-R isotherm equation also holds good for Cs sorption by RFPR. From the intercept and slope of these straight line plots, D-R isotherm parameters like q_m and β are calculated and the values are shown in Table 3-7.

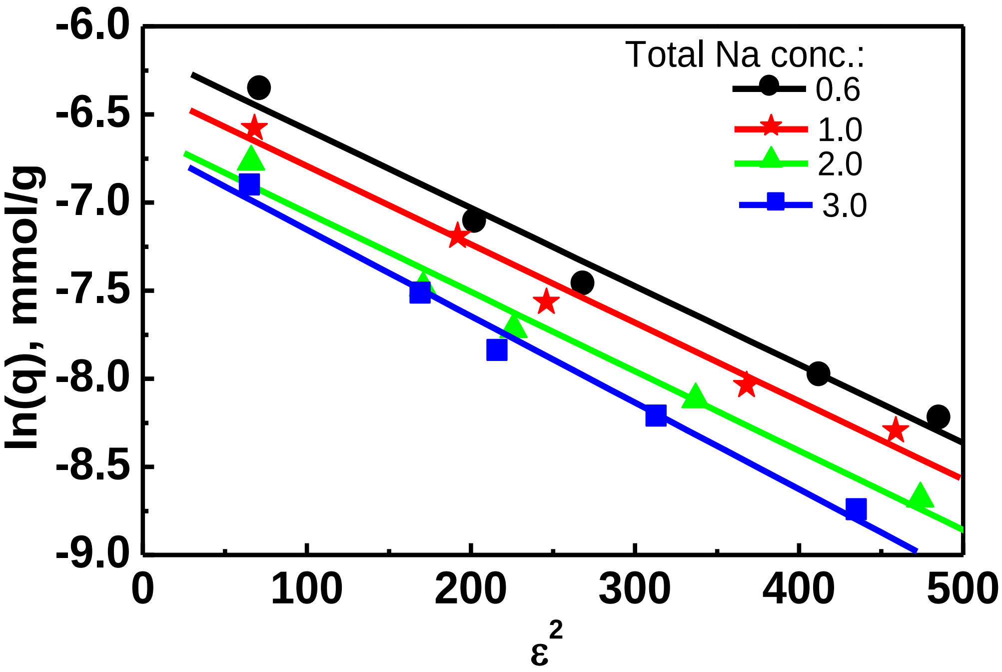

Figure 3-9: D-R isotherm plot for the Cs uptake by RFPR from solutions containing Cs concentration in the range of 1×10^{-4} to 0.1 M and having different Na concentrations.

Table 3-7: D-R isotherm parameters for Cs sorption by RFPR

Total Na* (M)	**q_m, (mmol/g)**	**β (mol^2/kJ^2)**	**E (kJ/mol)**
0.5	2.15	-0.0044	10.66
1.0	1.76	-0.0044	10.66
2.0	1.36	-0.0045	10.54
3.0	1.28	-0.0049	10.10

* The total Na in solution is due to the presence of *0.1 M NaOH and remaining $NaNO_3$, the solutions also contains ^{134}Cs tracer and varying Cs in the range of 1x10^{-4} to 0.1 M.*

As noted above, β is related to sorption energy and the mean free energy of sorption for Cs exchange (E) is calculated by using the following equation:

$$E = \frac{1}{\sqrt{-2\beta}} \qquad \ldots(13)$$

It can be seen that the β values and hence, mean free energy of sorption for Cs exchange (E), are constant for all the four isotherms (Table 3-7). The constant values of E can be explained by considering the fact that all the ion exchange sites of RFPR are initially occupied by Na ions as counter ions and then Na is replaced by Cs. The amount of energy released during replacement of one mol of Na by Cs is likely to be independent of the total numbers of Na or Cs ions present in solution. The E value therefore can be considered as a characteristic parameter of the particular reaction, (equation 14). The E value reported by Hassan et.al for the same ion exchange reaction using a similar resin, is in good agreement with the results of present study[55]. The q_m obtained from D-R isotherm represents the maximum Cs sorption capability of the resin and this is constant under the particular test conditions like constant Na ion concentration and pH.

3.4.6 Prediction of column loading from batch results

From application point of view, these batch results are directly useful for estimation of maximum loading of Cs on RFPR column under saturation conditions. Saturated column loading from test solution containing 0.6 M total sodium and varying Cs concentration in the range of 1.00×10^{-4} to 4.30×10^{-3} M was calculated using both the isotherm equations and the results are presented in terms of Cs loading per liter resin bed (Fig.3-10). The bed density of RFPR column (0.32 g/mL) was used for the conversion of Cs loading in terms of g/L. In order to validate the batch results, a series of column experiments were carried out and the results are discussed below.

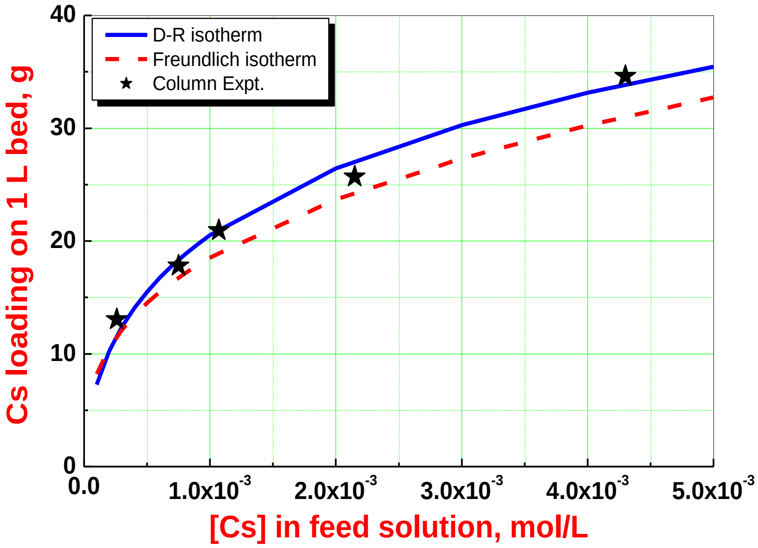

Figure 3-10: Maximum possible loading of Cs on 1 L RFPR column as a function of Cs concentration in solution containing 0.5 M $NaNO_3$+ 0.1 M NaOH; The loading predicted from D-R isotherm and Freundlich isotherm equation is indicated by blue (solid) and red (doted) line, respectively. The star is showing the values calculated from column run.

3.4.7 Mechanism of Cs sorption

Based on our earlier study, it is inferred that the phenolic OH group of RFPR is ionized to phenolate ion under alkaline conditions and then it participates in ion exchange reaction. The uptake of Cs ion by the resin in the presence of molar level of Na^+, indicates that Cs is preferentially replacing Na^+ in the resin phase as shown below:

$$R\text{-}\overline{O^-Na}^+ + Cs^+ = \overline{RO^-Cs}^+ + Na^+ \qquad \ldots(14)$$

The bar sign representing the resin phase, R is the resorcinol formaldehyde polymer, $-O^-$ is pheonolate ion. As per Eq.14 above, it is uni-uni molar ion exchange reaction. For low Cs concentration ($1.5\text{x}10^{-3}$ M or less), the plot of log K_d against log $[Na^+]$ gives a straight line with a slope of -1.20 (Fig.3-11), indicating that ideal Na^+-Cs^+ ion exchange relation holds good. For high Cs concentration, no such indication is obtained as saturation uptake of Cs is reached. In order to probe the ion exchange mechanism under high Cs bearing solution, efforts were made to measure the increase of Na concentration in solution with increase of Cs uptake. Results

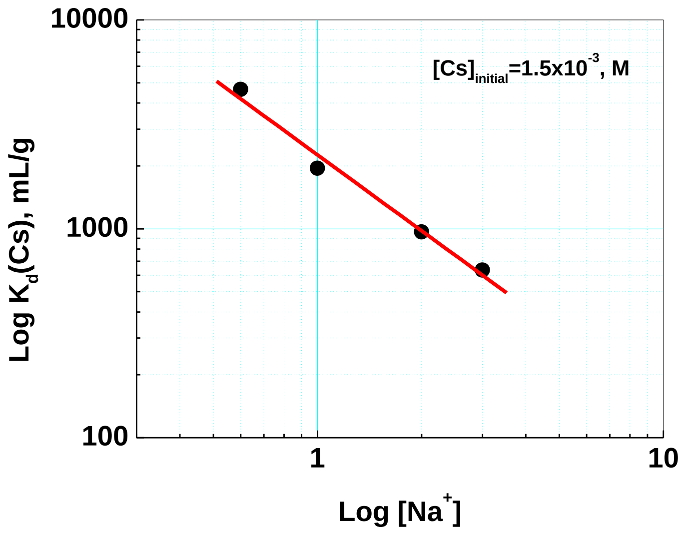

Figure 3-11: Effect of Na concentration in solution on Cs uptake by the RFPR

of this study are shown in Fig.3-12. The H^+ form resin (0.5 g) was equilibrated with 50 mL of 0.6 M (0.5 M $NaNO_3$+0.1 M NaOH+^{22}Na tracer) for 24 hours to convert it in Na -form. From the measurement of ^{22}Na activity before and after equilibration and initial Na concentration in solution (measured by ion chromatograph), the distribution of Na in resin phase and in solution was found to be 3 meq and 27 meq, respectively (Fig.3-12a and 3-12b). Since replacement of

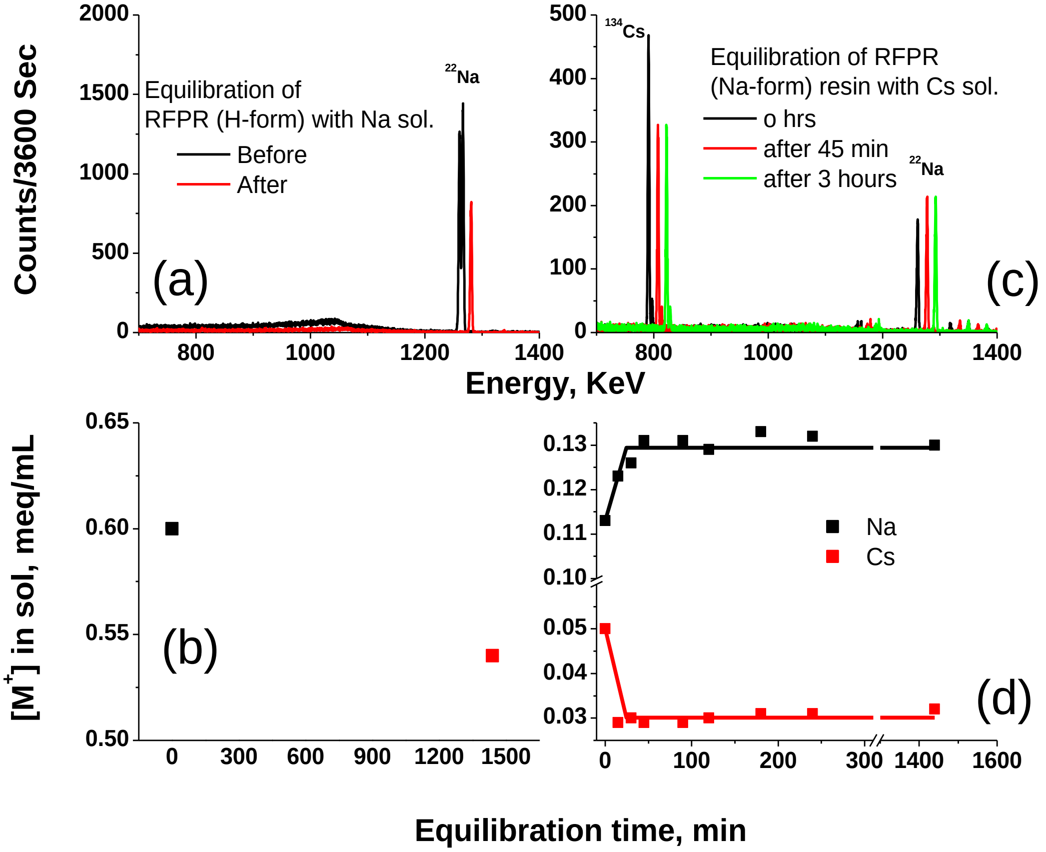

Figure 3-12: Uptake of Na and Cs by RFPR: (a) and (b) are gamma spectra and concentrations (meq/ml) of Na solution before and after equilibration of RFPR (H-form) with 0.6 M Na solution spiked with ^{22}Na tracer; (c) and (d) are the gamma spectra and Na and Cs concentration of in solution with the progress of equilibration of the Na-form resin with Cs solution spiked with 134Cs radiotracer. Gamma spectrum for “0” minute are in actual energy scale, other are shifted to 15 Kev for ease of representation.

Na by Cs in the resin phase will lead to only a marginal change of Na in solution, 40 mL of solution was withdrawn to minimize Na in external environment. Volume was then made up by addition of Cs solution (2.5 meq) and ^{134}Cs tracer. The mixture was kept under stirring conditions, samples (1 ml) were collected periodically and analyzed for Na and Cs by using HPGe detector coupled with 8K MCA. From the gamma spectrum shown in Fig.3-12c, it can be seen that Na concentration in solution is increased and Cs activity is decreased after equilibration of the Na-form resin with Cs solution. Fig.3-12d shows the concentration of Na and Cs ions in solution as a function of equilibration time.

It is seen that equilibrium Cs uptake (about 2.0 meq/g resin) is attained within 45 minutes and it occurred by the replacement of almost equimolar concentration of Na ions. Based on this results, it can conclusively be stated that uptake of Cs by RFPR occurred by replacement of Na^+ from resin phase, even when high concentration of Cs is present in solution.

3.4.8 Column tests for separation of Cs

In order to evaluate the Cs separation behavior of RFPR from high Cs bearing neutralized eluate and dissolved AMP solution, five column runs with neutralized eluate (composition: 0.1 M NaOH + 0.5 M $NaNO_3$ + ^{134}Cs tracer + varying Cs) and three column run with dissolved AMP solution were carried out.

Fig.3-13 represents results of column experiments for neutralized eluate solution. As mentioned earlier, chemical composition of the neutralized eluate solution was same for all the column runs and the Cs concentration was varied from 2.57×10^{-4} to 4.30×10^{-3} M. In the case of 2.57×10^{-4} M Cs bearing feed, which is the lowest Cs concentration used in the present study, the breakthrough of Cs occurred after 280 bed volumes. Thereafter, increasing amount of Cs was found in the effluent and the bed reached saturation after passing 475 bed volumes of waste. Based on the measured Cs activity in accumulated solutions and feed concentration, the maximum achievable loading on 1 L bed of RFPR was calculated and found to be about 13 g. The use of higher Cs bearing feed solution in subsequent column runs showed that breakthrough of Cs occurred earlier and the breakthrough curves become steeper. This is attributed to the fact that equilibrium Cs exchange capacity of the resin reached quickly in contact with the higher Cs concentration in the feed solution. This also explains the steeper breakthrough profiles also. The saturation loading of Cs was calculated for each of the column runs and the results are plotted as a function of Cs concentration in solution in Fig.3-10 along with their corresponding values estimated from batch results. It can be seen that estimated Cs loading from D-R isotherm (equation 11) is in good agreement with the results obtained from column studies. Results of the study are useful in predicting Cs loading on RFPR column from waste solutions of known composition.

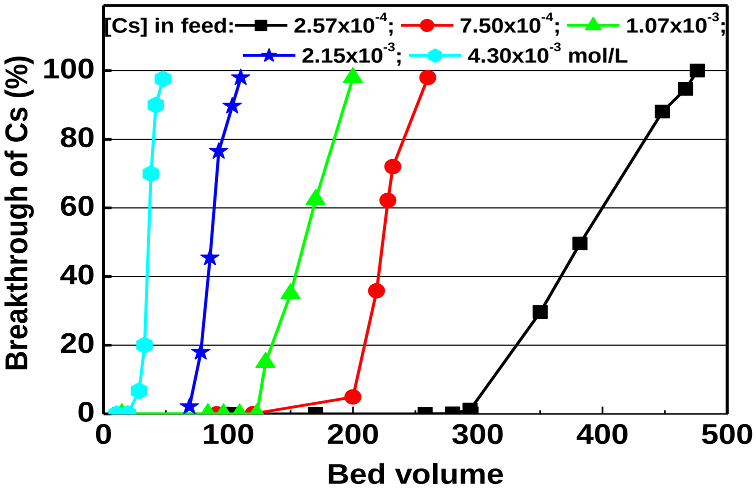

Figure 3-13: Cs separation behavior of RFPR column (Bed volume: 5 mL) from solutions containing 0.5 M $NaNO_3$+ 0.1 M NaOH and varying concentration of Cs at the flow rate of 4 bed volume per hour.

Three column runs were carried out using dissolved AMP solution as feed. In initial two column runs, Cs concentration in feed was kept at 1.07x10^{-2} M while 2.15x10^{-2} M was used for the third column. The results of column runs are shown in Fig.3-14. Results of the two column runs with 1.07x10^{-2} M Cs as feed confirmed that breakthrough behavior is reproducible. At breakthrough point, the loading of Cs^{+} in terms of ^{137}Cs on 1 L RFPR bed was estimated to be 1200 Ci for Run 1 (red line) and 1300 Ci for Run 2 (black line). The accumulated effluents were found to contain an equivalent of about 15 mCi/L ^{137}Cs activity. In the case of the third column, early breakthrough of Cs occurred, because of higher Cs concentration in feed. The estimated loading of Cs at breakthrough point is equivalent to about 1500 Ci per L of bed. Based on these results, it can conclusively be stated that ^{137}Cs can be effectively separated from the alkaline dissolved AMP solution using RFPR column. After the breakthrough point, the concentration of Cs^{+} ions in the effluent is seen to increase rather sharply. The continuation of

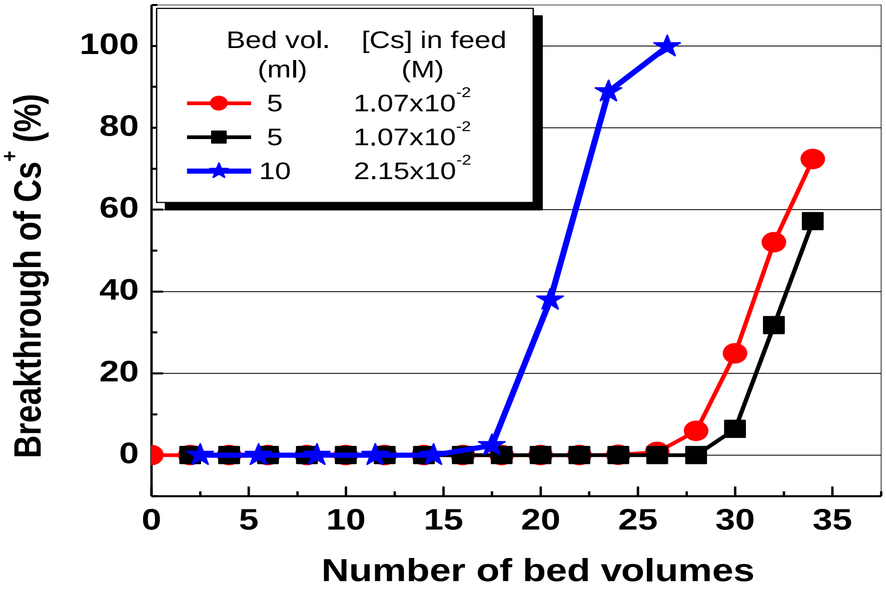

Figure 3-14: Loading of Cs^{+} on RFPR column from dissolved AMP solution

column run up to 60% breakthrough helped to achieve even higher loading of cesium, corresponding to about 1500 Ci of ^{137}Cs/L bed. However, such an extended operation beyond breakthrough would result in accumulated effluent containing as high as 2.8 Ci/L of ^{137}Cs activity. Comparison of column loading data at breakthrough and beyond with batch results show that somewhat higher loading is achieved in column runs. This is possibly due to the fact that RFPR column is conditioned with 1.0 M NaOH before use, leading to higher alkalinity prevailing in the column during loading operation. As reported earlier, higher alkalinity enhances the uptake of cesium by RFPR[11].

3.4.9 Recovery of Cs

The first two columns loaded with Cs from dissolved AMP solution was rinsed with 6 bed volumes of 0.1 M NaOH and 6 bed volumes of distilled water, respectively. After rinsing, elution was done using 20 bed volumes of 0.5 M HNO_3. In both the cases, complete elution of loaded cesium was achieved in 20 bed volumes of 0.5 N $HNO_{3,}$ as can be seen from the typical elution profile is shown in Fig.3-15. Considering the loading of Cs up to breakthrough point and complete elution of loaded Cs^+ as well as unexchanged Na^+ ions from RFPR in 20 bed volumes, the composition of eluate solution was calculated and is shown in Table 3-8. As compared to the dissolved AMP solution, there is 20% increase in ^{137}Cs activity but what is more significant is the absence of Na_3PO_4 and Na_2MoO_4 and 88% reduction in the content of Na which is now present as $NaNO_3$. The results obtained in this investigation thus prove the utility of ion exchange process for purification of ^{137}Cs-bearing dissolved AMP solution.

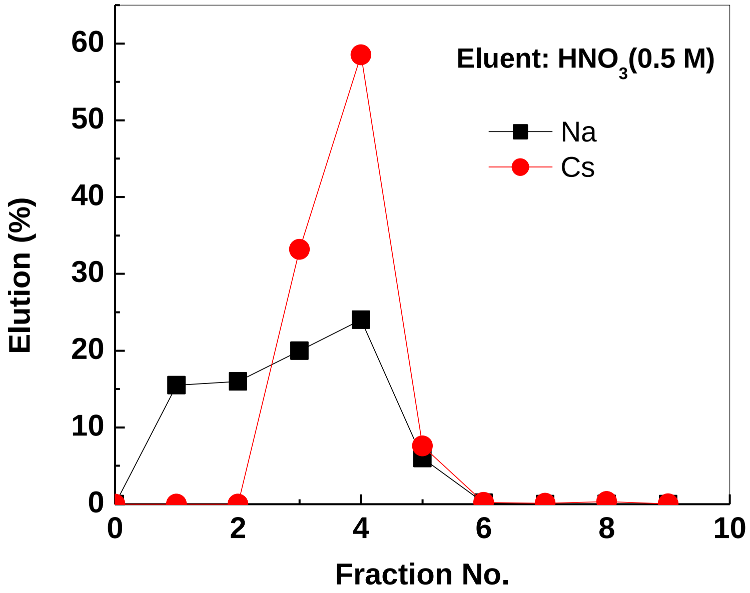

Figure 3-15: Elution profile of Cs and Na from RFPR column (Bed volume: 5 mL) at the flow rate of 4 bed volume per hour, fraction volume = 10 ml.

Table 3-8: Ion exchange purification of Cs^+ in dissolved AMP solution

	Cs-bearing dissolved AMP solution	**Eluate from RFPR column***
Cs (g/L)	1.4	1.7
Na (g/L)	17	2.1
Na/Cs (wt/wt)	12	1.2

**Loading up to breakthrough point, elution with 20 bed volumes of 0.5 N* HNO_3

The third column loaded with Cs from dissolved AMP solution was rinsed with 3 bed volumes of water and then eluated by passing 8 bed volumes (40 mL) of 0.1 M HNO_3 followed by 12 bed volumes (60 mL) of 0.5 M HNO_3. Results of elution are shown in Fig.3-16. This process of sequential elution of Na and Cs, developed earlier in our laboratory, is adopted to recover the Cs in chemically pure form[92].

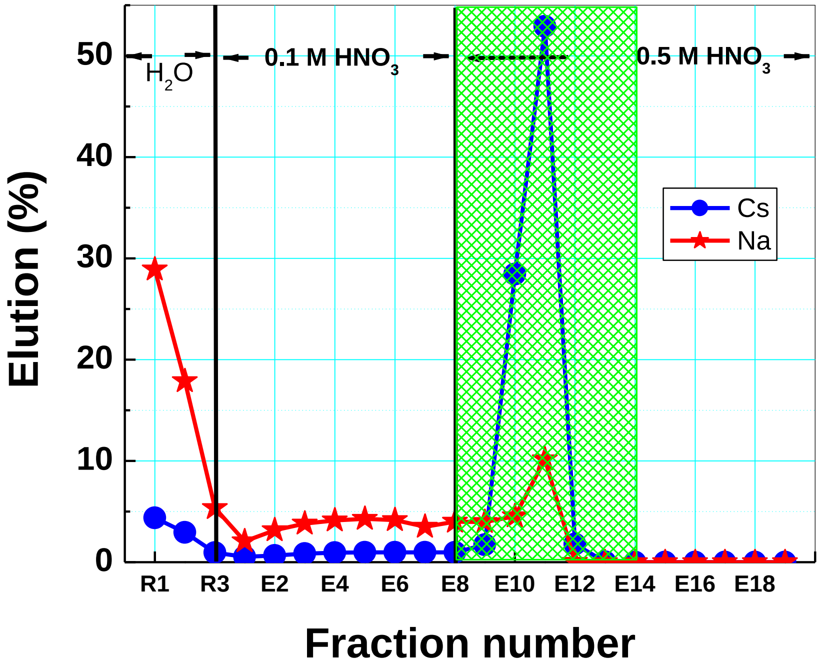

Figure 3-16: Elution profile of Cs and Na from RFPR column (Bed volume: 10 mL) at the flow rate of 4 bed volume per hour, fraction volume = 10 ml. The column was loaded with 0.6 g Cs from dissolved AMP solution containing 2.15×10^{-2} M Cs.

Sequential elution was also adopted for elution of loaded Cs from neutralized eluate and the results are shown in Fig.3-17. The elution profile is almost identical to that presented in Fig.3-16. From the Na and Cs concentration in the rinse, it can be stated that about 80% of un-reacted feed was removed during rinsing. This accounts for about 50% of the total Na present on the bed at the end of loading. Based on our earlier experience, rinsing with larger bed volumes of water was avoided to minimize hydrolysis of the loaded resin, which is basically a salt of weak acid and strong base. The use of dilute HNO_3 (0.1 M) during initial stages of elution removed about 30% of remaining Na ions, without elution of a significant amount of Cs ions. All the remaining Na and Cs were then eluted in 12 bed volumes of 0.5 M HNO_3.

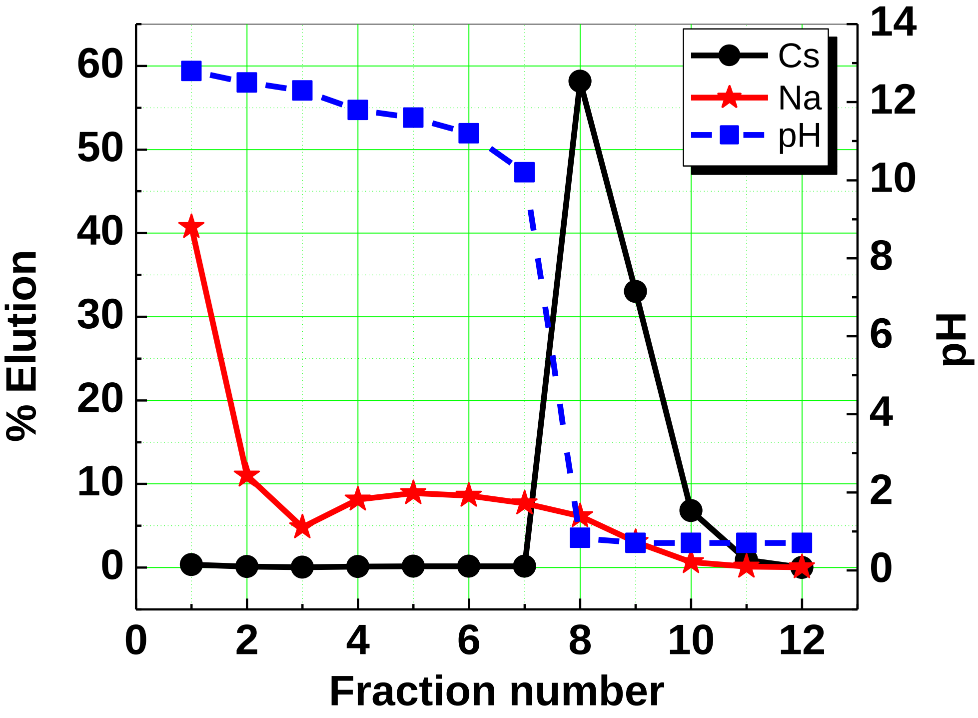

Figure 3-17: Elution profile of Cs and Na from RFPR column (Bed volume: 5 mL) at the flow rate of 4 bed volume per hour, fraction volume = 10 ml. The column was loaded with 0.06 g Cs from neutralized eluate containing 2.57×10^{-4} M Cs.

The observed elution of Na and Cs can be explained by considering the very high affinity of the resin for Cs ions. It can be noted that all the eluate solutions obtained during passing of 0.1 M HNO_3 are highly alkaline in nature. This suggests that the acid passed during 1^{st} phase of elution was utilized for neutralization of the bed and also for hydrolysis of some amount of Na-phenolate. Although the rate of hydrolysis of Cs-phenolate is higher than Na-phenolate, the higher affinity for Cs possibly overrules the hydrolysis as can be seen from the low Cs concentration in the eluate. Results of the study established that the adoption of sequential elution is useful for separation of a major amount of Na during initial stages of elution, thereby facilitating production of a low Na bearing Cs concentrate.

Table 3-9 shows the summary of Cs purification studies. It can be seen that the purified Cs solution obtained from both the waste streams are suitable for use in source preparation. Further, the very low Na content in solution generated from the processing of HLW makes it suitable for preparation of industrial irradiator sources.

Table 3-9: Composition of waste and purified Cs solution before and after ion exchange processing

	Alkaline ILW			**Acidic HLW**		
	ILW (as generated)	After primary separation	After purification	Waste (present study)	After primary separation	After purification
Cs (g/L)	0.0014 (0.05 Ci/L)	0.036 (1.25 Ci/L)	1.08 (37.8 Ci/L)	0.28 (10 Ci/L)	2.85 (100 Ci/L)	3.4 (120 Ci/L)
Na (g/L)	64	2.3	0.96	-	17	0.7
Na/Cs (wt/wt)	$4.5\text{x}10^4$	64	0.9	-	6	0.2

3.5 Summary of the results and conclusions

Results of present study on Cs recovery from acidic as well as alkaline waste streams, can be summarized as follows.

(1) Batch sorption data on Cs uptake by AMP-PMMA, prepared by coating of AMP powder on PMMA beads, show that Cs uptake by the sorbent remains unaffected even after coating on PMMA beads.

(2) Column behavior of the AMP-PMMA was found to be very good. It is inferred from column data that up to 800 Ci of ^{137}Cs can be loaded on 1 L bed of AMP-PMMA beads from radioactive waste solution containing 10 Ci/L of ^{137}Cs.

(3) Quantitative recovery of sorbed Cs from AMP-PMMA bed is possible by complete dissolution of AMP in NaOH solution and hence it can be concluded that the AMP-PMMA is a promising sorbent for recovery of Cs from acidic HLW.

(4) It is for the first time established that RFPR can be used for separation of Cs from high active alkaline waste streams.

(5) The Cs exchange isotherms of RFPR from solutions containing Cs concentrations in the range of 1×10^{-4} to 0.1 M have been evaluated for four different Na bearing solutions. All the isotherms have been found to follow Freundlich as well as D-R sorption equation. Cs uptake of RFPR calculated from the D-R isotherm equation was in good agreement with the values measured by conducting five column runs.

(6) The approach adopted for generation purified Cs solution includes higher loading of Cs on RFPR column followed by sequential elution of Na and Cs. The process has been showed promising for production of a concentrated ^{137}Cs solution containing very low

concentration of accompanying Na ions. The process also demonstrates the purified Cs solution production from the dissolved AMP solution. It was found that the Na/Cs ratio as low as 0.9 and 0.2 was obtained from alkaline ILW and acidic HLW solutions, respectively.

(7) The results of these studies show that ion exchange processes can be utilized for the recovery of high-purity ^{137}Cs from acidic HLW and also from alkaline ILW waste for use in radiation technology applications.

Chapter 4

Physicochemical properties of cesium borosilicate glasses containing TiO_2

Physicochemical properties of cesium borosilicate glasses containing TiO_2

4.1 Introduction

Development of borosilicate glass was first recorded in the late 19th century by German glassmaker Otto Schott and it was sold in Europe under the brand name "Duran" in 1893. In 1915, Corning glass works introduced Pyrex, a synonym for borosilicate glass. Thereafter rapid development has been noticed and quickly it became a ubiquitous material. The main reason behind this is that the borosilicate glass has a very low thermal expansion coefficient (3.3 x 10^{-6}/K), about one-third that of ordinary glass and high chemical resistance properties, leading to the widely use of borosilicate glass for kitchen glassware, thermometer glass and railroad lanterns and now in diverse fields including optical glass, glass to metal seal, etc.[93, 94]. However a scientific understanding of the glass network and its properties began only in early 1950. In 1955, Canadian scientists first experimentally established that HLW could be immobilized in glass[95]. This was followed by development of borosilicate matrix in UK (Fingal process) for vitrification of HLW[96]. In 1965, work on vitrification of HLW was started in India with emphasis on design and development of waste glass formulation and study of its properties including phase transformation, mechanical properties, radiation effects, chemical durability and volatilization[97]. A historical overview of the waste form development programme in nine countries including India was reviewed by Lutze and Ewing[98]. This highlights the fact that borosilicate glass has received the greatest attention in large scale immobilization of high level because of its excellent capabilities to accommodate almost all the elements of periodic table leading to a permanent and irreversible fixation of the nuclides in the vitreous matrix. Additionally, glass being a solid solution is not susceptible to inter-granular corrosion.

In-spite of these proven facts, borosilicate glass has not been considered for the preparation of ^{137}Cs based radiation sources. Such glasses are very simple as compared to the nuclear waste bearing glasses, as it will not have other fission products and actinides. It could be simple borosilicate glass containing a very few or no other additives. The basic differences in both the glasses are in terms of total alkali oxides content. The alkali oxide loading in the Cs glass should be significantly higher to meet the specific activity requirements. It is known that chemical durability of the borosilicate glasses decreases with the increase of alkali oxide loading. Further, volatilization of the Cs in preparation of such glasses is one of the major concerns. Taking inferences from nuclear waste glass development, it can be stated that the incorporation of various additives do play a major role in optimizing the properties of the glasses.

At the beginning of the work therefore feasibility of using simple alkali borosilicate glass was examined. The loading of alkali oxide in glass was fixed at 20 mol% including 2.5 mol% Cs_2O while the rest was Na_2O. Loading of 2.5 mol% Cs_2O is the minimum requirement for use of this glass as a radiation source in medical irradiators. A minimum amount Na_2O is necessary to make the glasses at relatively lower temperature. In the present context it is assumed that the preparation of the glasses will be carried out using the recovered Cs solution containing equal amount of Na and Cs (as shown in Table 3-11). This will correspond to the stated loading of Na_2O while incorporation of 2.5 mol% Cs_2O.

In order to improve the properties of the glasses, incorporation of some additives in small quantities can be considered essential. A number of studies have been carried out in this regards which have made it clear that the various additives played different roles in the glass network. Table 4-1 summarizes the effects of some additives on the change of properties of the resultant glasses[99]. In this chapter, the influence of TiO_2 on the Cs borosilicate glass is illustrated by evaluating physiochemical properties of the glasses incorporated with different amount of TiO_2. Physico-chemical properties like density, molar volume, glass transition temperature, chemical durability and Cs-volatilization behavior were evaluated as a function of TiO_2 concentration. In addition, the structural aspects of these glasses were also investigated using FTIR, ^{11}B MAS NMR spectroscopy and uv-visible spectro-photometry with a view to understand the role of TiO_2 on the physico-chemical properties of the glasses.

Table 4-1: Additives influence on the change of properties of borosilicate glasses

Name	***Formation temp.***	***Durability***	***Cs-loss (Volatilization)***
CaO	⬆	⬆	?
TiO_2	⬆	⬆	⬇
MnO	⬇	⬆	?
Al_2O_3	⬆	⬆	⬇
ZnO	⬆	⬆	?

4.2 Glass forming region of Na borosilicate system

Although sodium borosilicate glass can be obtained over a wide range of compositions as can be seen from the ternary diagram (Fig.4-1) representing glass forming region of the system, highlighting approximate compositional ranges of two commercial glass families[100] viz., Vycor glasses (area enclosed in magenta) and Pyrex type glasses (yellow shaded area), a limited region (SiO_2: 35-65, B_2O_3:10-20 and Na_2O:10-20, waste oxide: 15-30) has been used for the production of base glass for nuclear waste immobilization (area covered by black crossed lines)[98]. The glass forming region of interest in the present study is shown as circle filled in dark cyan color.

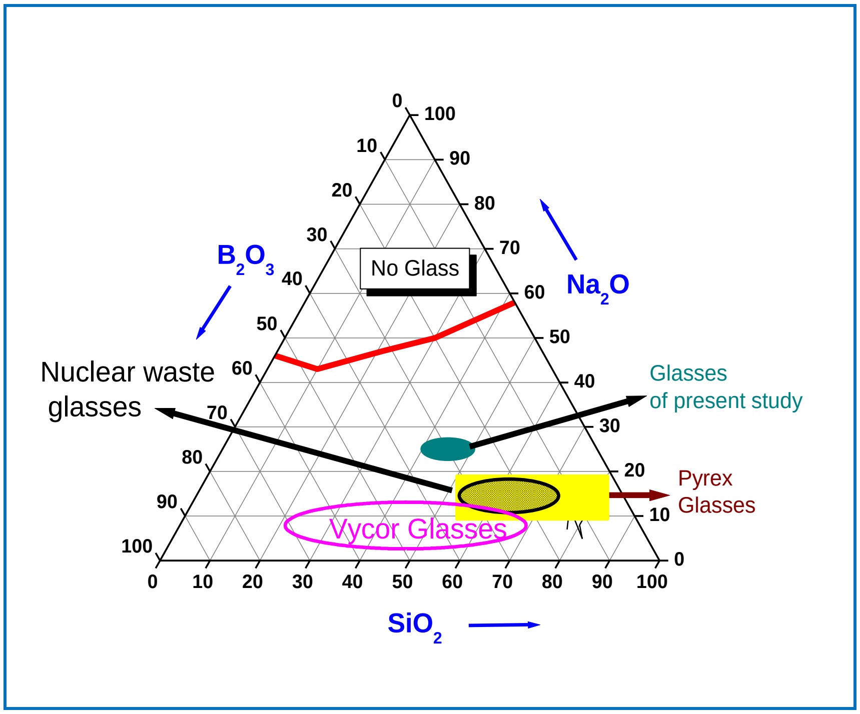

Figure 4-1: Ternary diagram of sodium borosilicate glass highlighting region of interest of some important class of glasses

4.3 Preparation of alkali borosilicate glasses

The characteristics of the simplified alkali borosilicate glasses prepared as per the formulation, 10 Cs_2O + 15 Na_2O + (75-x) SiO_2 + x B_2O_3, 'x' varied from 25-45 w% is shown in Table 4-2. It can be seen on the Table that the borosilicate glass containing $\geq$ 50 wt% of SiO_2 has pour temperature above 950°C. The chemical durability of the glasses in the series, as expected, are found to increase with the increase of SiO_2 concentration. From these results, it is clear that among the stated glasses that has low pouring temperature and Cs leach rate, #CBS-3 is the formulation considered as a baseline formulation for further investigations. Hereafter, it will be referred to as “base glass”.

Table 4-2: Characteristics of the Cs-borosilicate glasses prepared as per formulation (wt %) 10 Cs_2O + 15 Na_2O + (75-x) SiO_2 + x. B_2O_3

Batch No.	SiO_2 (wt%)	B_2O_3 (wt%)	Pour temp. (^oC)	Density (g/cm^3)	Leach rate (g/cm^2/d)	
					Na	Cs
CBS-1	50	25	> 950	-	-	-
CBS-2	45	30	950	2.46	1.7×10^{-3}	4.3×10^{-4}
CBS-3	40	35	900	2.47	3.0×10^{-3}	8.9×10^{-4}
CBS-4	35	40	900	2.48	3.8×10^{-3}	1.4×10^{-3}
CBS-5	30	45	900	2.49	4.0×10^{-3}	1.8×10^{-3}

4.4 Preparation of TiO_2 containing glasses

As mentioned above, the major thrust of this study is to improve the properties of the baseline glass by incorporating TiO_2. The additive can be incorporated in the glass either at the expense of B_2O_3 or SiO_2. In order to select the suitable one between the two alternatives, glasses were prepared adopting both the approaches and characterized (Table 4-3). Elemental (Na, Cs) leach rate for the glass (Ti-10A), prepared by incorporation of TiO_2 (10 mole %) at the expense of SiO_2, is found to be an order of magnitude higher than the base glass. Higher concentration of Si in leachate, however, indicates that the network dissolution also take place during leaching. It is known that SiO_2 decrease has a negative effect and TiO_2 increase has a positive effect on chemical durability[99]. The result clearly indicates that effect of SiO_2 is more dominant than TiO_2. On the other hand, the glasses prepared by incorporation of TiO_2 (10 mole%) with decrease of B_2O_3 showed higher chemical durability as compared to the base glass. Based on these results, the approach of incorporation of TiO_2 at the expense of B_2O_3 was selected and followed throughout the work. Five glasses of this series of molecular formula $(SiO_2)_{0.4}$ $(B_2O_3)_{0.35-x}$ $(Na_2O)_{0.175}$ $(Cs_2O)_{0.025}$ $(TiO_2)_x$, where x =0, 2.5, 5, 7.5 and 10, have been prepared and characterized as discussed below.

Table 4-3: Characteristics of the Cs-borosilicate glasses prepared from base glass by incorporating TiO_2

Batch No	**Batch composition (mole%)**					**Leach rate ($g/cm^2/d$)**			**pH of leachate**
	SiO_2	*B_2O_3*	*Na_2O*	*Cs_2O*	*TiO_2*	*Na*	*Cs*	*Si*	
Base glass	45	35	17.5	2.5	0	$3.0x10^{-3}$	$8.9x10^{-4}$	$3.1x10^{-5}$	9.35
Ti-10	45	25	17.5	2.5	10	$6.9x10^{-4}$	$5.9x10^{-5}$	$1.3x10^{-5}$	9.10
Ti-10A	35	35	17.5	2.5	10	$3.7x10^{-2}$	$2.0x10^{-2}$	$1.5x10^{-4}$	9.40

4.5 Chemical analysis of glass

The chemical analysis of the glasses was performed as per the procedure discussed in section 2.5.2. Experimentally determined concentrations of Na and Cs in the glasses were shown in Table 4-4. The error (standard deviation) associated with loss in wt % calculation for both the elements were found to be ± 2%. It is clear from Table 4-4 that both Na and Cs loss for 'base glass' is higher than all other glasses (Ti-2.5 to Ti-10). Among the four TiO_2 containing glasses, minimum loss for both Cs and Na was observed for the glass containing 5 mole% of TiO_2. Further, these results confirmed that 94% or more of both Na and Cs are present in all the glasses. Although other constituents in glass were not analyzed, it can be reasonably assumed that loss of boron will be lower than that of Cs. The Si and Ti content are assumed to be the same as batch composition.

Table 4-4: Chemical analysis (wt%) of Na and Cs in as melted glasses

Batch No	**Na_2O**			**Cs_2O**		
	Calculated	Expt.	Loss (%)	Calculated	Expt.	Loss (%)
'base glass'	15.39	14.36	6.7	10.00	9.0	10
Ti-2.5	15.33	14.77	4.0	9.96	9.4	5.6
Ti-5.0	15.26	14.88	2.5	9.92	9.5	4.2
Ti-7.5	15.20	14.71	3.2	9.88	9.3	5.9
Ti-10	15.14	14.20	5.8	9.83	9.2	6.4

4.6 General characteristics of the glasses containing TiO_2

4.6.1 Density and molar volume

Density of the glass samples were determined as per the procedure described in section 2.6. The measured density (g/cm^3) and calculated molecular weight (g) from batch composition of the glasses were used to calculate the molar volume (cm^3) of the glasses by using the following equation:

$$\text{Molar volume} = \text{Molecular weight} / \text{density}$$

Fig.4-2 shows the measured density and calculated molar volume of the glasses containing varying concentration of TiO_2. Density of the glasses was found to be similar within the limit of experimental error. The molar volume was also found to be almost same (27.5±0.3 cm^3).

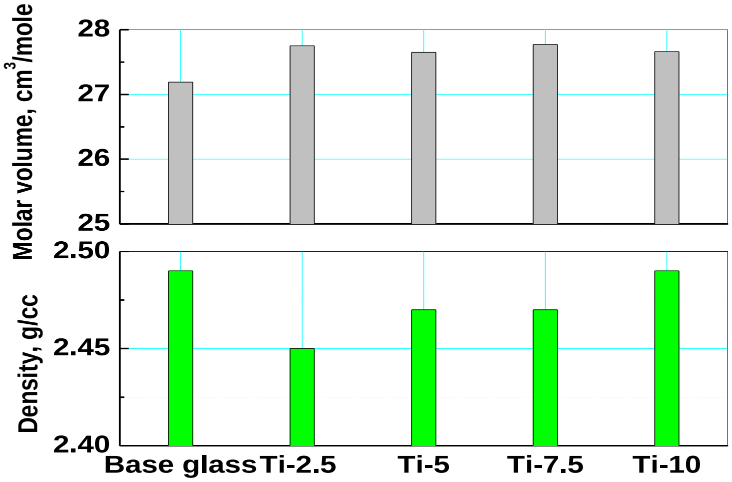

Figure 4-2: Density and molar volume of the Cs borosilicate glasses ($(SiO_2)_{0.4}$ $(B_2O_3)_{0.35-x}$ $(Na_2O)_{0.175}$ $(Cs_2O)_{0.025}$ $(TiO_2)_x$) containing different concentration of TiO_2,

4.6.2 XRD analysis

XRD patterns of the glass samples recorded with an X-ray diffractometer which uses CuKα radiation are shown in Fig.4-3. All the patterns showed a broad peak around a 2θ value

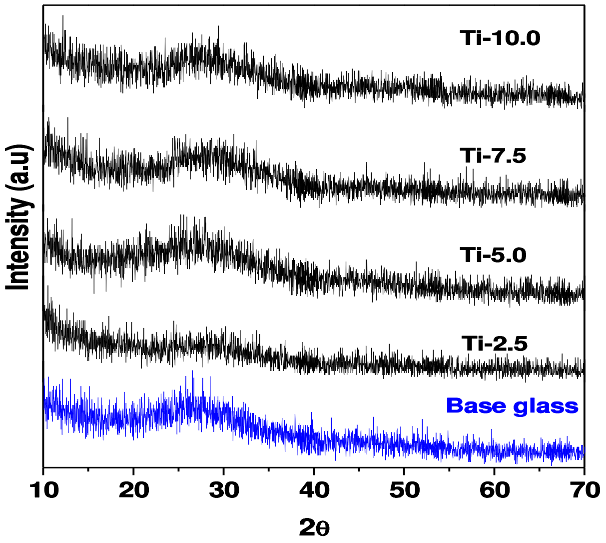

Figure 4-3: XRD profiles of the Cs borosilicate glasses of general formula $(SiO_2)_{0.45}$ $(B_2O_3)_{0.35-x}$ $(Na_2O)_{0.175}$ $(Cs_2O)_{0.025}$ $(TiO_2)_x$ with x varying from 0.0 to 10.0

of 25°, characteristic of the amorphous borosilicate network. Absence of sharp peaks clearly confirmed that no crystalline phases (within the detection limits of XRD technique) are present in these glasses.

4.6.3 Glass transition temperature

Glass transition temperature was determined from the onset of the first endothermic peak of DTA curve (Fig.4-4) generated at a heating rate of 10°C/min using setaram make TG-DTA instrument (section 2.9.4.2). The glass transition temperature of all the glass samples has been plotted as a function of TiO_2 concentration and is shown in Fig.4-5. It is found that the glass transition temperature decreases systematically with increase of TiO_2 concentration in glass. The observed variation can be explained based on the bond energy values of B-O and Ti-O bonds[101]. As the bond energy values are lower for Ti-O bonds compared to B-O bonds, replacement of B-O bonds by Ti-O bonds results in the decrease of average bond energy of the glass network, leading to reduction in glass transition temperature.

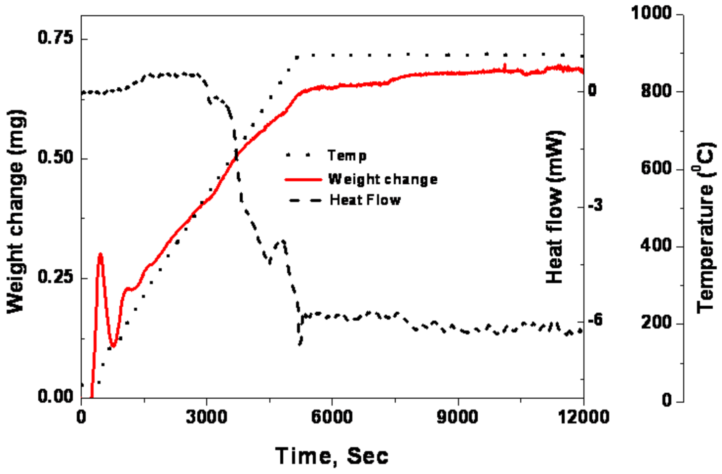

Figure 4-4: TG-DTA profile for the Cs-borosilicate glass containing 7.5 mole% TiO_2 (Batch No. Ti-7.5)

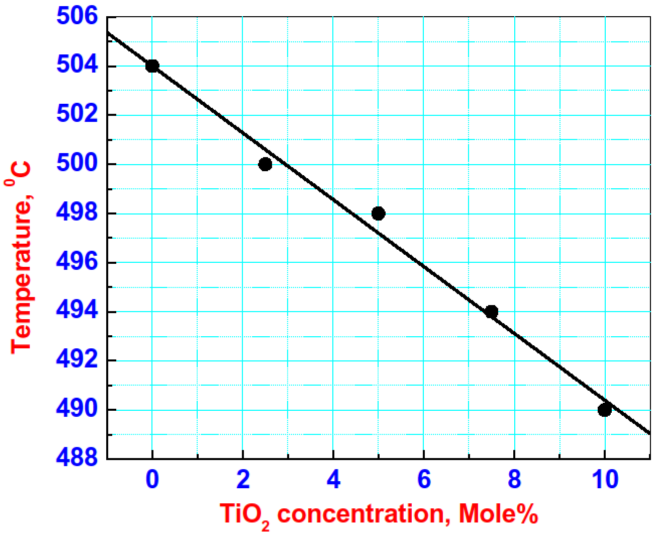

Figure 4-5: Glass transition temperature of Cs-borosilicate glasses containing varying amount of TiO_2, line is guided to eye

4.6.4 Chemical durability

Chemical durability is the property symbolizing the extent of resistance against hydrolytic attack and depends mainly on the nature of the constituents and their relative concentrations in glass[102, 103, 104, 105]. It is generally measured by conducting leaching tests. In the present study, leaching tests were performed as per the procedure described in section.2.7 for comparative evaluation of formulation. In brief, 1.0 g glass sample (-100+200 mesh ASTM) and 10 cm^3 of ultrapure water was heated in air-oven at 90°C for 24 hours, and the measured concentrations of Na, Cs, and Si in leachate were used to judge the chemical durability of the glasses. The normalized elemental leach rate of the glasses as a function of TiO_2 content is shown in Fig.4-6.

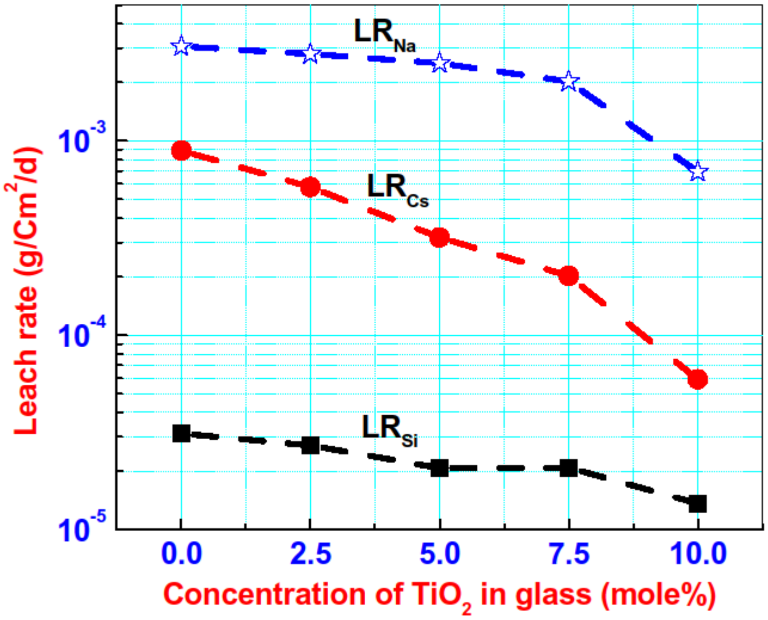

Figure 4-6: Leaching of Na and Cs from Cs-borosilicate glasses in distilled water at 90°C for 24 hours, lines are guided to eye, general formula of the glasses: $(SiO_2)_{0.4}$ $(B_2O_3)_{0.35-x}$ $(Na_2O)_{0.175}$ $(Cs_2O)_{0.025}$ $(TiO_2)_x$

The measured pH of leachate for the glasses was found to be within 9.35 to 9.10, highest for ‘base glass’, lowest for Ti-10 and almost same (9.20-9.25) for the other three glasses. The leach rate of Na, Cs and Si are found to be in the order: Na>Cs>Si. In detail, the Si concentration in the leachate for all the glasses is found to be almost same, and this has been attributed to the fact that network dissolution took place to the same extent for all the glasses during the course of leaching. Leaching pattern of Na and Cs can be explained by considering ion exchange reaction of glass and hydronium ions in which diffusion is the rate controlling step [103-104]. As Na^+ ion has a smaller ionic radius compared to Cs^+ ion, Na^+ ions have higher diffusion coefficient and mobility compared to Cs ions in the same glass matrix. This accounts for the increased leach rate of Na ions as compared to Cs ions from glass. In totality, the chemical durability of the glasses (with respect to Cs and Na leach rate) improved significantly due to incorporation of TiO_2 at the expenses of B_2O_3. This overall improvement of chemical durability is due to a combined effect of both TiO_2 increase and B_2O_3 decrease, as both factors are well known to improve the matrix durability[99, 106]. More specifically, it can be noted that the improvement of chemical durability with respect to Cs leach rate is more noticeable than Na. For example, the Cs leach rate was found to decrease almost linearly with increase of TiO_2 concentration and about 15 times lower Cs leach rate was noted for the Ti-10 glass (containing 10 mole% TiO_2) compared to the glass containing no TiO_2 ('base glass'). On the other hand, no improvement on Na leach rate, due to the presence of TiO_2 up to 7.5 mole%, was observed. The preferential leach rate of Na and Cs may possibly be due to the structural modification brought about by TiO_2 incorporation in the glass at the expense of B_2O_3. This aspect has been investigated in detail and is described in a later section of this chapter.

4.7 Volatilization of Cs

A large number of studies pertaining to the effect of TiO_2 on volatilization of Cs have been reported from various laboratories and the observations can be summarized as follows. Rastogi et al[107] reported that volatility of Cs can be reduced by using a little amount of $TiO_{2,}$

possibly due to the formation of thermally stable compounds such as Cs_2O-$4TiO_2$. The effect of TiO_2 on reduction of Cs-volatility was also observed by Kelly et al. during the preparation of glass from zeolite[108]. On the other hand, Gray[109] has shown that addition of TiO_2 in zinc borosilicate matrix increases the volatility of Cs. About 11% of Cs was found to be volatilized when 12 wt% TiO_2 was added to 76-183 glass. In 1981, Saidl et al. reported that the use of TiO_2 in borosilicate glass lowers Cs volatility[110]. It is to be noted that all the above studies have been carried out in connection with the incorporation of nuclear waste and no data for only Cs bearing borosilicate glasses are reported till date, to the best of authors' knowledge. Based on the above discussion it is clear that the role of TiO_2 in the extent of Cs losses due to volatilization is significantly dependent on the matrix composition. Hence, a systematic study on the extent of Cs-volatilization as a function of TiO_2 content in glass was performed.

In the present study, as described in section 2.8, different approaches were made to measure the extent of Cs volatilization as well as to provide an understanding on the volatilization behavior of Cs from borosilicate glasses as a function of TiO_2 content and the results are discussed below.

(a) Measurement of Cs volatilization loss in glass making

This method (described in section 2.8.1) in principle is a direct approach, as glass forming mixture is heated and the evolved glasses were collected and analyzed chemically. It is important that sample of evolved gas should have a measurable amount of volatilized species, so that a statistically reliable chemical analysis could be performed. In general, volatilization study with more glass (with higher batch size) generates a measurable amount of species. Otherwise, accuracy in analytical results can be improved by using radiotracer technique. In this method, as batch size used was 2 g glass, radiotracer technique was used. In addition, Cs analysis was performed after dissolving the glass sample in 40% HF and the analysis results was used to ascertain the material balance. For some selected batches, detailed elemental analysis in solutions of volatilized products was also carried out.

Table 4-5 shows the results of the extent of Cs volatilization during the glass formation. It can be seen that a maximum of about 4% of Cs was volatilized in the sample containing no TiO_2 ('base glass'). The loss of Cs was found to reduce from 4% to 1.5% (about 60% reduction) with the incorporation of 2.5 mole% of TiO_2. A further marginal decrease in Cs-loss was noted for the batch containing 5 mole% of TiO_2 and thereafter a trend reversal was observed. The loss of Cs was found to be about 2.8% for the last two batches containing 7.5 and 10 mole% of TiO_2. As compared to the base glass, all the batches with TiO_2 showed lower loss of Cs. A similar conclusion can also be arrived from the Cs concentrations in dissolved glass solution. The trend of Cs volatilization values obtained here compares to Table 4.4.

Table 4-5: Distribution of Cs in vapor and glass during formation of the Cs-borosilicate glasses

Batch No	***Concentration of Cs (%)***			***No. of tests***
	Dissolved glass (a)	Scrub solution (b)	Total (a+b)	
'Base glass'	95.95-96.15	3.55-3.99	99.85-100.13	4
Ti-2.5	97.92-98.81	1.53-1.55	99.47-100.35	2
Ti-5.0	96.27-97.84	1.39-1.48	99.24	2
Ti-7.5	96.76-97.55	1.93-2.80	98.70-100.35	2
Ti-10.0	96.21-96.35	2.64-2.82	99.03	2

The higher losses incurred in as melted glasses is possibly due to exposure of the glasses to elevated temperature for pouring. It is worth mentioning that more than 90% of the total Cs present in scrub-solution was obtained from the washing of the silica tube and a little amount was in the 1st bubbler (section 2.8.2). The Cs present in the 2nd bubbler was negligible and therefore it can be stated that no Cs escaped from the system. For all the tests, good mass balance of Cs was obtained, as it can be seen that > 99% of Cs was accounted for.

Result of detailed chemical analysis of the solutions generated from washing of the volatilization set-up is shown in Table 4-6. It can be seen that the volatilization loss of boron species is more significant after Cs. This also confirmed that Na is the least volatile element as compared to B and Cs and its volatilization loss for the glasses under investigation was found to be more or less same. Volatilization profile of B species was found to follow similar trend as described above for Cs.

Table 4-6: Elemental composition of the scrub solutions (in ppm) analyzed by ion chromatography

Total volume of scrub solution: 250 mL

Batch No	*Na*	*Cs*	*B*
Base glass	3.3	31.5 (32.7*)	10.7
Ti-5.0	4.4	9.2 (11.2*)	8.05 (7.1#)
Ti-10.0	4.6	20.7 (21.5*)	14.6

** calculated from the radiometric measurement of ^{137}Cs activity in solution (i) before and (ii) after glass formation and (iii) initial concentration of Cs in solution taken for glass making.*

 # analyzed using ICP-AES.

(a) Measurement of Cs volatilization by thermogravimetry method

As this method is highly sensitive with regard to the change of weight due to heating, it was used to study the Cs volatilization from preformed glasses. In this analysis, about 40 mg of glass sample in platinum crucible was heated under static air to 900°C at the heating rate of 10°C/min and then isothermal heating was continued at 900°C for 2 hours, using a Setaram make TG-DTA instrument. TG-DTA profile, corresponding to the glass sample containing 7.5 mole% TiO_2, is shown in Fig.4-4. It can be seen that a little weight gain was observed during the 1st heating sequence i.e., from 100-900°C and thereafter constant weight was recorded throughout the heating period (2 hours) at 900°C. The observations are in accordance with the results of volatility tests from simulated high level waste glass, reported by J. Harbour[111]. The experimentally observed TG-DTA profile for all the glasses under investigation was found to follow a similar pattern as shown in Fig.4-4. Based on these results, it is inferred that no loss of Cs, to the level of sensitivity of TG-DTA instrument, occurred from the preformed glasses.

(c) Chemical analysis method

It was seen that themogravimetry method, though very sensitive, did not yield any information about weight losses possibly due to very low quantity of the sample and lower experimental temperature. In the present study, therefore, higher quantity of sample was used and the volatile component was dissolved and analyzed chemically. As mentioned earlier, the heating of preformed glass is equivalent to soaking stage, which is the longest duration process in glass preparation and the glass at this stage endures minimum turbulence from froth formation/bubble evolution. The effect of temperature is more prominent at this stage, hence Cs volatilization loss in this period was measured and used as a representative parameter for comparing the effect of composition. In this study, preformed glass (batch size: 25 g) was heated for about 6 hours per day for 4 days and the amount of Cs volatilized during 6 hours of heating was obtained by analyzing the solutions obtained from washing the whole setup where Cs was deposited (section 2.8.2.2). Volatilization profile for two glass samples, viz., ‘base glass’ and Ti-5, were determined at three different temperatures (i.e., 900, 950 and 1000^oC).

The result of volatilization study is presented in terms of cumulative loss of Cs after 24 hours of heating in Table 4-7. It can be seen that the extent of Cs loss for both the glasses heated at 900^oC for 24 hours are very low and almost similar. However 950 and 1000^oC heated samples showed increasingly higher Cs losses. The influence of TiO_2 on suppressing Cs volatility is clearly seen.

Table 4-7: Cumulative loss of Cs (mg/cm^2) from the preformed Cs borosilicate glasses after 24 hours of heating at different temperatures

Glass sample	***Heating temperature (^{o}C)***		
	900	950	1000
Base glass	0.23	0.56	1.57
Ti-5	0.20	0.47	0.95

4.7.1 Discussion on Cs volatilization results

The loss of Cs due to volatilization during heating at elevated temperature may occur through several mechanisms, depending upon the composition of the melt and temperature. Thermal decomposition of $CsNO_3$ (taken as starting material for glass formation) takes place at around 400-600^oC, mainly through the following steps[112]:

$$2CsNO_3 \xrightarrow{414\,^{o}C} 2CsNO_2 + O_2$$

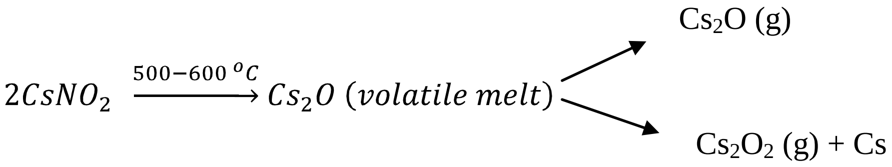

$$2CsNO_2 \xrightarrow{500-600\,^{o}C} Cs_2O\ (volatile\ melt) \rightarrow \begin{cases} Cs_2O\ (g) \\ Cs_2O_2\ (g) + Cs \end{cases}$$

Hence it is reasonable to assume that volatilization loss of Cs starts at around 500°C and continues up to fusion temperature of the glass. Since Cs metal is highly reactive with air, and our experiments were carried out under constant air flow conditions, it is quite possible that majority of the Cs can get converted to Cs(OH), which is the most volatile among all Cs compounds[113]. In addition, some amount of Cs may volatilize in the form of $Cs_2(BO_2)_2$ (g), Cs (BO_2) (g), as reported by Asano et al[114].

From the elemental composition profile of the scrub solution (Table 4-6), it can be inferred that some such compounds may form during formation of all the glasses under investigation. Some loss of Cs is also expected during soaking of the glass at 900°C for homogenization. The values in Table 4-5 represent the cumulative loss of Cs in glass making, starting from the decomposition of raw materials including soaking at 900°C for 2 hours. According to the results of Rudolph et al., the presence of B_2O_3 or TiO_2 in the melt is known to reduce Cs volatilization and the TiO_2 has been found to show pronounced effect compared to B_2O_3 in reducing the extent of Cs volatilization[115]. Hence in the present study, as TiO_2 is incorporated at the expense of B_2O_3, it is reasonable to conclude that the presence of TiO_2 is responsible for the decrease in the extent of Cs volatilization. Furthermore, the peculiar variation of Cs losses as a function of TiO_2 content in the glasses may possibly be due to the difference in the nature of interaction of Ti^{4+} ions with glass constituents, as TiO_2 is known to behave as a network former and modifier depending upon its concentration in the glass[116]. This information can be obtained by investigating the structural aspects of the glasses and the same has been described in the latter section of this chapter.

Further volatilization behavior of Cs at three different temperatures is presented in Figs. 4-7 and 4-8 in the form of cumulative Cs loss against square root of heating time. It can be considered that the nature of loss rate profile is a reflection of processes involved in volatilization. Elemental volatilization from glass melt, as in the case of present study in which all the glasses are in molten state at 900oC and above, occurred vide processes like (i) diffusion of Cs through the melt to surface, (ii) transport through melt/vapor interface and (iii) transport in the atmosphere[117]. It is therefore reasonable to assume that the volatilization profiles in Figs. 4-7 and 4-8 give an average picture of all the processes involved with the characteristic features of the rate controlling processes. For example, only one slope in rate loss profiles suggests that volatilization occurred predominantly through one type rate determining process. From the straight-line plots of cumulative Cs losses against square root of time, it can be stated that volatilization of Cs occurred predominantly through diffusion controlled process and the same can be expressed by equation 1 below[76]:

$$\mathrm{Q} = \mathrm{C}_0 . \sqrt{\frac{D}{\pi}} . \sqrt{t} \qquad \text{…(15)}$$

In equation 1, Q (mg/cm^2) represents the amount of Cs diffused from melt of unit surface area after t (h) time, C_0 (mg/cm^3) is the initial concentration of Cs in melt and D (cm^2/h) is diffusion coefficient (the quantity of material diffused through a unit area in unit time under a unit concentration gradient). Assuming negligible Cs loss takes place during glass preparation, the values of C_0 can be obtained from the measured density of the glasses and amount of Cs added in glass preparation. From the C_0 values and slope of the straight line plots (Figs 4-7 & 4-8), the values of diffusion coefficient were evaluated for all the glasses heated at different temperatures. As diffusion is a temperature dependent phenomenon, diffusion coefficient at any temperature can be expressed by the following equation[118]:

$$D = D_0 . e^{-\frac{E}{RT}} \qquad \ldots(16)$$

where R is universal gas constant and T is the absolute temperature. Calculated D values of the glasses are plotted as a function of 1/T and are shown in Fig.4-9. From the slope and the intercept of each line, the values of activation energy, E and D_0 for Cs diffusion from the glasses have been calculated (Table 4-8). The activation energy values for 'base glass' and Ti-5 glass were as found to be 513 and 360 kJ/mol, respectively. Interestingly, Cs loss is lower for Ti-5 glass even though the activation energy for Cs diffusion is lower than 'base glass'. Similar trend in weight loss and activation energy has also been reported for borosilicate glasses having different compositions by various authors[76,119]. The calculation of D_0 value for these glasses ('base glass' and Ti-5) showed that their differences are quite significant, (3.49 x 10^{12} cm^2/s for 'base glass' and 4.73 x 10^5 cm^2/s for Ti-5) and control Cs loss.

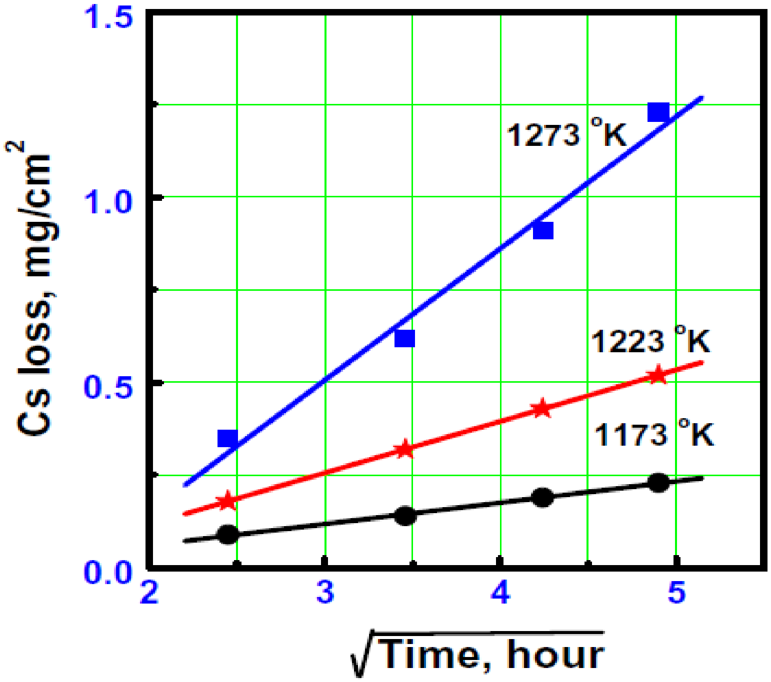

Figure 4-7: Cs loss profile as a function of square root of heating time for glass sample of molecular formula $(SiO_2)_{0.45}$ $(B_2O_3)_{0.35}$ $(Na_2O)_{0.175}$ $(Cs_2O)_{0.025}$ in dry air at different temperature

Table 4-8: Activation energy and pre exponential factor for Cs volatilization from the glasses

M_2O_x	E (kJ/mol)	D_0 (cm^2/s)
'base glass'	513	3.49×10^{12}
Ti-5	359	4.73×10^{5}

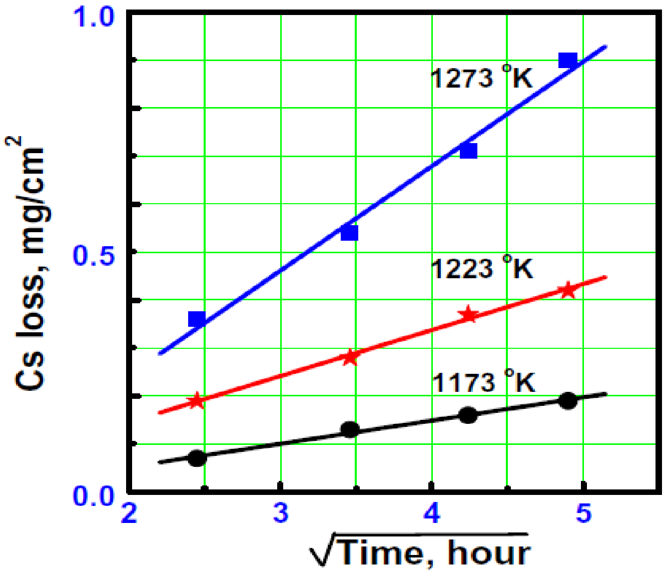

Figure 4-8: Cs loss profile as a function of square root of heating time for glass sample of molecular formula $(SiO_2)_{0.45}$ $(B_2O_3)_{0.30}$ $(Na_2O)_{0.175}$ $(Cs_2O)_{0.025}$ $(TiO_2)_{0.05}$ in dry air at different temperature

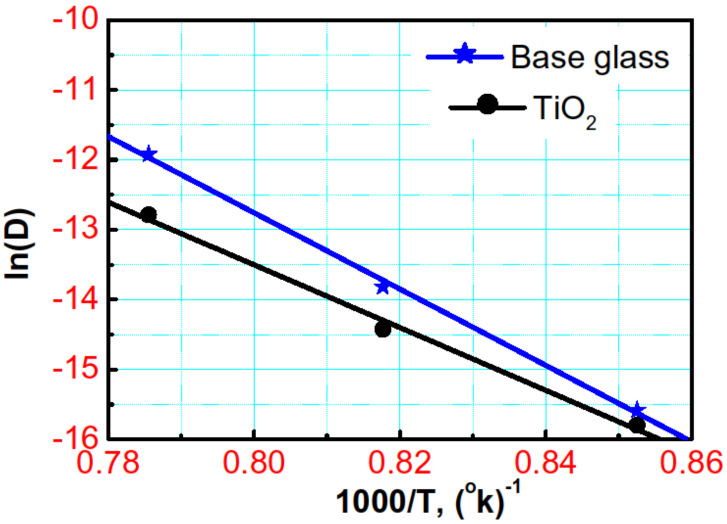

Figure 4-9: Plot of ln(D) against 1/T for the base glass and glass sample containing 5 mole% TiO_2

4.8 *Structural characterization of the glasses*

4.8.1 FTIR study

FTIR spectra of the glass sample was recorded from KBr pellets using a Fourier transform infrared (FT-IR) spectrometer (model: Jasco-660) with an average of 50 scan per spectrum at a resolution of 4 cm^{-1} are shown over the region of 440- 2000 cm^{-1} in Fig.4-10. The glass sample without any TiO_2 is characterized mainly by three peaks centered at 1408 cm^{-1}, 987 cm^{-1} and 454 cm^{-1}. The peak around 987 cm^{-1} also has a weak shoulder around 686 cm^{-1}. The peak around 1408 cm^{-1} is attributed to the B-O stretching vibration of BO_3 and BO_4 structural units present in the glass[120]. The broad peak around 987 cm^{-1} and weak shoulder around 686 cm^{-1} have arisen due to the asymmetric and symmetric stretching vibrations of Si-O-Si/Si-O-B linkages, respectively[121]. The peak around 454 cm^{-1} has arisen due to the bending

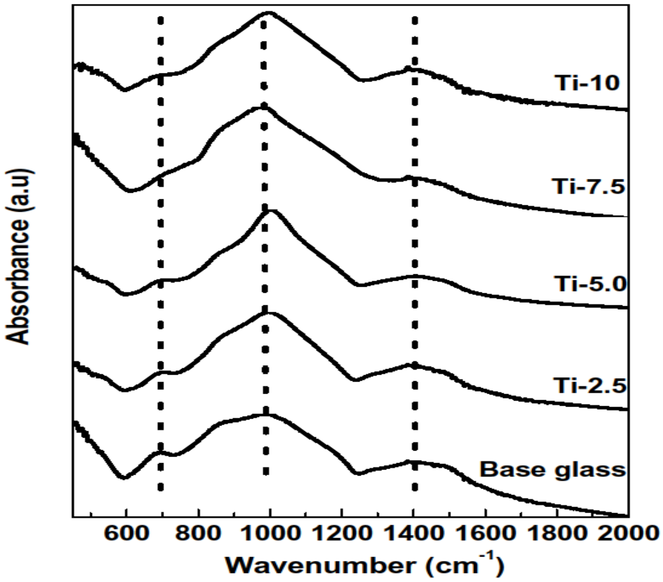

Figure 4-10: FTIR patterns of Cs-borosilicate glasses containing different amounts of TiO_2 over the region of 400-2000 cm^{-1}

vibration of Si-O-Si/Si-O-B linkages. Similar IR patterns were also observed for glass samples with different TiO_2 contents. No additional peak characteristic of Ti-O vibrations has been observed in these patterns due to the low IR activity of Ti-O bonds compared to the Si-O or B-O bonds. It is worth mentioning that with the incorporation of TiO_2, the line shape corresponding to asymmetric stretching vibration has been found to change significantly, as can be seen from Fig.4-11. For 2.5 mole% TiO_2 incorporation in the glass, there is significant narrowing in the line shape corresponding to 987 cm^{-1} peak (characteristic of Si-O-Si/Si-O-B asymmetric stretching vibration). Increase in TiO_2 content to 5 mole% resulted in further reduction of the line width of this peak. However for more than 5 mole% TiO_2 (i. e. for 7.5 and 10 mole% TiO_2) incorporation, line width began to increasing. The observed variations in the line width can be attributed to variation in the extent of strain/distortion associated with the borosilicate network with the addition of TiO_2. When a bridging oxygen atom gets converted to

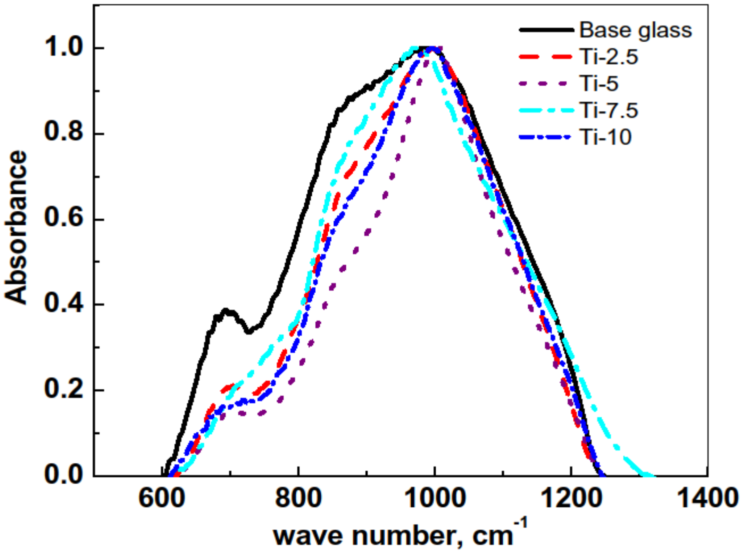

Figure 4-11: FTIR spectrum of Cs-borosilicate glasses containing different amounts of TiO_2 (normalized at peak 970-1010 cm^{-1})

non-bridging oxygen atom, the strain/distortion associated with the network decreases. This leads to decrease in line width of the IR absorption peak. However, above 5 mole% TiO_2, the line width increase has been attributed to the network forming action of TiO_2. The change in the behavior of TiO_2 from network modifier to network former is also reported by other investigators[122].

4.8.2 NMR study

^{11}B MAS NMR patterns for the glass samples loaded with different amounts of TiO_2 are shown in Fig.4-12. All the patterns are found to consist of less intense broad peaks around -3 ppm and sharp peak around -19 ppm along with side bands. Based on earlier ^{11}B MAS NMR studies[123], the sharp and broad peaks are respectively attributed to boron in tetrahedral (BO_4) and trigonal (BO_3) configurations. As ^{11}B is a quadrupolar nucleus (I = 3/2), boron in the trigonal coordination lacks cubic symmetry, and gives rise to a broad peak. Unlike this, cubic nature of the tetrahedrally coordinated boron structural units results in negligible quadrupolar coupling constant and thereby giving rise to a sharp NMR peak. The area under both the peaks was calculated and relative percentages of both BO_4 and BO_3 structural units have been determined and are given in Table 4-9. The relative concentrations of BO_4 structural units have been found to increase with the incorporation of 2.5 mole% TiO_2. However above 2.5 mole% TiO_2 incorporation, the relative concentration of BO_3 and BO_4 structural units remained more or less same. These results demonstrate that as TiO_2 content in the glass increases at the expense of B_2O_3 (upto 2.5 mole%), the boron network is affected initially. Further, the results prove that beyond 2.5 mole% TiO_2 incorporation the relative concentrations of BO_3 and BO_4 structural units are not responsible for the observed changes in the physical properties of the glass samples. With incorporation of TiO_2 up to 2.5 mole%, there exists a redistribution of the cations in the borosilicate network. However above 2.5 mole% TiO_2, Ti^{4+} ions do not have any interaction with boron structural units as revealed by the identical values of the relative concentration of BO_3 and BO_4 structural units. This is possible if Ti^{4+} ions interact with the silicon structural units present in the glass.

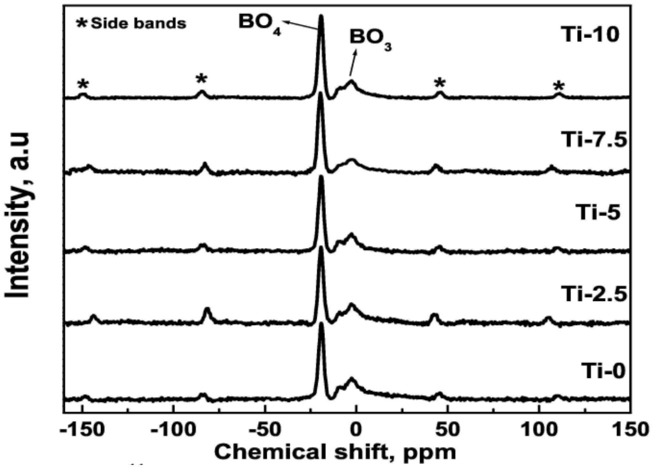

Figure 4-12 : ^{11}B MAS NMR profile of the glasses containing varying concentration of TiO_2

Table 4-9:: Concentrations of BO_4 and BO_3 structural units in the Cs-borosilicate glasses containing different concentrations of TiO_2 determined from ^{11}B MAS NMR profiles

Batch No	***Batch composition of B_2O_3 (mole%)***	***Relative concentration (%) in glass***	
		BO_4	**BO_3**
Ti-0	35.0	58	42
Ti-2.5	32.5	63	37
Ti-5.0	30.0	64	36
Ti-7.0	27.5	65	35
Ti-10.0	25.0	65	35

4.8.3 UV-Visible optical absorption study

Based on the FTIR and ^{11}B MAS NMR studies it is inferred that the relative concentration of non-bridging oxygen atoms changes with increase in the concentration of TiO_2 at the expense of B_2O_3 in the glass. Such changes in the relative concentration of non-bridging oxygen atoms result in change in the $E_{optical}$ values of the glass samples, and this can be followed by recording the uv-visible optical absorption spectrum of the sample. UV-VIS spectra were recorded from 800 to 200 nm with a thin plate of glass using Jasco spectrophotometer, (Model V-650), at a rate of 400 nm/minute scanning speed (section 2.9.7).

Fig.4-13 shows the uv-visible optical absorption spectrum of three representative glass samples. All the absorption curves are characterized by a broad onset over the region of 360 - 325 nm, which is characteristic of the glassy nature of the sample[124]. For glass sample without any TiO_2 ('base glass'), the onset of absorption is found to be around 325 nm. With incorporation of TiO_2, the onset of absorption was found to get red shifted for all the samples.

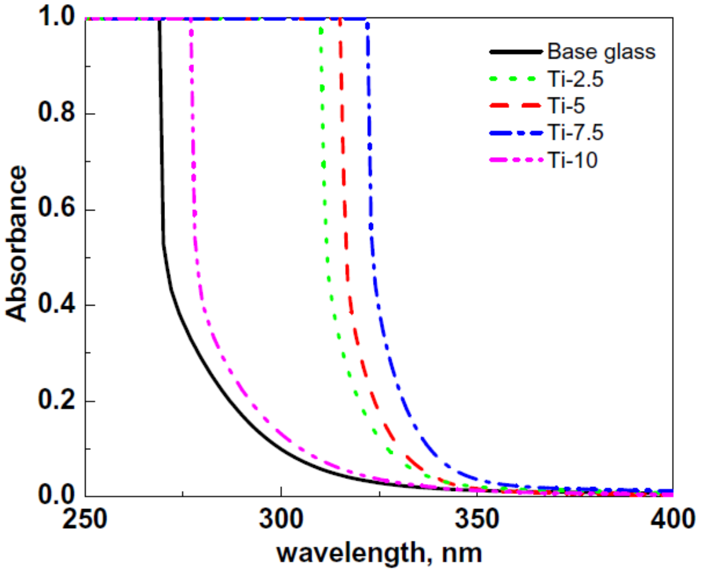

Figure 4-13: UV-visible optical absorption spectra of Cs borosilicate glasses containing different amounts of TiO_2.

As the onsets of absorptions are quite broad, attempt was not made to exactly calculate the onset wavelength of absorption. However the absorption coefficient (α) in these glasses can be related to energy gaps (optical gaps) in the glass by the power law suggested by Davison and Mott[125], which can be expressed as

$$\alpha h\nu = A(E - h\nu)^r$$

where, A is a constant and r can have values 2,3, ½ etc. For indirect transitions in glassy materials, value of r can be assumed to be 2. Hence in the plot of $(\alpha h\upsilon)^{1/2}$ versus hυ, known as extrapolation of the linear graph in the onset region to the x-axis can give the value of the optical gap in the glass. The Tauc plot (Fig.4-14) shows the variation of $(\alpha h\upsilon)^{1/2}$ as a function of hυ for the glasses. For glass sample without any TiO_2 content, the $E_{optical}$ value is found to be 3.60 eV. Incorporation of 2.5 mole% TiO_2 resulted in reduction in the $E_{optical}$ value namely to 3.52 eV. Further reduction of $E_{optical}$ value (3.42 eV) was noted for the glass containing 5.0 mole% of TiO_2. The $E_{optical}$ values for the glasses containing 7.5 and 10 mole% TiO_2, are comparable with that of the glass sample with 5 mole% TiO_2. The observed variation in the $E_{optical}$ values confirms that there is a change in the relative concentration of non-bridging oxygen atoms in the glass with incorporation of TiO_2. For glass containing 2.5 mole% TiO_2 the relative concentration of non-bridging oxygen atom is higher compared to the 'base glass' glass. The negative charge present in the non-bridging oxygen atoms facilitates the excitation of electrons to higher energy levels thereby decreasing the $E_{optical}$ value. For 5 mole% containing glasses, the decrease of $E_{optical}$ value indicated that some more non-bridging sites have been created due to incorporation of more TiO_2. However, the glasses containing more than 5 mole% TiO_2, no additional non bridging oxygen formation taking place as revealed from the comparable $E_{optical}$ values for all three glasses (Ti-5, Ti-7.5 and Ti-10). From these results it can be inferred that at higher concentration of TiO_2, Ti^{4+} mainly goes to the network rather than further modifying the network and increasing the concentration of non bridging oxygen atoms. In other words, Ti^{4+} acts as network modifier/former depending upon the concentration in glass. This fact was also confirmed from the FTIR and ^{11}B MAS NMR results described above.

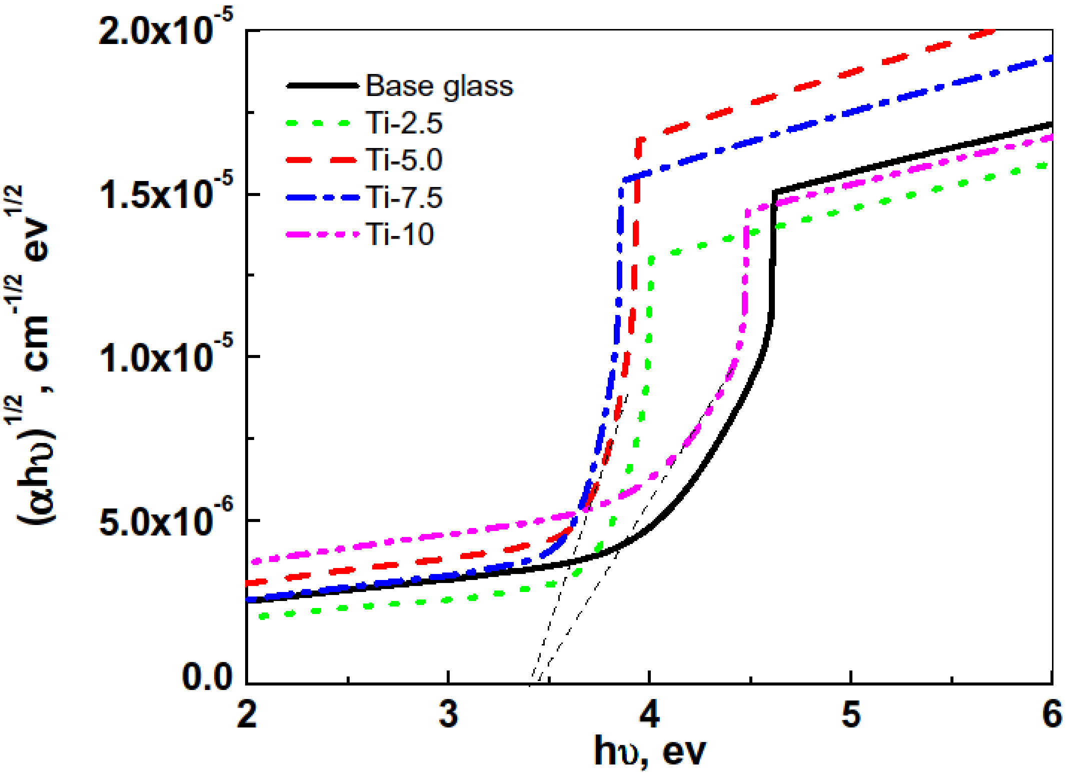

Figure 4-14: Tauc plots for Cs borosilicate glasses containing different amounts of TiO_2.

4.9 Discussion on Cs leaching and volatilization from structural aspect

The variation in the Cs volatilization and leaching behavior as a function of composition of the glass can now be explained with the help of structural information obtained from the results of FTIR, ^{11}B MAS NMR and uv-visible optical absorption studies. In base sodium borosilicate glasses containing Cs ('base glass'), both Na^+ and Cs^+ ions occupy the network modifying sites, viz., (Si-O^-) and BO_4^-. When part of B_2O_3 is substituted with TiO_2, initially (up to 2.5 mole% TiO_2), the relative concentration of BO_4 structural units increases as revealed by the ^{11}B MAS NMR studies. As a results of this, some of the alkali metal ions get attached to the non bridging oxygen atoms of Si or Ti, instead of BO_4^- structural units, which was also supported by FTIR studies (increase in number of non-bridging oxygen atoms) described above. The location of Cs/Na ions shift from the vicinity of BO_4^- structural units to that of Si/Ti structural units can be one of the possible reasons for the decrease of leach rate of alkali ions in the glass. It is also possible that there can be some preferential interaction of Cs and Na ions with the Si/Ti structural units and that may be the possible reason for the difference in leaching characteristics of Na and Cs ions from the glass. However in this study we do not have any evidence for such preferential interaction of Na and Cs ions with the glass structural units. Nevertheless, FTIR, ^{11}B MAS NMR and UV visible absorption studies revealed that the number of non bridging oxygen remained more or less constant after addition of 5 mole% TiO_2 or more. This confirmed that the excess TiO_2 is accommodated in glass network in forming silicotitanate type of cavity structural units where Cs^+ ions fit tightly, thus lowering lattice energy and in turn leading to lower leaching rate of Cs^+ ion.

The Cs volatilization behavior can also be explained to a certain extent by the structural information obtained from FTIR, ^{11}B MAS NMR and uv-visible optical absorption studies described above. Cs volatilization mostly occurs during the melting stage, as confirmed from Fig.4-4. It is assumed that the structural configurations existing at the melting stage remains the same of the glassy state as the structural configurations get trapped during the quenching of the melt. With the presence of Ti^{4+}, either at the network modifying or network forming sites, the interactions between the Ti^{4+} and Cs^+ ions exists and this can result in the lower Cs volatilization loss when compared to the glass without any TiO_2. However, the observed variation in Cs-volatilization loss for higher TiO_2 concentration could not be understood.

4.10 Summary of the results and conclusions

Results of present study on physico-chemical properties of Cs borosilicate glasses containing TiO_2 are summarized as follows.

1. The glasses prepared with incorporation of TiO_2 at the expense of B_2O_3 showed decrease in the extent of Cs volatilization.
2. The increase of TiO_2 content in glass resulted in improvement in chemical durability. This is attributed a combined effect of TiO_2 increase and B_2O_3 content decrease.
3. Based on the structural information obtained through FTIR, ^{11}B MAS NMR and uv-visible optical absorption studies, it is inferred that TiO_2 at lower concentration acts as a network modifier, while incorporation of more TiO_2 it goes to glass as network former.
4. Presence of TiO2 as network former affects the bonding nature of Na-O and Cs-O linkages in the glass.
5. From our studies, it can be concluded that 5 mole% TiO_2 incorporation in the glass gives the most suitable glass composition, possessing reasonably low leach rate and minimum Cs volatilization losses.

Chapter 5

Physicochemical properties of cesium borosilicate glasses containing divalent metal oxides

Physicochemical properties of cesium borosilicate glasses containing divalent metal oxides (CaO, BaO, MgO, SrO, ZnO)

5.1 Introduction

In chapter 4, the effect of TiO_2 on physicochemical properties of mixed alkali borosilicate glasses, Na_2O-Cs_2O-B_2O_3-SiO_2, was discussed. A similar approach was followed to evaluate the effect of different divalent oxides. It is well known that chemical durability of silicate/borosilicate glasses improve significantly in the presence of small amount of divalent oxides. For example, improvement of chemical durability of sodium silicate glasses in presence of CaO was first reported by Douglas et al[126] in early 1960. Later on, several oxides of divalent cations, like Zn, Ca and Ba have been used extensively to improve upon the chemical durability of borosilicate glasses for immobilization of high level waste [123, 127, 128]. Several studies were also carried out to establish the effects of the divalent modifiers on physicochemical and structural properties of borosilicate/aluminosilicate/silicate glasses[129, 130, 131, 132, 133, 134]. Most commonly studied physicochemical properties are chemical durability, softening temperature and density. It is revealed that among alkaline earth metal oxides the chemical durability of the sodium aluminosilicate glasses improved with the incorporation of MgO while CaO or BaO incorporation lead to highly durable borosilicate glasses[135, 136, 137]. Such variation in properties can be explained by the difference in behavior of the divalent cations in glass matrix.

Regarding Cs volatilization, a number of studies are available pertaining to vitrification of highly active nuclear waste [106-110, 138, 139]. These studies have revealed that the composition of the glass, including nature and concentrations of the constituents in waste, play a major role in the extent of Cs volatility. For example, the presence of Al, Ti, or Zn either in waste or as constituents of glass forming chemicals are known to suppress Cs volatility[140, 141] while the presence of chloride and technetium in waste accelerate volatilization of Cs[142, 143]. The nature of different Cs species getting volatilized from borosilicate glasses is also investigated by several authors[144, 145, 146]. These studies have confirmed that Cs can volatilize in the form of Cs_2O, CsOH, $CsBO_2$, $Cs_2(BO_2)_2$, and $NaCs(BO_2)_2$. In addition to the effect of the matrix composition on Cs volatilization, other factors like initial concentration of Cs, temperature, time and melt turbulence significantly influence the extent of Cs loss[115, 147]. It was found that studies on the volatilization of Cs as a function of divalent metal ion are very scarce. In view of the importance of such data and to generate an understanding on the subject, the volatilization behavior of Cs was investigated in detail during the course of this work.

In the present study, Physicochemical properties like density, molar volume glass transition temperature, Cs volatilization behavior and chemical durability of these glasses have been investigated with Cs containing borosilicate glasses having molecular formula $(SiO_2)_{0.45}$ $(B_2O_3)_{0.35-x}$ $(Na_2O)_{0.175}$ $(Cs_2O)_{0.025}$ $(CaO)_x$, where x =0 to 0.1 and $(SiO_2)_{0.45}$ $(B_2O_3)_{0.30}$ $(Na_2O)_{0.175}$ $(Cs_2O)_{0.025}$ $(MO)_{0.05}$, where M=Mg^{2+}, Ca^{2+}, Sr^{2+}, Ba^{2+} or Zn^{2+}. Structural aspects have been probed by using ^{11}B MAS NMR and FTIR techniques.

Major thrust of the work was to provide a detailed understanding on the leaching and volatilization behavior of Cs from borosilicate glasses containing different divalent metal oxides. Studies on Cs volatilization as a function of heating time and temperature helped in understanding the effect of composition. It was confirmed that the volatilization of Cs occurred predominantly through diffusion controlled process. From the temperature dependent volatility profiles of Cs, the activation energy and pre-exponential factor was calculated and found to be in the range of 300 – 500 kJ/mol and 10^3 - 10^{12} cm^2/s, lowest for ZnO and highest for CaO containing glasses. The interesting fact is that the pre-exponential factor and not activation energy control the Cs loss. The observed variations in the activation energy and pre-exponential factor have been explained by a unique model structure and possible interactions of Cs with different structural units that are formed due to incorporation of the different additives.

The elemental leach rate profiles of the glasses were determined by conducting leaching tests as a function of time. Structural alterations of the glasses before and after leaching were investigated by using FTIR and ^{11}B MAS NMR spectroscopy. Chemical durability of the glasses has been found to improve with incorporation of divalent modifier and this has been attributed to the formation of Ca^{2+} and Si rich layer at the outer surface of the glass, as inferred from SEM and EDX analysis with CaO containing glass. The possible role of molecular structure in controlling leaching of a complex glass system containing substantial amounts of Cs ions and CaO in varying concentrations was investigated. Based on the structural information obtained and with the help of derived model structure, the observed leaching behavior is also explained.

5.2 Glasses of present study

Altogether nine glasses including one base glass, four glasses containing varying concentration of CaO and four glasses containing of different divalent metal ions at 5 mole% were selected for this study. Nominal composition of the glass samples is given in Table 5-1. All these glasses were prepared in platinum crucibles (batch size: 50 g) by conventional melt quenching technique as per the process described in section 2.4.

Table 5-1: Nominal compositions of the Cs-borosilicate glasses (mole %) containing different divalent metal oxides

Batch No	**SiO_2**	**B_2O_3**	**Na_2O**	**Cs_2O**	**MO**
Ca-0	45	35	17.5	2.5	0.0
Ca-2.5	45	32.5	17.5	2.5	2.5 (CaO)
Ca-5	45	30	17.5	2.5	5.0 (CaO)
Ca-7.5	45	27.5	17.5	2.5	7.5 (CaO)
Ca-10	45	25	17.5	2.5	10.0 (CaO)
Mg-5	45	30	17.5	2.5	5.0 (MgO)
Sr-5	45	30	17.5	2.5	5.0 (SrO)
Ba-5	45	30	17.5	2.5	5.0 (BaO)
Zn-5	45	30	17.5	2.5	5.0 (ZnO)

5.3 Characterization of glasses

5.3.1 Chemical analysis of glass

Detailed chemical analysis of all the glasses containing CaO and the base glass were carried out and the results are given in Table 5-2 along with their nominal composition. Dissolution of glass samples and analysis of the dissolved glass were carried out as per the procedure discussed in section 2.5.2. Each analysis, starting from the dissolution was performed at least in duplicate and average results are presented. The variations in duplicate analysis results, varied from element to element, were observed to be around ±1% for Si and

Ca, ±5% for Na and Cs, and ±10% for B. Excluding the loss of the elements due to volatilization, the composition obtained are in accordance with batch composition.

Table 5-2: Chemical analysis results of the Cs-borosilicate glasses (wt %) containing different amount of CaO

Batch No		**SiO_2**	**B_2O_3**	**Na_2O**	**Cs_2O**	**CaO**
Ca-0	As added	40.8	33.8	15.4	10.0	0.0
	As measured	40.6	32.3	13.8	9.1	0.0
CBS-2.5	As added	41.0	31.5	15.5	10.0	2.0
	As measured	40.5	30.8	14.5	9.3	2.0
CBS-5	As added	41.2	29.2	15.5	10.1	4.0
	As measured	40.4	28.0	15.0	9.5	4.0
CBS-7.5	As added	41.4	26.9	15.6	10.1	6.0
	As measured	NM	NM	15.2	9.6	6.0
CBS-10	As added	41.6	24.5	15.7	10.2	8.1
	As measured	40.7	23.9	15.1	9.6	8.1

NM: Not measured

5.3.2 Density and molar volume

Density of the glass samples were measured by Archimedes method as described earlier (section 2.6). The experimentally measured density and calculated molar volume of the glasses containing varying concentration of CaO and the glasses containing different divalent metal oxides are shown in Fig. 5-1 and 5-2, respectively. Density of the glasses incorporated with different divalent metal oxides was found to increase with the increase of CaO incorporation at the expense of B_2O_3 and also with the increase of atomic weight of the incorporated divalent cation and can be represented as: Mg<Ca<Zn<Sr<BaO. The change in molar volume was

found to be almost the same (26.15±0.15 cm^3) and within the limit of experimental error. This suggests that the incorporated divalent cations are accommodated well within the interstitial voids in glass network. This result is in good agreement with that reported by Islam et al[136].

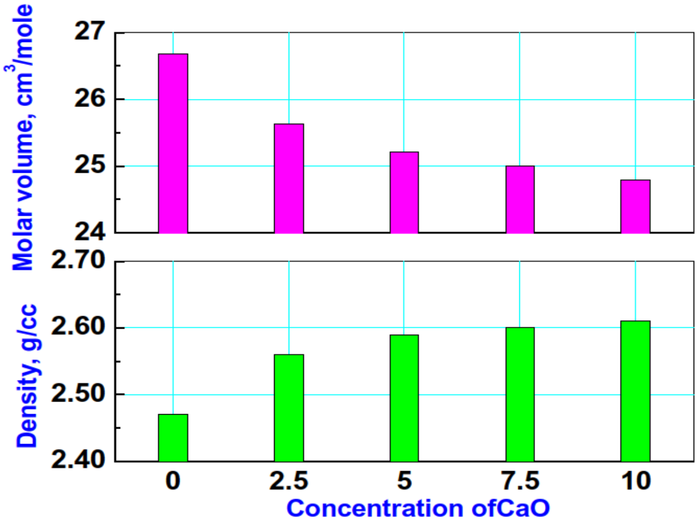

Figure 5-1: Density and molar volume of the Cs borosilicate glasses as a function of the incorporated CaO

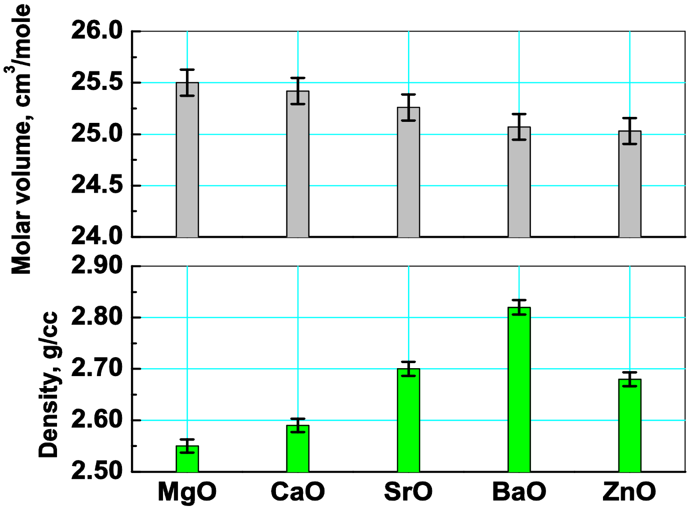

Figure 5-2: Density and molar volume of the Cs borosilicate glasses as a function of the incorporated MO in $(SiO_2)_{0.45}$ $(B_2O_3)_{0.30}$ $(Na_2O)_{0.175}$ $(Cs_2O)_{0.025}$ $(MO)_{0.05}$, where M=Mg^{2+}, Ca^{2+}, Sr^{2+}, Ba^{2+} or Zn^{2+}.

5.3.3 Glass transition temperature

Glass transition temperature was measured by differential scanning calorimeter (DSC-131, Setaram, France) in flowing Ar atmosphere, as per the procedure discussed in section 2.9.4.3. DSC patterns of all the glass compositions are found to be identical and a representative pattern for glass containing 5 mole% CaO is shown in Fig. 5-3. The values of glass transition temperature obtained from the DSC curves have been plotted as a function of composition in the inset of Fig. 5-3. The glass transition temperature of all the glasses was found to be same and within experimental errors. Value of T_g is a sensitive parameter which depends on the nature of the glass network. The fact that the T_g value is same for all the glass samples with different CaO content suggests that the glass network is not affected significantly by the CaO incorporation at the expense of B_2O_3 at these concentration levels. Further no crystallization is observed (up to 600°C) from the glasses as revealed by their DSC profiles.

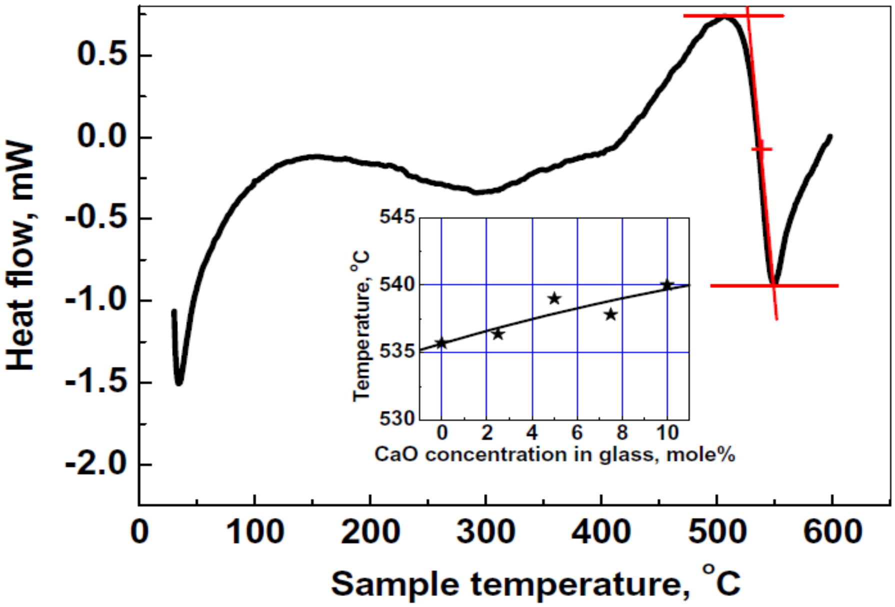

Figure 5-3: DSC pattern of the 5 mole% CaO containing Cs borosilicate glass sample, The inset plot represents values of glass transition temperature for the glass samples containing different amount of CaO

5.3.4 XRD study

XRD patterns of the glass samples (as melted) recorded showed a broad peak around a 2θ value of about 25°, characteristic of the amorphous borosilicate network. Absence of sharp peaks clearly confirmed that no crystalline phases (within the detection limits of XRD technique) are present in these glasses.

5.3.5 FTIR study

FTIR spectra of the glasses containing different amount of CaO are shown in Fig. 5-4 and 5-5 respectively. The glass sample without CaO is characterized by mainly three peaks centered at 1409 cm^{-1}, 987 cm^{-1} and 454 cm^{-1}. The peak around 1409 cm^{-1} is attributed to the B-O stretching vibration of BO_3 structural units present in the glass. The broad peak at around

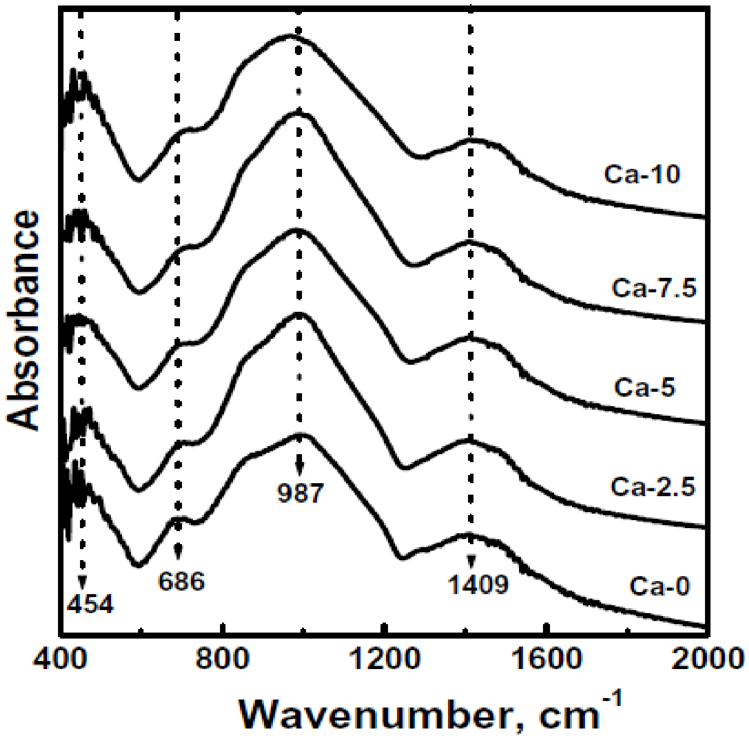

Figure 5-4: FTIR spectrum of Cs-borosilicate glasses containing varying concentrations of CaO over the region of 400-2000 cm^{-1}

987 cm^{-1} and weak shoulder around 686 cm^{-1} have arisen due to the asymmetric and symmetric stretching vibrations respectively of Si-O-Si/Si-O- B linkages present in the glass. The peak at around 454 cm^{-1} is due to the bending vibration of Si-O-Si/Si-O-B linkages.FTIR spectra of the CaO containing glasses were found to be almost similar to the base glass (without CaO), except for slight red-shift of Si-O-Si/Si-O-B asymmetric band (1000 to 970 cm^{-1}), and has been attributed to the weakening of the glass network. Further, line shape corresponding to the asymmetric stretching vibration of Si-O-Si/Si-O-B has been found to narrow with incorporation of CaO in glasses, as can be seen from Fig.5-5. The narrowing of line width signifies that strain/distortion associated with the borosilicate network gets reduced, which is possible when some bridging oxygen atom gets converted to non-bridging oxygen atom. It is therefore inferred that incorporation of CaO at the expense of B_2O_3, created more non-bridging oxygen atoms in glass. The non-bridging oxygen atoms can be created by formation of Si-O-Ca / B-O-Ca from Si-O-Si/B-O-B/Si-O-B bonds.

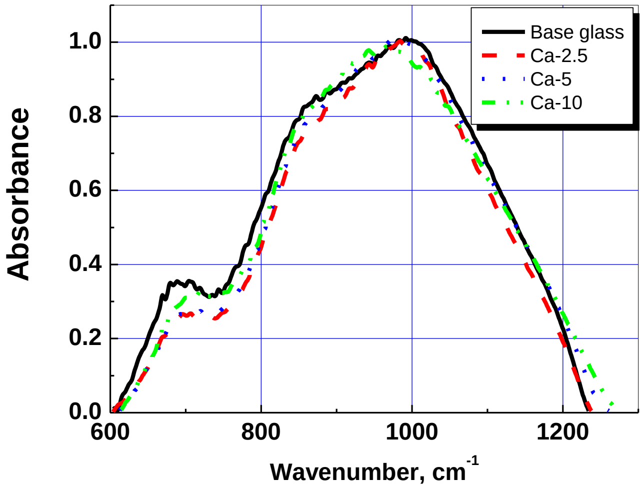

Figure 5-5: FTIR spectrum of Cs-borosilicate glasses containing varying concentrations of CaO (normalized at peak 970-1000 cm^{-1}

FTIR spectra (Figure 5-6) for the glasses containing divalent metal ions were found to be almost similar. For ZnO containing glasses, line shape corresponding to peak over the region of 400-600 cm^{-1} is found to be slightly different as compared to alkaline earth metal oxide containing glass. Vibration of ZnO_4 structural units in silicate glasses are characterized by peaks over the region of 400 to 600 cm^{-1} [148, 149]. In alkali silicate glasses, the existence of Zn^{2+} with tetrahedral coordination was confirmed from earlier X-ray, EXAFS and molecular dynamics study[150, 151]. In borosilicate glass also, presence of tetra coordinated Zn was confirmed through X-ray diffraction study[152]. The line shape change of the present FTIR study in the region of 400-600 cm^{-1}, though very weak, can be attributed to the overlapping of Si-O-Si bending modes with the vibrations of ZnO_4 structural units in the glass. Based on this result it was inferred that unlike alkaline earth metal ions, Zn^{2+} ions act as a network former and this may possibly be responsible for the lower loss of Cs by volatilization from ZnO glass.

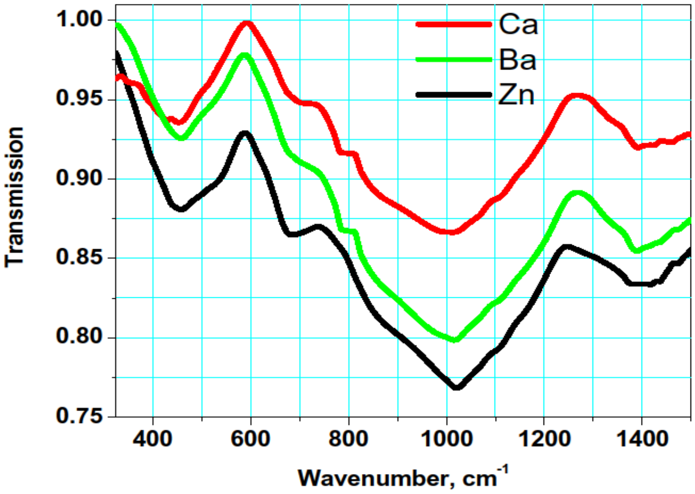

Figure 5-6: FTIR spectrum of the Cs-borosilicate glasses containing different MO, where M= Ca, Ba and Zn

5.3.6 ^{11}B MAS NMR study

^{11}B MAS NMR pattern of the glass samples containing different amount of CaO are shown in Fig. 5-7. All the patterns were found to consist of a less intense broad peak around -3 ppm and sharp peak around -19 ppm. The broad peak has been attributed to boron in trigonal (BO_3) and the sharp peak has been attributed to boron in tetrahedral (BO_4) configurations. In addition to this, few side bands are also observed which arise due to sample spinning.

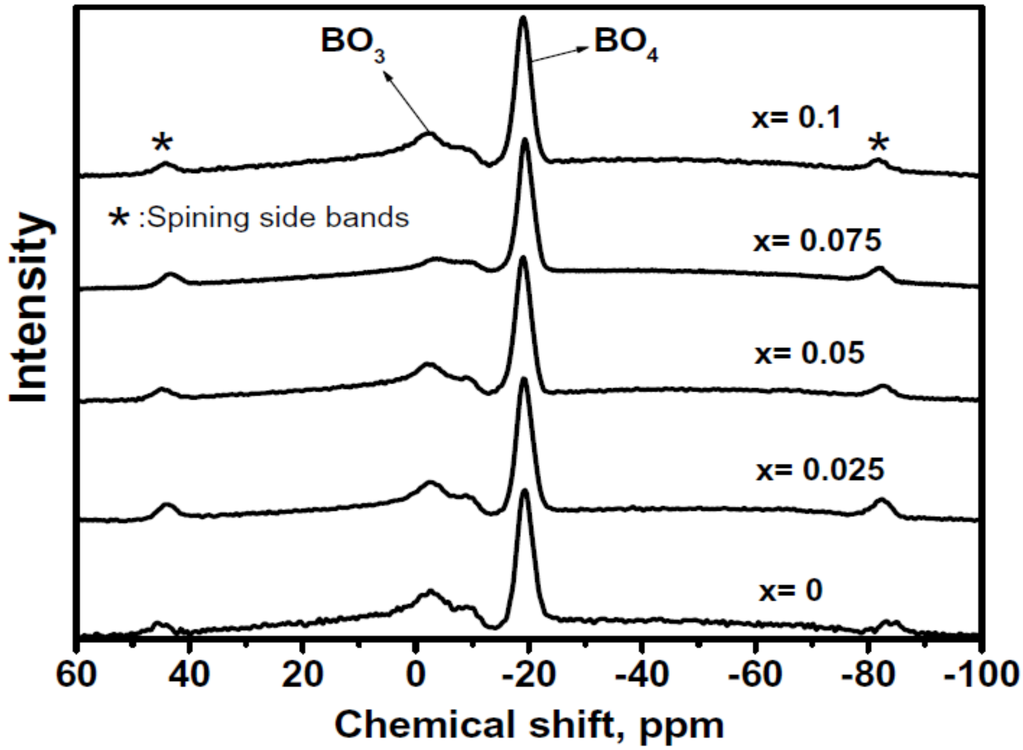

Figure 5-7: ^{11}B MAS NMR pattern of the Cs-borosilicate glasses of formula :$(SiO_2)_{0.45}$ $(B_2O_3)_{0.35-x}$ $(Na_2O)_{0.175}$ $(Cs_2O)_{0.025}$ $(CaO)_x$

Figure 5-8 shows the ^{11}B MAS NMR pattern of the glass samples containing different divalent metal oxides. In this case also, all the patterns are found to be similar as described above. The area under both the peaks has been obtained and the relative percentages of both

BO_4 and BO_3 structural units have been found to be 42±4 and 58±4 %, respectively. These values are in good agreement with the values calculated from well known model of Dell et al[153] assuming that the divalent ions act as a network modifier. The role of ZnO as a network former, as inferred from FTIR studies, is not reflected in the BO_3 and BO_4 values. These values are associated with some uncertainty due to loss of intensity corresponding to BO_3 structural units from its central transition under MAS. From the relative ratios of BO_3 and BO_4 structural units, it is inferred that these units are unaffected by the variation in the nature of the divalent cation in glass.

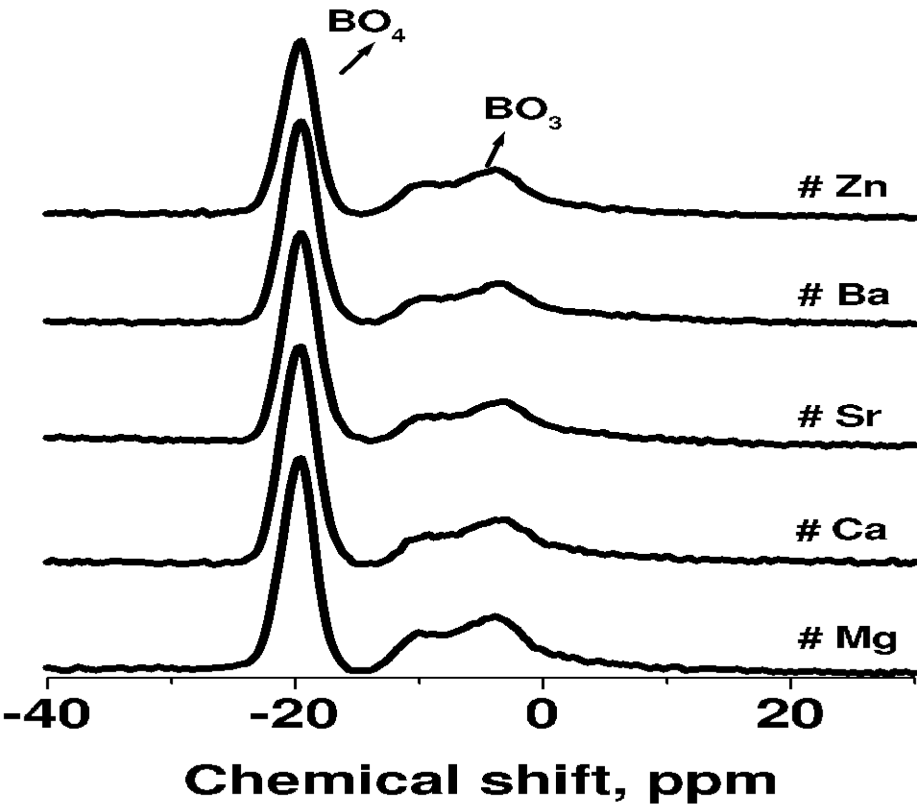

Figure 5-8: ^{11}B MAS NMR patterns of the Cs borosilicate glasses incorporated with different divalent cation (MO)

5.4 Volatilization of Cs

Among the three different methods of Cs volatilization study discussed in chapter 4, the heating of preformed glass followed by chemical analysis of the volatilized species has been found to be more suitable for evaluation of the effect of composition. In order to study the effect of CaO on the extent of Cs losses, three glass samples viz., Ca-0, Ca-5 and Ca-10, were used. Each glass in (25 g) alumina crucible was heated at 950°C for 30 hours at the rate of 6 h/d for 5 days. Results of this study are shown in Fig.5-9. It is clear that the glasses with CaO incurred higher volatilization loss of Cs than the base glass (without CaO) and loss of Cs increases with the increase of CaO loading in glass at the expense of B_2O_3. For all the glasses vaporization occurred through simple diffusion controlled mechanism as inferred from the straight line plot of Cs loss against square root of time[76]. As all the glasses are in molten stage

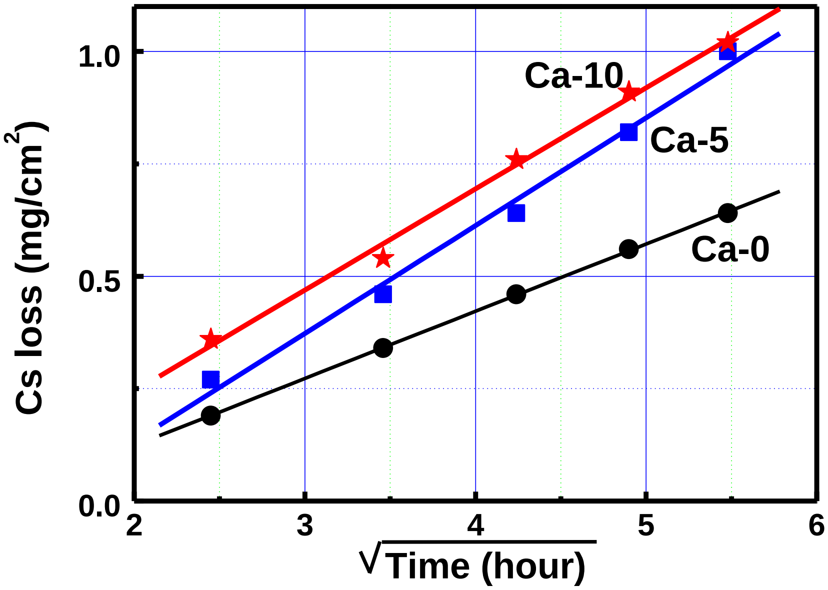

Figure 5-9: Loss of Cs from preformed Cs borosilicate glasses during heating at 950°C, Batch size: 25 g.

(at 950^{o}C) under the conditions of volatilization study and the extent of Cs volatilized is low enough with respect to the total Cs present in melt, it can be assumed that the matrix homogeneity remains intact throughout the course of volatilization study. Under this condition, the rate of diffusion is decided by the physiochemical properties, mainly viscosity of the melt. As the bond energy of Ca-O linkages is lesser than B-O linkages, it is expected that the viscosity of the glass melt will decrease with increase in CaO content at the expense of B_2O_3. Formation of lower viscous melt led to higher Cs losses for glasses containing CaO.

A similar study as mentioned above was carried out with four glass samples containing different divalent cations, viz., Mg, Ca, Ba and Zn. In this case, the glass samples were heated at 900^{o}C and the results are shown in Fig.5-10. Only for ZnO containing glass, the volatilization study was carried out in duplicate and the variations in values were found to be within 10%. For all the glasses, continuous loss of Cs was observed during the heating period

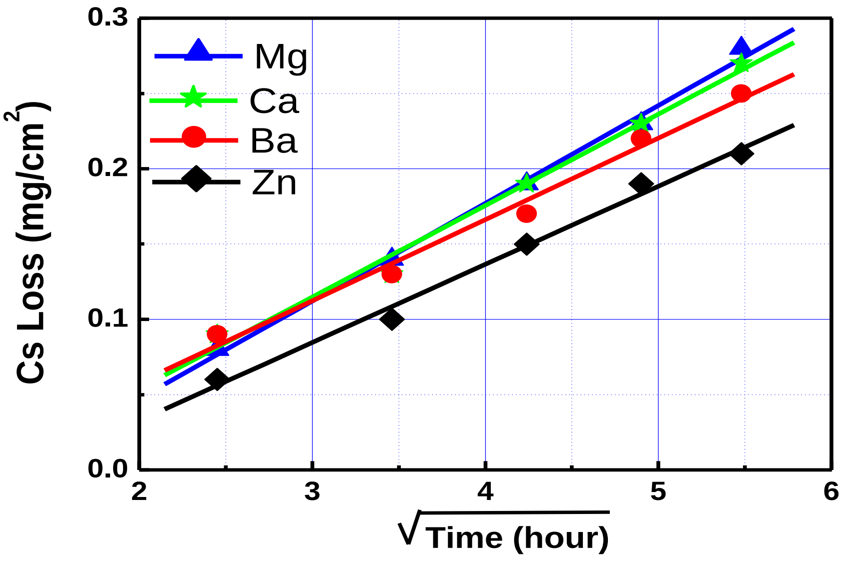

Figure 5-10: Cs loss from preformed borosilicate glasses incorporated with different divalent cations at 900^{o}C.

(~ 30 hours). Maximum loss of Cs occurred for the glass containing MgO and minimum for ZnO bearing glass. In terms of the lower loss of Cs, the glasses can be arranged as follows:ZnO<BaO≈CaO≈MgO . The Cs loss profile as function of square root of time showed a linear relationship indicating that the vaporization of Cs occurred through diffusion controlled mechanism.

The effect of temperature on Cs loss was investigated with four glass samples viz., glass samples containing 5 mol% either of CaO, BaO and ZnO and base glass. All the glass samples were heated at different temperatures namely 900, 950 and 1000°C and the cumulative loss of Cs after 24 hours of heating is given in Table 5-3. It can be seen that the extent of Cs loss for all the glasses heated at 900°C for 24 hours are in the range of 0.18 - 0.24 mg/cm^2. These marginal variations are within the limit of experimental errors and can be considered same. In other words, the influence of matrix formulation on Cs losses are not reflected for these glasses

Table 5-3: Cumulative loss of Cs (mg/cm^2) from the preformed Cs borosilicate glasses after 24 hours of heating at different temperature. General formula of the glasses: $(SiO_2)_{0.45}$ $(B_2O_3)_{0.3}$ $(Na_2O)_{0.175}$ $(Cs_2O)_{0.025}$ $(MO)_{0.05}$

MO	**Heating temperature, °C**		
	900	950	1000
ZnO	0.18	0.37	0.70
B_2O_3	0.23	0.52	1.23
BaO	0.22	0.63	1.49
CaO	0.24	0.77	2.31

samples heated at 900°C. However, 950 and 1000°C heated samples showed significantly higher Cs losses. Among the incorporated additives, the influence of ZnO in suppressing Cs volatility is clearly seen. Maximum loss of Cs occurred from the glass sample containing CaO. According to the lower Cs loss, the sequence of the incorporated oxides can be written as follows: ZnO < B_2O_3 < BaO < CaO. Observed variation in the Cs loss as a function of additives suggests that nature of additive plays a very important role in the extent of Cs loss from glass samples prepared at and above 950°C as can be seen from Table 5-3.

Further insight of the volatilization behavior was unveiled from the nature of the Cs loss profile presented in Figs. 5-11 to 5-14 in the form of cumulative Cs loss against square root of heating time. As observed for TiO_2 containing glasses (in section 4.7.1), only one slope in rate loss profiles was observed for all the glasses heated at temperatures 900 and 950°C.

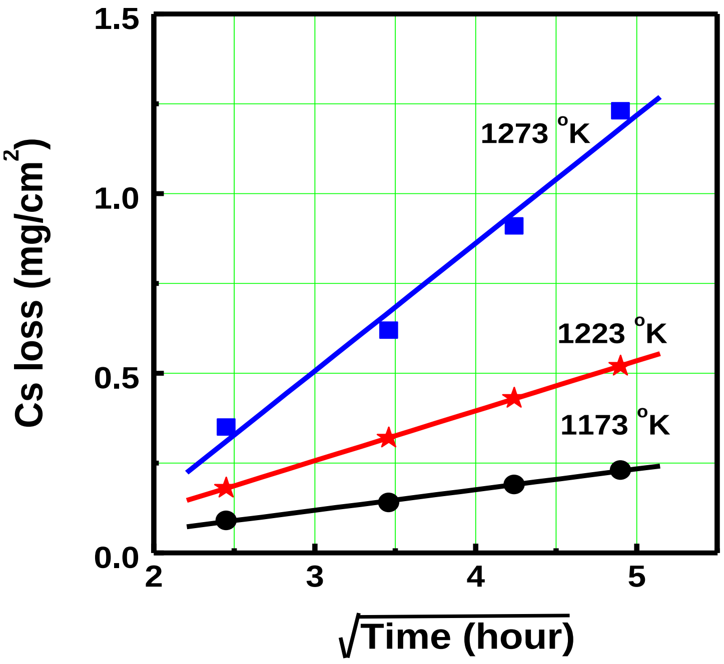

Figure 5-11: Cs loss profile as a function of square root of heating time for glass sample of molecular formula $(SiO_2)_{0.45}$ $(B_2O_3)_{0.35}$ $(Na_2O)_{0.175}$ $(Cs_2O)_{0.025}$ in dry air at different temperature

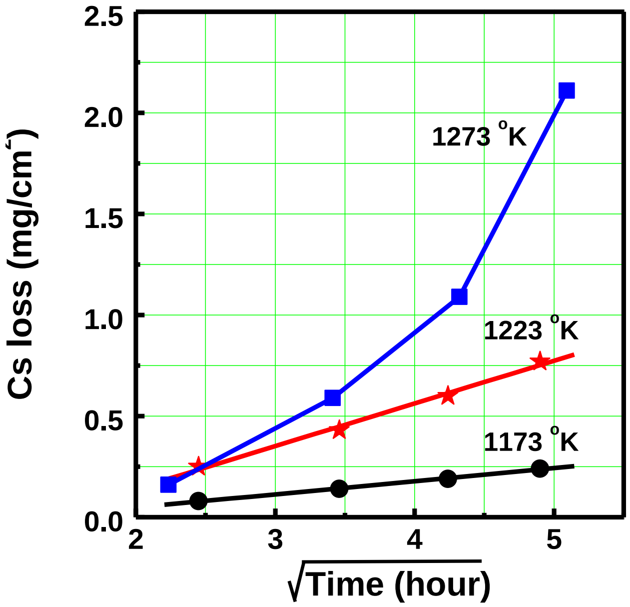

Figure 5-12: Cs loss profile as a function of square root of heating time for glass sample of molecular formula $(SiO_2)_{0.45}$ $(B_2O_3)_{0.3}$ $(Na_2O)_{0.175}$ $(Cs_2O)_{0.025}$ $(CaO)_{0.05}$ in dry air at different temperature

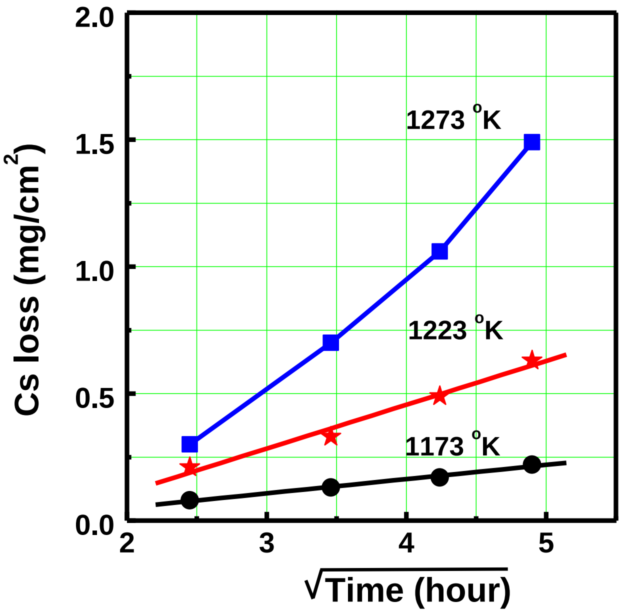

Figure 5-13: Cs loss profile as a function of square root of heating time for glass sample of molecular formula $(SiO_2)_{0.45}$ $(B_2O_3)_{0.3}$ $(Na_2O)_{0.175}$ $(Cs_2O)_{0.025}$ $(BaO)_{0.05}$ in dry air at different temperature

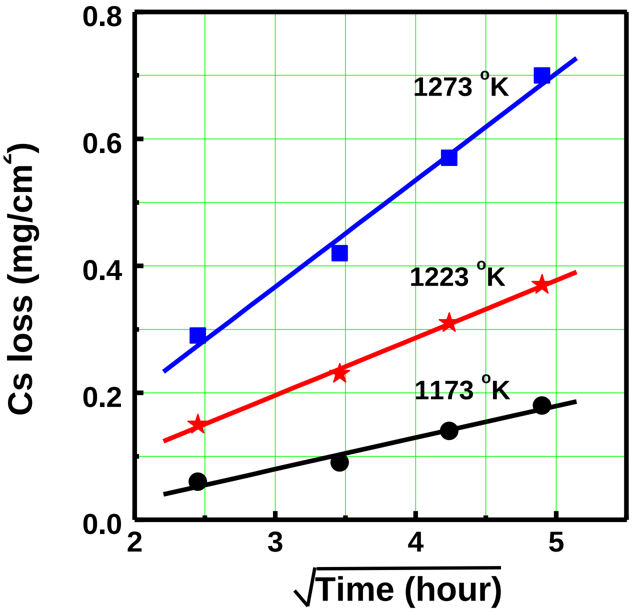

Figure 5-14: Cs loss profile as a function of square root of heating time for glass sample of molecular formula $(SiO_2)_{0.45}$ $(B_2O_3)_{0.3}$ $(Na_2O)_{0.175}$ $(Cs_2O)_{0.025}$ $(ZnO)_{0.05}$ in dry air at different temperature

The same is also true for the base glass and ZnO containing glass heated at 1000°C. This is attributed to the fact that volatilization occurred predominantly through one type rate determining process. In case of CaO and BaO containing glasses heated at 1000°C, the slope of the straight-line changed after approximately 15 hours suggesting that another process might be the rate controlling step. From the straight-line plots of cumulative Cs losses against square root of time, it can be stated that of Cs loss occurred predominantly through diffusion controlled process. The values of diffusion coefficients for all the glasses heated at three different temperatures were calculated adopting similar procedure as discussed in section 2.8.3 and D values are plotted as a function of 1/T and is shown in Fig. 5-15. From the slope and the intercept of each line, activation energy and D_0 values for Cs diffusion from the glasses have been calculated (Table 5-4). The activation energy values for all the glasses are in the range of

300 to 515 kJ/mol and was found to increase in the order ZnO<B_2O_3<BaO<CaO. The value of D_0 also followed the same trend, however, their magnitudes varied significantly in the range of 10^3 to 10^{12} cm^2/s. It is interesting to note that the Cs loss is lower when the activation energy for Cs diffusion is lower. Similar trends in weight loss and activation energy have also been reported for borosilicate glasses having different compositions by various authors[76, 117].The fact that low Cs loss corresponds to lower activation energy suggests that the D_0 value (pre exponential) is controlling the Cs loss. The Cs losses are found to increase with the increase of the D_0 value.

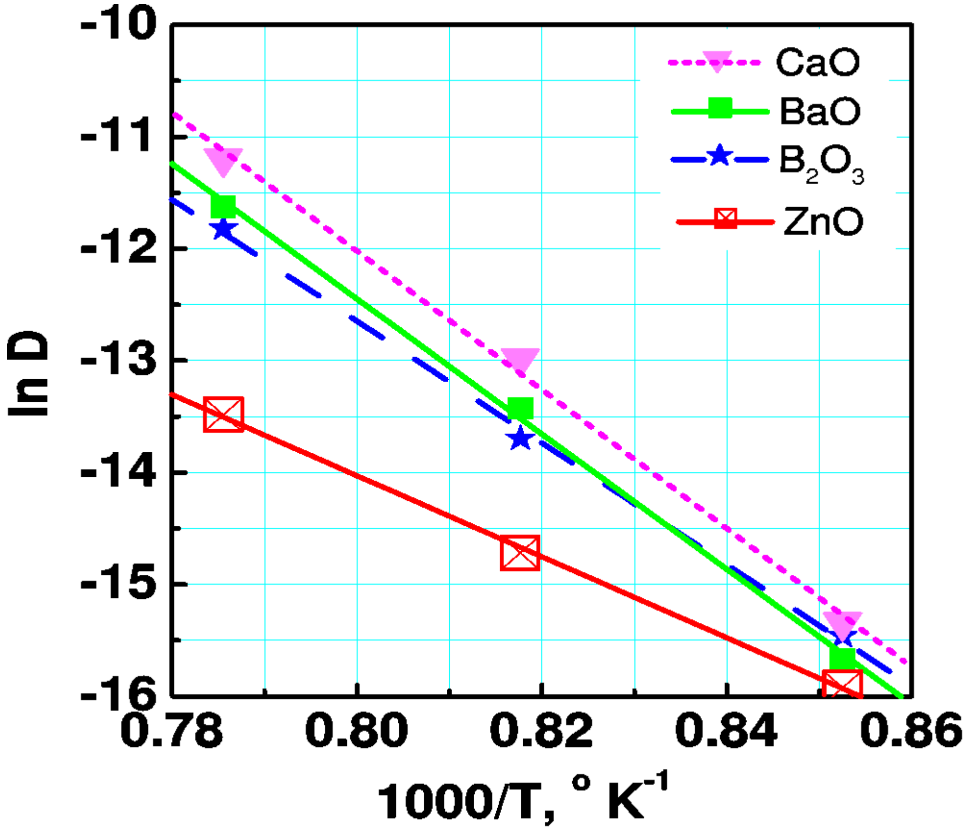

Figure 5-15: Plot of ln D vs 1000/T for Cs borosilicate glasses with different additives

Table 5-4: Activation energy and pre exponential factor for Cs volatilization from the glasses of general formula: $(SiO_2)_{0.45}$ $(B_2O_3)_{0.3}$ $(Na_2O)_{0.175}$ $(Cs_2O)_{0.025}$ $(MO)_{0.05}$

MO	**Cs taken for glass preparation (mg)**	**C_0 (mg/cm^3)**	**E (kJ/mole)**	**D_0 (cm^2/s)**
ZnO	2336	252.29	302 ± 10	9.8×10^{2}
B_2O_3	2358	232.03	452 ± 18	7.0×10^{9}
BaO	2223	250.75	502 ± 20	1.1×10^{12}
CaO	2378	246.36	515 ± 29	5.6×10^{12}

5.4.1 Discussion on Cs volatilization results

Although diffusion of any species from molten glass made of several oxides proceeds through a complex pathway, simple molecular interaction existing between the non-bridging oxygen and Cs^+ ions (diffusing ions) in glass is expected to significantly influence the observed variations in pre-exponential factor and activation energy values. This aspect has been considered to explain the variation in the pre-exponential factor and activation energy values in the present study. In general, the increase of ionic character of the O^-Cs^+ linkage results in a decrease of pre-exponential factor as well as activation energy. The covalent bond will have more energy and higher frequency. In order to find the nature of O-Cs linkages in the different glasses, structural elucidation of the glasses has been done by taking into consideration structural information of borosilicate glasses including possible inter linkages between different structural units. The base glass of the present study {molecular formula: $(SiO_2)_{0.45}$ $(B_2O_3)_{0.35}$ $(Na_2O)_{0.175}$ $(Cs_2O)_{0.025}$}is a simple alkali borosilicate glass with the atom ratio of Si:B:M:O=9:14:8:43, where M represents total alkali ions. For simplicity, it is assumed that each structural unit is built with 9 Si, 14 B, 8 M (alkali = Cs and Na) and 43 oxygen atoms. According to the model of Dell *et al*, sodium borosilicate glass containing Na/B < 0.5, all the alkali ions are utilized for charge neutralization of BO_4^- units[153]. The BO_4^- units can exist as diborate and reedmergnerite units. The base glass of this present study contains about 58% BO_4^- units, obtained from a ^{11}B MAS NMR (magic angle spinning nuclear magnetic resonance) study (Table 4-9). The 58% corresponds to approximately 8 out of every 14 B being present as BO_4^- . With these considerations, a model structural unit of the base glass is proposed which consists of interconnecting diborate and reedmergnerite groups and is shown in Fig.5-16.

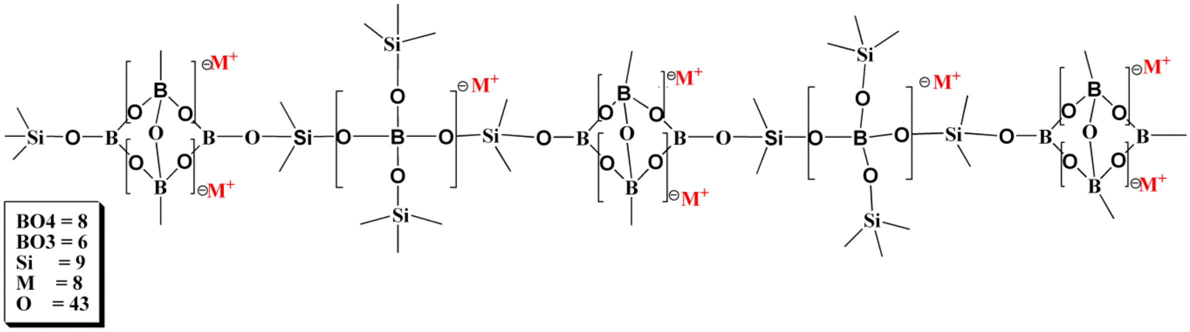

Figure 5-16: Model structural unit of the base glass

(*Atom ratio shown at the left side of the unit is as per molecular formula of the glass. Bonds represented without oxygen is part of extended network and have half contribution for this unit. The distribution* BO_4 *and* BO_3 *are taken from the results of* ^{11}B *MAS NMR study*).

Possible model structural units for other glasses are derived from this base model assuming that minimum changes are taking place in the presence of the variable oxide additive. As per molecular formula of Ca or Ba containing glasses, 9 Si, 12 B, 8 M, 1 Ca and 41 O are present and the measured concentration of BO_4^- units in these glasses was found to be about 64%. The structural unit of such glasses can be derived by subtracting 2 BO units from the base glass and adding 1 Ca and this is possible if 2 BO units are removed from one diborate as represented below in Fig.5-17. It can be seen that due to the formation of additional nonbridging oxygen by Ca^{2+}, the electron charge density on the BO_4^- ion will be greater and this will increase the covalent nature of the BO_4^- and Cs^+ interaction. This results in higher activation energy as well as higher pre-exponential values for Cs diffusion. This is in accordance with the increase of activation energy for Na^+ diffusion with the increase of Ca^{2+} or Ba^{2+} in borosilicate glasses as reported by different groups[154, 155], which has been explained by considering the dipole–dipole interaction between non bridging oxygen and Na^+ ions. The simple molecular interactions as indicated above are similar to the dipole-dipole interaction, however considering the nature of bonding helps to explain both the activation energy and pre-exponential factor.

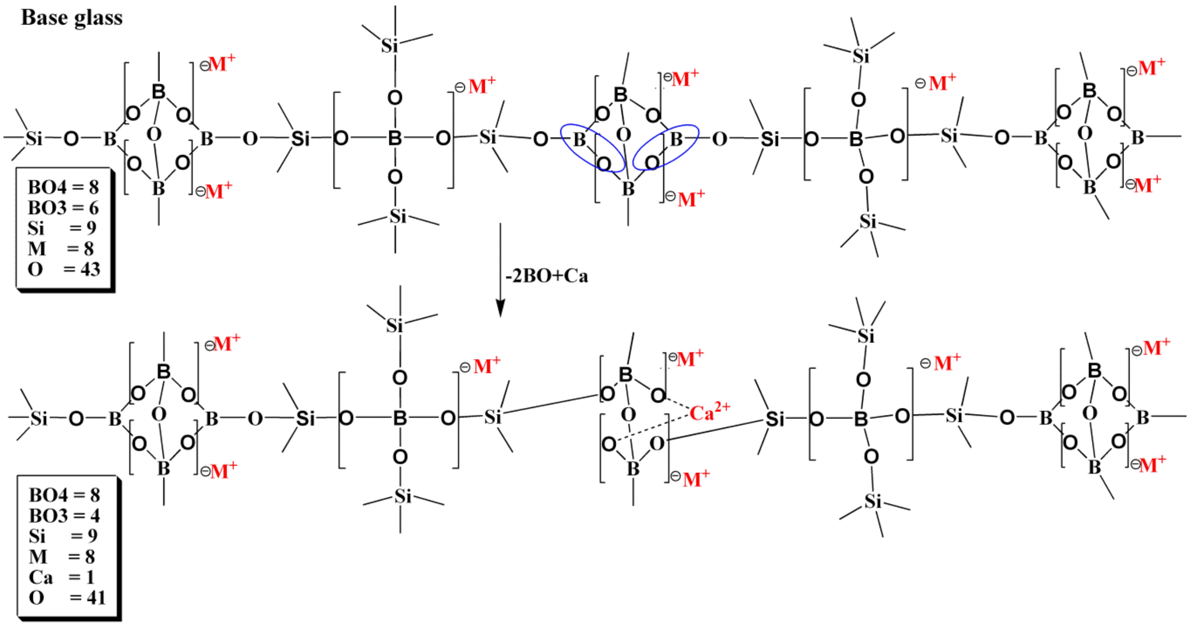

Figure 5-17: Model structural unit of the Cs borosilicate glass containing CaO along with its formation from base glass.

(*Atom ratio from molecular formula and distribution of BO_3 and BO_4 from ^{11}B MAS NMR results are shown at the left side of the each unit*).

Similarly, one might expect higher activation energies for glasses containing ZnO. However, the observed results of lowest activation energy and lowest pre-exponential factor for ZnO containing glass suggest that the behavior of Zn^{2+} is not similar to Ca^{2+}. This can be explained by considering the formation of ZnO_4^{-2} units in the glass. The proposed structural unit of this glass is indicated in Fig.5-18. It can be noted from Fig.5-18 that the total amount of BO_4^- units is reduced to 50% (from 58% in base glass). The experimentally measured BO_4^- concentration of about 54% supports this. In this configuration, two M^+ are attached to a single ZnO_4^{-2} as compared to base glass where two M^+ were associated with two BO_4^- units. Because of the bigger size of the ZnO_4^{-2} anion, its interaction with M^+ will be more ionic in nature when compared to the interaction between BO_4^- with M^+. This can explain the lower activation energy and lower pre-exponential factor for the Zn containing glasses. An alternative configuration would be to put Zn in place of B in the reedmergnerite unit and to remove one B and two O from the diborate unit which will also lead to the same final outcome.

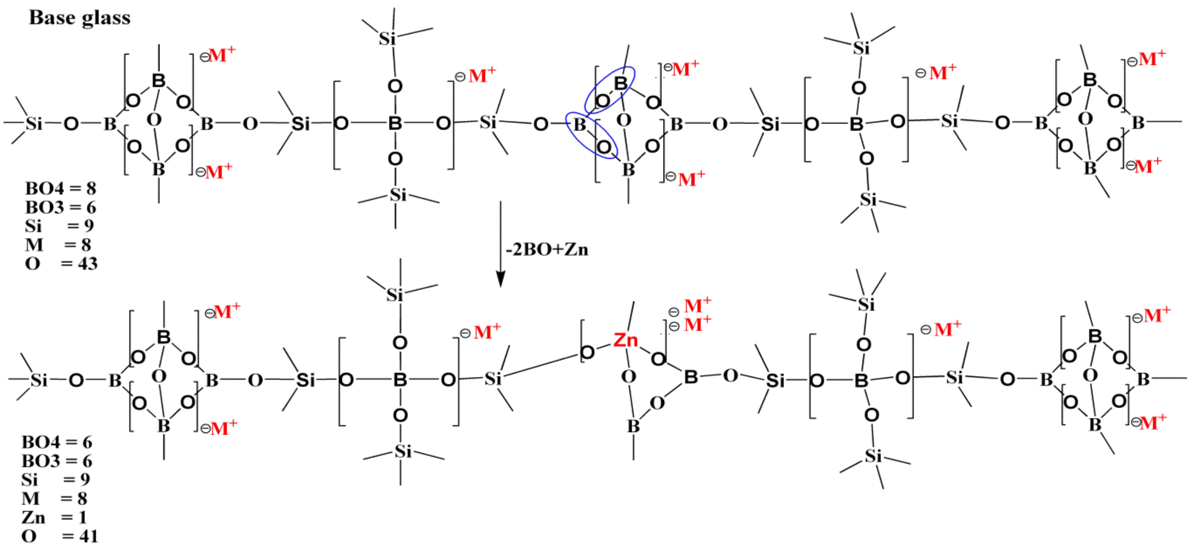

Figure 5-18: Model structural unit of the Cs borosilicate glass containing CaO along with its formation from base glass.

(*Atom ratio from molecular formula and distribution of* BO_3 *and* BO_4 *from* ^{11}B *MAS NMR results are shown at the left side of the each unit*).

5.5 Leaching study

5.5.1 Leaching tests in distilled water at 90°C for 24 h

Short duration leaching tests (24 h) were carried out for the comparative evaluation of formulation. The result of leaching tests for CaO containing and different divalent metal oxide containing glasses are presented in Fig. 5-19 and 5-20, respectively. Based on duplicate experiments, the variations in the values have been estimated to be around 10%. It can be seen from Fig.5-19 that both Na and Cs leach rate decrease significantly with increase of CaO incorporation at the expense of B_2O_3. For all the glasses, the leach rates for Na and Cs were significantly higher, whereas Si leach rate was found to remain the same. With respect to Na leach rate, a similar trend in durability was observed for borosilicate glasses of different composition by Chick et al[99]. It is noteworthy to mention that in the present study Na leach -

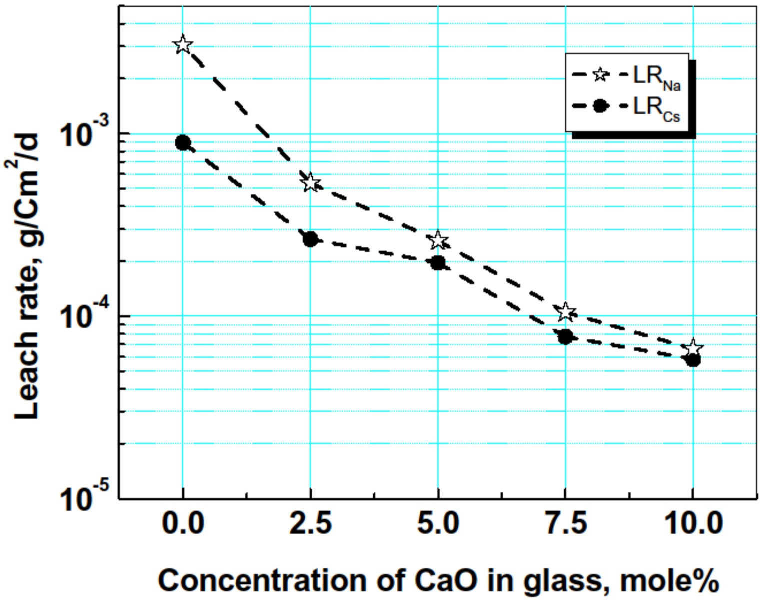

Figure 5-19: Leaching of Na and Cs from Cs-borosilicate glasses in distilled water at 90°C for 24 hours, lines are guided to eye.

rate of the glasses improved more than the Cs leach rate. For example, Na and Cs leach rates of the glass containing 10 mole% CaO were found to improve 45 and 15 times, respectively, as compared to those in base glass (Ca-0). The improvement in the durability of the glass can be explained by considering the cumulative effect of the decrease in B_2O_3 content and increase in CaO content in the glass.

Among the glasses containing different divalent metal cation, MgO glass showed highest leach rates for Na and Cs (Fig. 5-20). The Na and Cs leach rates for Zn oxide bearing glass were found to be marginally lower than MgO and higher than the glasses containing other oxides of group-II (Ca, Sr, Ba) metal ion. The glasses obtained by incorporating the other oxides of group-II (Ca, Sr, Ba) metal ion are similar with respect to their corrosion resistance to hydrolytic attack. According to lower leach rates of Na and Cs, the glasses can be arranged as follows: BaO ≅SrO < CaO < ZnO < MgO. The higher release of Na and Cs ion in leachate is reflected in the pH of the solution. As expected, highest pH (9.6) in leachate was observed for MgO bearing glass and lowest (9.2) for BaO containing glass. Interestingly, similar pH (9.4) was observed for ZnO and CaO containing glasses on dissolution, although the concentration of Na and Cs ions in leachate of ZnO glass is significantly higher than in CaO glass. This is possibly due to some ZnO leaching out and its amphoteric nature leading to reduction in pH of the medium. The dissolution rate for alkaline earth metal ions was found to increase from Mg to Ba. This can be explained by considering the rate of reaction of these alkaline earth oxides with water and the solubility of the corresponding hydroxides in water. It is known that the rate of reaction of these alkaline earth oxides with water increases as MgO<CaO<SrO<BaO and the solubility of the corresponding hydroxides increases as $Mg(OH)_2 < Ca(OH)_2 < Sr(OH)_2 < Ba(OH)_2$. It is interesting to note that the sequence of alkali ion leaching observed in the present study is reverse from that reported by Paul and Israd for sodium silicate and sodium aluminosilicate glasses containing different alkaline earth metal oxides[102, 134]. In order to understand the observed sequence of durability, detailed studies have been carried out and the results are discussed below.

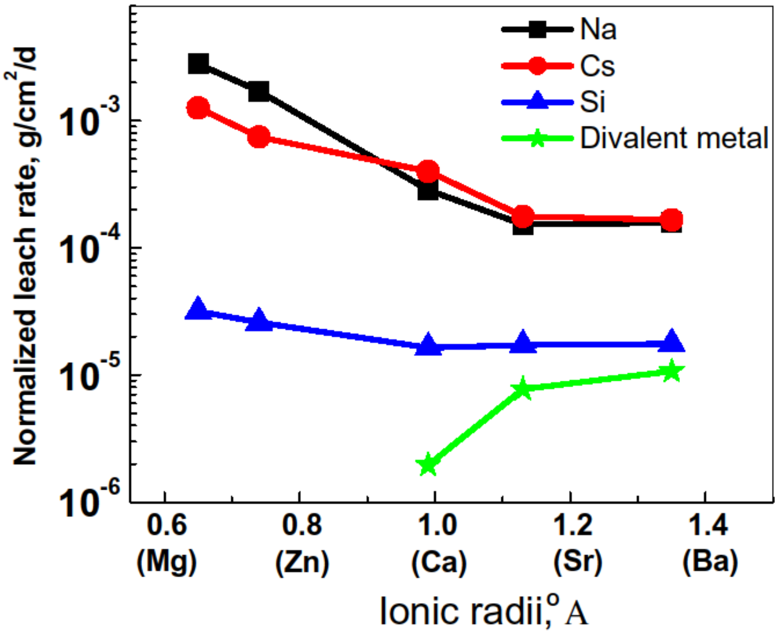

Figure 5-20: Elemental leach rates from the borosilicate glasses against the atomic radii of the incorporated bivalent cation (MO)

5.5.2 Leaching tests as a function of time

Detailed leaching tests, as a function of leaching time were conducted with the three glasses containing 0, 5 and 10 mol% CaO. Elemental leaching profiles of these glasses evaluated over a period of 7 days are shown in Fig. 5-21. The elemental leach rate was found to follow the order: Na>Cs ≈ B >> Ca ≈ Si (leach rate for Ca is not shown in the figure). The pH of leachates for all the samples was within 9.3 to 9.0, highest for base glass (Ca-0) and lowest for glass Ca-10, containing 10 mole% CaO. This lower pH, in-spite of the higher concentration of Na^+ and Cs^+ ions in leachate in the base glass can be attributed to neutralization of some alkali ions by the higher concentration of B in leachate. This lower pH also helped to restrict the silicate network dissolution, which can be inferred from the lower concentrations of Si in leachate. It is observed that for glass sample without any CaO, the amount of sodium leached out is around 50 % of total sodium present in the glass. Unlike this, the extent of leached out sodium is found to be only around 5 and 3 % for the glass samples containing 5 and 10 mol % CaO, respectively. From these results, it can be inferred that CaO plays crucial role probably by forming a protective layer around the surface of the glass[129]. In order to confirm this, SEM, XRD and structural studies have been carried out and the results are discussed below.

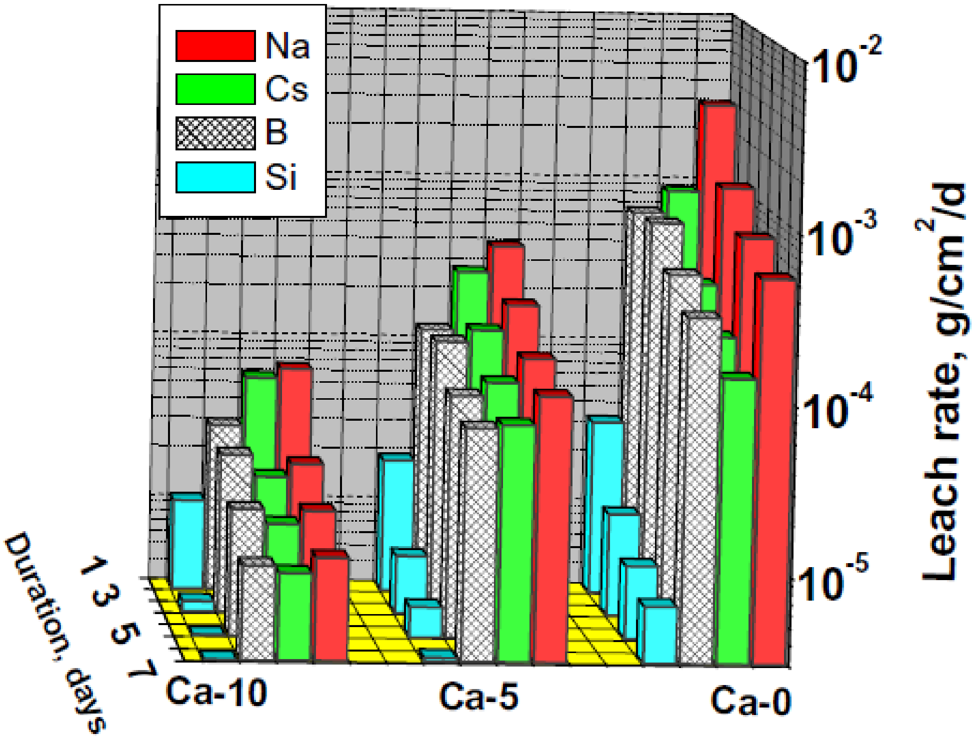

Figure 5-21: Elemental leaching profiles of the Cs borosilicate glasses containing varying concentrations of CaO as a function of leaching time. (*leaching in distilled water at 90°C*).

5.5.3 Discussion on leaching results

It is known that leaching of alkali ions from glass is the result of reaction between glass and water followed by transport of the ions[103]. The overall rate of the reaction depends on several factors like composition of glass, nature and composition of leachant, pH of leachant, reaction time, temperature, extent and nature of leached layer formation. Moreover, it is the cumulative result of the processes, like (i) ion exchange reaction of alkali ions and H_3O^+ in solution (ii) hydrolysis of Si-O/B-O bonds (iii) condensation of aqueous species at reaction inter-phases (iv) precipitation of secondary phases, etc[102-105]. The ion exchange reaction and network hydrolysis occurring during the leaching process can be generally expressed by the following reactions

$$\text{-Si-O-Na} + H_2O = \text{-Si-O H} + Na^+ + OH^- \qquad \ldots\ldots (17)$$

$$\text{-Si-O-Si-} + H_2O = 2\,(\text{Si-OH}) \qquad \ldots. (18)$$

5.5.4 Mechanism of leaching process

In order to identify the predominant process, leaching tests were conducted as a function of time and the results are presented in Figure 5-22. The amount of Cs leached out at 90°C from both the glasses followed a straight line relationship against square root of time which is a characteristic of a diffusion controlled process. Similar observations were also noted in the case of Na ion leaching.

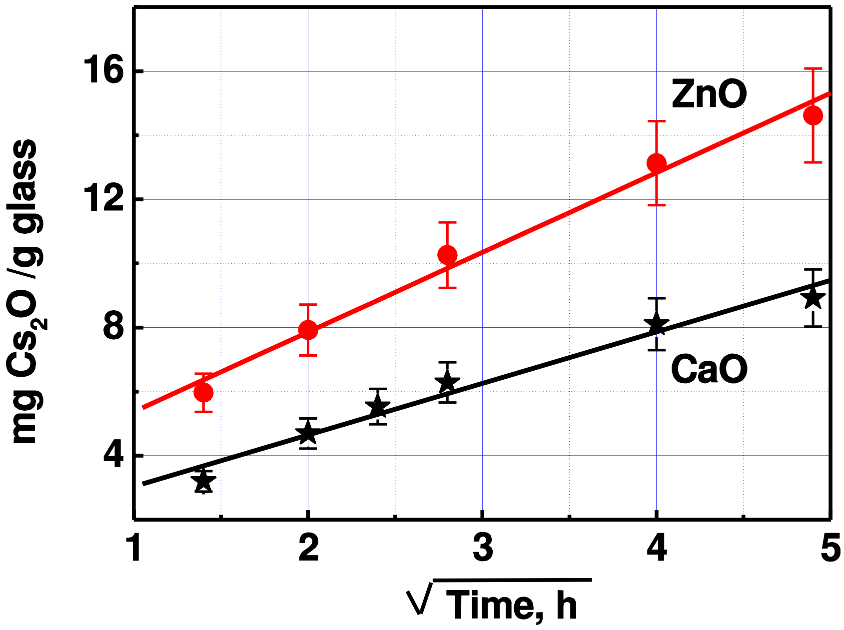

Figure 5-22: Kinetics of Cs extraction from ZnO and CaO bearing Cs-borosilicate glasses in distilled water at 90^{o}C

5.5.5 Identification of leached layer

The formation of leached layer if any will be more prominent in the sample leached for longer duration. The test was therefore carried out with the 5% CaO containing glass sample in bead form leached for 7 days. After leaching, the samples were washed in acetone, dried at 110 ^{o}C. A cross section of the bead was cut using diamond saw to observe and study the interface. Due to the charging/insulating nature of the sample, a thin gold coating (~50nm) was applied prior to loading the sample. Fig.5-23 shows the cross-sectional SEM image of 5% CaO containing glass sample leached for 5 days at 90°C. Three regions with distinctly different morphologies namely the resin, interface and bulk glass, can be seen from the image. The interface region was found to have a width of approximately 40-50 µm.

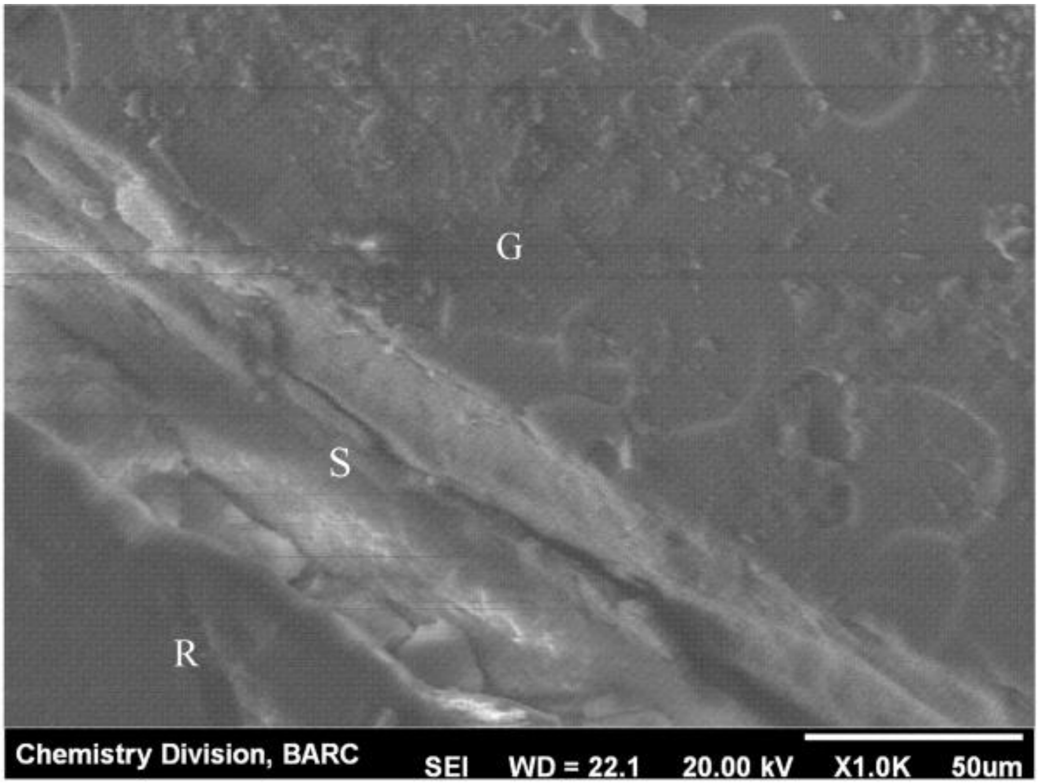

Figure 5-23: SEM micrograph of 5 mole% CaO containing glass sample (after 5 days leaching in distilled water at 90^{o}C). Here, G, S and R represents bulk glass, outer surface and resin, respectively

EDX analysis on the bulk glass showed the presence of all the elements whereas the interface region showed Ca, Si and Cs only (Fig. 5-24). Based on these results it is inferred that a calcium and silicon rich layer was forming at the glass surface and this layer is responsible for the improved leaching properties of the CaO containing glass sample.

The same is expected to be true for the other glasses of present study when another divalent metal ion was incorporated in place of CaO. As the measured rate of release of divalent metal ion from the glasses was found to increase from Mg to Ba and the relative stability of the M-SiO_3 (M-divalent metal ion) also increased in the same order, it can be stated that extent of leached layer formation is highest for BaO glass and lowest for MgO glass. This explains the sequence of Na and Cs leach rate among the glasses (MgO<CaO<SrO<BaO) investigated.

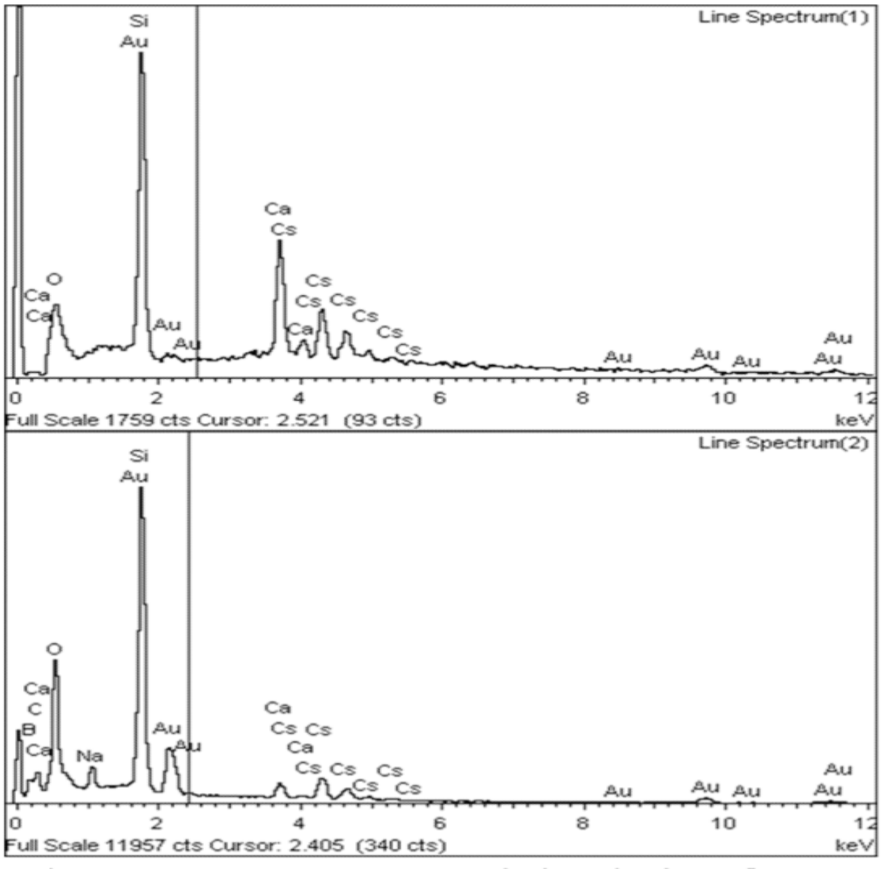

Figure 5-24: EDX spectra recorded at the interface. The line spectrum 1 and line spectrum 2 represent outer surface layer and bulk glass, respectively

5.5.6 XRD study of the leached glass samples

XRD pattern of the glass samples after 7 days of leaching were also recorded and the profile is shown in Fig.5-25 along with the corresponding glass sample before leaching. It is clearly evident that no crystalline phases are formed due to leaching, possibly due to the amorphous nature of leached layers.

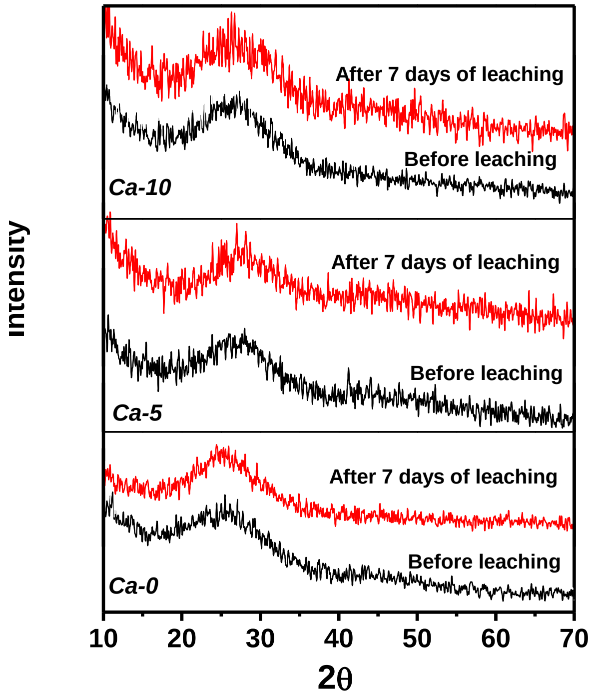

Figure 5-25: XRD pattern of the Cs-borosilicate glasses before and after leaching

5.5.7 FTIR study of the leached glass samples

Figure 5-26 shows the FTIR patterns of the base glass (Ca-0) samples obtained after leaching for different time periods. For the sake of comparison, spectrum of parent (unleached) glass is also shown. As compared to un-leached glass, the peak corresponds to asymmetric stretching vibrations of Si-O-Si/Si-O-B linkages blue-shifted from 987 to 1050 cm^{-1}. The shifting of the band has been attributed to the formation of more covalent Si-OH bonds at the expense of Si-O^{-} Na^{+} linkages. These Si-OH bonds are likely to be formed by the hydrolysis of the network as represented in equation 17. The peak corresponding to B-O stretching vibration also shifted from 1408 to 1535 cm^{-1} with significant reduction of the peak intensity. This is attributed to the combined effect of B-OH bond formation and dissolution of BO_4/BO_3 structural units during leaching. Substantial amount of boron concentrations in the leachate further confirm this. In other words, both boron and silicon structural units undergo significant hydrolysis. The noteworthy feature of these FTIR spectra is that the line width corresponding to 987 cm^{-1} peak has significantly reduced in leached samples (Fig. 5-26) compared to the parent glass, indicating a reduction in the extent of network polymerisation (more number of non-bridging oxygen are created during leaching).

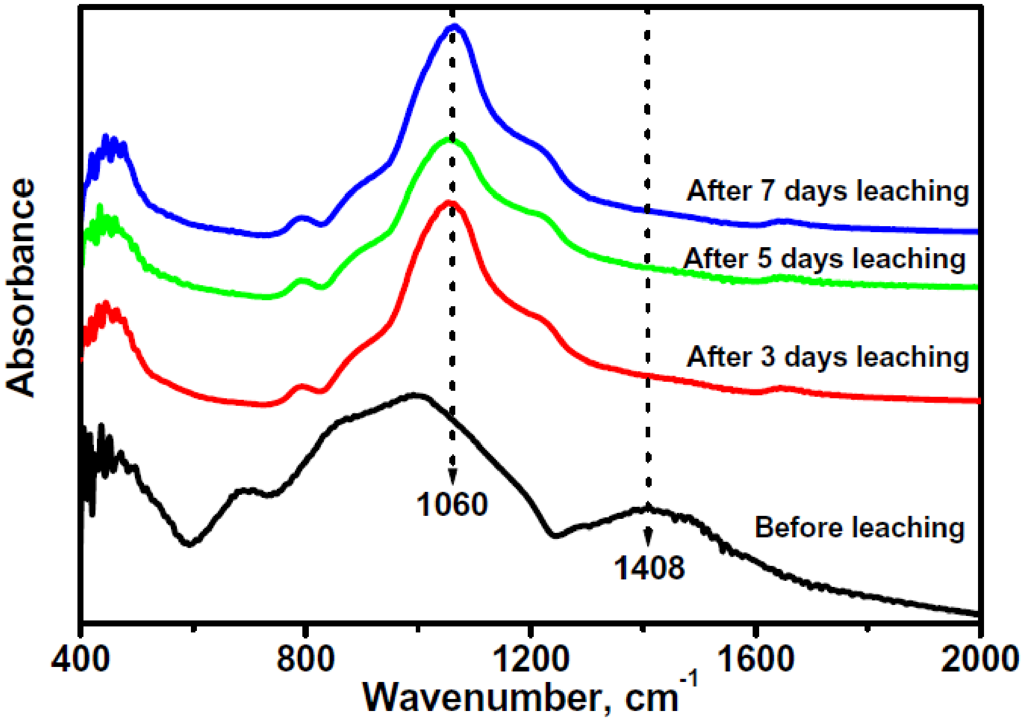

Figure 5-26: FTIR spectram of the base Cs-borosilicate glass without CaO before and after leaching

Fig.5-27 shows the FTIR pattern glass samples containing 5 mole% CaO (Ca-5) before and after leaching. The patterns are found to be identical as no change of the peak position and line shape corresponding to asymmetric Si-O-Si/Si-O-B vibrations was observed, even though there is a slight decrease in the line width corresponding to this peak. Similar observation is also noted for the glass containing 10 mole% CaO (Ca-10). Based on this results it is inferred that the extent of hydrolysis is significantly reduced for the glass samples containing CaO.

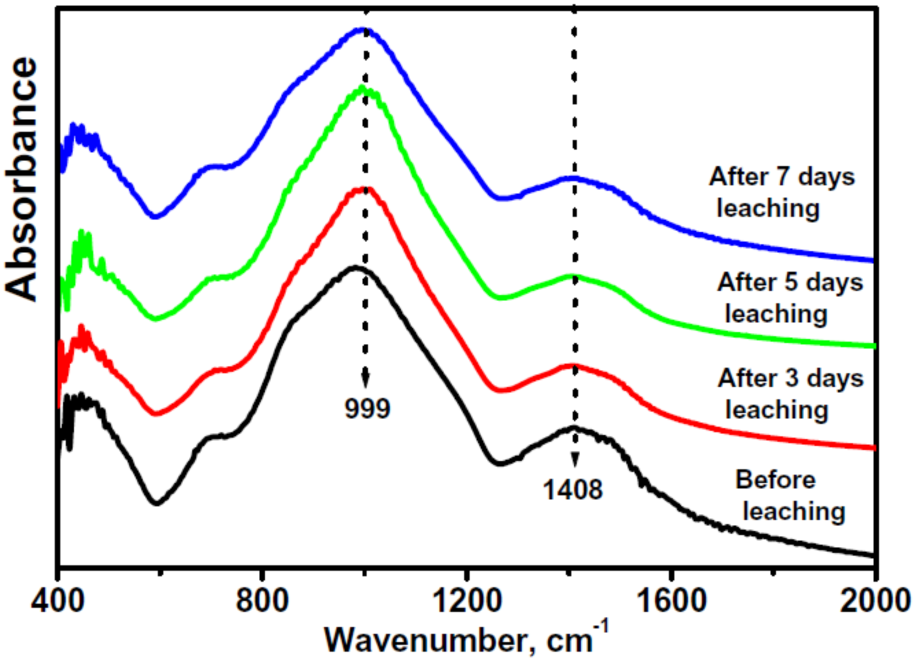

Figure 5-27: FTIR spectram of the Cs-borosilicate glass containing 5 mole% CaO before and after leaching

5.5.8 ^{11}B MAS NMR study of the leached glass samples

Figure 5-28 shows the ^{11}B MAS NMR patterns of leached and unleached glass samples with 5 mole% CaO and base glass (without any CaO). The ^{11}B MAS NMR patterns were found to be comparable for both the samples in terms of the peak position and line shape. Apparently, the relative intensity of peak corresponding to BO_4 structural units increases compared to BO_3 structural units in leached glass sample without CaO. As the leached volume fraction is substantial for glass sample without CaO and NMR gives an average picture of ^{11}B structural units present in leached and unleached fractions, it is not proper to compare the relative intensities of BO_3 and BO_4 structural units in the glass samples before and after leaching. Nevertheless it can be inferred that the BO_3 structural units are more susceptible for leaching compared to BO_4 structural units and that is reflected in the intensity profile. For glass samples containing $\geq$ 5 mole% CaO, the relative intensity of peaks corresponding to BO_3 and BO_4 structural units remained same before and after leaching (Fig.5-28) suggesting that the glass network is more stable against hydrolytic attack when CaO is present. These results are in conformity the FTIR studies.

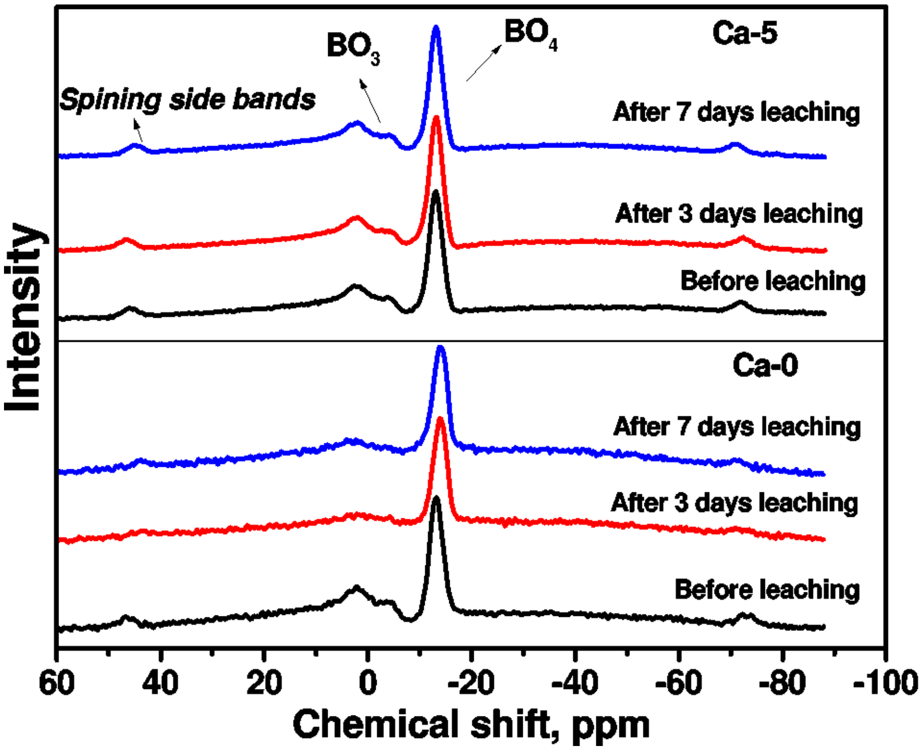

Figure 5-28: ^{11}B MAS NMR pattern of base (without CaO) and 5 mole% CaO containing glasses before and after leaching

5.6 Summary of the results and conclusions

Results of the present study can be summarized as follows:

1. Physiochemical properties of the Cs borosilicate glasses alter significantly due to incorporation of the different divalent cations. For example, density of the glasses increases with increase of atomic weight of the incorporated divalent cation. Chemical durability of the glasses was found to improve with the incorporation of CaO or BaO. However, it was found that the incorporation of CaO or BaO lead to higher volatilization loss of Cs. The incorporation of ZnO in glass helped to suppress the Cs volatilization loss.
2. Incorporation of CaO at the expense of B_2O_3 in Cs borosilicate glasses has been found to improve their leaching characteristics. Formation of protective amorphous layer at the interface enriched with Ca and Si, as revealed by the SEM and EDX studies, is responsible for the improved leaching characteristics of the glasses. It is established that diffusion controlled ion exchange is the rate controlling process for leaching of mobile Na/Cs ions from these glasses. According to lower leach rates for alkali metal ions, the glasses can be arranged as: BaO $\cong$SrO < CaO < ZnO < MgO. FTIR and ^{11}B MAS NMR studies confirmed that the borosilicate network remains unaffected during leaching for the glasses containing $\geq$ 5 mole% CaO.
3. It is confirmed that the Cs volatilization from the glass melt occurs through a diffusion controlled process. The extent of loss due to Cs volatilization increases with increase of CaO content in the glass. The observed sequence in terms of increasing loss of Cs was found to be: ZnO<BaO<CaO<MgO. Based on the results of this study, it is concluded that the addition ZnO to a simple alkali borosilicate glass is highly beneficial with

respect to a reduction of Cs volatility, while the effects of CaO or BaO incorporation are detrimental. Volatilization profiles for Cs from all the glasses followed a diffusion controlled process. Temperature dependence of Cs volatility profiles confirms that pre-exponential factor and not the activation energy for Cs diffusion influences the extent of Cs loss. The pre-exponential factor and activation energy for Cs diffusion in these compositions were found to be in the range of 10^3 to 10^{12} cm^2/s and 300 – 500 kJ/mol, respectively. A structural model based on the available structural information has been proposed and is used to explain the observed variation in the activation energies and pre-exponential factor for Cs diffusion.

4. In summary, although the incorporation of CaO showed mixed behavior, i.e., improvement in durability and higher volatilization of Cs, addition of about 5% CaO can be considered to draw the long-term beneficial effects of durability. On the other hand, incorporation of ZnO helped in reducing Cs volatilization significantly. Therefore, the glasses containing mixture of alkaline earth metal oxide CaO and ZnO could be considered for preparation of Cs source to draw the beneficial effects like long-term of durability and low Cs volatilization. This aspect was investigated and discussed in the next chapter.

Chapter 6

Development of borosilicate glasses for use as a source in radiation technology applications

Development of borosilicate glasses for use as a source in radiation technology applications

6.1 Introduction

Investigations on the effect of various additives on the physiochemical properties of glasses have been discussed in detail earlier (Chapter 4 and 5). These studies gave a clear insight that the different additives played specific roles in the glass network. It also revealed that no single additive could give a glass matrix suitable for use as gamma source in radiation technology application. One of the objectives of this thesis is to find a suitable glass formulation, which has the following properties (i) loading of $Cs_2O \geq 10$ wt% (ii) formation temperature $\leq 950^oC$ (iii) good chemical durability (iv) low Cs volatilization loss. Based on the results of our study, it is expected that the use of mixed additives will lead to glasses with desirable characteristics. With this vision, a series of Cs-borosilicate glasses containing more than one additive has been prepared and characterized. Based on these results, three glass formulations have been shortlisted and characterized in detail. Result of the study will help in selection of glass formulations to be used as radiation source in medical irradiators. Results of this investigation are presented in the first part of this chapter.

A little effort has been made in the second part of this chapter for preparation and characterization of glasses containing more than 10 wt% of Cs_2O. The glasses with higher loading of Cs_2O are required for use as gamma source in industrial irradiators. In the present study, preparations of such glasses were carried out by varying the Na and Cs oxides, keeping the total alkali oxides content constant. The base glass composition selected for this study is one of the optimized formulations shortlisted in first part of this chapter. Properties of the glasses measured include pour temperature, swelling factor, density, molar volume, Cs volatilization and chemical durability. This study describes the stated physicochemical properties including pour temperature, swelling factor, density, molar volume, Cs volatilization and chemical durability of the mixed alkali glasses. Based on these studies, Cs bearing glass containing 6 mole% (21 wt%) of Cs_2O and 14 mole% of Na_2O with formation temperature of 950°C or less and with good chemical durability has been proposed for possible use as a gamma source in industrial radiation technology applications.

6.2 Properties of glasses containing a single additive

Generally, additives in small quantities are incorporated in the glass to improve their properties. In our earlier investigations, the influences of some of the additives like TiO_2 and CaO were discussed in detail. In addition, effect of additives like MnO and ZnO were investigated and the results of chemical durability tests of such glasses are summarized in Table 6-1. For ease in comparison, the normalized leach rates of the glasses are represented as leach rate factors (f_{Na} and f_{Cs}) w.r.t #CBS-3 standard which is calculated as follows.

$$f_{Na} = \frac{\text{LR}-\text{Na (for \#CBS 3)}}{\text{LR}-\text{Na (for glass of \#CBS X)}} \qquad \ldots(19)$$

where X = batch number of the glass under evaluation

When this factor is >1 it indicates that the leach rate of the glass is less than the #CBS-3 glass i.e. the glass is more durable than #CBS-3. It is to be noted that all these additives were added by decreasing B_2O_3 content in the base glass.

Table 6-1: Effect of additives on Na and Cs leach rates of CBS glasses of general formulation: 2.5 Cs_2O + 17.5 Na_2O + 45 SiO_2 + (35-x) B_2O_3 + MO. The values in the table represent the factor by which leach rate of the different glass samples decrease with respect to the base glass.

MO added	**Leach fraction**	**mole% MO addition**			
		2.5	**5**	**7.5**	**10**
CaO	f_{Cs}	3.4^a	5.0^a	11.5^b	15.3^b
	f_{Na}	5.7	11.4	29.1	46.3
TiO2	f_{Cs}	1.5^a	2.8^b	4.4^b	15.0^b
	f_{Na}	1.1	1.2	1.5	4.4
MnO	f_{Cs}	1.0^a	1.3^a	1.2^a	2.0^a
	f_{Na}	1.0	1.6	1.4	2.0
ZnO	f_{Cs}	-	1.2^a	-	5.9^b
	f_{Na}	-	1.8	-	4.1

[#] Superscript 'a' and 'b' represent the formation temperature 900 °C and 950°C respectively. Na and Cs leach rate of CBS-3 glass (where x =0) are 3.0 x 10^{-3} and 8.9 x 10^{-4} g/cm^2/d respectively.

It can be seen from Table 6-1 that all the additives used in the present investigation are to some extent effective in improving the chemical durability of the product glasses. It is worth pointing out that CaO was most useful in improving the chemical durability of the product glasses. According to chemical durability enhancement, the additives can be arranged as CaO>TiO_2>ZnO>MnO. However, influence of the different additives on Na and Cs leach rates was found to vary significantly. For example, incorporation of CaO resulted in significantly more improvement in Na than in Cs leach rate. Whereas the reverse effect has been observed when TiO_2 was used as additive. It is noted that at least 7.5 mole% for CaO or 10 mole% for TiO_2 is required to produce glasses having an order of magnitude more chemical durability than the base glass. However, such glasses are formed at relatively higher temperature (950°C). The use of MnO and ZnO as additive had a marginal effect on the leach rate. Nevertheless, MnO helped in reducing the formation temperature but its use leads to more frothing during glass preparation. Based on our earlier investigations, it can be stated that additives like ZnO and TiO_2 are promising for lowering of Cs volatility. According to Cs volatility suppressing ability, the additives can be arranged as $ZnO \approx TiO_2 > CaO$.

6.3 Properties of glasses containing more than one additive

Based on the above discussion, it is clear that glasses with desirable properties can be obtained using a mixture of the additives and therefore a series of glasses were prepared using varying proportions of additives. A maximum of three additives were used at a time. Results of chemical durability tests of some selected formulations are shown in **Table 6-2.**

It can be seen from Table 6-2 that a few glasses which were formed at 900°C have an order of magnitude more chemical durability (wrt. Na leach rate) than the base glass and particularly, these glasses are obtained using as high as 25 mole% of additives (CaO, TiO_2 and MnO). In order to optimize the glass composition containing a total of 25 mole% of these three additives, a series of glasses were prepared by statistically varying the concentrations of these three additives and their characteristics are shown in Fig.6-1. It can be seen from Fig.6-1 that the glasses containing 12.5 mole% of TiO_2 are more durable in this series. However, formation temperature of such glasses was found to be relatively higher (950°C). Among the glasses formed at 900°C in this series, the #CBS-15 is one of the most chemically durable glasses.

Other than this series (containing 25 mole% additive), #CBS-28 is one of the glass formulations possessing relatively higher chemical durability. Based on this high durability, two glass formulations, viz., #CBS-28 and 15 are chosen for detailed studies. #CBS-40 was also under consideration because it has the highest durability among the ZnO containing glasses and it is also likely to suppress Cs volatility significantly owing to the combined influence of TiO_2 and ZnO. Detailed studies with these three formulations have been carried out and the results are described below.

Table 6-2: Properties of the Cs borosilicate glasses containing more than one additive

Batch No	**Additive concentration (mole %)**				**Properties**		
	CaO	TiO2	MnO	ZnO	Density (g/cc)	LR-Cs (g/cm2/d)	LR-Na (g/cm2/d)
CBS-25	5	5	0	0	2.58	4.3	4.5
CBS-26	5	0	5	0	2.59	9.2	7.5
CBS-27	0	5	5	0	2.57	4.5	3.2
CBS-41	0	5	0	5	2.62	4.1	3.5
CBS-42	5	0	0	5	2.57	3.2	4.2
CBS-28	**5**	**5**	**5**	**0**	**2.65**	**11.6**	**9.8**
CBS-40	**5**	**5**	**0**	**5**	**2.7**	**6.4**	**6.0**
CBS-30	5	7.5	7.5	0	2.8	7.7	9.6
CBS-15	**5**	**10**	**10**	**0**	**2.9**	**7.4**	**13.0**

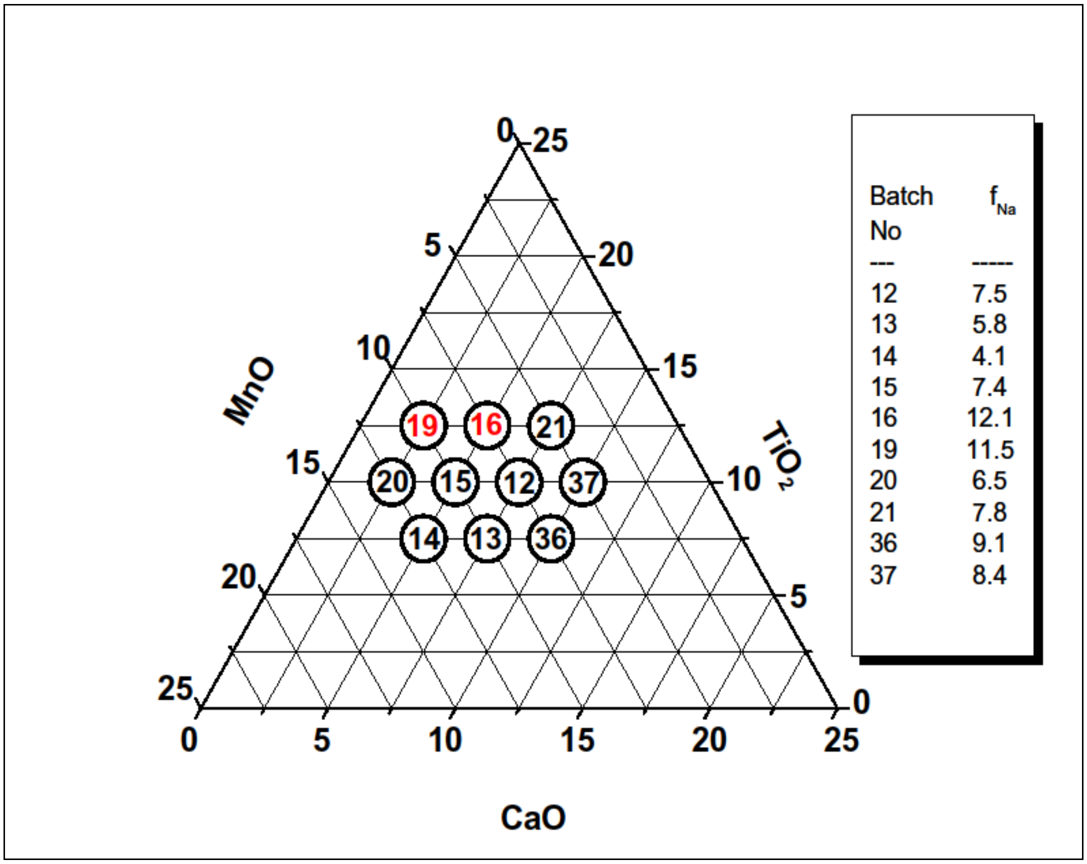

Figure 6-1: Optimization of CaO, TiO_2 and MnO_2 concentrations for the production of a chemically durable Cs-borosilicate glass containing constant levels of other oxides (mole %) 45 SiO_2-10 B_2O_3-15 Na_2O-10 Cs_2O. The number inside the circle represents batch number along with the corresponding chemical durability improvement index.

6.4 Detailed characterization of the shortlisted glasses

6.4.1 XRD patterns

Fig.6-2 shows the XRD pattern of the three shortlisted glasses. It can be seen that all the patterns consist of a broad peak around a 2θ value of about 25°, characteristic of the amorphous borosilicate network. Absence of sharp peaks clearly confirmed that no crystalline phases (within the detection limits of XRD technique) are present in these glasses.

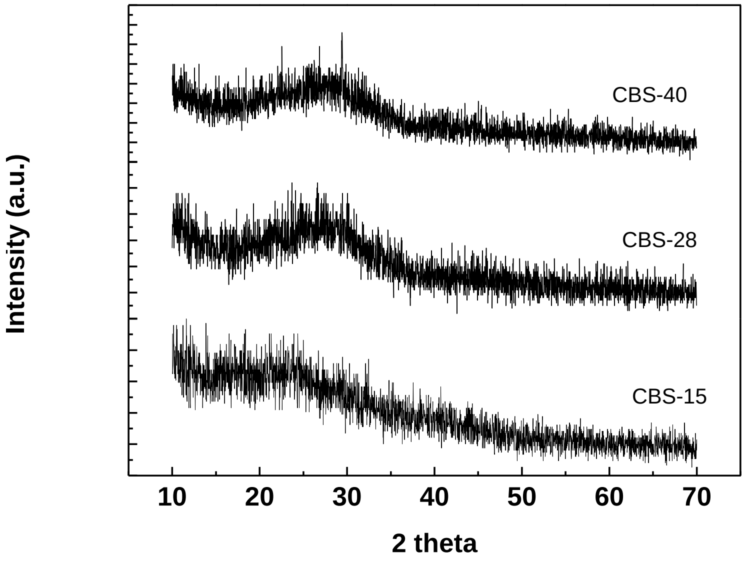

Figure 6-2: XRD patterns of the three shortlisted glasses

6.4.2 Leaching

Fig.6-3 shows the results of leaching tests as a function of leaching time. It can be seen that both the Na and Cs leach rates for all the glasses decrease slowly with the progress of leaching time upto 7 days and thereafter almost no change is observed. It is known that the leaching of alkali ions from the glasses occurs through ion exchange mechanism in which diffusion is the rate determining step. From our earlier studies it is established that the formation of Ca and Si leached leach layer, which acts as a diffusion barrier, is responsible for the reduction in the leach rates. Based on the results of these leaching tests, it can be concluded that all three formulations are equally good with respect to long term Na and Cs release behavior, even though Na and Cs leach rates for the glass #CBS-40 were found to be marginally higher during initial days.

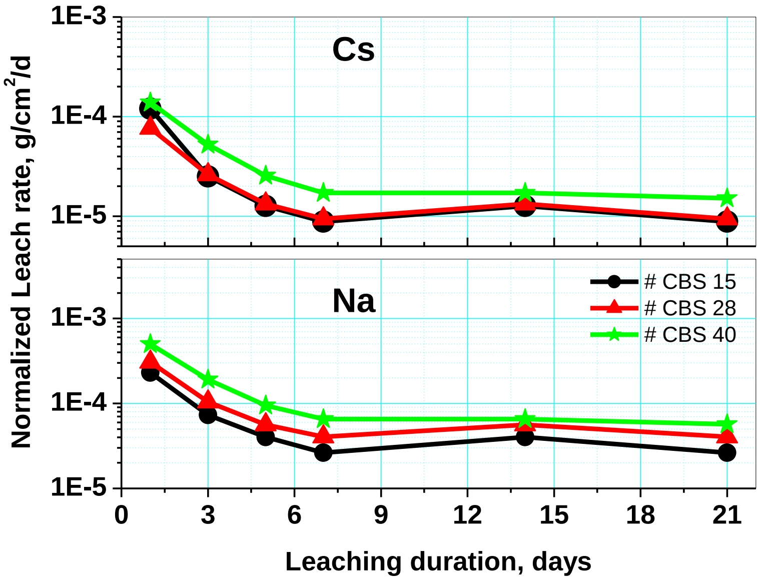

Figure 6-3: Na and Cs leach rates in distilled water at 90°C as a function of leaching time upto 21 days for the three shortlisted glasses.

6.4.3 Cs volatilization

The results of Cs volatilization study are shown in Fig.6-4, in the form of cumulative loss of Cs in glass making, including calcination, fusion and soaking. It is observed that minimum Cs volatilization occurred from the glass sample #CBS28, which contained 5 mole% each of TiO_2, CaO and MnO. The loss of Cs from glass sample #CBS15 is little more than that from #CBS28, possibly because of higher TiO_2 content in the glass [Inferred from this study described in Chapter 4]. Results of our earlier studies showed that TiO_2 and ZnO if added alone suppress Cs volatility. Therefore it was expected that, the glass #CBS40, which contains both TiO_2 and ZnO would show the lowest Cs volatilization loss. However this was not practically observed probably due to a behavioral change when the two additives were added together.

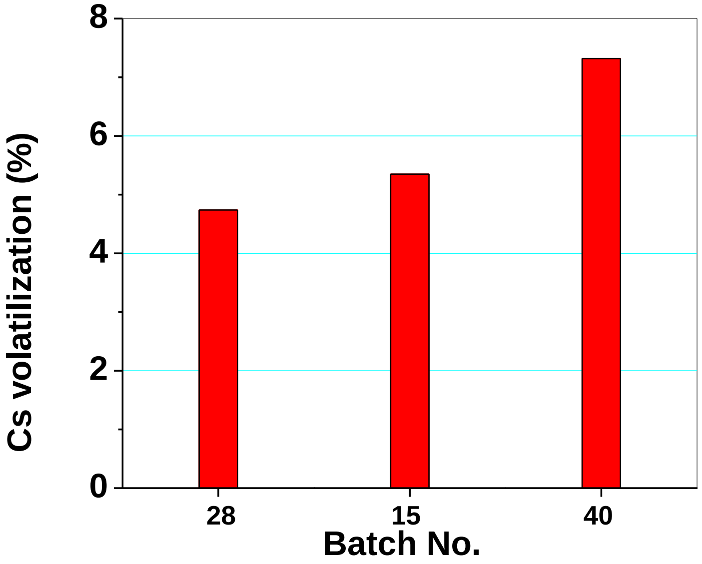

Figure 6-4: Cs volatilization loss during glass preparation including soaking at 950 ^{o}C for 4 hours.

Further to determine the Cs volatilization loss as function of soaking duration, the glass sample #15 was prepared at 900^{o}C from required amounts of starting materials (2 g batch) in a silica boat. Four such experiments with varying soaking time (4-10 hours) were carried out. Unlike earlier experiments, in this case no radioactive Cs was added and analysis of Cs was carried out using atomic emission spectroscopy (AES). Results showed (Fig.6-5) that the maximum loss of cesium due to volatilization was < 3% and it is found to be almost independent of fusion time in the range of 4-10 hours. This loss of Cs is slightly lower than the values obtained from 25 g glass batch (Fig. 6-4). The low Cs loss from inactive run can be attributed to (i) batch size and (ii) uncertainty associated with the analysis of Cs using AES and difference in soaking temperatures.

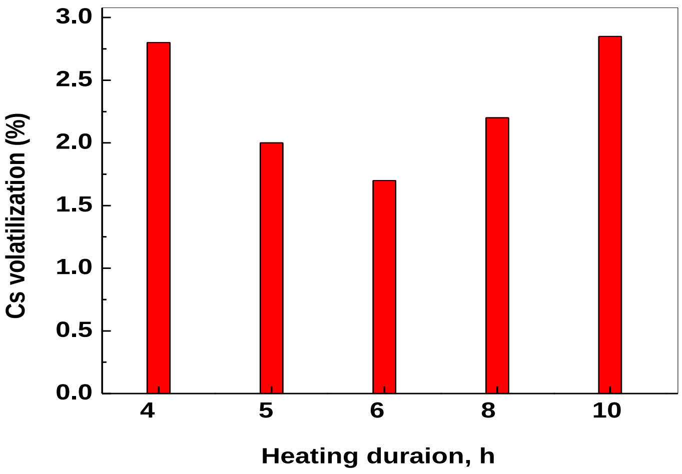

Figure 6-5: Cs volatilization during preparation of glass#15, as a function of soaking time. About 2 g glass was prepared in silica boat at 900°C.

6.5 Preparation of high Cs bearing glasses

As mentioned earlier, the preparation of high Cs bearing glasses were carried out by varying the Na and Cs concentrations on the #CBS-15, which is one of the shortlisted formulations for use as a source in medical irradiators. The detailed formulation of the #glass CBS-15 is shown in Fig.6-6**.** Eight glasses on the series were prepared and characterized. Glasses of this series can also be categorized as mixed alkali glasses.

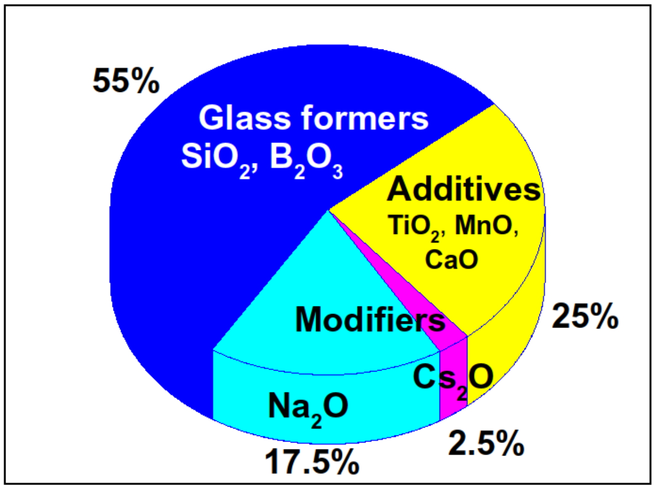

Figure 6-6: Composition of the glass used in Na and Cs variation study

6.6 Properties of high Cs bearing glasses

6.6.1 Formation temperature

Although it is evident that the incorporation of Cs_2O in place of Na_2O is directly reflected on the source strength, the preparation of the glasses with more Cs_2O is likely to be difficult. The higher ionic diameter of Cs compared to Na requires a higher temperature for incorporation into the network (fusion) and also for homogenization. In fact, the formation temperature of the glasses was found to be increase with the increase of Cs loading, as can be seen from Fig. 6-7. The calculated source strength of the glasses plotted in Fig. 6-7 was arrived at from Cs loading and specific activity of ^{137}Cs in waste (35 Ci/g). It can be seen that the loading of Cs_2O upto 4 mole% has no effect on the formation temperature as all these glasses are formed at around 900-930 ^{o}C. Glasses containing Cs_2O as high as 6 mol % can be prepared within 950 ^{o}C while glass preparation at concentrations of more than 6% Cs_2O needs a temperature of 1000 ^{o}C and above.

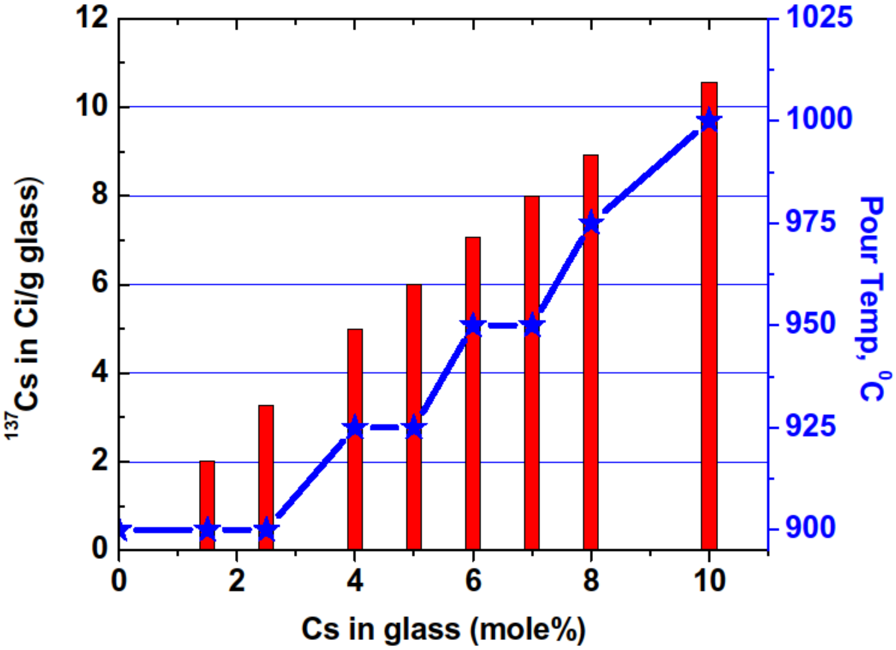

Figure 6-7: formation temperature and source strength of the glasses as a function of Cs_2O content in glass

6.6.2 Density and molar volume

Fig.6-8 shows the density of the glasses as a function of composition ratio of the substituted alkali cation. The density was found to increase linearly with the increase of Cs_2O loading. This is expected as the lighter Na_2O is replaced by a much heavier Cs ion. The molar volumes of the glasses also increased with the Cs_2O loading (Fig.6-8), which indicates that higher ionic diameter of Cs occupies more volume in the resulting glass.

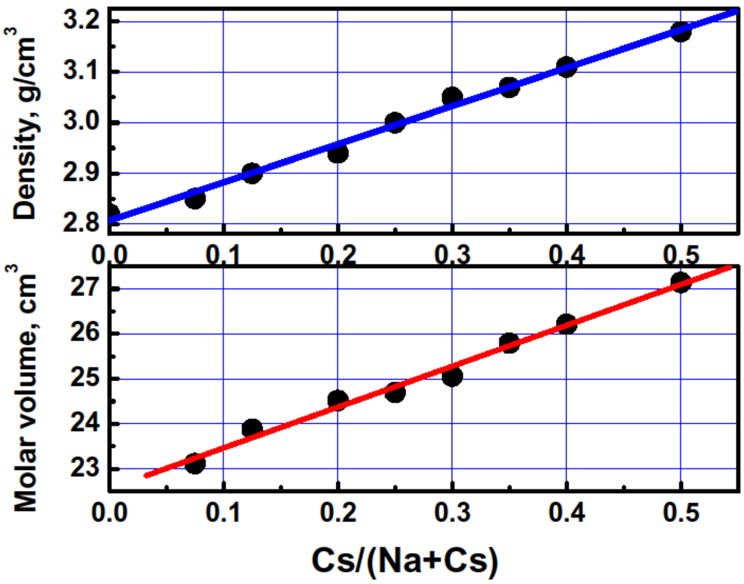

Figure 6-8: Density and molar volume of the mixed alkali Na-Cs borosilicate glasses

6.6.3 Swelling factor

Fig. 6-9 shows the swelling factor as a function of Cs_2O loading in glass. The swelling factor was calculated from the volume ratio of the glass melt (maximum volume level of the melt reached during melting) and the final product glass. The significance of representing swelling factor in this manner is that it directly indicates volume of melter required for production of a unit volume of glass. For example, swelling factor of 12 indicates that a melter of more than 12 liter operating capacity is required for production of 1 L of that glass. This parameter is therefore important from melter design point of view. It can be seen from Fig.6-9 that swelling factor decreases with the increase of Cs_2O loading. Highly violent reaction of molten Na_2O with other glass forming oxides may possibly result in higher swelling for high

Na_2O bearing glasses. Results of this study conclusively prove that the preparation of higher Cs bearing glasses is advantageous from swelling point of view.

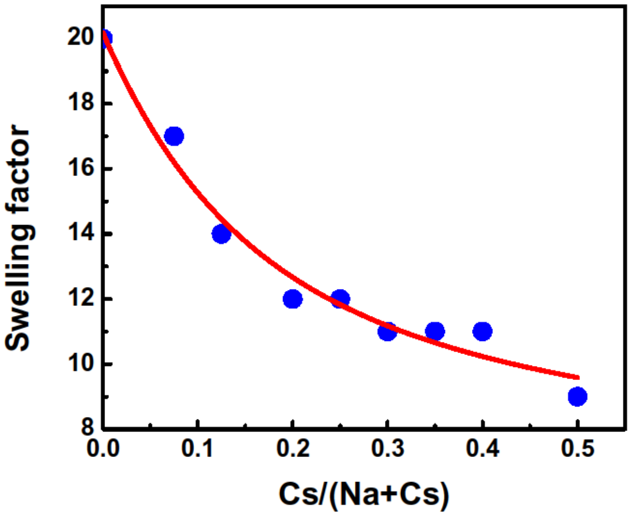

Figure 6-9: Swelling factor of the mixed alkali Na-Cs borosilicate glasses

6.6.4 Volatilization of Cs

Volatilization of Cs is one of the major concerns for the preparation of high Cs bearing glasses. This is mainly due to the high gamma radioactivity associated with the decay of ^{137}Cs. It is therefore desirable to evolve a formulation where volatilization loss is very low. It is known that Cs is highly volatile at elevated temperatures (> 514 ^{o}C) and composition of the melt can only play a little role in minimizing losses. Results of the present study presented in Fig.6-10 address the volatilization loss due to change of composition of melt and it is presented in terms of loss of weight (%). Admittedly, in addition to Cs, boron and Na are also volatilized during glass formation yet it is evident that Cs has maximum contribution on the measured weight loss. This is due to its highly volatile nature as well as its significantly higher molecular weight. The weight loss, (indirectly Cs volatilization) increases almost linearly with the increase of Cs_2O content in glass. This linear behavior is valid upto Cs_2O loading of 6 mole% only and the magnitude of weight loss varies within a narrow range, between 2 to 4 wt%. However, a significant loss of weight is noted for the glasses containing > 6 mole% Cs_2O.

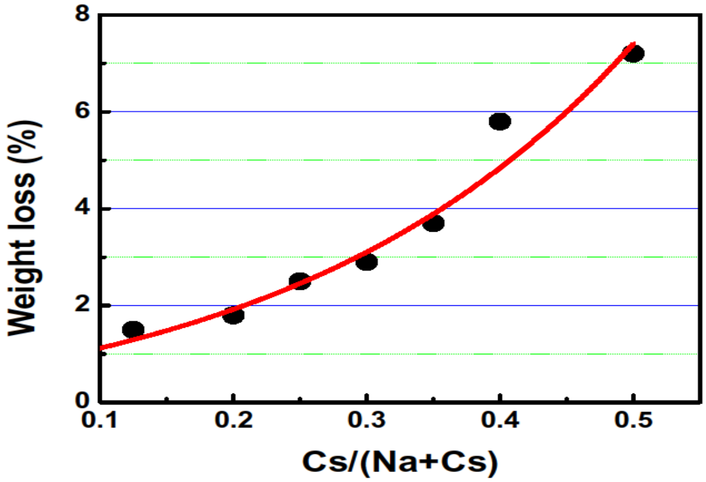

Figure 6-10: Cs volatilization of the mixed alkali Na-Cs borosilicate glasses

6.6.5 Leaching behavior

Fig. 6-11 shows the leaching behavior of the glasses as a function of Cs/(Na+Cs) molar ratio. The incorporation of Cs_2O up to 2.5 mole% at the expense of Na_2O in glass, results in significant decrease of Na leaching. However, incorporation of more Cs_2O thereafter does not affect Na extraction significantly. On the other hand, the extent of Cs extraction is found to increase slowly with the increase of Cs content in glass. In terms of overall chemical durability of the glasses, i.e., considering the total number of alkali ion extracted, the curve passes through a minimum at the alkali ion ratio (Cs/Na) of 0.1. This behavior of leaching is due to mixed alkali effect. Unlike simple borosilicate system, where large mixed alkali effects are generally observed, the effect in these glasses was seen to be marginal. This is possibly due to very complex formulation of the glasses. This study concludes that the glass containing 2.5 to 5 mole% Cs_2O is more chemically durable.

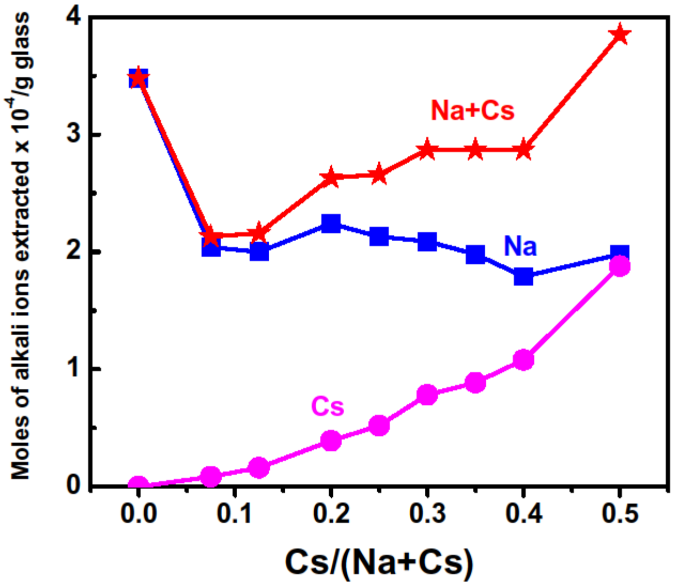

Figure 6-11: Leaching profile of Na and Cs from mixed alkali Na-Cs borosilicate glasses

6.7 Summary of the results and conclusions

Results of the present study can be summarized as follows:

(i) The properties of Cs-borosilicate glasses determined as a function of additive concentrations (Cao, TiO_2, MnO, ZnO) show that it is highly dependent on the nature and concentration of the additive incorporated.

(ii) The incorporation of mixed additive, helped in producing glasses with desirable characteristics such as low formation temperature and high chemical durability.

(iii) Based on the results of this study, three glass formulations have been shortlisted for possible application as a gamma source in medical irradiators.

(iv) The seven component glass formulation finalized for use as a source in blood irradiator, can be upgraded for application in industrial irradiators by incorporating more Cs_2O at the expense of Na_2O. Incorporation of Cs_2O results in glasses with improved physicochemical characteristics, viz., higher density, lower swelling factor and better resistance to hydrolytic attack.

(v) In line with our expectation, mixed alkali effect was observed for leaching of alkali ions as this phenomenon is related to the movement of alkali ions. Possibly due to complex formulation of the base glass, significant improvement in chemical durability is not obtained. Although it is small, advantage of the mixed alkali effect can be utilized for selection of the chemically durable formulation for the application.

(vi) Based on the formation temperature within 950^{o}C and good chemical durability, the highest Cs bearing glass containing 6 mole% (21 wt%) of Cs_2O and 14 mole% of Na_2O, can be selected for possible use as a gamma source in industrial radiation technology applications.

Chapter 7

Conclusions and plan of future work

Conclusions and plan of future work

7.1 Introduction

Investigations carried out in this thesis addressed to both the recovery of ^{137}Cs from nuclear waste and the immobilization of the recovered ^{137}Cs into borosilicate based glass matrix, the objective being to use the final product as a gamma source in radiation technology applications. A brief survey of literature pertaining to the recovery of Cs from nuclear waste streams revealed that solvent extraction based processes utilizing novel solvents like Calix[4]arene are most promising for recovery of ^{137}Cs in chemically pure form from nuclear waste. However, due to unavailability of such solvent, during this research work efforts were made to use the indigenously developed ion exchange resins instead of the exotic solvents for Cs recovery. Two ion exchange resins, viz., ammonium molybdophosphate and resorcinol formaldehyde polycondensate resin used in the present study for recovery of ^{137}Cs from acidic and alkaline waste streams, have been synthesized and extensively characterized earlier in our laboratory. Although deployment of the ion exchange process in plant scale treatment of intermediate level waste has also successfully been accomplished, it was found that the recovered ^{137}Cs is contaminated with substantial amount of Na and hence is not suitable for preparation of radiation source. Purification of the Cs solution has also been performed during this work. For the recovery of Cs from acidic high level waste, an integrated process schematic has been developed and demonstrated. The process steps include separation of Cs from acidic waste using ammonium molybdophosphate, recovery of Cs from AMP column by dissolution of AMP in NaOH and purification of Cs from dissolved AMP solution using RFPR. The important contribution of the present work lies in the final purification step which gave speeded up application of the recovered Cs in radiation technology applications).

The second part of the work was devoted to the preparation and characterization of borosilicate based glass formulation for immobilization of about 10 wt% Cs_2O. It can be noted that the loading of 10 wt% Cs_2O is the minimum requirement for use of the product glass as source in medical irradiators. Although borosilicate glass is known for a long time and it has extensively been used for immobilization of high level nuclear waste, the development of a chemically durable glass with high alkali oxides load including higher amount of Cs was a challenging task. Most importantly, volatilization of Cs during preparation of such glasses was also of concern. During the course of the present study, these aspects have been addressed by incorporating various additives alone and in combination in the glass network. In addition, effect of additives on the change in glass structure has been investigated in detail. Results of the study helped in finalizing suitable formulations and extended our understanding on the leaching and volatilization behavior of the glasses as a function of glass composition.

Detailed description of the above mentioned work and the results have already been discussed in earlier chapters. In this chapter, a summary of the present investigation along with highlights of the important contributions are presented.

7.2 Recovery of ^{137}Cs

The use of RFPR has been limited so far for the separation of ^{137}Cs from alkaline intermediate level waste. Present investigation, for the first time, examines the Cs separation behavior of the resin from high Cs bearing solution. The Cs exchange isotherms of RFPR from solutions containing Cs concentrations in the range of 1×10^{-4} to 0.1 M have been evaluated.

Further, column behavior of the resin from high Cs bearing solution has been evaluated by conducting five column runs using feed solution containing Cs concentration in the range of 2.57×10^{-4} to 4.3×10^{-3} M. These studies have established that the resins can be used for separation of Cs from high Cs bearing solution. The use of high Cs bearing solution helped in higher loading of Cs on the column. Further, adoption of sequential elution helped in separation of Na rich and Cs rich fractions. The Cs rich fraction was found to be a concentrated ^{137}Cs solution containing very low concentration of accompanying Na ions and hence useful for the preparation of radiation source. The extent of purification achieved by employing RFPR in two step ion exchange processes is summarized in Table 3-9.

Separation and recovery of ^{137}Cs from acidic solution was investigated using AMP-PMMA beads, prepared by coating of AMP powder on PMMA beads. The sorbent containing about 37 wt% AMP showed excellent Cs sorption behavior as revealed from batch and column study. It is inferred from column data that up to 800 Ci of ^{137}Cs can be loaded on 1 L bed of AMP-PMMA beads from radioactive waste solution containing 10 Ci/L of ^{137}Cs. Quantitative recovery of sorbed Cs from AMP-PMMA bed is achieved by dissolution of AMP in NaOH solution. Further purification of Cs from dissolved AMP solution is carried out by passing through RFPR column. Based on the results, an integrated process flowsheet (Fig. 7-1) is developed. It is established that the purified product solution will have a very low concentration of Na and Na/Cs ratio as low as 0.2. This solution can be used for the preparation of radiation source for industrial radiation technology application.

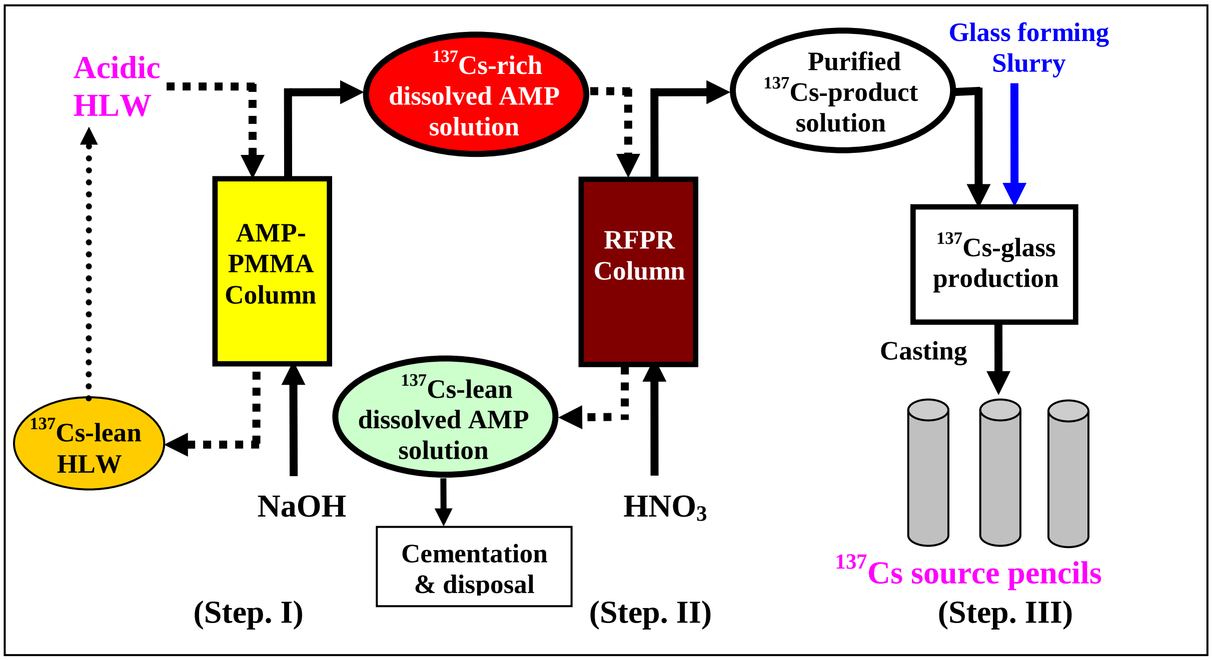

Figure 7-1: Process schematic for recovery ^{137}Cs from acidic HLW and production of source pencils

7.3 *Preparation and characterization of Cs borosilicate glasses*

In the preparation of Cs borosilicate glasses, initially, physico-chemical properties of the glasses as a function of incorporated TiO_2 concentration were investigated, with major emphasis on evolving the Cs volatilization profile. Although TiO_2 is a well known additive for reduction of Cs volatility, the extent of Cs volatilization and understanding of the phenomenon was of interest. It was found that addition of TiO_2 in a small quantity reduces Cs volatility, whereas higher TiO_2 in glass increased the Cs volatilization. Based on the structural information obtained through FTIR, ^{11}B MAS NMR and uv-visible optical absorption studies, it is inferred that TiO_2 initially acts as a network modifier and as a network former when increased TiO_2 is present. It is inferred that presence of TiO_2 as network modifier, affects the bonding nature of Na-O and Cs-O linkages in the glass, which in turn is responsible for suppression of Cs volatility. It is also confirmed that the addition of TiO_2 improves the chemical durability of the glasses.

Our understanding of Cs volatilization behavior improved after carrying out Cs volatilization studies with the incorporation of different additives like CaO, BaO, ZnO, as a function of temperature and time. It is confirmed that the Cs volatilization from the glass melt occurs through a diffusion controlled process. The observed sequence in terms of increasing loss of Cs was found to be: $ZnO<TiO_2< B_2O_3<BaO<CaO<MgO$. Based on the results of this study, it is concluded that the addition of ZnO to a simple alkali borosilicate glass is highly beneficial with respect to a reduction of Cs volatility, while the effects of CaO or BaO incorporation are detrimental. Temperature dependence of Cs volatility profiles confirms that pre-exponential factor and not the activation energy for Cs diffusion influences the extent of Cs loss. A unique empirical structural model has been proposed and is used to explain the observed variation in the activation energies and pre-exponential factor for Cs diffusion.

Incorporation of CaO and BaO at the expense of B_2O_3 in Cs borosilicate glasses has been found to improve their leaching characteristics. It is established that diffusion controlled ion exchange is the rate controlling process for leaching of mobile Na/Cs ions from these glasses. The results of SEM and EDX studies confirmed that the formation of protective amorphous layer at the interface enriched with Ca and Si is responsible for the improved leaching characteristics of the glasses. According to lower leach rates for alkali metal ions, the glasses can be arranged as: $BaO \cong SrO < CaO < ZnO < MgO$.

In summary, incorporation of CaO or BaO improves the durability but increases loss of Cs by volatilization. On the other hand, incorporation of ZnO or TiO_2 helped in reducing Cs volatilization significantly. Therefore, the glasses containing mixture of alkaline earth metal oxide CaO and ZnO and /or TiO_2 could be considered for preparation of Cs source to draw the beneficial effects like long-term of durability and low Cs volatilization.

The incorporation of mixed additives helped in producing glasses with desirable characteristics such as low formation temperature and high chemical durability. Based on the results of this study, three glass formulations have been shortlisted for the possible application as a gamma source in medical irradiators.

In the final part of the work, efforts were made to produce glasses for use as source in industrial irradiators. The feasibility of higher loading of Cs_2O at the expense of Na_2O was investigated on the seven component glass formulation (CBS-15) finalized for use as a source in blood irradiators. Incorporation of Cs_2O results in glasses with improved physicochemical characteristics, viz., higher density, lower swelling factor and better resistance to hydrolytic attack. In line with our expectation, mixed alkali effect was observed for leaching of alkali ions as this phenomenon is related to the movement of alkali ions. Possibly due to complex formulation of the base glass, significant improvement in chemical durability is not obtained. Although it is small, advantage of the mixed alkali effect can be utilized for selection of the chemically durable formulation for the application. Based on the formation temperature within $950^{o}C$ and good chemical durability, the highest Cs bearing glass containing 6 mole% (21 wt%) of Cs_2O and 14 mole% of Na_2O, can be selected for possible use as a gamma source in industrial radiation technology applications.

7.4 Future work

In the present work, various aspects involved in the immobilization of cesium in borosilicate glass have been discussed in detail. From the studies, it is clear that volatilization of certain extent of cesium in the above glass matrix is unavoidable as the glass samples are formed at higher temperatures of the order of 900°C and above. There are reports that immobilization of cesium can also be achieved in inorganic matrices like sodium zirconium phosphate (NZP) at relatively low temperatures like 450^{o}C by adopting microwave heating technique [156]. Because of low processing temperature, it is expected that Cs volatility in this process would be significantly lower compared to that involved in the immobilization in borosilicate glass matrix. Reported studies [157], [158][157-158] on Cs incorporated NZP materials also revealed that the, Cs leach rate from the matrix is comparable with that of the borosilicate glasses reported in this work. In view of this it is absolutely necessary to perform a detailed comparative study on the various aspects involved in the two immobilization processes along the respective final product characteristics. It is proposed to investigate this aspect as a future work

It is also planned that further work will be dedicated on the development of high Cs bearing matrices for use in industrial irradiators. As it is quite evident from this study that loading of higher amounts of Cs (> 6 mole %) in borosilicate matrix needs higher formation temperature which in turn will increase the Cs volatilization. The use of small amount of Li in place of Na could be an option to make the glasses at relatively lower temperature. Alternatively, feasibility of using phosphate based glasses, mainly alumino-phosphate and iron phosphate based glasses will be explored in the future with a view to accommodate large amounts of alkali oxides.

During the course of thesis work, two important questions pertaining to the role of TiO_2 and ZnO in glass network could not be addressed**.** It is known that as the role of the cation changes in the glass, its coordination environment also changes. For examples, Ti^{4+} is known to have octahedral configuration when it is in the network modifying positions. However, as the role changes to network former, the coordination number changes to four. In order to confirm this fact with glass samples of present study, detailed Raman and Ti K edge EXFAS measurements needs to be carried out. In a similar fashion change in the role of Zn^{2+} ions in the glass with respect to change in composition also needs to be understood by carrying out EXAFS measurements. Such studies can give valuable information regarding the cation distribution in the glass. This will be quite useful for predicting and understanding the physico-chemical properties of different glass compositions.

As an extension of this work, in future, it is also proposed to carry out ^{17}O and ^{133}Cs NMR studies on these glasses to get idea regarding the nature of different oxygen and Cs environments in the glass matrix. It is expected that the advanced techniques like ^{17}O multi quantum magic angle spinning (MQMAS) NMR can distinguish between the oxygen atoms in the close vicinity of different cations like Cs^+, Na^+, Zn^{2+}, Ca^{2+}, Ti^{4+} etc., in addition to bridging and non-bridging oxygen atoms. The information on this aspect will be helpful for understanding the composition dependent changes in the network modifying and network forming actions of some of the above mentioned cations. Even though ^{133}Cs is quadrupolar nucleus with a spin value 7/2, it has got very low quadruple moment. This result in sharp line NMR line shapes and hence can be used to identify the changes in the Cs environment as the composition changes in the glass.

Publications from present investigation

Journal

1. D. Banerjee, M.A. Rao, J. Gabriel and S.K. Samanta, ‘Recovery of Purified Radiocesium from Acidic Solution using Ammonium Molybdophosphate and Resorcinol Formaldehyde Polycondensate Resin’, Desalination 232, 172-180, 2008.
2. D. Banerjee, V. Sudarsan, A. Joseph, R.K. Mishra I.J. Singh, P.K. Wattal and D. Das, ‘Role of TiO2 on Physico-Chemical Properties of Cesium Borosilicate Glasses’, J. Am. Ceram. Soc. 93 [10] 3252–3258, 2010.
3. D. Banerjee, V. Sudarsan, A. Joseph, I.J. Singh, J. Nuwad, C.G.S. Pillai, P.K. Wattal and D. Das, Physicochemical properties of Cs borosilicate glasses containing CaO, J. Nucl. Mater. 413, 177–182, 2011.
4. D. Banerjee, A. Joseph, V. Sudarsan, P.K. Wattal and D. Das, Effect of composition and temperature on volatilization of Cs from borosilicate glasses, J. Am. Ceram. Soc. (95 [4] 1284–1289 (2012).
5. D. Banerjee, M. A. Rao and P.K. Wattal, Separation and recovery of Cs from high active waste simulant using resorcinol formaldehyde polycondensate resin: Batch and column studies, Sep. Sci.Technol. (Accepted).
6. D. Banerjee, V. Sudarsan, P.K. Wattal and D. Das, Role of structural groups on chemical durability of high Cs bearing sodium borosilicate glasses containing CaO, Phys. Chem. Glasses. (accepted).

7. D. Banerjee, V. Sudarsan, A. Joseph, P.K. Wattal and D. Das, Evaluation of the suitable divalent cations for the preparation of Cs-borosilicate glasses for use as a gamma source, Phys. Chem. Glasses. (communicated).
8. D. Banerjee, Annie Joseph, V. Sudarsan, P.K. Wattal and D. Das, ^{137}Cs based borosilicate glass source for radiation technology applications. Glass Technology, (communicated).

Conferences

1. D. Banerjee, Annie Joseph, I.J. Singh, P.K. Wattal and D.Das, 'Development of ^{137}Cs based borosilicate glass source in radiation technology applications', NUCAR-2011, Visakhapatnam, Feb-22-26, 2011.

2. R.K. Gupta, Sugilal Gopalakrishnan, S.B Patil, Piyush Srivastava, Jyoti Jha, K.N.S. Nair, D. Banerjee, "Wealth from Waste – Demonstration of Selective Removal of Cesium from Radioactive Wastes for Producing Blood Irradiator Source Pencils', - 11626, WM Symposia, USA, Jan-2011

3. D. Banerjee, A. Joseph, I.J. Singh and P.K. Wattal, 'Effect of Bivalent Cations on the Physicochemical Properties of Cs-Borosilicate Glasses', Proc. ISMC-2010. Mumbai, Dec7-11, 2010.

4. D. Banerjee, I.J. Singh, P.K. Wattal, 'Evaluation of Cs-borosilicate glass formulation on the basis of mixed alkali effect for use as a source in radiation technology applications', Proc. of International Workshop & Symposium on Synthesis and Characterization of Glass/Glass-ceramics (IWSSCGGC-2010), Pune, India, July 7-10, 2010.

5. Amar Kumar, P.S. Dhami, Tessy Vincent, S.B. Patil and D. Banerjee, ‘Recovery of Valuable Fission Products from Radioactive Waste’, Proc. *Peaceful Uses of Atomic Energy – 2009, New Delhi, Oct 1-3, 2009*

6. D. Banerjee, M.A. Rao and S.K. Samanta, ‘Column Loading and Elution Behavior of Rubidium during Ion Exchange Separation of Cesium from Alkaline Radioactive Waste’, Proc. of DAE-BRNS Symp. on Emerging Trends in Sep. Sci. Technol. SESTEC – 2008, University of Delhi, Delhi, March 12-14, 2008, page -173.

7. D. Banerjee, M.A. Rao, J. Gabriel and S.K. Samanta, ‘Evaluation of some Process Variables for the Separation of ^{137}Cs from Acidic Solution using Ammonium Molybdophosphate’, Proceedings of DAE-BRNS Symposium on Emerging Trends in Separation Science and Technology, SESTEC – 2006, Mumbai, Sept. 29-Oct. 1, 2006, page -260.

8. D. Banerjee, M.A. Rao and S.K. Samanta, ‘Ion Exchange Purification of ^{137}Cs after Caustic Dissolution of ^{137}Cs-loaded Ammonium Molybdophosphate’, Proceedings of DAE-BRNS Symposium on Emerging Trends in Separation Science and Technology, SESTEC – 2006, Mumbai, Sept. 29-Oct. 1, 2006, page -262.

9. D. Banerjee, M.A. Rao, and S.K. Samanta, ‘Purification and Concentration of ^{137}Cs Separated from Nuclear Waste for Use as a Radiation Source after Immobilization in Vitreous Matrix’, Nuclear and Radiochemistry Symposium (NUCAR-2005), Guru Nanak Dev University, Amritsar, March 15-18 (2005), Proceedings, p. 331.

References

[1] Feasibility of Separation and Utilization of Cesium and Strontium from High Level Liquid

[2] A. Dash, S.K. Saxena, M. Venkatesh, Cesium-137 brachytherapy sources, NAARRI Bull. 9, 79–86, 2005.

[3] H.J. Bhabha, Conference on Development of Atomic energy for peaceful purposes in India, New Delhi, Nov. 1954.

[4] S. Ramakrishna Iyer, Gamma radiation sources, IANCAS Buletin, , 15 (4), 1999

[5] AERB /SS 3 1990 testing and classification of sealed sources, 1990.

[6] International standard, ISO-9978-Radiation protection-sealed radioactive sources, leak test method, 1992

[7] D.D. Sood, A.V.R. Reddy and N. Ramamoorthy, Fundamental of radiochemistry, Ch 12, Production and separation of isotopes, Indian association of nuclear chemists and allied scientists. 2000.

[8] Y.D. Parmar and .V.S. Sastry, Gamma radiation sources for radiation processing plants, IANCAS Bulletin, , vol. IV (2), 2005.

[9] C. P. Kaushik and J.G. Shah, Challenges in development of matrices for vitrification of high level radioactive waste, BARC News letter, May-June 2000.

[10] D. Banerjee, S.K. Samanta, (2003) Proc. 14th Annual Conference of Indian Nuclear Society and 1st BRNS Conference on Nuclear Fuel Cycle, (INSAC 2003), IGCAR, Kalpakkam, Paper no. G 14, 2003.

[11] M.A. Rao, D. Banerjee and S.K. Samanta, Removal of Cesium from Aluminium Decladding Waste by Selective Ion Exchange, Nuclear and Radiochemistry Symposium (NUCAR-2005), Guru Nanak Dev University, Amritsar, March 15-18 (2005), Proceedings, p. 353, 2005.

[12] M.E. Meek and B.F. Rider “Compilation of fission product yields” NEDO-12154, Class I, 71 NED 41, January 1972.

---

[13] W. W. Schulz, L. A. Bray, Solvent Extraction recovery of Byproduct ^{137}Cs and ^{90}Sr from HNO_3 Solutions—A Technology Review and Assessment, *Separation Science and Technology*, 22 (2&3), 191-214, 1987.

[14] A. Clearfield, Inorganic Ion Exchangers, Past, Present, and Future, *Solvent Extraction Ion Exchange*, 18(4), 655-678, 2000.

[15] V. Kourim, J. Rais, B. Million, Exchange properties of Complex Cyanides-I: Ion Exchange of Cesium on Ferrocyanides, *J. Inorg. Nucl. Chem.*, 26, 1111-1115, 1964.

[16] B.F. Judson, R.L. Moore, H.H. van Tuyl and R.W. Wirta, Chem. Eng. Symp. Ser. (A.I.Ch.E)Vol.55, 23, 1959

[17] L.M. Lee and L.L. Kilpatrick, Rept.DP-1636, A Precipitation Process for Supernate. Decontamination, E.I. du Pont Nemours & Co. Aiken, SC, 1982

[18] J. Rais, P. Selucky, M. Kyr, Extraction of Alkali-Metals into Nitrobenzene in Presence of Univalent Polyhedral Borate Anions, *Journal of Inorganic Nuclear Chemistry*, 38, 1376, 1976.

[19] V.N. Ramonovsky, Management of accumulated high level waste at the amyak production Association in the Russian Federation' in issues and Trends in Radioactive waste management, Proc. International conference, IAEA, Vienna, 2003, 360.

[20] V. N. Romanovsky, U.S.-Russian Cooperative Program in Research and Development of Chemical Separation Technologies, Chemical Separations in Nuclear Waste Management, G. R.Choppin, M. K. Khankhasayev, H. S. Plendl (eds), DOE/EM-0591, Battelle Press, Columbus OH, 2002.

[21] R. S. Herbst, J. D. Law, T. A. Todd, V. N. Romanovskii, V. A. Babain, V. M. Esimantovski, B. N. Zaitsev & I. V. Smirnov, Development and Testing of a Cobalt Dicarbollide Based Solvent Extraction Process for the Separation of Cesium and Strontium From of Acidic Tank Waste, *Separation Science and Technology*, 37(8), 1807-1831, 2002.

[22] C. J. Pederson, The discovery of crown ethers, *Science*, 241, 536, 1988.

[23] I. H. Gerow, G. E. Smith, and M. W. Davis, Extraction of Cesium (+1) and Strontium (+2) from Nitric Acid Solution using Macrocyclic Polyethers, *Separation Science and Technology*, 16(5), 519-548, 1981.

---

[24] J. W. McDowell and G. N. Case, Selective Extraction of Cesium from Acidic Nitrate Solutions with didodecylnaphthalenesulfonic acid synergized with bis(tert-butylbenzo)-21-crown-7, *Anal.Chem.*, 64, 3013, 1992.

[25] E. A. Filippov, Application of Crown ethers and Ferrocyanide-Based Inorganic Material for Cesium and Strontium Recovery from High-Level Wastes, Proceedings of Waste Management '92, Tucson, Arizona, 1992.

[26] S.R. Izatt, R.T. Hawkins, J.J. Christensen, R.M. Izatt, Cation Transport from Multiple Alkali Cation Mixtures using a Liquid Membrane System containing a Series of Calixarene Carriers, *Journal of American Chemical Society*, 107, 63, 1985

[27] Z. Asfari, C. Bressot, J. Vicens,C. Hill, J.F. Dozol, H. Rouquette, S. Eymard, Veronique. L. B. Tournois, Doubly Crowned Calix[4]arenes in the 1,3-Alternate Conformation as Cesium-Selective Carriers in Supported Liquid Membranes, *Anal. Chem.*, *67* (18), 3133, 1995.

[28] J. F. Dozol, N. Simon, V. Lamare, H. Rouquette, S. Eymard, B. Tournois, D. De Marc and R. M. Macias, A Solution for Cesium Removal from High-Salinity Acidic or Alkaline Liquid Waste: The Crown Calix[4]arenes, *Separation Science and Technology*, 34(6&7), 877-909, 1999.

[29] P. V. Bonnesen, L. H. Delmau, B. A. Moyer, and R. A. Leonard, A Robust Alkaline-side CSEX Solvent Suitable for Removing Cesium from Savannah River High Level Waste, *Solvent Extraction and Ion Exchange*, 18 (6), 1079–1108, 2000.

30 M . A. Norato, M. H. Beasley, S. G. Campbell, A. D. Coleman, M. W. Geeting, J. W. Guthrie, C. W. Kennell, R. A. Pierce, R. C. Ryberg, D. D. Walker, J. D. Law and T. A. Todd, Demonstration of the Caustic-Side Solvent Extraction Process for Removing 137Cs from High-Level Waste at Savannah River Site, *Separation Science and Technology*, 38(12&13), 2647-2666, 2003.

[31] P. V. Bonnesen, T. J. Haverlock, N. L. Engle, R. A. Sachleben and B. A. Moyer, Development of Process Chemistry for the Removal of Cesium from Acidic Nuclear Waste by Calix[4]arene-crown-6 Ethers, in ACS SYMPOSIUM SERIES 757, Calixarenes for Separations, G. J. Lumetta, R. D. Rogers, A. S. Gopalan (eds), American Chemical Society, Washington, DC, 2000.

---

[32] V.N. Ramonovsky, R&D activity on portioning in Russia, in fifth OECD/NEA information exchange meeting on actinides and fission product portioning and transmutation, SCK-CEN, Mol, Belgium, 1998.

[33] J. van R. Smit, The AMP process for cesium separation I. Adsorption of cesium on ammonium 12- Molybdophosphate, Report AERE-R-3884, AERE, Harwell, 1961.

[34] K. Terada, H. Hayakawa, K. Sawada and T. Kiba, Silica gel as a support for inorganic ion-exchangers for the determination of caesium-137 in natural waters, Talanta, 17, 955–963, 1970.

[35] Y. Onodera, H. Mimura, T. Iwasaki, H. Hayashi, T. Ebina and M. Chatterjee, A New Granular Composite with High Selectivity for Cesium Ion Prepared from Phosphomolybdic Acid Hydrate and Inorganic Porous Material, *Separation Science and Technology*, 34, 2347–2354, 1999.

[36] A. Nakaoka, H. Yokoyama, M. Fukushima and S.Takagi, Rapid determination method of radiocesium in sea water by cesium-selective resin, *J. Radioanal. Chem*., 56, 13–24, 1980.

[37] I.I.L. Cunha and L. Sakai, Determination of cesium-137 in water by ion exchange, *J. Radioanal. Nucl. Chem.,*131, 105–109, 1989.

[38]T.A. Todd, N.R. Mann, T.J. Tranter, F. Sebesta, J.John and A. Motl, Cesium sorption from concentrated acidic tank wastes using ammonium molybdophosphate-polyacrylonitrile composite sorbents, *J. Radioanal. Nucl. Chem*., 254(1) 47–52, 2002.

[39] C.J. Miller, A.L. Olson and C.K. Johnson, Cesium Absorption from Acidic Solutions Using Ammonium Molybdophosphate on a Polyacrylonitrile Support (AMP-PAN), *Separation Science and Technology*, 32, 37–50, 1997.

[40] H. Mimura, M. Saito, K. Akiba and Y. Onodera, J.Nucl. Sci. Technol., 38 (2001) 872–878.

[41] J.D. Law, R.S. Herbst and T.A. Todd, Integrated AMP–PAN, TRUEX, and SREX testing. I. Extended flowsheet testing for separation of surrogate radionuclides from simulated acidic tank waste, *Separation Science and Technology*, 37(6), 1353–1373, 2002.

[42] J. Gabriel, G.J. Shah and T.P. Valsala, Spherical AMP composite ion exchange material for treatment of acidic intermediate level waste, Proc. Nuclear and Radiochemistry Symposium (NUCAR 2003), Bhabha Atomic Research Centre, Mumbai, 2003, p. 321, 2003.

---

[43] T. A. Todd, K. N. Brewer, D. J. Wood, P. A. Tullock, N. R. Mann & L. G. Olson, Evaluation and Testing of Inorganic Ion Exchange Sorbents for the Removal of Cesium-137 from Idaho Chemical Processing Plant Acidic Tank Waste, *Separation Science and Technology*, 36(5&6), 999-1016, 2001.

[44] R. G. Anthony, R. G. Dosch, D. Gu, and C. V. Philip, Use of Silicotitanates for Removing Cesium and Strontium from Defense Waste, *Ind. Eng. Chem. Res*., 33, 2702-2705, 1994.

[45] Z. Zheng, C. V. Philip, And R. G. Anthony., Ion Exchange of Group I Metals by Hydrous Crystalline Silicotitanates, *Ind. Eng.Chem. Res.*, 35, 4246-4256, 1996.

[46] J.P. Bibler, and R.M. Wallace, Preparation and properties of cesium specific resorcinol-formaldehyde ion exchange resin. Savannah River Laboratory: Aiken, SC, DPST-87-647, 1987.

[47] J.P. Bibler, R.M. Wallace and L.A. Bray, Testing a new cesium-specific ion exchange resin for decontamination of alkaline high-activity waste. Proc. Waste Management Symp., Post, R.G. (Ed.), Vol. 2, 747, 1990.

[48] S.K. Samanta, M. Ramaswamy, and B.M. Misra, Studies on cesium uptake by phenolic resins, *Separation Science and Technology,* 27 (2), 255-267, 1992.

[49] A. Favre-Réguillon, B. Dunjic, N. Dumont, and M. Lemaire, Design of ion-exchange resins selective of caesium. Synergistic effect of macrocycle in phenolic resins, *Separation Science and Technology,* 36 (3), 367-379, 2001.

[50] A. Favre-Réguillon, B. Dunjic, M. Lemaire, and R. Chomel, Synthesis and evaluation of resorcinol-based ion-exchange resins for the selective removal of cesium, *Solvent Extraction and Ion Exchange,* 19 (1), 181-191, 2001.

[51] S.K. Samanta and B.M. Misra, Ion exchange selectivity of a resorcinol-formaldehyde polycondensate resin for cesium in relation to other alkali metal ions *Solvent Extraction and Ion Exchange,* 13 (3), 575-589, 1995.

[52] S.K. Samanta, T.K. Theyyunni and B.M. Misra, Column behaviour of resorcinol-formaldehyde polycondensate resin for radiocesium removal from simulated radwaste solution. *Journal of Nuclear Science and Technology,* 32 (5), 425-429, 1995.

---

[53] P.D. Ozarde,; S.K. Samanta and K. Raj, *Management of intermediate level wastes from past reprocessing using cesium-specific resorcinol formaldehyde resin,* International Conference on Issues and Trends in Radioactive Waste Management, December 9-13, International Atomic Energy Agency, Vienna, Austria. 2002.

[54] D.Banerjee, T.P.Valsala, M.S. Sonawane, S. Chattopadhyay, U. Dani, A.K. Singh, and I.J. Singh, Treatment of Intermediate level liquid waste of reprocessing origin-PREFRE, Tarapur, BARC Newsletter Founder's Day Special Issue, 2011.

[55] N.M. Hassan, K. Adu-Wusu, J.C. Marra, Resorcinol - Formaldehyde adsorption of cesium from Hanford waste solutions: Part I. Batch equilibrium study. *Journal of Radioanalytical and Nuclear Chemistry,* 262 (3), 579-586, 2004.

[56] N.M. Hassan and K. Adu-Wusu, Cesium removal from Hanford Tank waste solution using resorcinol-formaldehyde resin. *Solvent Extraction and Ion Exchange,* 23 (3), 375-389, 2005.

[57] S.K. Fiskum, S.T. Arm, M.J. Steele and M.R. Thorson, Spherical resorcinol-formaldehyde performance testing with Hanford tank waste. *Solvent Extraction and Ion Exchange,* 26 (4), 435-452, 2008.

[58] F.G. Smith, S.Y. Lee, W.D. King and D.J. McCabe, Comparisons of crystalline silicotitanate and resorcinol formaldehyde media for cesium removal by in-tank column processing. *Separation Science and Technology,* 43 (9-10), 2929-2942, 2008.

[59] C.A. Nash and S.T. Isom, Characterization of spherical resorcinol-formaldehyde resin cesium adsorption with batch contact tests. *Separation Science and Technology* 45 (12), 1822-1827, 2010.

[60] M.R. Duignan and C.A. Nash, Removal of cesium from Savannah river site waste with spherical resorcinol formaldehyde ion exchange resin: Experimental tests. *Separation Science and Technology,* 45 (12), 1828-1840, 2010.

[61] E. Lamb, Cesium-137 Source Material for an Irradiator, US DOE Report No. CONF-800964-1, Oak Ridge National Laboratory, USA, 1980.

[62] H. Farrar IV, G. Subbaraman, C. C. Conners and J. P. Page, 'The Cesium-137 Agricultural Commodities Irradiator', pp. 551-56 *in Proceedings of Waste Management Symposium*, Vol-1, Edited by P. G. Roy, Tuscon, Arizona, 1985.

---

[63] L. Roberts, Radiation accident grips Goiania, *Science*, 238, 1028-1031, 1987

[64] A.F. Rupp, Radioisotope program (8000) progress report for Dec1971, ORNL-TM-3677 (1972).

[65] A.Olomble, C. Perebaskine and A. Raggenbass, French patent P.V. No. 21,960, No. 1,478,340 (1976).

[66] S. Enomoto, S.Maeda and M.Senoo, *Int.J. Appl.Radiat.Isot*. 32, 595-599, 1981.

[67] D.M. Strachan and W.W. Schulz, Glass and ceramic materials for the immobilization of megacurie amounts of pure Cs-137, ARH-SA-246, Altantic Richfield Handford company, Richland, Washington, 1976

[68] A.E. Ringwood, S.E. Kesson, N.G. Ware, W. Hibberson, A. Major, Immobilisation of high level nuclear reactor wastes in SYNROC, *Nature* 278, 219–223, 1979.

[69] H.Abe, A. Satoh, K. Nishida, E. Abe, T.Naka, M.Imai, H.Kitazawa, Electrochemical immobilization of Cs in single-crystalline SYNROC, *J. Solid state chemistry*, 179, 1521-1524, 2006.

[70] F.Bart, S.Sounilhac, J.L. Dussossoy, A. Bonnetier and C. Fillet, Development of new vitreous matrices for conditioning cesium, Environmental issues and waste management technologies VI. P-352

[71] S. Enomoto, S. Maeda, M. Senoo, A simplified method for preparation of ^{137}Cs pollucite γ-ray source, *The International Journal of Applied Radiation and Isotopes*, 32 (8), 595–599, 1981.

[72] J. van R. Smit, W. Robb and J.J. Jacobs, Cation Exchange on Ammonium Molybdophosphate-I The. Alkali Metals, *J. Inorg. Nucl. Chem*., 12, 95-103, 1959.

[73] Hans bach and Dieter Krause (ed.), Analysis of the composition and structure of glass and glass ceramics, Spinger, 1999.

[74] A. E. Greenberg, R. R. Trussell, L. S. Clesceri and M. A. H. Franson, '*Standard methods for the examination of water and waste water*', 16th edition, American Public health Association, Washington, DC, 1985.

---

[75] ASTM Standard Test Methods for Determining Chemical Durability: Product Consistency Tests (PCT), ASTM-C-1285-94.

[76] L. F. Oldfield and R.D. Wright, "*Advances in glass Technology*, Pt-1, Technical papers of the VI International Congress on glass", Washington, DC, USA, Ed. *The Am. Ceram. Soc*., 1962.

[77] G.F. Noll, Radiation detection and measurement, John Wiley and sons Inc.

[78] S. Jeyakumar, V. V. Raut and K. L. Ramakumar, 'Simultaneous Determination of Trace Amounts of Borate, Chloride and Fluoride in Nuclear Fuels Employing Ion Chromatography after their Etraction by Pyrohydrolysis, *Talanta*, 76, 1246-51, 2008.

[79] B.D. Cullity, Elements of X-ray diffraction, Addison-Wilson Publishing Comp. Inc., U.S.A, 1959.

[80] H.P. Klug, L.E. Alexander, X-ray diffraction procedures, Wiley-Interscience Publication, New York, 1974.

[81] P. Boolchand, Insulating and semiconducting glasses, Series on directions in condensed matter physics, Vol.17, World scientific, Singpoor, 2000.

[82] E. R. Andrew, A. Bradbury and R. G. Eades, *Nature*, 183, 1802, 1959.

[83] I. J. Lowe, Phys. Rev. Lett., 2, 285, 1959.

[84] R.W. Cahn, P. Haasen, E.J. Kramer, Material Science and Engineering: Characterisation of Materials, VCH Publisher Inc., New York, 1991.

[85] W. Zhou, Z. L. Wang, Scanning microscopy for nanotechnology: Techniques and applications, Springer science and business media, New York, 2006.

[86] J. van R. Smit, W. Robb and J.J. Jacobs, *J. Inorg. Nucl. Chem*., 12, 104-112, 1959.

[87] Standard Methods of Chemical Analysis, N.H. Furman (Ed.), 6th Edition, Vol. 1, p. 815, D.Van Nostrand Co., Inc., New York, 1962.

[88] D. Banerjee., M.A. Rao and S.K. Samanta, Evaluation of Amberlite IRC-718 Chelating Ion Exchange Resin in Loading-Elution-Regeneration Cycles for Separation and Recovery of Strontium from Alkaline Radioactive Waste. *Sol. Extr. Ion Exch.* 26: 687-698, 2008.

[89] Pauling, The nature of the chemical bond, 2nd Edn., Cornell university Press, p 350, 1948.

---

[90] M.M Dubnin and I.V. Raushkevich (1947) Proc. Acad. Sci. USSR Phys. Chem. Sect. 55, 331.

[91] M. Polanyi, Verh. Deutch. *Phys. Ges*. 16:1012, 1914.

[92] M.A Rao and S.K. Samanta, Sequential Elution of Sodium and Cesium from Resorcinol Formaldehyde Polycondensate Resin, Proceedings of BRNS-DAE National Symposium on Nuclear and Radiochemistry, Mumbai, Feb 10-13, 295. 2003.

[93] M. V. Dyadenko and I. A. Levitskii, ‘Glass for fiber optics (Review)’, *Glass and Ceramics*, 65 [9-10] 310-315, 2008.

[94] I. W. Donald, ‘Preparation, properties and chemistry of glass- and glass-ceramic-to-metal seals and coatings’, *J. Mater. Sci.,* 28 [11] 2841-2886, 2006.

[95] L.C. Watson, A.M. Aikin and A.R. Bancroft, The permanent disposal of radioactive waste by incorporation in glass. Treatment and storage of high level radioactive waste, IAEA, Vienna, 37, 1963.

[96] M.N. Elliot, J.R. Grover and W.H. Hardwick, Fixation of radioactive waste in glass, Part II, Ibid, 381.

[97] J. Mukerji, Fixation of high level atomic waste in glass for ultimate disposal, part-I, General aspect, *J. Sc. Ind. Res*. 33(6), 397-405, 1974.

[98] W. Lutze, *Radioactive waste forms for the future*, Edited by W. Lutze and R. C. Ewing, pp.1-161 in Chapter-1, North-Holland, Amsterdam, 1988.

[99] L. A. Chick, B. F. Pieple, G. B. Mellinger, R. P. May, W. J. Gray and C. Q. Buckwalter, ‘The Effects of Composition on Properties in an 11 Component Nuclear Waste Glass System’, US DOE Report No. PNL-3188, Pacific Northwest Laboratory, WA, USA , 1981.

[100] Uhlig's Corrosion Handbook, 3rd edition, R. Winston Revie (ed), Wiely.

[101] V. Dimitrov and T. Komatsu, Correlation Between Optical Basicity and Single Bond Strength of Simple Oxides and Sodium Containing Oxide Glasses, *Phys. Chem. Glasses: Eur. J. Glass Sci. Technol. B,* 49 [1], 33–40, 2008.

[102] H. Scholze, Chemical durability of glasses, *J. Non-Cryst. Solids* 52, 91-103, 1982.

---

[103] L. L. Hench, D. E. Clark and J. Campbell, High Level Waste Immobilization Forms, *Nucl. Chem. Waste Manage.*, 5, 149-73, 1984.

[104] A. Paul, Chemical Durability of Glasses: A Thermodynamic Approach, *J. Mater. Sci.*, 12, 2246-68, 1977.

[105] P.B. Adams, Glass corrosion, *J. Non Cryst. Solids*, 67, 193-205, 1984.

[106] D. C. Stewart, '*Data for Radioactive Waste Management and Nuclear Applications*', P-185, John Wiley & Sons, 1985

[107] R. C. Rastogi, J. D. Sehgal, K. Chandra and K. T. Thomas, 'Investigation of Materials and Methods for the Fixation of Low and Medium Level Radioactive Waste in Stable Solid Media', BARC Report No. BARC-400, Bhabha Atomic Research Centre, India, 1969.

[108] J. A. Kelly, Evaluation of a Glass as a Matrix for Solidification of Savannah River Plant Waste, US DOE Report No. DP-1382, Savannah River Laboratory, USA , 1975.

[109] W. J. Gray, Volatility of Some Potential High Level Radioactive Waste forms, *Radioact. Waste Manage.*, 1[2], 147-69, 1980.

[110] J. Saidl, In chemistry and Process Engineering for HLW Solidification, pp. 621-27 *in Proceedings of International Seminar Julich*, Edited by J. R. Odo, Kernforschung sanlange, Julich, Conc, 1981.

[111] J. R. Harbour, Volatility of Simulated High Level Nuclear Waste Glass by Thermogravimetry Analysis, *J. Am. Cearm. Soc.*, 75 [3], 507-13, 1992.

[112] J. W. Mellor, *A comprehensive Treatise on Inorganic and Theoretical Chemistry*, Vol. II, pp. 813, Longmans, Green and Co, London, New York, Toronto, 1948.

[113] F. Z. Roki, C. Chatillon, M. N. Ohnet and D. Jacquemain, Thermodynamic Study of the CsOH(s,l) Vaporization by High Temperature Mass Spectrometry, *J. Chem. Thermodynamics*, 40, 401–16, 2008.

[114] M. Asano and Y. Yasue, Vapour Species Over Na_2O-B_2O_3-SiO_2-Cs_2O Glass, *J. Nucl. Sci. Technol.*, 22 [12], 1029-32, 1985.

---

[115] G. Rudolph, J. Saidl, S. Drobnik, W. Guber, W. Hild, H. Krause and W. Muller, 'Lab Scale R&D Work on Fission Product Solidification by Vitrification and Thermite Process', pp. 655-79 *in Proceedings of Symposium on Manage. of Radioactive Waste from Fuel Reprocessing* , Jointly Edited by OECD Nuclear Energy Agency and IAEA, Paris, 1972.

[116] B. Mysen and D. Neuville, Effect of Temperature and TiO_2 Content on the Structure of $Na_2Si_2O_5$-$Na_2Ti_2O_5$ Melts and Glasses, *Geochim. Cosmochim, Acta,* 59 [2], 325-42, 1995.

[117] M. Cable, and M. A. Chaudhry. Volatilization from soda-lime-silica melts at one atmosphere and reduced pressures, *Glass Technology,* 16 (6), 25-134, 1975.

[118] W. D. Kingery, H. K. Bowen, and D. R. Uhlmann, Introduction to Ceramics, Vol. 232. Wiley-Interscience, New York, 1976.

[119] T. Zhang, William G. Fahrenholtz, Signo T. Reis and R. K. Brow, Borate Volatility from SOFC Sealing Glasses, *J. Am. Ceram. Soc.*, 91 [8] 2564–2569, 2008.

[120] S. D. Ross, *Inorganic Infrared and Raman Spectr*, pp. 148 -260, McGraw-Hill, New York, 1972.

[121] V. Sudarsan, V. K. Shrikhande, G. P. Kothyal and S. K. Kulshreshtha, Structural Aspects of B_2O_3 Substituted (PbO)0.5(SiO2)0.5 Glasses, *J. Phys.:Condens, Matter,* 14, 6553-65, 2002.

[122] L. A. Farrow and E. M. Vogel, Raman Spectra of Phosphate and Silicate Glasses Doped with the Cations, Ti, Nb and Bi, *J. Non Cryst. Solids*, 143, 59-64, 1992.

[123] R. K. Mishra, V. Sudarsan, C. P. Kaushik, K. Raj, S. K. Kulshreshtha, and A. K. Tyagi, Effect of BaO Addition on the Structural Aspects and Thermophysical Properties of Sodium Borosilicate Glasses, *J. Non-Cryst. Solids,* 353 [16–17], 1612–7, 2007.

[124] V. K. Shrikhande, V. Sudarsan , G. P. Kothiyal, S. K. Kulshreshtha, Photoluminescence and Structural Studies on Na_2O–PbO–SiO_2 Glasses, *J. Non Cryst. Solids,* 353, 1341–45, 2007.

[125] N. F. Mott and E. A. Davis, *Electronic Processes in Non-Crystalline Materials*, 2nd Edition, pp. 272-300, Clarendon Press, Oxford, 1979.

[126] M.A. Rana, R.W. Douglas, The reaction between glass and water. Part I. Experiment methods and observations, *Phys. Chem. Glasses*. 2, 179-195, 1961.

---

[127] R. P. Turcotte and J. W. Wali, Devitrification behaviour in a zinc borosilicate nuclear waste Glass, Report PNL-2247, Battelle, Pacific Northwest Laboratories, March, Richland, Wa.99352, 1078.

[128] N.E. Bibler, W.G, Ramsey, T.F. Meaker, J.M. Pareizs, Durabilities and microstructures of radioactive glasses for immobilization of excess actinides at the Savannah River site, Proceedings of the 1995 MRS Fall Symposium; Boston, MA, USA; 27-30 Nov. 1995, Materials Research Society, Pittsburgh, PA, United States.

[129] D.E. Clark, M.F. Dilmore, E.C. Ethridge and L.L. Hench, Aqueous corrosion of soda-silica and soda-lime-silica glass, *J. Am. Ceram. Soc.*, 59 [1-2], 62-65, 1976.

[130] B.M.J. Smets, M.G.W. Tholen and T.P.A. Lommen, The effect of divelent cations on the leaching kinetics of Glass, *J. Non-Cryst. Solids*, 65, 319-332, 1984.

[131] I.A. Levitsk, S.A. Gailevich and I.S. Shimchik, The effect of bivalent cations on the physicochemical properties and structure of borosilicate glasses, *Glass and Ceramics*, 61, 73-76, 2004.

[132] H. Miyoshi, D. Chen, H. Masui, T. Yazawa and T. Akai, Effect of calcium additive on structural changes under heat treatment in sodium borosilicate glasses, *J. Non Cryst. Solids*, 345 & 346 99-103, 2004.

[133] M. Arbab, V.K. Marghussian , H. Sarpoolaky and M. Kord, The effect of RO oxides on microstructure and chemical durability of borosilicate glasses opacified by P_2O_5, *Ceramics International,* 33, 943–950, 2007.

[134] J. Wu and J. F. Stebbins, Effects of cation field strength on the structure of aluminoborosilicate glasses: High-resolution ^{11}B, ^{27}Al and ^{23}Na MAS NMR, *J. Non-Cryst. Solids*, 355, 556–562, 2009.

[135] J.O. Israd and W. Muller, Influence of alkaline earth ions on the corrosion of glasses, *Phys. Chem. Glasses*, 27 [2], 55-58, 1986.

[136] *M.M.* Islam, D. Holland, A.P. Howes, C.R. Scales, The effect of divalent additions on the structure of a mixed alkali borosilicate glass for high level waste immobilization, *Phys. Chem. Glasses*, 3, 137-145, 2010.

---

[137] R. K. Mishra, K. V. Sudarsan, P. Sengupta, R. K. Vatsa, A. K. Tyagi, C. P. Kaushik, D. Das, Kanwar Raj, Role of Sulfate in Structural Modifications of Sodium Barium Borosilicate Glasses Developed for Nuclear Waste Immobilization, *J. Am. Ceram. Soc.*, 91[12] 3903–3907, 2008.

[138] H. Kamizono, S. Kikkawa, S.Tashiro, H. Nakamura and H. Kanazawa, Air contamination by cesium in a canister containing nuclear waste glass, *J. Nucl. Mater.*, 149 113-16, 1987.

[139] R.W. Goles, and G J. Sevigny. Off-Gas Characteristics of Defense Waste Vitrification Using Liquid-Fed Joule Heated Ceramic Melters, PNL-4819 UC-70, Pacific Northwest Laboratory, Richland, Washington. 1983.

[140] M.H. Langowski, J.G. Darab and P.A. Smith, Volatility Literature of Chlorine, Iodine, Cesium, Strontium, Technetium and Rhenium; Technetium and Rhenium Volatility Testing, US DOE Report No. PNNL-11052, Pacific Northwest National Laboratory, USA, 1996.

[141] H. Kamizono, S. Kikkawa, Y. Togashi, S. Tashiro, Volatilization of ^{137}Cs and ^{106}Ru from Borosilicate Glass Containing Actual High-Level Waste, *J. Am. Ceram. Soc.*, 72 (8), 1438–41, 1989.

[142] B. P. Spalding, Volatilization of Cesium-137 from Soil with Chloride Amendments during Heating and Vitrification, *Environ. Sci. Technol*., 28 [6] 1116–23, 1994.

[143] B.P.W. Cains, K.C. Yewer, and S. Waring. Volatilization of Ruthenium, Caesium and Technetium from Nitrate Systems in Nuclear Fuel Processing and Waste Solidification, *Radiochemica Acta*, 56, 99-104, 1992.

[144] M. Asano, T. Kou and Y. Yasue, Mass Spectrometric Study of Vaporization of Cesium-Containing Borosilicate Glasses, *J. Non-Cryst. Solids*, 92 [2-3], 245-60, 1987.

[145] M. Asano, T. Harada and Y. Mizutani, Vaporisation of glasses in the R2O-Cs2O-B2O3-SiO2 (R= Li, Na, K and Rb) system, *J. Mater. Sci*., 26, 399-406, 1991.

[146] D. W. Bonnel, E. R. Plante and, J.W. Hastie, Vaporization of Simulated Nuclear waste Glass, *J. Non-Cryst. Solids*, 84, 268-75, 1986.

---

[147] B.G. Parkinson, D. Holland, M.E. Smith, A.P. Howes and C.R. Scales, Effect of minor additions on structure and volatilization loss in simulated nuclear borosilicate glasses, *J. Non-Cryst. Solids*, 353 [44-46], 4076-83, 2007.

[148] S. M. Salem, E. M. Antar, E. A. Mohamed, Structural and dielectric properties of Li_2O–ZnO–BaO–B_2O_3–CuO glasses, *J. Mater. Sci*., 46, 1095–1102, 2011.

[149] S. Bale, S. Rahman, A.M. Awasthi, V. Sathe, Role of Bi_2O_3 content on physical, optical and vibrational studies in Bi_2O_3–ZnO–B_2O_3 glasses, *J Alloys Compd*., 460, 699-703, 2008.

[150] A.B. Rosenthal and S.H. Garofalini, Molecular dynamics simulation of amorphous zinc silicate, *J. Non-crystl. Solids*, 87, 254-258, 1986.

[151] A.B. Rosenthal and S.H. Garofalini, Structural role of zinc oxide in silica and soda-silica glasses, *J. Am. Ceram. Soc*., 70, 821-826, 1987.

[152] G. Ennas, A. Musinu, G. Piccaluga, A. Montenero, G. Gnappi, Structure and chemical durability of zinc-containing glasses, *J. Non-crystl. Solids*, 125, 181-185, 1990.

[153] W.J. Dell and P.J. Bray, ^{11}B NMR studies and structural modelling of Na_2O-B_2O_3-SiO_2 glasses of high soda content, *J. Non Cryst. Solids*, 58, 1-16, 1983.

[154] G. Malow and W. Lutze, Sodium Diffusion in borosilicate glasses. Part 1. Influence of glass composition, *Phys. Chem. Glasses*, 16 113-18, 1975.

[155] R.K . Mishra, Sumit Kumar, B.S. Tomar, A.K. Tyagi, C.P. Kaushik, Kanwar Raj, V.K. Manchanda, Effect of barium on diffusion of sodium in borosilicate glass, *J. Hazardous Materials*, 156 129–134, 2008.

[156] A.H. Naik, N.V. Thakkar, V.R. palkar, S.R. Dharwadkar, K.D. Singh Mudher and V. Venugopal, Radiochim. Acta, 94, 335-338, 2006

[157] A.H. Naik, S.B. Deb, A.B. Chalke, M.K. saxena, K.L. Ramakumar, V. Venugopal and S.R. Dharwadkar, J. Chem. Sci. 122(1), 71-82, 2010.

[158] B.E. Scheetz, D.K. Agarwal, E. Breval and R.Roy, Waste Manage. 14 (4), 489-505, 1994.